Fundamentals of Cosmic Physics, 1986. Vol. 11, pp. 1–278
0094–5846/86/1103-0001$18.50/0

The Stellar Initial Mass Function

JOHN M. SCALO
University of Texas

Contents

1. INTRODUCTION

1.1 Overview

A basic result from the theory of stellar evolution is that the structure and evolution of a star of given chemical composition is controlled by its mass. Numerical solutions of the equations of stellar evolution have demonstrated that this conclusion remains valid even in advanced evolutionary phases; the influence of initial composition, and probably rotation rate and magnetic field strength, are secondary in comparison. Once the mass of a star is specified, we can in principal calculate such quantities as its luminosity, radius, and radiation spectrum at any point in its history, and attempt to predict such things as the mass of newly-produced metals and the kinetic energy which it will inject into the interstellar medium during its lifetime. Since in many applications the integrated appearance and effects of a large number of stars are of primary interest, and because most of the relevant quantities are sensitive to mass, it is necessary to specify the relative fraction of stars in different mass intervals. The frequency distribution of stellar masses at birth, the so-called "initial mass function", or "IMF", is therefore an especially important function, particularly in evolutionary or population synthesis modeling of galaxies (see Tinsley, 1980 for a comprehensive review). In effect, the stellar mass distribution is the link between stellar and galactic evolution.

Observational determinations of the IMF and its possible variations in space and time also provide a fundamental constraint on theories of star formation. Most stars form in groups within large interstellar cloud structures, and the observed IMF contains information on how mass is partitioned and possibly redistributed among protostellar cloud fragments, and on the manner in which these processes depend on local and global conditions. Theories for the form of the IMF are numerous, ranging from simple analytic arguments to probabilistic models to numerical hydrodynamic calculations. Although the importance of the many physical mechanisms which may control the IMF remain unclear, the theoretical studies are important as a chain in the link between stellar and galactic evolution. It is unlikely that, in the foreseeable future, we will be able to observationally constrain the dependence of the mass distribution on such parameters as metal abundance, ambient radiation spectrum, thermodynamic state and magnetic field strength in the interstellar medium, and so on. The theories, no matter how qualitative, allow us to at least make an educated guess as to how the mass distribution might depend on local and global conditions.

On the other hand, the extensive theoretical literature on the IMF presents a bewildering jumble of approaches and ideas, usually motivated by empirical evidence which is either extremely uncertain or subject to ambiguous interpretation. Furthermore, empirical IMFs are often presented as power law approximations which admit a large number of theoretical interpretations. As an example one can consider the range of physical mechanisms which were purported to account for Salpeter's (1955) power law approximation to the IMF, often "predicting" exponents in amazingly close agreement with the Salpeter value of -2.3. It is my present feeling that the IMF represents the result of a number of nonlinear physical processes operating over a wide range of spatial scales whose detailed modeling lies beyond present-day theoretical capabilities. One has only to consider the fact that the most ubiquitous nonlinear process of all, turbulence, still defies our physical understanding, even at the terrestrial level, to see that a realistic physical theory of the IMF may lie in the distant future. For these reasons, and because of space limitations, I confine this review to the empirical and semiempirical evidence and its uncertainties. It is such evidence which will ultimately provide some insight into the dominant physical processes which determine the IMF.

The purpose of the present review is to collect and present the available observational evidence relating to the stellar mass distribution. The remainder of this section introduces the problematical definition of the stellar mass distribution as a probability density, discusses the use of parameterized distribution functions, and gives a few examples of practical manipulations. Observational evidence is discussed in Sections 2 through 7. Section 2 is a detailed presentation of the direct observational determination of the IMF from counts of field stars in the solar neighborhood. Some of the quantities which are discussed include the luminosity function, the mass-luminosity relation, stellar lifetimes as a function of mass, and the stellar birthrate history in our galaxy. A new estimate of the field star mass spectrum is given, as well as a critical assessment of the sources of

error. An alternate method which is in principle more straightforward is the determination of luminosity functions and mass distributions in clusters of stars, which is the subject of Section 3. The available information concerning open clusters of various ages, OB associations, groups of pre-main sequence stars, and globular-clusters is selectively reviewed, and the problem areas, which are for the most part very different from those encountered in the field star IMF, are delineated. We are most interested in variations in the IMF among these individual objects, especially open clusters, and the degree to which the group mass spectra agree with the estimate for field stars. In Section 4 determinations of the luminosity functions of bright stars in nearby galaxies are presented and compared. The major goal here is an answer to the questions of whether the IMF varies among galaxies, and if any variations are correlated with galactic properties. Sections 5 through 7 present a review of the numerous indirect methods and arguments which have been proposed to infer variations or uniformity of the IMF in space and time. Most of these methods rely either on an interpretation of the integrated light (e.g., colors, line strengths) of galaxies or theoretical models for the chemical evolution of galaxies. These sections emphasize the methods, problems, and uncertainties encountered, although an attempt is made to synthesize the available data into a coherent and consistent picture.

Previous reviews which discuss parts of this material have been given by Tinsley (1980), Burki (1980), Lequeux (1981), Scalo (1978), Miller and Scalo (1979), Silk (1978), and Zinnecker (1981). The work of Zinnecker contains an especially thorough discussion of theories for the IMF. The book by Mihalas and Binney (1981) is an excellent source of background material.

1.2 Definitions

A satisfactory definition of the IMF must be general enough to encompass all plausible possibilities for its behavior, yet precise enough so that practical determinations of stellar mass distributions can be meaningfully related to the definition and to theories of star formation. These conflicting requirements lead to serious and unresolved difficulties which are fundamental in nature, and it will be useful to begin with a clear recognition of these problems.

If nothing at all were known about star formation and we sought the simplest possible conceptual model on which to base a definition of the IMF, we might visualize stars forming individually at random positions throughout the galactic disk at a constant total rate. If the value of the stellar mass at any of these uncorrelated positions is a random variable distributed according to some probability density $f_0(m)$, one can think of each position as a realization of a stochastic time process $m(t)$, and the collection of positions constitutes a statistical ensemble. If the process is stationary in time and homogeneous in space, then a consistent and unambiguous definition of $f_0(m)$ can be given: $f_0(m)dm$ is the fraction of stars in any volume of space which have masses in the interval m to $m+dm$ at birth. In practice the fraction of stars counted in each mass interval would have to be corrected for the dependence of lifetime on mass in order to obtain the *initial* mass distribution, but the correction is straightforward in principle, especially since it was assumed that the total birthrate is constant. It is seen that this conceptual ideal for the star formation process leads to an operationally viable yet mathematically consistent definition. This was only possible because the star formation process was assumed to be a stationary homogeneous ergodic process.

Stars are not formed independently, but instead in groups, or clusters. To accommodate this fact, the meaning of the IMF must be revised. Assume that each cluster represents an independent realization of the star formation process and thus the IMF. Individual clusters will differ in their mass distributions because of stochastic variations, but the ensemble average over a large number of clusters will be meaningful. An empirical estimate of the IMF defined in this way could be obtained again from counts of field stars, assuming they are former members of disrupted clusters, or by trying to average a number of individually determined cluster mass distributions.

However, a little thought shows that no consistent and practical definition of the IMF is possible if the form of this function has varied systematically with time or position in the galaxy. Consider the collection of field stars in the solar neighborhood, which contains objects originally formed in a large number of clusters and associations of stars over a range of times and positions in the galaxy. The problem with this sample is that the age of an observed star is limited by its lifetime, which is a sensitive function of mass. The field stars with masses like the sun's or smaller live for $\gtrsim 10^{10}$yr and were mostly formed at locations very distant from their current positions, while very massive stars can have ages no greater than $\sim 10^7$yr and are observed near their birthsites. This means that if we construct the frequency distribution of masses of field stars we will only obtain a proper ensemble average if the IMF represents a process which is stationary in time and homogeneous in space. Any spatial or temporal variations in the IMF which are not stochastic will result in an empirical IMF which has only an indirect relation to either the true space-time ensemble average IMF over the history of the galaxy or the spatial ensemble average of any particular time, and there is no way to "correct" the empirical IMF without some theoretical model for how the IMF varies. Furthermore one cannot derive the "average" IMF over the entire age and dimensions of the galaxy because the range of ages and birthsites depends on mass, so a detailed model of stellar migration would be required.

There is no *a priori* justification for assuming that the IMF is constant in time or space. The IMF is actually a conditional probability whose form may depend on metal abundance, gas density, turbulent velocity, or some other property of the interstellar medium, and several of these properties have certainly varied with time and position in our galaxy.

An alternate approach which could in principle circumvent some of these problems is to determine the average frequency distribution of stellar masses for a large sample of star clusters and associations which all have about the same age. The resulting IMF would then be a spatial ensemble average at a particular time interval in the past. By using collections of groups with different ages we could test whether the IMF is a stationary process and, if it isn't, estimate its time dependence. Unfortunately a number of considerations preclude the practical application of this program. For example, each age group would offer us different ranges of stellar masses because of the effects of stellar evolution on the upper mass limit of a cluster (the turnoff mass) and the fact that the lower mass limit (actually absolute magnitude limit) to which we can identify cluster members is a function of the cluster's distance from the sun. Optimistically, then, we can only hope to use cluster samples to determine the form of the mass spectrum over a number of mass intervals, each of which would correspond to a different time in the past. These segments could not be combined to give $f(m)$ over the entire range of stellar masses without again assuming that the IMF is a stationary and homogeneous process. Even the construction of a composite cluster IMF over a limited mass range for groups with about the same age is not straightforward, since it is not clear how to weight each cluster or correct for different upper and lower mass limits if, as seems likely, there are cluster-to-cluster fluctuations in the IMF. These matters are discussed in detail in Section 3.

We are therefore left in the uncomfortable position of having no means of obtaining an empirical mass distribution which corresponds to a consistent definition of the IMF and which can be directly related to theories of star formation without introducing major assumptions. The best we can do at present is to attempt an estimate of the IMF by assuming it to be constant in space and time, and then examine the nature of the fluctuations of this function among individual groups of stars, and search for evidence regarding systematic variations with position and time in our own and other galaxies.

We define the *mass spectrum* of stars $f(m)$ such that $f(m)dm$ is the number of stars formed at the same time in some volume of space with mass in the interval m to $m+dm$ at birth. It is a differential frequency distribution. The phrase "at birth" is somewhat ambiguous, especially for massive stars, but we are generally referring to the mass of a star when it settles onto the hydrogen-burning main sequence. We are clearly excluding giants, central stars of planetary nebulae, stellar remnants, and protostellar gas clouds. The mass spectrum may be defined in this way for an individual cluster, in which case it represents a realization of $f(m)$, or for a sample of clusters or field stars. In the latter case $f(m)$ is an ensemble average, but this average is only meaningful if the function does not depend on time or spatial position.

The units of $f(m)$ are defined entirely by the desired normalization. It is usually convenient to treat $f(m)$ as a standard probability density function, so that

$$\int_{m_l}^{m_u} f(m)dm = 1,$$

where m_l and m_u are the lower and upper mass limits which may also be functions of time, and

$$\int_{m_1}^{m_2} f(m)dm$$

is the fraction of stars with masses between m_1 and m_2. In some applications, however, we will normalize to the total number of stars in some volume or in some cylinder directed through the disk of a galaxy. In other applications, especially the mass spectra in clusters and the luminosity functions of galaxies, the normalization will be arbitrary, since we are for the most part concerned with the shape of the mass spectrum.

The upper and lower limits of $f(m)$, m_l and m_u, are parameters generally believed to have current values around $m_u \approx 100$–500 and $m_l = 0.05$–0.1. (All masses will be given in units of solar masses in what follows.) The upper limit may be related to the effectiveness of radiation pressure relative to gravity at large masses, although other effects have been suggested, while the lower limit is dictated by the ability of degenerate electron conduction to cool the stellar core before nuclear reactions can commence. These subjects were reviewed in Scalo (1978), and more recent developments on the value of m_u can be found in papers by Lamers, Paerels, and de Loore (1980), Maeder (1980), Hutchings (1980), Chiosi and Greggio (1981), and Walborn (1982). The recent interest in the object R136, located in the 30 Doradus nebula of the Large Magellanic Cloud (see, e.g., Chu and Daod 1984 and references therein) emphasizes the uncertainty in m_u.

It is convenient in practice to replace the mass spectrum $f(m)$, the fraction or number of stars born per unit mass interval dm, by another function which gives the fraction or number of stars born per unit logarithmic (base ten) mass interval $d\log m$. We refer to this function as the *mass function* $F(\log m)$, related to $f(m)$ by

$$F(\log m) = (\ln 10) m\, f(m). \tag{1.1}$$

When referring to the number of field stars in a specially-defined area of the galactic disk integrated over the history of the galaxy (assuming a constant mass function) this function is given the special symbol $\xi(\log m)$ and is referred to as the "initial mass function" for reasons which will be explained in Section 2 below. In most applications $\xi(\log m)$ and $F(\log m)$ can be thought of as equal within a scale factor. The well-entrenched term "IMF" will be used in a more general sense here to refer to either the mass spectrum or mass function, a practice which should not cause confusion. The empirical estimates in Sections 2 through 7 will, for consistency's sake, be uniformly expressed as the number of stars per unit log m.

Other quantities of interest are the cumulative number distribution, which is the fraction of stars more massive than m:

$$g_n(>m) = \int_m^{m_u} f(m)dm = \int_{\log m}^{\log m_u} F(\log m)d\log m \tag{1.2}$$

and the cumulative mass distribution, which is the fraction of the mass of all stars contained in stars more massive than m:

$$g_m(>m) = \frac{\int_m^{m_u} mf(m)dm}{\int_{m_l}^{m_u} mf(m)dm} = \frac{\int_{\log m}^{\log m_u} mF(\log m)d\log m}{\int_{\log m_l}^{\log m_u} mF(\log m)d\log m} \tag{1.3}$$

Note than $g_n(>m)+g_n(>m)=g_m(>m)+g_m(<m)=1$.

Averages and all higher moments (variance, skewness, kurtosis, etc.) of the mass distribution can be readily defined, but will not ordinarily be encountered in this work.

Extremely useful parameters are the *indices* of the mass spectrum and mass function, defined as

$$\gamma(m) = \left.\frac{\partial \log f(m)}{\partial \log m}\right|_m \tag{1.4}$$

and

$$\Gamma(m) = \left.\frac{\partial \log F(\log m)}{\partial \log m}\right|_m \tag{1.5}$$

These are the logarithmic slopes of $f(m)$ and $F(m)$ evaluated at mass m. For power law mass spectra, these indices are independent of mass. For example, the classical Salpeter field star initial mass function has an index $\Gamma \approx -1.3$, and the corresponding mass spectrum

has $\gamma = \Gamma - 1 \approx -2.3$. The lognormal field star IMF fit by Miller and Scalo (1979) has $\Gamma \approx -(1+\log m)$.

The literature contains a great variety of nomenclature for the mass spectrum, mass function, and their indices, so one must exercise some care in the interpretation of published results.

While in most applications the IMF can be treated as a univariate distribution, in some applications, for example involving binary stars, we must consider the joint distribution $f(m_1, m_2)$ in which m_1 and m_2 may be dependent. An example is the frequency distribution of mass sums or ratios in binary systems (see Trumpler and Weaver 1953). The joint distribution of masses is also important in judging the feasibility of Type I supernova mechanisms which involve binary interactions (Miller and Chevalier 1985).

It is commonly necessary to calculate the frequency distribution $h(y)$ of some function of mass, say $y(m)$. The transformation is simply

$$h(y) = f(m)/|dy/dm| \tag{1.6}$$

where m and $|dy/dm|$ must be expressed in terms of y. This transformation is central to all derivations of $f(m)$ because for practically all stars we cannot directly observe the mass, but some quantity which is thought to be well-correlated with mass; this quantity is nearly always the absolute magnitude in some broad-band filter system, such as the absolute visual magnitude M_v. In this case $h(y)$ is proportional to the "luminosity function" $\phi(M_v)$, which gives the number of stars per unit magnitude interval per volume of space.

The consideration of the IMF as a probability distribution has some important immediate consequences which are not generally appreciated. Several of these statistical effects have been discussed by Elmegreen (1984). Consider an interstellar cloud which is forming stars at a constant rate B with a constant mass spectrum $f(m)$, normalized to unity. At a time Δt after star formation began, the expected number of stars more massive than some mass m' is

$$N(>m') = B\Delta t \int_{m'}^{\infty} f(m)dm,$$

where the upper mass limit for $f(m)$ has been taken as infinite for simplicity. The time at which the expected largest mass is m', $\Delta t(m')$, is thus given by setting $N(>m')=1$. Comparing two masses m_1 and m_2, with $m_2 > m_1$, for a power law $f(m) \propto m^{\gamma} (\gamma \neq -1)$ this gives $\Delta t(m_2)/\Delta t(m_1) = (m_1/m_2)^{\gamma+1}$. For example, if $\gamma = -2$, the first $10 M_{\odot}$ star is expected to form 10 times later than the time at which the first $1 M_{\odot}$ star appears. For the lognormal IMF of Miller and Scalo (1979), this factor is 43 (Elmegreen 1984). The important point is that one expects high mass stars to form latest in a cluster due to this purely statistical effect alone. There is fairly convincing evidence that star formation proceeds from small to large masses in several clusters and regions of current star formation, as discussed in more detail in Section 3. The above discussion suggests that one could estimate the appropriate value of γ in a region of current star formation, such as the Taurus complex, by comparing the mean ages of stars in two or more mass intervals. This approach might provide a valuable check on the IMF obtained from star counts in such regions, especially when the total number of objects is too small to directly construct a meaningful IMF. In general the procedure is more complicated than in the example given above, because the star formation rate may not have been constant. However, it may be possible to estimate $B(t)$ in the regions of interest, as in the study of Cohen and Kuhi (1979).

Additional consequences of the probabilistic nature of $f(m)$ which can account for a number of observational results, such as the correlation of cloud mass with maximum mass of associated stars found by Larson (1982) and the fact that OB associations appear unbound while open clusters are bound, are discussed by Elmegreen (1984).

One additional simple yet significant consequence of the statistical nature of $f(m)$ is that we should not be too surprised at the appearance of a "gap" between the two largest masses observed in a cluster. The probability that a star has a mass greater than xm_1 is

$$\int_{xm_1}^{\infty} f(m)dm,$$

or $x^{\gamma+1}$ for a power law $f(m)$. Thus we might see a more or less continuous distribution of masses up to m_1 in a cluster, no stars from m_1 to xm_1, and then N stars more massive than xm_1. The probability of this event for a power law $f(m)$ is $x^{N(\gamma+1)}$ if the masses of consecutively formed stars are independent. For example, if $\gamma = -2$, the probability of a factor of three gap in mass with N stars above the gap is 3^{-N}.

1.3 Parameterized mass distributions

In most applications of the IMF to astrophysical problems, it is natural to seek a simple analytical formula which can provide an approximation to the real IMF. This procedure is so commonly applied in the study of size distributions (see Soo 1967; Fuchs 1974; Williams 1964; Sedunov 1974) and lends itself so readily to theoretical derivations and practical applications of the IMF, that the properties of a few of the more commonly adopted distribution functions are summarized here.

The most commonly adopted form is the power law distribution

$$f(m) = Am^{\gamma} \tag{1.7}$$

This distinctive property of the power law mass spectrum is that it has no preferred scale (except for the lower and upper mass limits); it is also rarely, if ever, encountered in any real natural or artificial systems. However, often the data are so uncertain that a power law fit is adequate especially because of the ease with which it can be integrated. Normalization to unity gives.

$$A = \begin{cases} \dfrac{1+\gamma}{m_u^{1+\gamma} - m_l^{1+\gamma}} & \gamma \neq -1 \\ \ln^{-1}\left(\dfrac{m_u}{m_l}\right) & \gamma = -1. \end{cases} \tag{1.8}$$

When $\gamma = 0$, this is the uniform distribution. Other common forms are the gamma distribution

$$f(m) = \frac{1}{\beta\alpha\Gamma(a)} m^{a-1} \exp(-m/\beta) \tag{1.9}$$

where $\Gamma(\alpha) = \int_0^{\infty} y^{a-1} e^{-y} dy$, $\alpha > 0$, and the mean mass is $\langle m \rangle = \alpha\beta$; the exponential distribution ($\alpha = 1$ in the gamma distribution)

$$f(m) = \frac{1}{\langle m \rangle} \exp(-m/\langle m \rangle); \tag{1.10}$$

the Rayleigh distribution

$$f(m) = \frac{1}{\pi \langle m \rangle^2} m \exp(-\pi m^2/4\langle m \rangle^2); \tag{1.11}$$

and of course the normal or Gaussian distribution

$$f(m) = \frac{1}{(2\pi)^{1/2}\sigma} \exp[-(m - \langle m \rangle)^2/2\sigma^2] \tag{1.12}$$

where σ^2 is the variance. Since size and mass distributions are rarely symmetrical, it is common in such studies (see Fuchs 1974, Edwards 1976, and Soo 1967 for examples from aerosol size distributions, May 1974 for other examples) to use the lognormal distribution

$$\begin{aligned} f(m)dm &= F(\log m) d\log m \\ &= \frac{1}{(2\pi)^{1/2} \log \sigma_1} \exp[-(\log m - \langle \log m \rangle)^2 / 2(\log \sigma_1)^2] d\log m \end{aligned} \tag{1.13}$$

where $(\log \sigma_1)^2 = \langle (\log m - \langle \log m \rangle^2 \rangle$ is the variance in log m.

A more complicated, but still very useful, parameterized distribution is the "generalized Rosin–Rammler" function (Williams 1965),

$$f(m) = B\, m^{\gamma} \exp(-\mathrm{A} m^{s}) \tag{1.14}$$

in which one of the four parameters A, B, γ, s, can be eliminated by normalization in favor of $\langle m \rangle$. The case $s = 0$ gives a power law while $s = 1$ gives a gamma distribution. Multimodal distributions are also sometimes required to fit measured size and mass distributions.

It is important to realize that, while the resemblance of a mass distribution to some analytic parameterized function may yield clues to the formation and evolution of the system, it is generally the deviations from the idealized form which give the most unique constraints. Especially in the study of size and mass distributions, it is generally true that a large number of theoretical models can be imagined which will result in a given simple distribution function. However it is rare to find size distributions in nature which tend to some common simple form. The processes governing the evolution of the distribution function are often so varied and complex that a universal equilibrium distribution, simple or not, is unlikely to exist. Parameterized mass distributions should therefore be regarded primarily as useful tools for predicting the integrated properties of a large number of stars, such as the spectrum or metal enrichment of a galaxy.

1.4 Examples of practical applications

Before we begin to discuss attempts to estimate the IMF, it will be useful to see how this function enters into the calculation of various integrated properties of a group of stars, which could be a star cluster or a galaxy. This exercise is meant to motivate the subsequent sections by introducing a few of the many astrophysical applications in which the IMF plays a central role.

Assume that stars in some region of space are born at a total rate $B(t)$, which may vary with time in an arbitrary manner. The star formation rate per unit volume per unit mass interval at time t is then $f(m)\, B(t)$. (The mass spectrum $f(m)$ can be assumed to possess an implicit time dependence, as long as it is realized that in that case we have no way of empirically estimating its form for the reasons described in Section 1.2) Stars spend nearly their entire lives burning hydrogen near the main sequence and we can usually neglect all subsequent phases of evolution as short-lived by comparison. We therefore associate a lifetime $\tau(m)$ with each star of mass m. At any time T after star formation began, the total number of main sequence stars per unit volume will be

$$N_*(t) = \int_{m_0(t)}^{m_u} \int_{T-\tau(m)}^{T} f(m)B(t)dmdt + \int_{m_l}^{m_0(T)} \int_0^T f(m)B(t)dmdt \tag{1.15}$$

where $m_0(T)$ is the mass at which $\tau(m) = T$. The integration limits reflect the fact that stars with $\tau(m) < T$ have already died. The total mass of main sequence stars at time T, $M_*(T)$ is given by the same expression but with a factor of m in both integrands.

Theoretical estimates for the rate of occurrence of stellar events such as supernovae and planetary nebulae depend on the IMF. For example, if all stars more massive than some limit m_{SN} explode as supernovae at the end of their lives, and $\tau(m_{SN}) < T$, then the supernova rate per unit volume at time T will be

$$R_{SN}(T) = \int_{m_{SN}}^{m_u} f(m)B(T-\tau(m))dm. \qquad (1.16)$$

The time delay in the birthrate reflects the fact that the deathrate of stars of a given mass depends on the birthrate a main sequence lifetime ago. If we knew $f(m)$ we could estimate the currently-known quantity m_{SN} from observed supernova rates. In practice, it is quite difficult to carry out this procedure because of uncertainties in the supernova rate as well as the birthrate history and IMF.

We can also write down an expression for the frequency distribution of masses of stars in a particular evolutionary stage. If a star of mass m spends a time $\tau_p(m)$ in evolution prior to the phase of interest and $\tau_i(m)$ is the duration of the phase, then to be observed in that phase at time T, this star must have been born between times $t_1 = T-\tau_p(m)$ and $t_2 = T-[\tau_p(m)+\tau_i(m)]$. The desired mass distribution is then

$$N(m) = \int_{t_2(m)}^{t_1(m)} f(m)B(t)dt. \qquad (1.17)$$

This expression has been used to study problems associated with mixing in red giants (e.g. Scalo and Miller 1979) and the rate of planetary nebula formation (Papp, Purton, and Kwok 1983). Similarly, the predicted luminosity function of white dwarfs, for a given set of white dwarf cooling calculations, depends on the IMF (see D'Antona and Mazzitelli 1978 for such a calculation).

The mass spectrum also partly controls the evolution of the interstellar gas density and abundances of the elements in a galaxy. If each star of initial mass m ejects a mass $m_{ej}(m)$ near the end of its life, then the net rate of change of the mass density of interstellar gas due to stellar processes will be

$$\frac{d\rho}{dt} = \int_{m_0(T)}^{m_u} m_{ej}(m)f(m)B[T-\tau(m)]dm - \int_{m_l}^{m_u} mf(m)B(T)dm \qquad (1.18)$$

where the first term accounts for mass ejection from dying stars and the second term gives the total mass being formed into stars at the time T. If the ejected mass $m_{ej}(m)$ contains a fractional abundance

$Z^A_{ej}(m)$ of an element A, then the net rate of enrichment of the abundance by mass of this element in the interstellar medium at time T, $Z^A(T)$, is given by

$$\frac{d[Z^A(T)\rho]}{dt} = \int_{m_0(T)}^{m_u}$$

$$\times Z^A_{ej}(m)m_{ej}(m)f(m)B[T-\tau(m)]dm - Z^A(T)\int_{m_l}^{m_u} mf(m)B(T)dm.$$

Such equations form the basis for the study of galactic chemical evolution (see Tinsley 1977, 1980 for comprehensive reviews). In order for such equations to be useful, the dependence of m_{ej} and Z_{ej} on stellar mass must be reliably known from stellar evolution calculations.

We can calculate the total luminosity of a group of main sequence stars in some wavelength interval, say the visual band, by assuming that we know the mass-luminosity relation $l_v(m)$ from empirical or theoretical studies. The result is

$$L_v(T) = \int_{m_l}^{m_0(T)}\int_0^{\tau(m_0)}$$

$$\times l_v(m)f(m)B(t)dmdt + \int_{m_0(T)}^{m_u}\int_{T-\tau(m)}^{T} l_v(m)f(m)B(t)dmdt.$$

Later evolutionary phases could be treated by including the time dependence of $l_v(m,t)$ for each mass. A similar expression for the blue luminosity can be used to calculate the evolution of the B–V color of a star cluster or galaxy, and can be combined with the expression for $M_*(T)$ to study the mass-to-light ratio, for an assumed mass spectrum and birthrate history. Expressions such as these form the basis for the study of galactic photometric evolution, and can in principle be compared with real galaxies in an effort to determine the birthrate and/or the IMF.

We can also estimate the total radiation emitted by H II regions in galaxies. Since H II regions result from the ionization of interstellar neutral hydrogen by ultraviolet radiation with $\lambda < \lambda_H = 912Å$, the total ionizing radiation rate per unit volume will be

$$L_{uv}(T) = \int_{m_d(t)}^{m_u} \int_{T-\tau(m)}^{T} \int_0^{\lambda_H} s(\lambda,m) l(m) f(m) B(t) d\lambda dm dt$$
$$+ \int_{m_l}^{m_d(T)} \int_0^{\tau(m_d)} \int_0^{\lambda_H} s(\lambda,m) l(m) f(m) B(t) d\lambda dm dt. \quad (1.21)$$

where $l(m)$ is the total (bolometric) luminosity of a star of mass m and $s(\lambda,m)$ its relative spectral distribution normalized such that

$$\int_0^{\infty} s(\lambda,m) d\lambda = 1.$$

A similar expression can be used to calculate the radiation emitted in any wavelength interval. The function $s(\lambda, m)$ must come from observed spectra of nearby stars of all relevant masses and/or from model atmosphere calculations. A match to a galaxy spectrum in a number of wavelength regions, usually including spectral line strengths, can yield constraints on the IMF and/or birthrate, and this procedure is usually referred to as population synthesis.

These equations are usually simplified by assuming that $f(m)$, m_l, and m_u are independent of time, and by adopting simple analytically integrable forms for $f(m)$ and $B(t)$. An exponential form of $B(t) \propto e^{-t/\tau}$ is especially popular. Much can also be learned by adopting simple analytic forms for $\tau(m)$, $l(m)$, etc. Power laws like $l(m) \propto m^{4}$ and $\tau(m) \propto m^{-3}$ have often been used in illustrative work. More sophisticated studies use theoretical stellar evolution calculations to estimate the stellar properties in detail, include time delays in the birthrate, and treat other processes and properties not considered above. For examples the reader is referred to Talbot and Arnett (1971), Searle, Sargent, and Bagnuolo (1973), Larson and Tinsley (1978), Dwek and Scalo (1979), and Chiosi and Matteucci (1982).

One general and important result which emerges from all the above expressions is that the predicted values of all quantities except abundances of primary metals depend on both the mass spectrum *and* the birthrate history $B(t)$, even if $f(m)$ is independent of time and space and all the other quantities are known. It is difficult to think of any galactic evolution problem which does not involve $f(m)$ and $B(t)$ together, and there is usually no straightforward and unambiguous

method for disentangling their effects. (The predicted absolute abundances of primary metals do not depend much on $B(t)$, but are very sensitive to the chemical evolution model, e.g., the importance of infall, radial flows and galactic winds, as discussed in Section 6.) This is a recurring and severe problem in galactic evolution studies. Since we cannot directly measure $B(t)$ (but see Section 2.6 below), a reliable observational or theoretical determination of the mass spectrum and its possible dependence on local or global properties of galaxies would greatly improve our understanding of the chemical, photometric, and spectral similarities and differences among galaxies. In many cases the procedure is reversed, and the observed integrated properties are used, along with some assumption or (rare!) independent evidence concerning $B(t)$ in order to constrain the form of the mass spectrum. Given the number of and uncertainties in the input quantities like $m_{ej}(m)$, $Z^{A}_{ej}(m)$, and $B(t)$, these indirect IMF estimates carry low weight, but taken together suggest some interesting possibilities. We return to these indirect methods for estimating the mass spectrum in Sections 5 through 7. First we must examine the large body of data which can be used to estimate the mass spectrum directly from star counts.

2. THE FIELD STAR INITIAL MASS FUNCTION

2.1 Definitions and procedure

A primary method for estimating the stellar mass function is to determine the frequency distribution of luminosities for field stars in the solar neighborhood, convert this to a distribution of masses using an adopted mass-luminosity relation, and then correct the distribution for the stars which have died during the history of the disk. This approach was used in a pioneering paper by Salpeter (1955). The resulting mass function will be referred to as the *field star initial mass function*, often abbreviated IMF, and will be denoted $\xi(\log m)$. Several complications and assumptions arise in practice, and so it is important to understand the steps involved in the procedure. The discussion given here parallels and updates the derivation of the field star IMF given by Miller and Scalo (1979, hereafter MS). Comparisons with earlier determinations can be found in MS.

The term "field stars" loosely refers to the stars in the solar neighborhood which are not presently in clusters. The size of the "neighborhood" varies greatly according to the absolute magnitude range being studied and the method used to obtain distances, varying from about 40 pc for samples of lower-mass ($\lesssim 2M_\odot$) stars with reliable trigonometric parallaxes, to about 5 kpc for massive ($\gtrsim 10M_\odot$) stars whose distances are established by spectroscopic parallaxes. Since the fraction of nearby stars which are members of clusters is negligible, the term "field" stars is appropriate, except for massive stars, most of which can still be found in clusters and associations because of their youth.

The field star IMF is often referred to as the "local" or "solar neighborhood" IMF because the star counts on which it is based can only sample nearby regions of space. It should be understood that these terms are misleading for stars with masses less than around $2M_\odot$. The random peculiar velocities of disk stars, typically 20–40 km s^{-1}, are large enough that most stars with main sequence lifetimes greater than 10^9yr, corresponding to $m \sim 2$, have wandered over a considerable fraction of the galactic disk during their lives, assuming a roughly uniform age distribution. For this reason the field star IMF for lower-mass stars reflects the average IMF of a significant fraction of the entire galactic disk, no matter how small the sample volume of the star counts. In addition, the solar neighborhood contains (at least) two populations, one corresponding to a local spiral arm, the other to an underlying well-mixed disk population (see Mould 1982; also Clube 1983). For $m \gtrsim 3$, on the other hand, we observe most field stars near their place of birth, and the derived IMF can be considered local, with a sampling scale $\sim$ 1–5 kpc.

Similarly, the mass function at mass m derived from star counts represents an average of the IMF over a time equal to the lifetime of stars with mass m. For low mass stars with $m \lesssim 1$ the IMF is a time average over the entire history of the disk, while for $m \gtrsim 3$, the average only covers the past 10^8yr. For these reasons, if the IMF has varied significantly with time or with position in the galaxy, the field star IMF derived from star counts has a complex physical meaning, since it refers to averages over spatial and time scales which depend on mass, as discussed in Section 1.2. We are therefore forced to assume that the field star IMF is independent of location in the disk for $m \lesssim 2$, and independent of time for all masses. Relaxation of these assumptions would require the determination of more parameters,

such as the IMF index as a function of time, or the slope of some adopted relation between IMF and galactocentric distance. We return to these questions in Sections 5–7 below.

The fundamental observational quantity which is used to estimate the field star IMF (or just IMF in what follows) is the *luminosity function* $\phi(M_v)$, which gives the number of stars of all types (not just main sequence stars) observed at absolute visual magnitude M_v per unit magnitude per unit volume. Many determinations of the luminosity function are based on blue or photographic magnitudes rather than visual magnitudes, but most of the calibrations which will be required to determine the IMF are based on M_v, and so we will always transform blue or photographic magnitudes into M_v.

The luminosity function can be transformed into a mass function $\phi_{ms}(\log m)$, which is the number of *main sequence* (actually core hydrogen-burning) stars at mass m per unit interval of log m, per unit *area*. The number per unit area, that is, integrated perpendicular to the galactic disk, is used because of a bias that would be introduced into the number per unit volume by the fact that stars are distributed differently perpendicular to the disk according to their mass; more massive stars are more concentrated to the midplane of the disk. The function $\phi_{ms}(\log m)$ is called the present-day mass function, or PDMF for short, because it refers only to those stars which can be observed today. The relation between $\phi(M_v)$ and $\phi_{ms}(\log m)$ is

$$\phi_{ms}(\log m) = \phi(M_v) \left| \frac{dM_v}{d \log m} \right| 2H(M_v) g_{ms}(M_v) \tag{2.1}$$

The factor $|dM_v/d\log m|$ transforms the luminosity function into a mass function. A relation between M_v and mass (mass-luminosity relation) is also required for substitution in $\phi(M_v)$. It should be noted that the mass-luminosity relation used does not imply a unique relation between mass and luminosity; it does not refer to the luminosity of a star on the zero-age main sequence, but the average luminosity of hydrogen-burning stars of all ages at a given mass. This choice approximately compensates for the effect of the brightening of stars during their main-sequence lifetime, an effect which is discussed further below. The term $2H(M_v)$ is the result of integrating the luminosity function perpendicular to the disk, assuming an exponential spatial distribution in this direction with scale height $H(M_v)$ at each

M_v. The last factor, $g_{ms}(M_v)$, is the fraction of stars at a given M_v that are on the main sequence; it corrects the observed luminosity function for the presence of stars which have exhausted hydrogen in their cores and are now in a later evolutionary phase.

PDFM does not reflect the frequency distribution of stellar masses at birth because of the effects of stellar evolution. Stars with masses $m \lesssim 1$ have lifetimes as large as the age of the disk, so for these masses the PDMF counts all stars ever born, and is a time integral of the IMF over the past $\sim 10^{10}$yr. However, more massive stars have smaller lifetimes, and so we only observe some fraction of the stars ever born. This fraction decreases with increasing mass. In order to derive the IMF, we must correct the PDMF for this effect. The correction, which we now derive, involves the lifetimes of stars as a function of mass and the star formation rate as a function of time in the disk.

Define a stellar *creation function* such that $C(\log m,t)d\log m\, dt$ is the number of stars born per unit area in the galactic disk in the mass range $\log m$ to $\log m + d\log m$ during the time interval t to $t+dt$, averaged over a suitably large region centered on the sun. The term creation function is used to emphasize the dependence on both mass and time, and to avoid confusion with the "birthrate", which is used below. The creation function can be related to the PDMF as follows. All stars with main-sequence lifetimes $\tau(m)$ greater than the age of the galactic disk T_0 are still on the main sequence, so the observed number of these stars is

$$\phi_{ms}(\log m) = \int_0^{T_0} C(\log m,t)dt, \quad \tau(m) \geqslant T_0. \tag{2.2}$$

It is useful to denote by $m(t)$ the stellar mass which corresponds to lifetime t. The above expression is then valid for $m < m(T_0)$. For stars with main-sequence lifetimes $\tau(m) < T_0$, we only see those stars born within the last $\tau(m)$ years, since all stars born between $t=0$ and $t=T_0-\tau(m)$ have evolved off the main sequence. Therefore,

$$\phi_{ms}(\log m) = \int_{T_0-\tau(m)}^{T_0} C(\log m,t)dt, \quad \tau(m) < T_0 \tag{2.3}$$

These equations can be simplified by assuming that the creation function is a separable function of mass and time

$$C(\log m,t) = F(\log m)B(t), \tag{2.4}$$

where $B(t)$ is the total stellar birthrate per unit area of the disk at time t, normalized such that

$$\int_0^{T_0} B(t)dt = T_0\bar{B}, \tag{2.5}$$

with $\bar{B}$ the average birthrate over the history of the disk. The quantity $T_0\bar{B}$ is the total number of stars ever formed in the galactic disk. It is usually stated that the assumption of a separable creation function is made mostly for the sake of convenience and simplicity, since there is very little theoretical or observational evidence for or against this assumption. However, it should be recalled from Section 1.2 that the assumption is mandatory if we are to have a practical and consistent definition of the IMF. In this case, we can write

$$\phi_{ms}(\log m) = F(\log m)T_0\bar{B}, \ \tau(m) \geqslant T_0. \tag{2.6}$$

The quantity on the right represents the number of stars per unit area and per unit log m with $\tau > T_0$ which have ever formed, and essentially defines the units of the field star IMF, $\xi(\log m)$:

$$\xi(\log m) = F(\log m)T_0\bar{B}. \tag{2.7}$$

For a time-independent mass function $F(\log m)$, then, $\xi(\log m)$ is equivalent to the mass distribution at birth, within a normalizing constant. It is useful to introduce the "relative birthrate" $b(t)$ as the ratio of the birthrate at time t, $B(t)$, to the birthrate $\bar{B}$ averaged over the past history of the disk. The normalization condition on $b(t)$ is

$$\int_0^{T_0} b(t)dt = T_0.$$

In these terms, the creation function is

$$C(\log m,t) = F(\log m)\bar{B}b(t) = \frac{\xi(\log m)}{T_0}\, b(T), \tag{2.8}$$

and the IMF is given in terms of the observable present-day mass function by

$$\xi(\log m) = \begin{cases} \phi_{ms}(\log m)T_0 \Big/ \int_{T_0-\tau(m)}^{T_0} b(t)dt, & \tau(m) < T_0 \\ \phi_{ms}(\log m), & \tau(m) \geqslant T_0 \end{cases} \tag{2.9}$$

Notice that for $\tau(m) \ll T_0$ the first expression becomes

$$\xi(\log m) = \phi_{ms}(\log m)\frac{T_0}{\tau(m)}\frac{I}{b(T_0)}, \; \tau(m) \ll T_0 \tag{2.10}$$

This equation is valid for $m \gtrsim 2$ and shows that the shape of the upper part of the IMF is independent of $b(t)$.

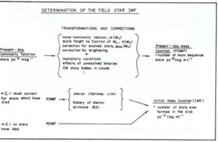

FIGURE 1 Steps involved in the derivation of the field star IMF.

The assumption of a separable creation function then divides the determination of the IMF into two problems: (1) Estimate the present-day mass function $\phi_{ms}(\log m)$ from the observed present-day luminosity function. For stars with masses so small that $\tau(m) \gtrsim T_0$, this determines the IMF; (2) Estimate the history of the relative stellar birthrate $b(t)$ and the age of the galactic disk T_0. If we assume that $\tau(m)$ is a known function, then the form of $b(t)$ and the value of T_0 tell us the factor by which the presently observed number of stars ϕ_{ms} at each mass $> m(T_0)$ must be increased to account for stars which have died. The procedure is shown schematically in Figure 1. We begin with the crucial estimate of the luminosity function, discuss quantities required to convert to the PDMF, and then discuss the stellar life-times and birthrate history needed to finally obtain the IMF.

2.2 Determination of the luminosity function

The most important function entering the derivation of $\phi_{ms}(\log m)$, and hence the IMF, is the luminosity function $\phi(M_v)$. Because of its central importance and because of several developments which were not apparent at the time of the review given by MS, a fairly complete review and update is given here.

2.2.1 *Methods*

All methods for determining the luminosity function of field stars involve counting the number of stars as a function of apparent magnitude m and estimating distances to these stars by various means. From this, the absolute magnitudes and space densities can be calculated. Detailed expositions of some of the methods and references to the large body of earlier work can be found in Trumpler and Weaver (1953), van Rhijn (1965), McCuskey (1966) and Mihalas and Binney (1981, ch. 4) and only a brief summary will be given here.

The most direct method for obtaining the luminosity function (LF in what follows) is the use of trigonometric parallaxes, π, which can only be measured reliably for nearby ($d \lesssim 20$–50 pc) stars. Stars are usually chosen for parallax measurement on the basis of large proper motion μ, so the star counts $N(m, \pi)$ must be corrected for the omission of stars with small μ, a correction which becomes very large at small μ. At μ smaller than some limit, a stellar kinematical approach is used to correct for incompleteness instead. Finally, corrections must be made for parallax measurement errors. This method was used by van Rhijn (1925), Starikova (1960), Muzzio (1973), Mazzitelli (1972), Wielen (1974), Armandroff (1982), and Upgren and Armandroff (1981). The latter four works used Gliese's (1969) catalogue and its supplement, which is believed nearly complete out to 20 pc (Upgren and Armandroff 1981), at least for $M_v \lesssim 9$, and so incompleteness is not a problem for the relatively brighter portion of the LF derived from this catalogue.

Early in this century, when the number of measured parallaxes was quite small, another approach, called the method of mean parallaxes, was used. Comparison of the distributions of proper motions and tangential velocities inferred from radial velocity distributions resulted in counts $N(m, \mu)$. Assigning mean parallaxes $\pi(m, \mu)$ to each (m, μ) cell from the little available direct parallax data, and assuming a probability distribution function for π about the mean, gave a most probable parallax for each mean parallax. Summing over μ at fixed m then allowed an estimate of $N(m, \mu)$, and $\phi(M)$. Van Rhijn (1936) used this method. Table 2 of McCuskey (1966) shows how well these first two methods agree, at least for $M_v \gtrsim 0$.

A third method, also designed to avoid the use of parallax measurements, is called the method of mean absolute magnitudes, and was applied by Luyten (1938, 1968), Wanner (1972), and Chiu (1980). The method involves blink surveys for stars with large proper motion ($\mu > 0.5$/yr) brighter than some limiting apparent magnitude. The counts $N(m, \mu)$ are then corrected for magnitude scale calibration, inclusion of binary stars, incompleteness due to unblinked sky areas, and μ measurement errors. One can then write $f(m, \mu, M) = N(m, \mu)\phi(M|m, \mu)$, where the last factor is to be determined. A new function $H = m + 5 + 5 \log \mu$, called the reduced proper motion, is then introduced. This function is useful because it is an intrinsic stellar property independent of distance, since it can be rewritten $H = M - 5.7 + 5 \log v_T$ where v_T is the tangential velocity. Luyten shows that $\phi(M|m, \mu)$ can be replaced with a function $\psi(M|H)$. The definition of H shows that if there exists a mean value of v_T for each M, independent of distance, then a linear relation between mean absolute magnitude $\bar{M}$ and H will exist. Stars of known parallax showed this to be the case, so $\psi(M|H)$ could be constructed by assuming a Gaussian form of

$$\psi(M|H) \propto \exp - [M - \bar{M}(H)]^2 / 2\sigma^2.$$

With $N(m, \mu)$ and $\psi(M|H)$ in hand, $f(m, \mu, M)$ can be obtained. Summing over μ and correcting for incompleteness due to the omission of small μ stars gives a function $g(m, M)$ which, when summed over m and divided by the volume element, finally gives the luminosity function. Published LFs using this method include Luyten (1938, Bruce Proper Motion Survey). Luyten (1968, Palomar Survey), and Wanner (1972, Lowell Survey). Wanner (1972) discusses the details of the computational methods and the resulting uncertainties. A recent discussion by Schmidt (1983) emphasizes the strong sensitivity of the LF on the adopted $\bar{M}(H)$ relation. As pointed out by Schmidt, this sensitivity, the fact that Luyten's LF for $M_v > 14.7$ was based on an extrapolation of the $\bar{M}(H)$ relation to fainter magnitudes, and the conclusion that the LF for $M_v > 12$ is based primarily on high-velocity stars (see also Gilmore 1983), suggest that the LF is not reliable for $M_v > 12$. A proper motion method to determine the LF which does not require the $\bar{M}$–H calibration has been reported (Kipp, 1981) to give good agreement with Luyten's (1968) LF.

All three of the above methods are restricted to relatively small distances and hence sample only very small numbers of intrinsically bright stars. In order to extend the luminosity function to greater volumes, luminosities based on spectroscopic and/or photometric criteria must be used. A major problem here, besides the distance calibration, concerns fluctuations in space density and interstellar absorption, so one must obtain a space density as a function of distance for each spectral class. Details can be found in Mihalas and Binney (1981). The method has been used by several investigators. Bartaya and Kharadze (1977) have used over 10,000 MK spectral types from the Abastumani catalogue in a LF determination. Cruz-Gonzalez *et al.* (1974), Lequeux (1979), Garmany, Conti, and Chiosi (1982), Bisiacchi, Firmani, and Sarmiento (1983), Humphreys and McElroy (1984), Van Buren (1985), and Vanbeveren (1985) used spectroscopic parallaxes in studies of very massive stars. Photometric parallaxes have been used primarily for the faint end of the LF, notably by Weistrop (1972), Chiu (1980, hybrid with $\bar{M}$ method), Reid (1982), Reid and Gilmore (1982), and Gilmore and Reid (1983).

The method used by McCuskey (1956) and Upgren (1963), while still relying basically on spectroscopic parallaxes, is considerably different than those described above, and I will refer to it as the method of "spectral groups". For a given spectral group, i.e. a given spectral type-luminosity class interval, the stellar density $D_s(r)$ as a function of distance is related to star counts $A_s(m)$ as a function of apparent magnitude through an integral equation of the form $A_s(m) \propto {}_0\int^{\infty} r^2 D_s(r)\, \phi_s(M)\, dr$, where $\phi_s(M)$ is the LF for that spectral group. To solve for $D_s(r)$ it is *assumed* that $\phi_s(M)$ for each group is a Gaussian, with mean and variance coming from other data, usually luminosities of stars in open clusters. In this case $\phi(M,r)$ summed over all the groups is linearly proportional to $D_s(r)$ with coefficients which can be calculated from the error function. A more detailed presentation can be found in McCuskey's (1966) review. Since the method must assume a value for M for each spectral group, it is referred to as a "spectroscopic parallax" method here. The assumption of Gaussian $\phi_s(M)$ for each group is basically *ad hoc*, and in fact we know that $\phi_s(M)$ for several spectral type intervals is more like a power law. The effect of non-Gaussian $\phi_s(M)$ on the result has not been investigated.

A different approach to estimating the luminosity function has been used in applications where one wishes to separate two groups of stars on the basis of kinematic criteria. In such studies (Schmidt 1975, Chiu 1980, Eggen 1983) a sample of stars with proper motions exceeding some limit and apparent magnitudes brighter than some limit is constructed. The sample limits introduce biases which can be reduced using the "V_m method" of Schmidt (1968, 1975). Distances are estimated for each star either by trigonometric, photometric, or spectroscopic parallax. The maximum distance to which each star *could* be seen, r_m, is calculated from its absolute magnitude and the apparent magnitude limit of the sample. The corresponding maximum volume is $V_m = 4\pi r_m^3/3$. Each star in a particular M_v range contributes V_m^{-1} to the luminosity function, so $\beta \sum V_m^{-1}$ for all sample stars in this M_v range gives the value of luminosity function, where β is the sky fraction sampled. Chiu (1980) and Eggen (1983) have used variations of this method to estimate the LF of disk stars and halo stars, following the work of Schmidt (1975) on the halo LF. Details and refinements can be found in these papers.

Variations in the shape of the LF with distance from the sun, with galactic longitude, and with distance z above the galactic plane (for

$z \lesssim 500$ pc; see Gilmore and Reid 1983) are surprisingly small (see Figure 5, Figure 6, and Table IX in McCuskey 1966, and the discussion of OB stars given in Section 7 below), and the actual variations from region to region, at least in the solar neighborhood, may amount to no more than 50% (see, however, Chiu 1980). More recent comparisons of the LF of north and south galactic pole samples by Kipp (1983) and of galactic models with deep star counts by Pritchet (1983) and Bahcall and Soniera (1984) support this contention. Variations in the LF do appear for distances $\gtrsim 100$ pc from the galactic plane, but these are due to an increasing admixture of Population II stars (see Upgren 1983a). The reasonable agreement between LFs derived independently using different methods and for different volumes of space lead to the conclusion that there exists a meaningful average luminosity function which represents the disk population in the solar neighborhood. We assume this to be so in the present section.

2.2.2 *Comparison of luminosity function determinations*

In order to graphically compare the large number of LF determinations and to estimate uncertainties, the entire range of M_v has been divided into four slightly overlapping portions: $-7 < M_v < -1$ (spectral types O and B, Figure 2), $-2 < M_v < 5$ (late B to early G stars, Figure 3), $4 < M_v < 11$ (late F to early M stars, Figure 4), and $9 < M_v < 17$ (lowest mass M stars, Figure 5). Table I lists the 15 LF determinations plotted; for each source the table gives the method used, the range is M_v covered, the figures in which they are shown, the symbol used in the figures to represent that determination, and a few comments. In the figures, determinations based on the $\bar{M}$–H method are connected by dashed lines, those based on spectroscopic or photometric parallaxes by solid lines, and those based on trigonometric parallaxes by dot-dashed lines. Eggen's (1983) disk LF estimates based on the V_m method are not connected for the sake of clarity. Upper and lower limits quoted in the references are not included because they would confuse the visual display for the faintest stars and, in any case, are very uncertain.

All photographic LFs were converted to visual LFs using $\phi(M_v) = \phi(M_{pg})\, |dM_{pg}/dM_v|$, with a set of linear relations of the form (see, e.g., Allen 1973 for data sources)

$$M_v = a(M_{pg} + b) \tag{2.11}$$

TABLE I
Luminosity function determinations

Source	Method	Min. M_v	Max. M_v	Figures	Symbols	Remarks
Luyten (1939)	M	−0.8	18.1	2,3,4	△	Bruce Proper Motion Survey, complete to $M_v = 13.4$
Luyten (1968)	M	−0.8	18.1	2,3,4	▲	Palomar Proper Motion Survey, complete to $M_v = 15.3$
Wanner (1972)	M	2.8	15.3	2,3,4	▼	Lowell Proper Motion Survey, complete to $M_v = 13.4$
Chiu (1980)	M, phot. π	4.5	12.5	3,4	□	Hybrid method; results shown are for Chiu's model A
Reid (1982)	phot. π	7.5	12.5	3,4	◆	So. gal. pole, 50 pc. sample
Reid and Gilmore (1982)	phot. π	9	16	3,4	×	So. gal. pole, 100 pc. sample, machine-counted
van Rhijn (1965)	trig. π, spec. π, μ	−5.5	13.4	1–4	○	Average of 3 methods, from van Rhijn (1939)
Upgren (1963)	spectral groups	−0.8	5.3	2,3	▽	No. gal. pole, 100 pc sample.
McCuskey (1956, 1966)	spectral groups	−1.7	6.2	2,3	◇	LF from assumed Gaussian LF for each of several groups, for both Upgren and McCuskey
Bartaya and Kharadze (1977)	spec. π	−5.5	6.2	1,2,3	+	Ambastumi Catalogue of spectral types
Cruz-Gonzales *et al.* (1974)	spec. π	−5.8	−0.4	1	▼	Counts by spectral type
Garmany *et al.* (1982)	spec. π	−7	−4	1	×, △	Spectral type O stars, complete to ~2.5 kpc
Armandroff (1982); Upgren and Armandroff (1981)	trig. π	1	13	2,3,4	•	Gliese (1969) catalogue and supplement; complete to 20 pc
Muzzio (1973)	trig. π	3	13.6	2,3,4	■	Parallaxes of large-μ (nearby) stars. Required incompleteness corrections
Eggen (1983)	trig. π, phot. π	3	16.5	2,3,4	*	Large-μ (nearby) stars with V_m method of Schmidt (1975)

where the constants a and b are given for 4 separate magnitude ranges (not the same as the ranges used in the figures) in Table II. In plotting Muzzio's $\phi(M_B)$ I used $M_B = M_{pg} + 0.11$. The LFs taken from Chiu's (1980) study represent averages of his tabulated LFs for the regions SA 51, SA 57, and SA 68. Chiu's method, which is a combination of photometric parallax for $B-V \le 1.3$ and the method of mean absolute magnitudes for $B-V > 1.3$ along with a V/V_{max} test, required matching a star density model of the form

$$\rho(r,z) \propto r^{-n} \exp(-z/z_0).$$

Results are shown for his "model A" ($n=2$, $z_0 = 300$ pc). Chiu prefers his model B ($n=4$, $Z_0 = 500$ pc), but notes that it must represent the higher-velocity disk component. His model B results falls below model A by 0.7 in $\log \phi(M_v)$ at $M_v = 4.5$, by about 0.4 for $6.5 \le M_v \le 8.5$, and by about 0.1 at $M_v = 12.5$.

TABLE II
Parameters for convertion of M_{pg} to M_v

Range in M_v	a	b
<1	0.94	0.17
1 to 6	0.85	0.28
6 to 8.9	0.83	0.50
>8.9	0.95	−0.90

The results shown for McCuskey's (1956) work using the "spectral group" method were taken from McCuskey (1966), who gives the average $\log \phi(M_{pg})$ for 9 regions studied, using an updated absolute magnitude scale for each spectral class. The results of Upgren's (1963) study of stars toward the north galactic pole using the same method were also taken from McCuskey (1966), who revised the mean absolute magnitudes and dispersions.

Wielen's (1974) LF based on Gliese's catalogue of nearby stars is not shown, but is very similar to the updated version of Upgren and Armandroff (1981) and Armandroff (1982) which is shown in the figures. For these last two references only their "separate component" case is shown; their "combined magnitude" case which treats binaries as single objects gives a LF which is generally smaller by roughly 0.02 to 0.1 in $\log \phi(M_v)$, with differences increasing with larger M_v. Also not shown is the LF determination of Wielen, Jahreiss, and Krüger

(1983) which is also based on Gliese's catalogue and its supplement, but with different volumes for stars in each of 4 M_v intervals. However their result is very similar to the Upgren and Armandroff LF for the M_v range in common ($1 < M_v < 13$). Wielen *et al.* (1983) give a LF outside this range, but the result is based on less than 5 stars at each M_v. It should be noted that Luyten's (1968) LF continues to $M_v \approx 22$; however Gilmore (1983) has presented evidence showing that this tail in Luyten's LF is due to the inclusion of high velocity stars at faint apparent magnitudes, a possibility which was recognized by Luyten. Schmidt (1983) also discusses this problem and suggests that high-velocity stars become a problem for $M_v > 12$.

We now discuss each M_v range in more detail, and attempt to settle on an adopted luminosity function.

The range $M_v < -1$

The brightest part of the luminosity function presents severe difficulties for the determination of the IMF. First, the number of intrinsically bright stars is very small and the statistical uncertainties correspondingly large. As emphasized by Garmany, Conti, and Chiosi (1982, hereafter GCC), the LF recommended by McCuskey (1966) and used by MS only surveys a roughly 1 kpc region containing about 45 O stars ($m \gtrsim 20$) and only 5 stars earlier than 07 ($m \gtrsim 30$), yet the LF is given to $M_v = -6$ ($m \approx 60$). This criticism is not quite correct, since MS also compared McCuskey's LF with independent data on the space densities of 2883 O and early B stars derived by Torres-Peimbert *et al.* (1968). The agreement was satisfactory within the large uncertainties (see MS, Figure 5). Nevertheless, the number of O stars used in the LF was indeed very small. Van Rhijn (1965) considers his LF (open circles in Figure 2) as very uncertain for $M_v \lesssim -3$ because of the small number of stars. Bartaya and Kharadze (1977) give a spectroscopic LF (plus signs in Figure 2) which extends to $M_v \approx -5.5$, but do not give sufficient information on the number of stars used in each M_v interval. The problem of obtaining a sufficiently large sample of early-type stars which is complete to some limiting apparent magnitude or distance has been attacked more recently in the studies of Lequeux (1979), GCC, and others. (See Section 2.6.4 below).

A second problem arises because the basis of the method used here to estimate the IMF is the assumption that the luminosity function can be transformed to a mass function, i.e., that there is a one-to-one correspondence between M_v and mass, once a correction for post-hydrogen-burning phases of evolution is applied. This is not true, especially for massive stars. In an H–R diagram with M_v and $\log T_e$ as coordinates, a star of given initial mass evolves to the right and upward during core hydrogen burning, even though an evolutionary track in the $M_{bol} - \log T_e$ plane may be roughly horizontal. This occurs because the core hydrogen-burning phase covers a large range in T_e, and the bolometric correction becomes smaller in absolute value at lower T_e, as more of the total stellar flux shifts into the visible part of the spectrum. For example, a $40 M_\odot$ star may evolve from an early O star on the zero-age main sequence to a B0 star by the end of core hydrogen-burning (e.g. Brunish and Truran 1982a), so the bolometric correction will change by over a magnitude. The bolometric magnitude contributes further to this effect, brightening by ~ 0.5–1 mag. This means that a horizontal cut through the M_v–$\log T_e$ diagram at given M_v will contain stars with a range of masses, from the zero-age mass corresponding to that M_v downward. Application of the mass-luminosity relation to convert the LF to a mass function will therefore overestimate the number of massive stars, i.e. the mass function will be too flat.

There is no completely satisfactory way to circumvent this dilemma. Lequeux (1979), Garmany *et al.* (1982) and others (see Section 2.6.4) have avoided the use of a luminosity function altogether by comparing the positions of stars in the M_{bol}–$\log T_e$ plane with theoretical evolutionary tracks to assign masses. This method suffers from the necessity of adopting very uncertain calibrations of bolometric corrections and effective temperatures with spectral type and from the large uncertainties in theoretical calculations of high-mass stellar evolution (e.g. mass loss rates and convective overshoot). On the other hand, this method is more sensitive to IMF variations than is the method which relies on the LF. The results of this approach are discussed later.

In order to use directly the visual luminosity function, which is the basic observable, we must correct the luminosity function for the effect of brightening during the core hydrogen-burning phase. This problem was discussed in detail by MS (Appendix), who derived a general expression for the correction factor, $\varkappa$. The expression can be evaluated if the dependence of M_v on age for each mass is given. In principle this information is contained in theoretical evolutionary tracks, but, because there is no way to extract this much detail from the large number of published evolutionary calculations, a simple brightening law was adopted. According to this assumed law, M_v decreases linearly with time, decreasing by an amount $\Delta M_v(m)$ by the end of the main sequence lifetime, for each mass m. MS show the results of numerical solutions for $\varkappa(\log m)$ for two constant values of $\Delta M_v = 0.75$ mag and 1.0 mag, and verified the result using a simulation. The basic features are that the correction factor is near unity for $m \lesssim 0.8$, since these stars have not had time to brighten, decreases rapidly as mass increases from 0.8 to $2.0 M_\odot$, and then flattens out for larger masses (see MS, Figure 14). The asymptotic value at $m \gtrsim 4$ depends on $\Delta M_v(m)$ but not the birthrate history. The reader is referred to MS for details. The important conclusion is that a simple but fairly accurate approximation is given by simply replacing the relation between mass and zero-age luminosity by the relation found using instead the luminosity of a star of average age. This is just what will be done in Section 2.3.1. below.

We can therefore use the visual luminosity function to derive the mass function, although it should be remembered that an approximation is involved. The question remains: What is the visual luminosity function? The most extensive sample of O-type stars available at the time of this writing was that of GCC. The catalogue contains 427 O stars our to a distance of 2.5 kpc. C. Garmany kindly made available M_v data for all the stars in the GCC catalogue. The sample was checked for completeness by plotting the cumulative number distribution as a function of distance, following GCC, and also by examining the distribution of apparent magnitudes. There is no compelling evidence for incompleteness except for the faintest stars ($-4.5 \leq M_v \leq -3.5$). The LF was constructed by dividing the stars into one magnitude M_v intervals and dividing by a limiting volume of $3.5 \times 10^9 \text{pc}^3$ (assuming a scale height of 90 pc—the scale height will cancel out when we convert the LF into a mass function). The LF is shown in Figure 2 (crosses), along with $N^{1/2}$ uncertainties. Also shown for comparison is the LF from the same data but binned in half-magnitude intervals. The discrepancy with other estimates around $M_v \approx -5$ (based on smaller samples) should be noted. It should also be remembered that the GCC catalogue contains only O

stars, and so at $M_v \sim -4$ to -5 a significant number of stars which have evolved to somewhat cooler effective temperatures during core hydrogen-burning are omitted. This incompleteness effect is obvious from Figure 2 at $M_v \approx -4$, but the effect on the slope of the LF for $M_v \lesssim -5$, where the data was adopted, is uncertain, except that inclusion of the B stars may steepen the LF. That the effect may be significant is suggested by the work of Bisiacchi, Firmani, and Sarmiento (1983), Vanbeveren (1984), and Humphreys and McElroy (1984), as discussed in more detail in Section 2.6.2 below.

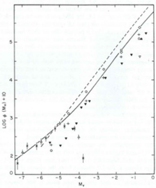

FIGURE 2 Determinations of the luminosity function of bright stars. Sources of data are given in Table I.

After the present comparison was completed Humphreys and McElroy (1984 hereafter HM) presented a visual LF for a much larger sample of 5044 stars which includes all spectral type B stars and supergiants with MK spectral types and luminosity classes, as well as the O stars from the GCC catalogue. The resulting LF is parallel to the LF adopted here for $-7.5 \leq M_v < -5.5$. The LF published by HM is larger than our adopted LF by a factor 2–3 in this magnitude range. Most of the difference is due to the fact that HM adopted a scale height of 200 pc (Humphreys, personal communication), which is a factor of 2.2 larger than the value adopted here in deriving a LF from the GCC value; I feel that the choice of 90 pc for the scale height is more appropriate for massive stars (see Section 2.3.2 below). In any case, since the scale height will cancel out in the construction of the IMF from the LF, the HM result can be regarded as consistent with the presently adopted LF over this magnitude range, except for a difference of 20–50 percent due to their inclusion of later spectral types. The HM LF flattens and eventually turns over for $M_v \geq -5.5$, suggesting serious incompleteness, as they point out; I have partially avoided this problem by extrapolating the adopted LF to fainter magnitudes so that it joins smoothly with the other LF estimates at fainter magnitudes. Because of the inclusion of supergiants of later spectral types, HM were able to extend their LF to $M_v = -9.5$; their LF steepens for $-9.5 \leq M_v \leq -7.5$ compared to the $-7.5 \leq M_v \leq 5.5$ range. However, I have not used these brighter stars in deriving the IMF because most of them are evolved supergiants whose evolution is very poorly understood.

Although we postpone a discussion of spatial variations in the IMF until Section 7, it should be noted here that the *shape* of the LF from the GCC catalogue showed no significant difference when stars toward and away from the galactic center were compared.

At fainter magnitudes the results of McCuskey (1956, 1966), Upgren (1963), and Luyten (1968), as well as the continuation of the LFs of Bartaya and Kharadze (1977) and van Rhijn (1965), are plotted. Also shown is the LF derived from the counts of stars as a function of spectral type given by Torres-Peimbert *et al.* (1974), using the relation between M_v and spectral type given in MS. Notice that because the counts represent vertical slices through the H–R diagram, the LF is only meaningful if at each spectral type most of the stars are near the main sequence. The adopted LF in this M_v range, shown as a solid line, basically joins the GCC LF at $M_v \leq -5$ with the McCuskey (1956, 1966) LF at $M_v > -2$, and passes through the van Rhijn and Bartaya and Kharadze results at intermediate luminosities. The LF which was used by MS (essentially the one recommended by McCuskey 1966), shown by the dashed line, is larger than the adopted relation by a factor of about 2 over most of the M_v range. The discrepancy apparently arises because of a different transformation between M_{pg} and M_v used by McCuskey, which was not noticed by MS. The uncertainties in this M_v range are at least ± 0.3 in log ϕ, judging from the scatter in the various determinations and the uncertainty in the distances (from an M_v-spectral type calibration) of the brighter stars not in clusters. The treatment of interstellar extinction may also introduce considerable uncertainty, as indicated by the work of Van Buren (1984).

The range $-2 < M_v < +5$

Published luminosity functions in this M_v range come from a variety of methods. The scatter among these determinations is quite large, from about 0.3 in log $\phi(M_v)$ at $M_v = 2$, to 0.5 or more at larger and smaller M_v. Without attempting any reconciliation, the LF adopted here is basically McCuskey's (1956, 1966, open diamonds in Figure 3) for $M_v \leq 2$ and Armandroff's (1982, filled circles) for $M_v \geq 2$. The scatter suggests an uncertainty of about $\pm 0.15 - 0.2$ in log $\phi(M_v)$ for this M_v range.

The range $4 < M_v < 10$

In this range of M_v a major question has recently centered on the difference between the LFs of Wielen (1974), which is based on Gliese's (1969) catalogue of nearby stars with measured trigonometric parallaxes, and Luyten (1968), which is based on proper motion data (M–H method) in the range $6 < M_v < 10$. Wielen's densities are smaller by a factor as large as two in this magnitude range. The LF of Wanner (1972) using the same method as Luyten but a different proper motion catalogue, shows an even larger LF than Luyten's over the range $4 \leq M_v < 9$. The LFs of Muzzio (1973), Eggen (1983), Chiu (1980), van Rhijn (1965), Reid (1982), and Reid and Gilmore (1982) also fall below Luyten's function in this magnitude range even though

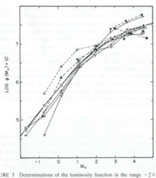

FIGURE 3 Determinations of the luminosity function in the range $-2 < M_v < +5$. Sources of data are given in Table I.

the last four results are based on photometric parallaxes. Upgren's (1963) LF which used the method of spectral groups is consistent with a dip at $M_v = +6$, but this is the faintest point and may suffer from incompleteness. McCuskey's $\phi(M_{pg})$ shows no dip, but his recommended $\phi(M_v)$ from the same data does indicate a dip at $M_v = +7$, the faintest luminosity included. The LF of Starikova (1960, inadvertently omitted from the graphical comparison), who used trigonometric parallaxes of stars with $m_v < 6.0$, agrees well with most results based on other methods. This LF does show a dip, but at $M_v \sim 8-9$ instead of at $M_v \sim 7$ as found from Gliese's catalogue, even though Starikova used some of Gliese's early data for faint stars. Eggen's (1983) LF based on a combination of distance indicators and the V_m method also shows a dip at this fainter luminosity. The origin of these discrepancies is not known.

A convincing demonstration of the reality of the dip has been given by Upgren and Armandroff (1981) and Armandroff (1982), who presented a detailed study of the completeness of Gliese's (1969) catalogue and its supplement (Gliese and Jahreiss 1979). According to Upgren and Armandroff, the lack of a dip in Luyten's LF may be due to uncertainties in the calibration of the method of mean absolute magnitudes and also because Luyten apparently smoothed his results in an unspecified manner. That the smoothing was important can be seen in the recent reanalysis of Luyten's LF by Kipp (1983), which shows a dip at $M_v \approx 6$ in both the north and south galactic pole samples.

In an independent study Reid (1982) used photometric parallaxes of bright M dwarfs, calibrated by trigonometric parallaxes, to derive the LF in the range $7 < M_v < 12$ for 122 stars. The results agree fairly well with Wielen's function, showing the factor of two deficiency relative to the Luyten function at $M_v \sim 7$. However Reid suggests that the difference may be due to different sampling volumes, and the possibility that the proper motion surveys included some misclassified dwarfs.

More indirect support for the dip comes from a comparison of models with the observed color distribution of disk stars (Bahcall and Soneira 1983), and with deep star counts by Armandroff (1982), Pritchet (1983a, b), Bahcall and Soniera (1984), and Gilmore (1984).

The presence of such a real feature in the LF, and possibly the mass function, could provide a valuable constraint on theoretical work, and so it is important to ask whether the feature could be a local fluctuation. At $M_v = +8$ there are about 5×10^{-3} stars pc^{-3} mag^{-1}, so the total number of stars between $M_v = +7$ and $+9$ is around 300 within the 20 pc survey radius, and a local fluctuation of a factor of two is very unlikely in such a volume. Besides, Chiu (1980) and others find a similar dip even though they surveyed a larger volume of space using different methods. Gilmore (1984) points out that modeling of color distributions and deep star counts require the dip to be present over distances of at least 1 kpc. A related analysis of star counts by Bahcall and Soniera (1984) gives the same result. With these comments in mind we give low weight to the results based on proper motions, and to the spectroscopic parallax results of Bartaya and Kharadze (1977), for which details are unavailable.

In adopting a "best" LF in the interval $4 < M_v < 11$ the following

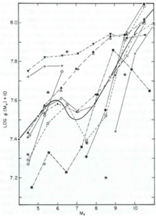

FIGURE 4 Determinations of the luminosity function in the range $4 < M_v < 10$. Sources of data are given in Table I.

considerations were made. First, I assume that the dip in the LF is real. The value of M_v at which the minimum occurs and the amplitude of the dip varies somewhat between the determinations which show it, but I adopted the dip minimum at $M_v = 7$, a full width of 2 mag, and an amplitude of 0.1 in log $\phi(M_v)$. (These last two numbers are measured with respect to a baseline of constant ϕ.) This amplitude is intermediate between the results of Upgren and Armandroff and van Rhijn (0.05–0.09) and Chiu and Muzzio (0.1–0.2). The

amplitude of Eggen's (1983) dip, ~ 0.6, is much larger, and his dip appears at $M_v \approx 8.5$. The Upgren and Armandroff LF is given the highest weight because of the simplicity of the method used and the demonstrated completeness of the sample.

For the increasing part from $4 \leq M_v \leq 6$ most of the determinations (including Luyten) agree well on the slope, and the adopted relation was passed through the Upgren and Armandroff results at $M_v = 4$ and 5. Past the dip, good agreement between most results is not reached until $M_v = 10$, so the adopted LF was basically extrapolated from the value adopted at $M_v = 8$ through Upgren and Armandroff's result at $M_v = 10$. The explanation for the larger values found in Reid's 50 pc sample using photometric parallaxes compared to Reid and Gilmore's 100 pc sample using a similar method, but automated star counting, is not clear.

The uncertainty in this M_v range can be roughly estimated as ± 0.15 in log $\phi(M_v)$, and probably smaller at $M_v \sim 10$.

The very faint stars: $M_v > 10$

The LF for the lowest mass stars is important, not only to complete the IMF, but because the form of the LF at faint magnitudes can indicate whether we should expect to see a large number of non-stellar "black dwarfs" using the Space Telescope (e.g. Staller and de Jong 1981). Such objects could conceivably account for the "missing mass", which is the term used to refer to the likely difference between the local mass density determined by dynamical arguments and the density of observed objects (see Bahcall 1984). A basic question is: Does the LF have a maximum at faint magnitudes? This question has a long and rather muddled history, which is worth reviewing.

At very faint magnitudes there has long been a controversy over the possible existence of a large number of low-velocity *dM* stars ($M_v \gtrsim 10$) which would have escaped detection in proper motion surveys such as Luyten's. Sanduleak (1964, 1965) gave the first evidence for such an excess by a factor of about three. Later work by Weistrop (1972), Murray and Sanduleak (1972), Pesch (1972), Gliese (1972), and Jones (1972) presented supporting evidence for this hypothesis. In particular Weistrop's (1972) photometrically-determined LF gave an excess of a factor of 5–10 relative to Luyten's function, and Murray and Sanduleak (1972) found a large density and small velocity dispersion for 21 M stars near the north galactic pole, explaining why the stars had been missed in proper motion surveys. A similar conclusion was reached by Gliese (1972) for 75 stars near the south galactic pole.

These results seemed encouraging because they might account for the "missing mass" deduced by Oort (1965) from the motions of stars perpendicular to the galactic plane. However Weistrop (1976a) and Faber *et al.* (1976) discovered systematic errors in Weistrop's (1972) original photographic photometry, in the sense that colors were too red, luminosities too faint, distances too small, and thus densities too large. Weistrop (1976b) found similar errors in Sanduleak's (1965) photometry. Studies by Koo and Kron (1977) and Weistrop (1977), and by Warren (1976), invalidated the results of Murray and Sanduleak (1972) and Gliese (1972), respectively. Jones and Klemola (1977) also found no evidence for an excess of very faint stars in the direction of the north galactic pole. Even though an excess of a factor of 5–10 is therefore untenable, a number of more recent papers (e.g. Pesch and Sanduleak 1978; Staller, Thé, and Bochem-Becks 1981; Alcaino and Thé 1982) have maintained that a low velocity *dM* star population with an excess of a factor of about three does exist.

A detailed study of this question by Reid (1982) and Reid and Gilmore (1982) shows that subjective classification of colors or spectral types can artificially enhance the inferred *dM* density, and they find no evidence for any enhancements in their data. In fact, they find a rapid decline in the LF for $M_v \geq 13$, as shown in Figure 5. Gilmore (1984) also finds a maximum in the LF using infrared data for another field. Notice that every LF determination shown gives a peak in log $\phi(M_v)$, although the position of the peak varies from $M_v = 10.5$ (Chiu) to 13.4 (Luyten and Eggen). Although some of this behavior can be ascribed to incompleteness, it seems unlikely that such different methds would give similar results.

An interesting alternative approach to this question was presented by Probst and O'Connell (1982), who made an infrared search for very low-mass stars in binaries with white dwarf companions using JKH photometry of composite energy distributions in the white dwarfs. These authors find that the LF must decline steeply for $M_v > 14$, in agreement with the LF determinations. More recent work by Probst (1983b) confirms this result.

A novel method to study the turnover problem has been suggested

by Herbst and Dickman (1983, see also Herbst and Sawyer, 1981). The idea is to use nearby dark clouds of known distance (e.g. Taurus, Sco-Oph) to obtain an absolute magnitude-limited sample. The sample will be small, but possibly large enough to distinguish between

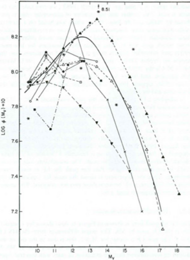

FIGURE 5 Determinations of the luminosity function of faint stars. Sources of data are given in Table I.

a turnover in the LF and a continued increase to very faint magnitudes.

Since there no longer seems to be any strong evidence for excess low-velocity M dwarfs, and because of the LF result of Reid and Gilmore (1982), which does not involve any kinematic criteria, and the indirect result of Probst and O'Connell (1982), we conclude that the peak is real. This implies that the number of non-stellar objects predicted by Staller and de Jong (1981), which was based on a continuously increasing mass function, may be a gross overestimate, unless these substellar objects are formed by processes much different than those which give rise to thme stellar IMF. Searches for low-mass stellar and substellar objects using a variety of techniques (see the review by Probst 1983b, also Boeshaar and Tyson 1983; Marcy 1983; McCarthy 1983; Karimabadi and Blitz 1984) will help resolve this question, and future Space Telescope and HIPPARCHOS (see Crézé 1983; Upgren 1983b) observations will probably decide the issue once and for all.

In adopting a LF in this region, the peak was placed at $M_v = 12.5$, a compromise between the published values, the Probst and O'Connell (1982) result, and the fact that the Upgren and Armandroff LF is still rising between $M_v = 12$ and 13. The position of the peak could be in error by at least ± 0.5 mag. The value of $\log \phi(M_v)$ at the peak was taken as 8.2, with an uncertainty of perhaps ± 0.15. Note however that Eggen (1983) finds the value of $\log \phi$ at the peak to be 8.5. The adopted LF for the rising portion is basically a "middle of the road" choice which connects with the peak. The uncertainty may be only ± 0.1 in $\log \phi$ in this region. Past the peak the LF is much more uncertain. Since the slope here is about the same for Luyten and for Reid and Gilmore, a LF between these two was adopted. The uncertainty here is larger, at least ± 0.2.

2.2.3 *Adopted luminosity function*

The LF adopted here is shown in Figure 6. Also shown for comparison is the LF used by MS. The major differences from the MS LF are: 1. The new LF is flatter for $M_v \leq 5$; this is due to the use of the GCC O star catalogue and the small number of stars used by MS. It should be remembered that the exclusion of stars with spectral types later than 09.5 in the sample may contribute significantly to the flat-

tening (see Section 2.6 below and Bisiacchi *et al.* 1983; Humphreys and McElroy 1984). 2. The new LF is larger by a factor of 1.6 to 2 in the range $-4 \leq M_v \leq -1$ because of the different conversion between $\phi(M_{pg})$ and $\phi(M_v)$, and the weight given to the LF determination of Bartaya and Kharadze (1977), which MS overlooked. 3. The LF has a "dip" which sets in at $M_v \approx 7$ and extends out to $M_v \approx 9$. The position and amplitude of the dip are uncertain, but its existence is now established by a number of independent investigations as discussed earlier. MS basically gave large weight to Luyten's LF in this M_v range 4. The adopted LF has a maximum at $M_v \approx 12$–13 and decreases significantly for fainter stars. As noted above, this behavior appears in nearly all LF determinations for faint stars, but the position of the peak and the rate of decline are very uncertain.

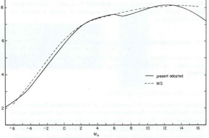

FIGURE 6 Adopted luminosity function (solid line) compared with luminosity function used by Miller and Scalo (1979, dashed line).

After this work was complete, several new discussions of the LF appeared. The reanalysis of Luyten's data by Kipp (1983) gives good agreement with Luyten (1968), and shows how Luyten's smoothing probably disguised the dip at $M_v \approx 6$. Wielen *et al.* (1983) presented a LF based on Gliese's catalogue and its supplements, but with different limiting volumes for 4 separate M_v classes. For $1 \leq M_v \leq 13$ their LF agrees well with the presently adopted LF (± 0.10 in $\log \phi$). Outside this range the sample contains less than 5 stars at each M_v and is more uncertain. The main difference is that their LF is flat for $14 \leq M_v \leq 17$, while the present LF declines. However, the weight of evidence discussed earlier supports the declining LF, with albeit large uncertainties. Schmidt (1983) has attempted to improve the LF determinations based on proper motions by requiring that the quantity H (see Section 2.2.1 above) is larger than some limit. This corresponds to a limiting absolute magnitude, and so provides a means of obtaining an M_v-limited sample. Schmidt gives a LF for $13.5 \leq M_{pg} \leq 18.5$, but, as he notes, the points at $M_{pg} = 13.5$ and 14.5 are very sensitive to the minimum H adopted, and the points at $M_{pg} = 16.5$, 17.5, and 18.5 represent only 5, 4, and 1 stars respectively. A much larger sample will be required to obtain a reliable LF using this method.

2.3 Conversion to the present-day mass function

The relation between the LF and the PDMF is given by Eq. 2.1. In this section we discuss the various quantities required to obtain the PDMF.

2.3.1 *The mass-luminosity relation*

A basic ingredient in the conversion of the luminosity function to a mass distribution is the relation between mass and absolute visual magnitude (since the LF has been determined essentially in terms of M_v), the so-called mass-luminosity relation. Direct determinations of mass and M_v are possible only for visual binaries with accurately-known trigonometric parallaxes and high-quality orbital solutions, and for double-lined spectroscopic binaries in which spatial resolution allows determination of the inclination. Unfortunately, the number of such systems which yield trustworthy main sequence masses is quite small. The sample can be enlarged by including eclipsing binary systems whose light curves show two minima and in

which spectral lines of both components can be cleanly resolved. In these cases the masses and radii are obtained directly, while values of M_v must be derived indirectly, for example using the empirical relation between color index (or spectral type), visual surface brightness, and M_v (Barnes, Evans and Moffett, 1978).

These matters are discussed in the comprehensive review by Popper (1980) who has critically examined the available information and presented lists of masses and M_v (and other derived properties) for the three types of systems named above. Popper's lists are quite selective in terms of the quality of data and ranges of parameters required for admission; the masses are generally estimated to be accurate within 20 percent and most of the values of M_v carry uncertainties between 0.10 and 0.25 mag. The most uncertain masses are for the eclipsing systems with spectral types hotter than about B6 ($M_v \lesssim -1$). Although a few minor alterations were made here (e.g. Anderson, 1983), no systematic literature search was made to update or add to Popper's tables. Results for all main sequence (luminosity class V) stars from Popper's Tables 2, 4, 5, 7 and 8 are shown in Figure 7. The data represent 23 stars in visual binary systems, 81 in resolved spectroscopic systems, and 81 eclipsing systems. Six of the stars from eclipsing systems are probably contact binaries according to Popper, and so their measured masses may not reflect their original masses; these stars are shown as plus signs in Figure 7. Also shown because it contains the star with the lowest measured mass is the resolved astrometric system Ross 614A and B. The inferred apparent magnitude of the secondary given by Lippincott and Hershey (1972) and Probst (1977) are in good agreement. Other astrometric companions with very small estimated masses certainly exist (e.g. G24–16, $m \approx 0.07$–0.11, Hershey 1978), but are not seen visually and so cannot be placed in Figure 7, and some of these objects may of course not be stellar.

The solid line in Figure 7 is the mass-M_v relation adopted by MS (their Figure 2), which was based mostly on the compilations of Lacy (1977) for visual and eclipsing binaries, and Cester (1965) for spectroscopic systems. Although there is some overlap between the Popper (1980) sample and the earlier sample, there are significant differences due to increase in information and the more stringent restrictions which Popper imposed on the spectroscopic systems. In particular, the data on high mass stars now comes almost entirely from

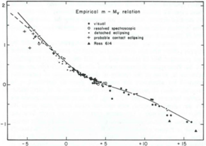

FIGURE 7 Empirical mass-luminosity relation from binary star data. Solid line is relation used by Miller and Scalo (1979); dashed line is modification adopted in present work.

eclipsing binaries while the MS relation was based primarily on spectroscopic binaries and a relation derived from theoretical stellar models. It is therefore encouraging that the determinations judged accurate by Popper agree well with the MS relation. However, it should be noted that the relation for bright stars ($M_v \lesssim -2$, $m \lesssim 10$) is still quite uncertain for a number of reasons. Popper points out that the published masses for most of these stars are probably too small by up to 20 percent, but there are many additional problems such as the scale of bolometric corrections and the ambiguity introduced by the likelihood of mass transfer in the most massive stars. Nevertheless, the results suggest that the MS relation should be altered in the sense of smaller masses at a given M_v. The final adopted relation at high masses is shown by the dashed line, which is consistent with other considerations to be discussed presently. The relation for $M_v \gtrsim 12$ is also uncertain because of the small number of data points. The slope of the relation in this region is important in converting to

the PDMF and IMF, as emphasized recently by D'Antona and Mazzitelli (1983); we return to this point below.

It is important to realize that the stars for which direct mass determinations are available do approximate a sample of stars of average age at any given mass $\gtrsim 5M_\odot$, assuming the star formation rate has been roughly constant over their main sequence lifetimes. Since stars brighten while on the main sequence, this means that the data give the relation between mass and *average* luminosity, not zero-age luminosity. The distinction is crucial because it is the average core hydrogen-burning luminosity which must be used to approximately correct for brightening, as discussed in Section 2.2.2 above. The situation is not so satisfactory for the higher-mass stars because they evolve through different luminosity classes during core hydrogen-burning, while the data shown in Figure 7 include only luminosity class V stars. It might be possible to better define the relation by including stars of all classes and using theoretical evolutionary tracks to estimate weights for each class, but no such procedure will be attempted here.

Equally important information comes from the semi-theoretical mass-M_v relation. This relation is obtained by combining stellar evolution calculations with scales of bolometric corrections and effective temperatures to convert the theoretical luminosities to M_v. The principle uncertainties are at large and small masses. For high-mass ($m \gtrsim 5$–10) stars, mass loss rates, degree of convective overshoot from the convective core into the radiative envelope, and the effects of rotation on the interior structure may influence the $m-M_v$ relation. Of these, only mass loss has been included in a number of independent studies, but with a very uncertain parameterization of the mass loss rate (see, for example, Andriesse 1983 and references therein). The effects of overshoot have been studied in a few papers, but realistic calculation requires a detailed dynamic and nonlocal theory of turbulent convection. A recent review of high-mass stellar evolution is given by Maeder (1984). For low-mass stars the structure of the outermost layers provides an important boundary condition on the nearly-adiabatic convective structure of the bulk of the star. The major difficulties are the sensitivity of the radius, and effective temperature, to the structure of the radiative atmosphere, especially the treatment of molecular opacity, and the possible importance of convective overshoot in the radiative atmosphere. For both the highest and lowest masses the empirical scale of bolometric corrections and effective temperatures remain uncertain (see Conti 1984 for a review of the observed properties of massive stars).

For purposes of constructing the IMF it is necessary to use theoretical properties at an evolutionary phase midway between the zero-age model and hydrogen exhaustion, yielding an initial mass–mean luminosity relation. Such a relation was compiled by Tinsley (1980) using theoretical models of Mengel *et al.* (1979) and Alcock and Paczynski (1978) in the range $0.8 \leq m \leq 10$, and those of Chiosi, Nasi and Sreenivasan (1978) with "maximum" (large) mass loss rates for $m \leq 20$. Tinsley's results are shown as open circles in Figure 8. The results for $m \geq 0.6$ ($\log m \leq -0.22$) were based on a combination of observed and theoretical relations presented by Veeder (1974), which are uncertain. Further cool dwarf model atmosphere calculations are sorely needed to better establish the relations between color and bolometric corrections for these low-mass stars.

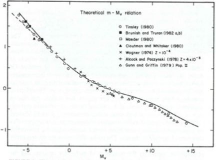

FIGURE 8 Theoretical mass-luminosity relation from stellar evolution models. Solid line is relation used by Miller and Scalo (1979); dashed line is modification adopted in present work.

Also shown are $m = 15$ and 30 models with $Z = 0.03$ from more recent calculations by Maeder (1980, open squares), and $m = 15$, 30 and 40 models with $Z = 0.02$ by Brunish and Truran (1982a, b, filled squares). Both sets of models include mass loss with different parameterizations but the results are relatively insensitive to the adopted mass loss rates. The bolometric correction-effective temperature calibration used is that given by Popper (1980), extrapolated to higher effective temperatures. Further calculations which could be used to construct mass-M_v relations at large masses are given in a list of references in Brunish and Truran (1982a, p. 248, footnote); more recent calculations can be found in, e.g. Falk and Mihalas (1983) and Doome (1983).

The good agreement with the MS relation, which in turn fits the observed mass-M_v relation well, must be tempered by the fact that most theoretical models which allow for convective overshoot in the convective cores of relatively massive stars give luminosities during core hydrogen burning which are significantly larger than those obtained by neglecting overshoot. (Overshoot also may significantly affect stellar lifetimes as discussed in Section 2.4 below.) The $m = 15.6$ overshoot model of Cloutman and Whitaker (1980) was overluminous by about a factor of two. Their model is shown, after converting to M_v using Popper's (1980) bolometric correction scale, as the filled triangle in Figure 8. A more recent calculation (Cloutman 1983) using a variable mixing length derived from a statistical turbulence model gives very similar results. Maeder's (1976) models for a range of masses, which employ a different formulation of the overshoot estimate, indicate that the brightening in M_v due to overshoot is only about 0.2 mag at $m = 3$, and this brightening decreases with decreasing mass. Therefore, convection probably introduces a significant uncertainty only for $m \gtrsim 3$. Further calculations using Maeder's recipe for overshoot by Maeder and Mermilliod (1981) and Matraka, Wasserman and Weigert (1982) show a roughly constant brightening of 0.2–0.3 mag between $4M_\odot$ and $9M_\odot$, or about 20–30% in luminosity. Figure 9, from Maeder and Mermilliod (1981), shows how the brightening in M_{bol} varies with effective temperature at the end of core hydrogen-burning (i.e. with mass) for three different values of a parameter α_c, which is the ratio of mixing length to pressure scale height in the nonlocal mixing length theory used by Maeder, and is a measure of the importance of convective overshoot. The shaded boxes are estimates of the brightening required for open

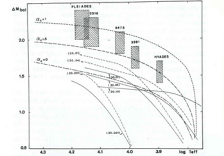

FIGURE 9 Brightening in M_{bol} at the end of core hydrogen-burning due to convective overshoot as a function of effective temperature for various values of the overshoot parameter α_c and composition, from Maeder and Mermilliod (1981). Shaded boxes are estimates of brightening required for open clusters in five age groups.

clusters in five age groups. Maeder and Mermilliod's comparison indicates that substantial overshoot brightening occurs. Calculations of the evolution of stars of masses $m = 20$, 60 and 100, including mass loss and a simple, but perhaps realistic, parameterization of the degree of overshoot, have been presented by Bressan, Bertelli and Chiosi (1981). Their results contradict the calculations just described, in that the effect of overshoot on the luminosities (but not the lifetimes) is very small, both for models with and without mass loss; typically overshoot was found to decrease the mean luminosity by ~ 0.05–0.15 mag. The discrepancy, apparently unnoticed in the literature, is unresolved at present. Because of the more realistic treatment of overshoot by Cloutman and Whitaker (1980), Cloutman (1983), Maeder (1976), Maeder and Mermilliod (1981), and Matraka *et al.* (1982), and the facts that the overshoot brightening effect gives better agreement with the (uncertain) binary star

data for massive stars in Figure 7, and that convective overshoot can better account for the observed broad main-sequence band for massive stars (see Meylan and Maeder 1982; Chiosi 1983), the revised m–M_v relation at high masses will continue to be used.

Given the uncertainties in convective overshoot, mass loss, and the bolometric correction scale, it still appears that the general form of the adopted mass-M_v relation is reasonably secure, with uncertainties in mass at a given luminosity around 0.1–0.2 in the logarithm, or 20–60%. Convective overshoot and bolometric corrections seem to be the most severe problems which require further study. The m–M_v relation is most uncertain for the brightest stars, where the adopted relation may misestimate mass at a given M_v by 50% or more. This is also suggested by the binary data of Figure 7.

It is important to notice that the theoretical mass-M_v relation terminates at $m = 60$, even though higher-mass stars almost certainly exist and theoretical calculations for high mass objects are available (e.g., Maeder, 1980). The problem is that the models give bolometric luminosities, while the bolometric corrections needed to convert to M_v are unknown for these masses. Detailed calculations of model atmospheres could in principle alleviate some of the problem, but the calculations are extremely difficult because of uncertainties associated with ultraviolet line blanketing and the effects of stellar winds on the radiative transfer. For lack of a better procedure, I have simply linearly extrapolated the adopted relation to $M_v = -7$.

The uncertainty in the $m(M_v)$ relation at small masses has been recently emphasized by D'Antona and Mazzitelli (1983). In an earlier paper (D'Antona and Mazzitelli, 1982), these authors derived a theoretical mass-luminosity relation for low-mass stars which becomes very flat for $m \lesssim 0.09$ and $M_{bol} \gtrsim 11.5$. In a later paper (D'Antona and Mazzitelli, 1983), they suggest that this flattening sets in at a corresponding $M_v \approx 13$, and that this is consistent with the available visual binary data. They correctly emphasize that the IMF derived from the LF, being proportional to $|dM_v/d\log m|$, would be greatly altered if this is correct. In particular, the maximum in the LF at $M_v \approx 13$ would in that case *not* imply a turnover in the IMF, which may continue to increase with decreasing mass. I believe this assertion is unlikely. First, if their $m(M_{bol})$ relation for $Y = 0.25, Z = 0.02$ (D'Antona and Mazzitelli, 1982, Figure 3) is adopted, the flattening only sets in at $\log m \approx -0.90$, $M_{bol} \approx 11.8$. The effective temperatures of the models less massive than this are very small

(≤ 3000 K) and would be smaller if molecular opacity had been included in the atmospheres of the theoretical models. The bolometric corrections for such stars are almost certainly smaller than -3, and so the corresponding M_v must be at least 15, well past the peak in the luminosity function. This can be seen in Figure 1 of their 1983 paper, where the extreme change of slope occurs at the plotted position of the two faintest visual binary data points, which have $M_v \approx 16$ (see Figure 7). Second, inspection of Figure 7 shows that it is true that the four faintest visual binary points might be consistent with a flattening at $M_v > 13$, but the eclipsing system at $M_v \approx 13$ and the data for Ross 614, while more uncertain, do not support this idea, and might even suggest a steepening of the $m(M_v)$ relation. The most extreme adjustment to the $m(M_v)$ relation which appears possible is to disregard the eclipsing binary data and force the relation to pass through the four faintest visual binary points; the resulting IMF would be (roughly) flat for $m < 0.5$, but could not continue to increase with $\Gamma \approx -1.3$ as suggested by D'Antona and Mazzitelli (1983). I conclude that their work does correctly identify a major previously neglected source of uncertainty in the IMF, but that the resulting consequences are probably not as extreme as they suggest. We shall proceed to use the linear m–M_v relation adopted in Figures 7 and 8, but the possibility of a flatter relation must be kept in mind.

D'Antona and Mazzitelli (1983) also suggested that the dip in the LF at $M_v \approx 7$ may not reflect a dip in the IMF if the m–M_v relation has a strong inflection point at this M_v. In fact $|dM_v/d\log m|$ does have a maximum (≈ 15.6) at $M_v \approx 7$ (see Table IV), but this flattening is insufficient to erase the dip in the corresponding IMF, and there is no suggestion from the theoretical m–M_v relation for a significantly flatter slope in this region; if anything, the theoretical models would suggest a slightly steeper relation. The observational data are too scarce in this small magnitude interval to make any definitive statements, but the position of the two unresolved spectroscopic systems at $M_v \approx 5$, which have well-determined masses and magnitudes, suggests that if a flattening occurs between $M_v \approx 6$ and 9, it would have to set in very abruptly and cover a very small mass interval ($0.5 \leq m \leq 0.8$), which seems unlikely on theoretical grounds.

In constructing halo field star and globular cluster mass functions, it is necessary to estimate the mass-M_v relation for Population II stars. Such an estimate was given by Gunn and Griffin (1979), based on the blue envelope of Veeder's (1974) $M_{bol}-(V\text{–}K)$ diagram, bolometric corrections from Veeder, and a theoretical mass-M_{bol} relation taken from Copeland, Jensen, and Jorgensen (1970) for a metal abundance $Z = 10^{-4}$, extrapolated from $m = 0.25$ to $m = 0.1$. Gunn and Griffin's results are shown as the open triangles in Figure 8. Also shown are results derived from Wagner's (1974) evolution calculations at $Z = 10^{-3}$ for masses between 0.65 and 2.5 (crosses), and Alcock and Paczynski's (1978) calculations at $Z = 4 \times 10^{-4}$ for masses $2 \leq m \leq 10$ (plus signs). Popper's (1980) bolometric correction scale was used (even though the scale will differ somewhat at low Z), and the plotted points again refer to the phase midway between the zero-age model and hydrogen exhaustion. The result for $m \gtrsim 1$ are not relevant to today's halo population in our galaxy, but may be useful in deriving mass distributions from luminosity functions in nearby dwarf irregular galaxies which have mean metal abundances smaller than those of Population I stars of our galaxy ($Z \approx 0.02$) by factors of perhaps 3 to 30. For $m < 1$, it is seen that for a given M_v the corresponding mass for $Z = 10^{-3}$ is smaller than the disk Z relation by around 20–30%, a result which is due essentially to the smaller atmospheric line blanketing in the low-Z models. From these considerations it appears that the Population II m–M_v relation should not differ much from the relation adopted for the disk.

In estimating a mass function from a luminosity function, the uncertainty in the m–M_v relation enters in three ways. First, it causes uncertainty in the mass range identified with each M_v range. From the comparisons and discussion given above, the uncertainties in log m in various ranges of M_v given in Table III were estimated; they are uncomfortably large (~ 40–60%) for $M_v \lesssim -2$ and $M_v \gtrsim +12$. The uncertainties for $16 < M_v < -5$ are only guesses, since there are no data, observational or theoretical, for these extremes. Secondly, the slope of $m(M_v)$ converts each unit of M_v interval into a unit interval of log m. The quantity $|dM_v/d\log m|$ is uncertain by no more than 30% over most of the range of M_v, which is smaller than the uncertainty in the luminosity function itself, and in other quantities which we shall discuss shortly. An exception occurs for $M_v \gtrsim 13$, where the m–M_v relation may be flatter, i.e. $|dM_v/d\log m|$ larger (D'Antona and Mazzitelli, 1983), as discussed above. It is also important to note that, because $|dM_v/d\log m|$ is large at all masses, a small error in the slope of the LF results in a much larger error in the PDMF and IMF. For example, for massive stars an error in $d\log\phi(M_v)/dM_v$ of ε results in an error in the slopes of the PDMF and IMF of about 5ε. Third, the relation used here connects a mass with the luminosity of a star of average age, which automatically (but approximately) corrects the LF for brightening during the core hydrogen-burning phase. The theoretical brightening in M_v is large and uncertain for the most massive stars because it depends on the importance of mass loss and convective overshoot as well as the scale of bolometric corrections and effective temperatures. The resulting uncertainty in the m–M_v relation cannot be easily estimated.

TABLE III
Estimated uncertainties in the mass-luminosity relation

M_v range	Uncertainty in log m	Range in log m for adopted $m(M_v)$
< -5	± 0.2:	> 1.4
-5 to -2	± 0.15	$0.9 - 1.4$
-2 to $+1$	± 0.1	$0.4 - 0.9$
$+1$ to $+5$	± 0.05	$0.0 - 0.4$
$+5$ to $+12$	± 0.1	$-0.5 - 0.0$
$+12$ to $+16$	± 0.15	$-1.1 - 0.5$
$> +16$	± 0.2:	< -1.1

2.3.2 *Stellar scale heights*

The spatial distribution of main sequence stars perpendicular to the galactic plane is known to depend on spectral type, or equivalently mean age, in the sense that younger stars are more closely confined to the disk midplane. A favored explanation for this behavior is that stars are born with a small velocity dispersion from a thin layer of interstellar gas, but are heated due to gravitational scattering by interstellar clouds (Spitzer and Schwarzschild, 1951). Detailed calculations (Wielen 1977; Villumsen 1983) show that the velocity dispersion in this model increases with time as $[1 + (t/\tau_0)]^n$, where τ_0 is a constant and the exponent $n \approx 1/3$–$1/2$ is somewhat uncertain. Since stellar lifetimes increase strongly with decreasing mass, the low-mass stars are older on the average than higher-mass stars, and so have diffused further from the galactic plane. Although the theory cannot presently predict the form of the z-distribution and its detailed dependence on stellar age, it does predict that stars with lifetimes in excess of the age of the galactic disk ($M_v \gtrsim +6$) should all have about the same mean z-thickness, a result which provides a useful check on the $H(M_v)$ relation inferred from observations.

The z-distributions for stars of various spectral types are usually modeled by an exponential function with scale height H. This is the origin of the term $2H$ in the conversion from LF to PDMF in Eq. (2.1). Observationally, a number of determinations of stellar z-density distributions are available in the literature (see MS and especially Gilmore and Reid 1983 for references). Several problems arise in practice, however. First, as emphasized by Gilmore and Reid (1983), the data often require a two- or more-component model. This problem is not serious because we are only interested in distances less than about 500 pc from the plane. But even close to the plane an exponential function often does not provide a very good fit to the data (MS), which are usually too noisy for an analytic representation. Finally, for faint stars ($M_v \geq 8$) there is almost no information. Despite these problems, a characteristic relation between H and M_v does emerge for $M_v \leq 8$. The relation adopted by MS and here is shown in Figure 10. The scale height is taken as constant at 90 pc for $M \leq 1$ and constant at 325 pc for $M_v \geq 6$. The only available results for the latter range (Faber *et al.* 1976; Gilmore and Reid 1983) are consistent with a scale height of around 300 pc, but the uncertainties are large. The theoretical considerations given above suggest that H should remain constant with M_v for $M_v \geq 6$, consistent with the adopted relation. In fact, Wielen's (1977) calculation of the rms deviations of stars perpendicular to the galactic plane as a function of age agrees well with the adopted relation over the entire range, assuming that the mean age equals halt the main sequence lifetime. The indicated uncertainties in $H(M_v)$ in Figure 10 are only rough estimates, but vary from 20 to 30%.

One point which should be noticed is that the value of M_v at which the steep rise in $H(M_v)$ occurs is quite significant. For the adopted relation it occurs over a range of M_v (3 to 5) in which the $m(M_v)$ relation is very flat, and m only increases by about 50% over this range; i.e., H changes by a factor of three over a range in log m of only 0.17. Any significant fluctuation in the derived mass function in this range ($1 \leq m \leq 1.4$) must therefore be regarded with caution. Furthermore, $M_v = 5$ corresponds to the stellar mass which has a lifetime about equal to the age of the disk, so the sharp rise in $H(M_v)$ occurs just in the region of the mass function which depends most crucially on the assumed stellar birthrate history. Star densities are usually determined for stars of a given spectral type. The conversion used here is given in MS (Section 11c and Figure 2). Uncertainties of greater than 0.3 mag in this conversion would significantly increase the estimated uncertainty in $H(M_v)$ in the range

$3 \le M_v \le 5$. For these reasons, $H(M_v)$ in the mass range 1–$2M_\odot$ can have important effects on the PDMF and IMF.

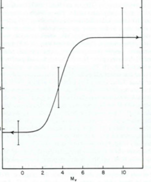

FIGURE 10 Adopted relation between stellar scale height and absolute visual magnitude; indicated uncertainties are rough estimates.

2.3.3 *Correction for non-main sequence stars*

The final factor which converts the LF into a mass function if $g_{ms}(M_v)$, the fraction of stars which are on the main sequence at a given M_v. This factor corrects the LF for the presence of evolved stars. For example, at $M_v = 0$ both A0 V and K III stars contribute to the LF.

The correction is only significant for $M_v \le 4$, but is poorly determined, especially for the brightest stars. Figure 11 shows several estimates of $g_{ms}(M_v)$ taken from Salpeter (1955), Sandage (1957), Schmidt (1959), Upgren (1963), and McCuskey (1966). Recently Mamon and Soneira (1983) have given an analytic representation which is shown as a dashed line in Figure 11. Most of the estimates agree fairly well, except for Salpeter (1955) at $M_v < -2$ and Upgren (1963). There is little basis for choosing between these results, and the scatter must simply be treated as a source of uncertainty. The relation adopted here is shown as a solid line. The dip at $M_v \approx 0$ represents the effect of G–K giants, an effect also seen in the values of Salpeter, Schmidt, and Upgren. The reason for the increase in g_{ms} for $M_v < -4$ is that the star counts on which the LF in this region is based (GCC) only include stars earlier than B0, so no correction for

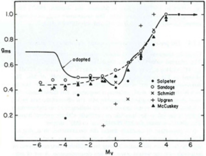

FIGURE 11 Estimates of the fraction of stars which are in the core hydrogen-burning phase as a function of absolute visual magnitude. Dashed line is from Mamon and Soneira (1983). Solid line is relation adopted in present work.

later-type supergiants is needed. On the other hand, the adopted corrections for massive stars are still uncertain, since it is not possible at present to say what fraction of O stars are post-main sequence objects. The fraction which are massive post-core hydrogen-burning objects may be as large as 10–20% (see Falk and Mihalas, 1973). Carrasco *et al.* (1979, see also Lequeux, 1979) proposed that a large fraction of O stars are evolved old population objects; arguments against this possibility have been presented by Pawlocisz and Herbst (1980), Tobin and Kilkenny (1981), and GCC. The fraction of stars in the GCC sample which are luminosity class V is only 0.2 at $M_v = -6$ and 0.3 at $M_v = -5$, but because massive stars evolve so far from the zero-age main sequence during core hydrogen-burning, these numbers cannot be used to estimate the fraction in later evolutionary phases. For these reasons the adopted values of g_{ms} for $M_v < -4$ must be considered extremely uncertain. At $M_v \geq 12$, the correction g_{ms} is slightly smaller than unity because of the presence of white dwarfs ($g_{ms} = 0.85$ to 0.97 according to Mamon and Soneira, 1983), but I have ignored this correction here. The uncertainty in g_{ms} is probably around 20–40% for $-4 \leq M_v \leq +3$, and only 10% for $M_v \geq 4$.

2.3.4 *The present-day mass function and uncertainty estimates*

Using the relations discussed above, we can now construct the PDMF. The adopted values of $\log m$, $\log \phi(M_v) + 10$, $|dM_v/d \log m|$, $2H(M_v)$, $g_{ms}(M_v)$, and $\log \phi_{ms}(\log m)$ are given in Table IV. The resulting PDMF is plotted in Figure 12 and compared with the PDMF of MS. The differences mostly just reflect the difference in adopted LF, but for $m \geq 10$ the adopted $m(M_v)$ relation is important. For these masses, the mass at any M_v is smaller than used by MS. The effect of the new $m(M_v)$ relation on the MS result can be seen by shifting the four highest-mass points to the left so that they line up vertically with the present masses. The effect is to make the MS PDMF (and so IMF) *steeper*.

It is important to carefully assess the uncertainties in $\phi_{ms}(\log m)$. The error estimates are necessarily subjective, since most often they must be based on the scatter among the published determinations of quantities and the weight given to each determination. A set of estimates for the contribution to the error in $\log \phi_{ms}(\log m)$, $\varepsilon(\log \phi_{ms})$, due to uncertainties in $\phi(M_v)$, $m(M_v)$, and $|dM_v/d \log m|$ is shown in Figure 13. Without explaining in excessive detail the basis for all the

choices (some of which were discussed earlier), the essential features will be summarized.

TABLE IV
Present-day mass function

M_v	$\log m$	$\log \varphi(M_v) + 10$	$\lvert dm/d \log m \rvert$	2H	g_{ms}	$\log \varphi_{ms}(\log^{-1} m\ \mathrm{pc}^{-2})$	$\varepsilon(\log \varphi_{ms})$
−7	1.80:	2.02	5.3	180	0.7:	−5.15	0.48
−6	1.62	2.40	5.3	180	0.7:	−4.78	0.39
−5	1.43	2.73	5.3	180	0.7:	−4.44	0.36
−4	1.26	3.28	5.3	180	0.54	−4.01	0.35
−3	1.08	3.95	5.3	180	0.50	−3.37	0.33
−2	0.90	4.57	5.3	180	0.50	−2.74	0.28
−1	0.72	5.20	5.8	180	0.49	−2.09	0.28
0	0.54	5.82	6.4	180	0.44	−1.47	0.27
1	0.40	6.40	7.1	185	0.60	−0.70	0.32
2	0.27	6.84	8.1	210	0.71	−0.08	0.32
3	0.16	7.20	9.2	300	0.86	+0.57	0.33
4	0.07	7.38	10.6	465	1.0	1.07	0.32
5	−0.01	7.52	12.8	590	1.0	1.40	0.26
6	−0.08	7.60	15.4	635	1.0	1.59	0.24
7	−0.14	7.50	15.6	650	1.0	1.50	+0.27, −0.21
8	−0.21	7.60	15.0	650	1.0	1.59	0.26, −0.20
9	−0.27	7.76	13.5	650	1.0	1.70	0.25, −0.19
10	−0.35	7.95	11.6	650	1.0	1.83	0.24, −0.16
11	−0.44	8.07	10.4	650	1.0	1.88	0.21, −0.16
12	−0.54	8.18	10.0	650	1.0	1.88	0.24
13	0.65	8.18	10.0	650	1.0	1.88	0.23, −0.26
14	−0.75	8.04	10.0	650	1.0	1.85	0.24
15	−0.85	7.84	10.0	650	1.0	1.65	+.29, −0.36
16	−0.96	7.57	10.0	650	1.0	1.38	+.41, −0.49
17	−1.06:	7.25	10.0	650	1.0	1.06	0.68

1. The uncertainty in the adopted LF $\phi(M_m)$ at each integer M_v between −7 and +17 was judged on the basis of the number of and scatter among independent determinations, as well as the weight given to certain determinations. For example, high weight was given to the LF of Upgren and Armandroff (1981) for $2 \leq M_v \leq 12$ because it is based on a straightforward counting of stars with known trigonometric parallaxes comprising a sample which has been shown to be essentially complete out to 20 pc. Lower weight was given to the LFs of Luyten (1938, 1968) and

Wanner (1972) which used the $\bar{M}$–H method, because of the complexity of the method and the number of determinations with which these results disagree. The estimate of $\epsilon(\log \phi) = \pm 0.2$ at $M_v = -7$ and -6 ($\log m = 1.80$ and 1.62) was altered to $(+0.3, -0.2)$ at $M_v = -5$ because spectral type B stars, excluded from the GCC catalogue, may make a substantial contribution at this luminosity. Most the detail in the estimate is largely irrelevant to the total error, and is in any case very uncertain. The basic feature is that the uncertainty in $\log \phi(M_v)$ is around ± 0.1 to ± 0.15 for $0.2 \leq m \leq 8$, and increases to about 0.2 or larger outside this mass range. Notice that while the LF is a significant source of uncertainty, it is probably not the dominant source for most masses.

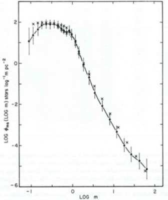

FIGURE 12 Present day mass function (PDMF) with uncertainty estimates. Crosses represent the PDMF derived in Miller and Scalo (1979).

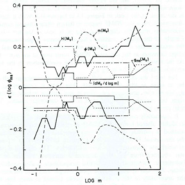

FIGURE 13 Estimates for contributions to the uncertainty in the PDMF due to the factors entering its derivation.

2. The uncertainty due to errors in the mass-luminosity relation, $m(M_v)$, dominate the other sources except in the mass range $0.15 \leq m \leq 0.8$. The error estimate was made by first judging the uncertainty in $\log m$ at a given M_v, $\epsilon(\log m)$, from Figures 7 and 8 and the considerations discussed in Section 2.3.1, and then multiplying by the average slope $d \log \phi_{ms}/d \log m$ at the corresponding $\log m$. At the largest masses ($m \gtrsim 25$, $M_v < -5$), $\epsilon(\log m)$ is large (0.1, 0.15, 0.2 at $\log m = 1.43, 1.62, 1.80$ respectively), because of lack of binary data and

problems with mass loss and convective overshoot, and the slope is moderately large (~ 2), giving the large contribution at the highest masses. At smaller masses the estimated $\varepsilon(\log m)$ decreases to about ± 0.05 to ± 0.07, but the PDMF becomes extremely steep, with a slope which increases from about 3.5 at $m = 10$ to 5.9 at $m = 1.6$. This is the cause of the peak in Figure 13 at $\log m = 0.2$. With a further decrease in mass the PDMF begins to flatten while $\varepsilon(\log m)$ remains reasonably small; the slope of $\phi_{ms}(\log m)$ is zero at $\log m = -0.54$. Finally, at the smallest masses, $\varepsilon(\log m)$ becomes larger because of the small number of visual binaries with well-known masses, and the slope increases as the estimated PDMF turns over at $\log m \lesssim -0.8$. At the lowest mass shown ($m = 0.09$), the contribution to the total error is as large as ± 0.6 in $\log \phi_{ms}$.

For $m \gtrsim 1$ the error in the IMF due to mass uncertainties will not be as large as that in the PDMF. The IMF is proportional to $\phi_{ms}(\log m)/\tau(m)$, and since $d\phi_{ms}/d\log m$ and $d\tau/d\log m$ have opposite signs, the contribution to the total error is somewhat smaller. The total errors will be reduced by 0.03 to 0.08 in the logarithm.

It is generally not recognized that this same source of error exists, in slightly altered form, if the PDMF is estimated using the alternate method of counting numbers of stars between evolutionary tracks in the theoretical *H–R* diagram (e.g. Lequeux, 1979 and GCC), results of which are discussed in Section 2.6.4 below. The mass of a given star obtained from the *H–R* diagram is uncertain because of the bolometric correction and effective temperature scales needed to obtain M_{bol} and T_e from M_v and spectroscopic data, and because of the uncertainty in the evolutionary tracks related to mass loss and convective mixing, and this, along with the steep slope of the PDMF, results in a substantial uncertainty in the IMF at any mass. These are essentially the same considerations which enter the theoretical mass-*mean* M_v relation, or the more detailed treatment of main sequence brightening described in MS. A more detailed error analysis of both approaches which explicitly includes the effects of errors in the bolometric correction and effective temperature scales and the uncertainty in the topology of the evolutionary tracks would be useful.

3. Uncertainty in the scale height $H(M_v)$ is a large source of error in the range $0.14 \lesssim m \lesssim 0.8$. The estimates shown assume that the actual scale height (or factor which gives the correct surface density if the z-

distribution is not exponential) of stars with $m \lesssim 0.8$ ($M_v \geq 6$) is in the range 250–520 pc, the adopted value being 325 pc. This adopted possible upper limit may be somewhat large and pessimistic; if H is in the range 250–400 pc, scale height uncertainties will be approximately equal to or less than those attached to the LF.

Notice that there is no scale height uncertainty for the three largest masses because the stellar sample (GCC) was limited only in distance from the sun in the plane of the galaxy, and so directly gives the number per unit area. We divided these numbers by $2H$ to obtain a luminosity function per unit volume for consistency and comparison with other data, but multiplied the LF by $2H$ to find the PDMF.

4. Contributions to $\varepsilon(\log \phi_{ms})$ by $|dM_v/d\log m|$ and g_{ms} are relatively small, $\lesssim 0.1$, and so we shall not discuss the detail exhibited in Figure 13, most of which can be understood by examination of Figures 7, 8 and 11. However, it must be emphasized that the estimated uncertainty in $|dM_v/d\log m|$ at masses $\lesssim 0.2 M_\odot$ does *not* incorporate the recent suggestion of a flatter m–M_v relation at low masses by D'Antona and Mazzitelli (1983). As discussed earlier, I find that the most extreme flattening consistent with the observational data would lead to a roughly flat PDMF (and IMF) for $m \lesssim 0.5$.

The total uncertainties listed in Table IV, along with their decomposition into various contributions shown in Figure 13, are somewhat different than the earlier error estimates by MS (Table IV). The present values of $\varepsilon(\log \phi_{ms})$ are smaller for most masses, and the positive and negative values are more nearly equal. The major differences are: (a) the greater weight given by MS to the possibility that the scale heights at $m \lesssim 1$ could be very large, ~ 700–800 pc, but not smaller than 300 pc, and (b) a severe underestimate of the uncertainty due to the $m(M_v)$ relation for $\log m < 0.8$.

The subjectivity of the present error estimates is a problem, and the reader may wish to modify them accordingly. I am fairly confident that the estimate of the error due to $m(M_v)$, which is dominant over a wide range of masses, can be better quantified and perhaps reduced by a more careful study. There is also room for improvement in the luminosity function around $M_v = -5$ to -4 by inclusion of later spectral types and improved theoretical models, and over the entire range $-5 \leq M_v \leq -2$ where the number of published LF determinations are small. Future Space Telescope and HIPPARCHOS observations should substantially improve our knowledge of the luminosity function, its possible variations, and stellar scale heights, over the entire range of stellar masses. All those programmes will be necessary for any substantial improvement in the determination of the present-day mass function and IMF.

2.4 Stellar lifetimes

For stars with $m \gtrsim 1$, the conversion of the PDMF to the field star IMF requires knowledge of the main sequence core hydrogen-burning lifetime as a function of mass. It is a well-known and useful feature of stellar structure that the main sequence lifetime of a star can be easily estimated to within a factor of around three for most masses. This occurs because the time it takes to burn all the hydrogen in the core is just the mass of the core divided by the luminosity, both averaged over the main sequence lifetime, divided by the energy release per gram of hydrogen burned. The mass of the core can be estimated from straightforward considerations to within a factor of around 1.5 (see e.g., Stothers, 1972). Perhaps because of the simplicity of the argument, it has become common lore that a numerical evolutionary calculation can give hydrogen-burning lifetimes with much better accuracy than this, perhaps as good as 10%. This supposition is incorrect. The time evolution of the luminosity and hydrogen-burning core mass depend on a number of factors, including the treatment of convection in the core for $m \gtrsim 1.5$, the rate of mass loss as a function of stellar parameters in more massive stars, and the possible effects of rotation in altering the luminosity and in driving mixing, which could increase the effective mass of the core. As we shall see, some of these effects can lead to significant changes in calculated lifetimes.

Even without these complications, it has proven surprisingly difficult to obtain lifetimes from independent numerical calculations which agree better than about 10–30% for the same helium and metal abundances. Evidently the lifetimes in certain mass ranges may depend on details of the input physics (opacities, energy generation rates, equation of state), surface boundary conditions, timestep and spatial resolution, and even numerical algorithms. Tinsley (1980) and MS had noted the slight discrepancies between independent sets of calculations performed for the same composition.

The accuracy of the lifetimes also depends on the proper choice of composition. MS used approximate relations for the dependence of luminosity on mass, nuclear energy generation rate, and opacity, and simple scaling laws for the dependence of the energy generation rate and opacity on hydrogen, helium and metal abundances (X, Y, and Z) in different mass ranges to estimate the dependence of lifetime on composition. At $Z = 0.02$ and $Y = 0.25$, changes in Y by ± 0.05 and in Z by ± 0.01 resulted in a change in $\tau(m)$ of less than 20% for $m > 10$. The compositions of disk stars probably span a similar range, but since the IMF refers to a large group of stars, the spread in Y and Z will not be very important if the appropriate *mean* composition is used. This mean will depend somewhat on mass, since the age range of stars with $m \lesssim 1.2$ is comparable to or greater than the timescale for changes in Y and Z. A reasonable choice for Z might increase from 0.01 at $m \approx 1$, to 0.02 at $m \approx 1.4$, to 0.025 for $m \gtrsim 2$, using the age-metallicity relation derived by Twarog (1980a, b). These values are probably uncertain by no more than 20%.

Based on these considerations, it was decided to investigate the $\tau(m)$ relation and its uncertainties in more detail before proceeding with the calculation of the IMF. A large number of stellar evolution calculations are available which can be used to construct such a relation. Three recent independent compilations of $\tau(m)$ for stars with metal abundances appropriate to the galactic disk ($Z \approx 0.01$–0.02) based on different selections of the published models have been given by MS, Tinsley (1980), and Bahcall and Piran (1982), and these relations are shown in Figure 14. The values of lifetimes for stars with $m \lesssim 1.0$ are not required; all we need to know is that their lifetimes are in excess of any estimate for the age of the galactic disk. The Bahcall and Piran result is given as an analytic fit:

$$\log \tau(m) = 10.0 - 3.6 \log m + 1.0 \log^2 m, \quad 10^{-1} < m < 10^2$$
$$\log \tau(m) = 6.3 \qquad m \geq 10^2,$$

which is discontinuous at $m = 10^2$. The MS result can be fit by a similar expression (Scalo and Miller, 1979) which falls below the relation of Tinsley, which in turn is below the relation of Bahcall and Piran. It might be noted that the numerical results used by MS were obtained 5 to 14 years before the calculations used by Tinsley. Although Bahcall and Piran report that their formula fits all the available calculations within 10%, it is clear from the difference between the three compilations shown that the uncertainty must be larger than this; the spread between the upper and lower curves in Figure 14 is around 30–50%. Some of this scatter is due to differences in assumed composition, but most of it presumably reflects the differing details of the (mostly) independent evolutionary codes.

For the massive stars, the results of Maeder (1980, $Z=0.03$) and Brunish and Truran (1982a, $Z=0.02$), which include mass loss with somewhat different parameterizations and absolute values, are shown as crosses and plus signs respectively. The lifetimes are relatively insensitive to the metal abundance for the range in Z of interest here (see below). The two results are in excellent agreement for the two masses in common ($m=15$ and 30). Maeder's work allows us to estimate lifetime up to $m=240$.

The main sequence lifetimes of stars with $m \gtrsim 1.5$ are uncertain by an additional 30–70% due to the difficulty in accurately calculating the extent of convective cores for models with these masses. Stars of smaller mass burn hydrogen by the less temperature-dependent proton–proton cycle rather than the CNO cycle, and therefore do not have significant convective cores. Maeder (1975, 1976), Roxburgh (1978), and Cloutman and Whitaker (1980) have pointed out that the ability of turbulent convection to diffuse, or "overshoot", into overlying stable radiative regions can significantly increase the size of the convective core and thus the hydrogen-burning lifetimes. None of the models used to construct the smoothed relations in Figure 14, nor the calculations of Maeder (1980) and Brunish and Truran (1982a, b), take this effect into account.

It remains a fact of life that there exists no satisfactory theory of turbulent convection which can accurately treat convective overshoot. Nevertheless, we can examine the available calculations and try to estimate the effect on the lifetimes. Probably the most detailed treatment of the problem to date is that of Cloutman and Whitaker (1980; see also Cloutman, 1983). Using Reynolds averaging to obtain an equation for the transport of turbulent kinetic energy, it was found that the mixed core of a $15.6M_\odot$ model is larger by about $3M_\odot$ than non-overshoot calculations would indicate, and that the main-sequence liftime was correspondingly larger by about 50%. Similar

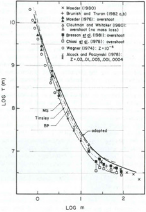

FIGURE 14 Estimates of the core hydrogen-burning lifetime as a function of mass.

results for lower-mass models were obtained by Maeder (1976) using a very different and more approximate approach to the overshoot estimate, with lifetimes extended by 25–35% for masses of 1.25 to 3. These lifetimes, as well as those calculated without overshoot, are shown as filled (Maeder) and open (Cloutman and Whitaker) triangles in Figure 14, with the upper symbols representing the models which included overshoot. Notice that the Cloutman and Whitaker lifetime without overshoot is in good agreement with the lifetimes from Maeder (1980) and Brunish and Truran (1982a) at $m=15$. Further calculations, using Maeder's (1976) overshoot prescription, have been presented by Matraka *et al.* (1982) for intermediate-mass stars. The results (not shown in Figure 14) give a lifetime extension ranging from 33% at $m=4$ to 22% at $m=9$. Evolutionary calculations designed to study the combined effects of overshoot and mass loss in massive stars by Bressan *et al.* (1981), using a very simple parameterized treatment of overshoot, are shown as filled squares (results quoted by Garmany *et al.*, 1982). The corresponding lifetimes without overshoot (Chiosi *et al.*, 1978, open squares) are smaller than in other calculations, but the extension of the lifetimes due to overshoot found by Bressan *et al.* is similar to the Cloutman and Whitaker result, with some evidence for a decreasing effect above $m=30$. Until turbulent convection can be treated in a more detailed manner (e.g., Marcus, Press, and Teukolsky, 1983; Chan and Sofia, 1983), these results must be considered tentative. Nevertheless, unless all these calculations have severely overestimated the efficiency of overshoot, they strongly suggest that the adopted main-sequence lifetimes of stars with $m>1.2$ should be increased by 25–50%. This result is supported by the fact that models with significant internal mixing can better explain the observed large width of the main sequence band for massive stars. The comparison of theoretical isochrones, with and without overshoot, with composite cluster color-magnitude diagrams by Maeder and Mermilliod (1981) shows that the mixed cores of stars with masses $>2M_\odot$ should be larger than indicated by classical models by about 20–40%.

The dependence of $\tau(m)$ on metal abundance is also of concern for the reasons given above. Although the mean metal abundance Z has probably increased by no more than a factor of four during the history of the disk (see Twarog 1980a, b), we present results for a larger range in Z for completeness, and because of the possibility of deriving IMFs in the Magellanic Clouds, where the mean metal abundances may be as low as 0.002 to 0.005. Some relevant results are shown in Figure 14. The vertical lines with hatch marks are from Alcock and Paczynski (1978) and represent, from top to bottom, $Z=0.03$, 0.01, 0.001, and 0.0004. The filled circles at lower masses are from Wagner (1974) for $Z=10^{-4}$. It is seen that the uncertainty in mean metal abundance in disk stars of different masses ($0.01\leq Z\leq 0.03$) only introduces an uncertainty of less than 10% at any mass.

It should also be noticed that at $m=2$ and 3, Alcock and Paczynski's (1978) lifetimes for $Z=0.03$ are larger than those of Maeder (1976, no overshoot, lower filled triangles) at the same Z by about 30%. Maeder's lifetimes at smaller masses also fall below the three compiled relations shown. A comparison of various calculated lifetimes at the same mass and metal abundance indicates that the variations in the input physics and numerics among various stellar evolution codes and the uncertainty in helium abundance leads to a total spread of around 30–50% in $\tau(m)$.

In constructing the field star IMF, it was decided that the systematic increase in lifetimes due to overshoot at the convective core boundary found by Maeder (1976), Cloutman and Whitaker (1980), and Bressan *et al.* (1981) should be accounted for. The adopted $\tau(m)$ relation, shown in Figure 14 as the dark solid line, is basically that of Tinsley (1980) for $m<1.2$. For $1.2\leq m\leq 30$, Tinsley's lifetimes were smoothly increased in accordance with the overshoot calculations of Maeder and Cloutman and Whitaker by 20% at $m=1.5$, 30% at $m=3$, and 50% at $m=30$. For $m>30$, the adopted lifetimes are those of Maeder (1980) increased by about 20% and smoothed. The adopted lifetimes are listed in Table V. The uncertainty in lifetime is optimistically estimated at around 40% for $m\gtrsim 1.5$ and 20% for smaller masses. Since the IMF estimate for $m\gtrsim 1.5$ involves division of the present-day mass function by $\tau(m)$, this uncertainty will be directly reflected in the IMF for these masses. Note that the adopted $\tau(m)$ is larger than the relation used in MS by factors between about 1.5 and 2 over nearly the entire mass range. This will turn out to be a significant contribution to the difference between the IMF to be given in Section 2.6 and the earlier IMF or MS, which is as large as a factor of 3–4 at some masses.

TABLE V

Stellar lifetimes

$\log m$	$\log \tau(m)$	$\log m$	$\log \tau(m)$	$\log m$	$\log \tau(m)$
1.80	6.69	0.90	7.65	0.16	9.40
1.62	6.77	0.72	8.00	0.07	9.69
1.43	6.88	0.54	8.42	−0.01	10.02
1.26	7.08	0.40	8.78	−0.08	10.30
1.08	7.32	0.27	9.13		

2.5 History of the stellar birthrate

For a given mass m, the PDMF $\phi(\log m)$ gives the present number of stars around $\log m$ per pc^2. None of these stars can be more than $\tau(m)$ years old, so to calculate the IMF, that is, the number of such stars *ever* formed, we must correct the PDMF for stars around $\log m$ which have died. For a constant birthrate, this correction factor will obviously be $T_0/\tau(m)$. For a time dependent birthrate, Eq. (2.10) shows that when $\tau(m) \ll T_0$ the correction contains an additional factor $1/b(T_0)$, where

$$b(T_0) = \frac{B(T_0)}{\langle B(t) \rangle} \tag{2.13}$$

is the ratio of the present birthrate to the past average birthrate. We refer to $b(t)$ as the "relative birthrate". Notice that the *shape* of the IMF in this short-lifetime limit is independent of the detailed history of $B(t)$, depending only on its recent and past average values. Because of this property, which applies to stars with $m \gtrsim 2$, the IMF can be determined if we can obtain even gross information on the birthrate history, as long as we are willing to accept the assumption that the IMF is independent of time and spatial position.

For masses in the range $1 \lesssim m \lesssim 2$, i.e. $\tau(m) \sim T_0$, the situation is much more difficult because the conversion between PDMF and IMF, Eq. (2.9), depends on the detailed form of the birthrate history. For this reason it is currently impossible to accurately estimate the form of the IMF in the $1–2M_\odot$ range.

Our main concern, then, is the value of the relative birthrate $b(T_0)$. There are a large number of possible approaches to this problem. Most of these were critically reviewed in MS, and only those which yield quantitative constraints on $b(T_0)$ will be reviewed here. A list of all the methods is given in Table VI, which is a revised version of a table given in Scalo and Miller (1980). The methods have been divided into three groups on the basis of reliability (the judgment is somewhat subjective). The first group yields results whose uncertainties can be evaluated, the second group those which give only rough limits on $b(T_0)$ and/or whose uncertainties cannot be readily evaluated, and the third group contains methods which are either essentially indeterminate because of large uncertainties or contain too

TABLE VI
Constraints on the stellar birthrate history

Method	$b(T_0) = B(T_0)/\langle B(t) \rangle$
Continuity of the IMF	0.18–2.5
Counts of H II regions	0.06–1.5
Age distribution from isochrones	0.4 –1.0
Age distribution from Li in dwarfs	≥0.5
Age distribution from Li in red giants	0.5 –2
Age distribution from Ca H and K	≥1:
Kinematics of planetary nebulae	≤2–3
Formation rates of white dwarfs and planetary nebulae	0.3 –10:
Yields of nucleosynthesis	≥0.3
Formation rates of supernovae	
Radioactive nuclides	
Chemical evolution constraints	indeterminate
Initial mass function of open clusters	

many free parameters. Here we discuss only the primary group of determinations.

2.5.1 *Continuity of the IMF*

A relatively straightforward determination of $b(T_0)$ can be obtained by assuming that the IMF must be continuous between 1 and $2M_\odot$. If the birthrate was much larger in the past, the correction factor to the PDMF for $m \gtrsim 2$, $T_0/b(T_0)$, will be very large (for a given T_0), and the resulting IMF at $m \approx 2$ may be much larger than its value at $m = 1$, where it is independent of the birthrate, and so the derived IMF will show a "bump". Likewise, if $T_0/b(T_0)$ is too small, the $m \approx 2$ value will be much smaller than at $m \approx 1$, and the IMF will show a "dip". If the uncertainties in the PDMF and T_0 can be evaluated, the fitting procedure yields a range of possible values for $b(T_0)$. The method is illustrated schematically in Figure 15 for a power law true IMF. Schmidt (1959) was the first to emphasize that an IMF which is continuous between $m = 1$ and 2 requires that the ratio of present birthrate to past average birthrate cannot be very small. Tinsley (1977) used this method to estimate an upper limit on $T_0/b(T_0)$ of 80×10^9yr, which corresponds to a lower limit on $b(T_0)$ of 0.11 to 0.19 for

$9 \times 10^9 \leq T_0 \leq 15 \times 10^9$yr. Tinsley favored 20×10^9yr as a more realistic upper bound, or a lower limit $b(T_0) \approx 0.4$ to 0.8, but she did not consider the upper limit on $b(T_0)$ because she required that the birthrate be a decreasing (or constant) function of time.

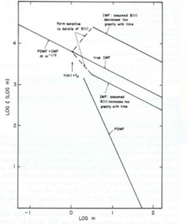

FIGURE 15 Schematic illustration of the effect of errors in the assumed stellar birthrate history on the derived IMF, assumed here to be a continuous power law with $\Gamma = -1/2$.

The problem was reconsidered in more detail by MS. Allowing for the various uncertainties, the allowed range in $T_0/b(T_0)$ is 6×10^9yr to 50×10^9yr. For the same range in T_0 as above, this gives $0.18 \lesssim b(T_0) \lesssim 2.5$, the result given in Table VI. In other words, the past average birthrate may have been at most about 5 times larger or 3 times smaller than the present birthrate. However these extremes come from pushing all the uncertainties to their estimated limits. For this reason MS, as did Tinsley, favored a range $0.5 \lesssim b(T_0) \lesssim 2$ as more realistic. Therefore if the IMF is reasonably continuous in the range 1–$2M_\odot$, the birthrate over the past 10^7–10^8yr cannot be much different than the average birthrate over the history of the disk. This does *not* imply that the birthrate was necessarily a smooth function in the past; large variations may have occurred more than 10^8yr ago, but these variations do not affect the form of the IMF for $m \gtrsim 2$. For example, the result is consistent with a strictly constant birthrate, an exponentially decreasing birthrate with a large star formation burst during the last 10^8yr, or a wildly fluctuating birthrate in which the present time happens to fall near the mean value. We shall see that stellar age distributions can give more detailed information on $B(t)$ back to ~ 4–6×10^9yr ago.

The above method assumes that the birthrate is continuous between $m \approx 1$ and 2. There have been frequent suggestions that the mechanism of star formation may be different for large and small masses, so that an abrupt change in the IMF might in fact occur in this mass range. As we shall see in Section 2.6.3 below, the IMF may in fact be bimodal to some degree, and if this is so, the continuity constraint on $b(T_0)$ is not valid. It turns out, however, that other methods for estimating limits on $b(T_0)$ give results which will allow us to estimate just how discontinuous the IMF could be.

2.5.2 *Counts of radio* HII *regions*

The current birthrate of *massive* stars can be estimated from observations of radio HII regions, since the radio luminosity is related to the number of ionizing Lyman continuum photons emitted by massive stars, and this number is approximately known as a function of mass (see Mezger and Smith, 1976; Smith, Biermann and Mexger, 1978). The calculation involves some uncertain parameters, such as the average length of time an HII region is detectable as a radio source.

The conversion to a *total* birthrate requires an assumed initial mass function, which itself depends on the birthrate history. MS tried to evaluate the uncertainties and concluded that the result is consistent with $0.06 \leq b(T_0) \leq 1.5$. This method therefore gives a useful upper limit, but the uncertainties render it less useful than some other methods in providing a lower limit. A more detailed discussion of these problems has been recently presented by Gusten and Mezger (1984).

2.5.3 *Stellar age distributions*

In principle the most direct method for obtaining the birthrate history is the distribution of stellar ages. A larger or smaller birthrate in the past would be reflected by larger or smaller numbers of old stars relative to the number of young stars. Because stellar lifetimes vary with mass, a correction must be applied to the age distribution to obtain $B(t)$, as discussed in detail by Tinsley (1974). In practice, the method is difficult to apply because of selection effects and the uncertainty of stellar ages based on, for example, theoretical isochrones, velocity dispersion, or CaII emission strength. Since the time of the review by MS there have appeared several studies which have improved the reliability of these birthrate determinations, and so we briefly discuss these developments.

1. Twarog (1980a, b) has presented a comprehensive study of the ages and metallicity distribution of about 1,000 spectral type F main sequence stars. For each star, effective temperature is obtained from the Hβ strength while M_v and metallicity are estimated from uvby photometry. A comparison with theoretical isochrones in the *H–R* diagram for the appropriate metallicity yields an age estimate for each star. The apparent age distribution was then corrected for the dependence of scale height on age and stellar evolution effects to provide a strong lower limit on the ratio of the present birthrate to the average past birthrate of $b(T_0) > 0.4$. The requirement that the age distribution be consistent with the observed metallicity distribution gives a most probable value in the range $2/3 \leq b(T_0) \leq 1$. One of the main problems with this method, as emphasized by Tinsley (1977), is that the age distribution depends not only on $B(t)$, but also on the IMF in the $1–2 M_\odot$ range where it is poorly determined. Further discussion can be found in Twarog (1980b).

2. The strength of Ca H and K emission lines in late-type main sequence stars is known to be correlated with age, younger stars exhibiting stronger emission. In principle, this correlation can yield ages more accurate than those obtained from theoretical isochrones for F and G stars near the main sequence, if the relation can be reliably calibrated (Barry *et al.*, 1981). Vaughan and Preston (1980) have given a progress report on their study of Ca H and K emission in a large number of nearby (distance < 25 pc) stars. One estimate of the birthrate history can be obtained by comparing the number of stars which have emission strengths comparable to stars in the Hyades cluster (age $\sim$ few $\times 10^8$yr) to the number with solar-like strengths (age $\sim$ few $\times 10^9$yr). Using 185 F–G stars and after correcting for difference in volume densities associated with the different velocity dispersions of the two groups, Vaughan and Preston find that $\sim 11–14\%$ of these stars have been formed within the age of the Hyades, which is probably 4–10% of the lifetime of the galactic disk. Even though the ages of the Hyades and the disk are uncertain, this still strongly suggests a nearly constant, or even increasing, birthrate.

One puzzle in the data concerns an apparent gap in the age distribution at $\sim 10^9$yr, corresponding to intermediate emission strengths. The ages and velocity dispersions of these stars show that they formed over a substantial fraction of the galactic disk, so the result implies either that the birthrate history in the disk suffered a large global change, that the emission strength is significantly affected by some parameter other than age, or that the age-emission strength calibration is in error. Barry *et al.* (1981) have given a recalibration of this relation based on the sun and six open clusters with estimated ages. In the cluster M67 they find a bimodal distribution of emission strengths, similar to the Vaughan and Preston result for field stars. Another indication that the bimodal distribution in the field stars is not due to the birthrate history comes from Duncan's (1981) study of lithium abundances in F–G main sequence stars and subgiants. Duncan finds some anomalous stars with strong lithium lines (young) yet weak Ca H and K emission, suggesting that a second parameter is involved. Until this effect is explained, the birthrate history implied by the field star survey must be regarded cautiously.

3. Stars with masses less than about $2 M_\odot$ have convective envelopes while on the main sequence. As a result, the surface abundance of lithium is continuously reduced as convection transports it to

depths hot enough for destruction by the reaction $^7Li(p,\alpha)^4He$. For a constant temperature at the base of the convective envelope the Li abundance would be an exponentially decreasing function of time. For example, the observed solar Li abundance implies a destruction timescale $\sim 1\times10^9$yr. Although current standard stellar models are incapable of accounting for such a short destruction timescale because they neglect convective overshoot and possibly turbulence in radiative zones (see Straus, Blake, and Schramm, 1976; Schatzman, 1977; see Cayrel *et al.* 1984, for a recent discussion of problems involved in accounting for the observed correlation of Li abundance with effective temperature), the existence of a correlation of Li abundance with age is well-established observationally (e.g. Zappala, 1972).

Duncan (1981) has carried out a detailed study of lithium in over 100 field F5–G5 dwarfs and subgiants. The lithium depletion timescale is obtained using the sun and three clusters with estimated ages. When applied to a sample of 79 field stars closer than 16 pc, this calibration gives a flat age distribution. After correcting for the correlation between velocity disperson and age, Duncan finds a birthrate history which has only decreased by less than a factor of two over the past $4-5\times10^9$yr.

4. A similar method for estimating the variation of the birthrate involves Li abundances in red giants. As stars ascend the red giant branch for the first time, the surface Li abundance is diluted as the deepening convective envelope mixes whatever Li was left in the outer layers at the end of main sequence evolution with Li-free material in the deeper layers. The dilution factor is about 30, increasing somewhat with decreasing mass (see Iben, 1967). Since the red giant lifetime is short compared to the age of a star, one can attach an age to each red giant with known Li abundance. A large sample of red giant Li abundances therefore gives an estimate of the age distribution, and hence the birthrate history. A birthrate which has decreased with time will give fewer young red giants with relatively large Li abundances than will an increasing birthrate.

Scalo and Miller (1980) compared theoretical Li abundance frequency distributions for different assumed birthrates with the observed abundance distribution of 35 giants studied by Lambert, Dominy, and Sivertsen (1980). Allowing for uncertainties associated with the small sample size, the comparison suggests $0.5 \lesssim b(T_0) \lesssim 2$. A greatly enlarged data base consisting of Li abundances in several hundred giants will soon be available (Sneden, 1985, personal communication).

It is worth noting that stellar age distributions directly sample the birthrate history back to $3-6\times10^9$yr ago, with a resolution of perhaps $0.5-1\times10^9$yr, unlike the IMF continuity constraint and counts of radio H II regions, which only directly sample the birthrate in recent times ($<10^8$yr ago).

2.5.4 *Other galaxies*

Estimates of star formation rates in galaxies other than our own are very uncertain because they must be based on integrated properties of the stellar population, and involve a rather large number of assumptions and parameters. Nevertheless, these estimates provide a valuable check on the galactic birthrate histories inferred from the methods described above. The dependence of UBV colors on birthrate history, IMF, and other quantities is discussed in Larson and Tinsley (1978); a study extending this work to other colors, particularly the far-ultraviolet, is given in Rocca-Volmerange *et al.* (1981), and additional work is summarized in Section 5.3.

A good example of the considerations involved is the study of over a hundred disk galaxies by Kennicutt (1983), discussed in more detail in Section 5.7 below. The observational data consists of integrated $H\alpha$ and red continuum fluxes, as well as UBV photometry. The basic idea is that the $H\alpha$ luminosity is directly related to the Lyman continuum photon flux, and therefore measures the number of massive ($\gtrsim 10M_\odot$) stars capable of providing photoionization. Using theoretical evolutionary tracks and stellar atmospheres, and an adopted IMF for the massive stars, the ultraviolet luminosity of theoretical models can be calculated. The birthrate of the massive stars then follows by requiring agreement with the observed $H\alpha$ flux. The *total* present birthrate depends on the form of the IMF at smaller masses. This is constrained by the red continuum flux, which comes mainly from low mass red giants. For an assumed IMF and $B(t)$, predicted continuum colors can be computed, again using theoretical evolutionary tracks and atmospheres, and compared with the observed colors. Separation of the effects of the IMF and the birthrate history is obviously a severe problem here, as it is in nearly all methods for estimating these functions.

The past average birthrate for each galaxy can be computed as the mass of stars in the disk divided by its age, and, combined with the current birthrate estimate, gives $b(T_0)$. A check on the result comes from using this $b(T_0)$ to predict the UBV colors of the galaxy.

Following this procedure, Kennicutt (1983) finds that $\langle b(T_0)\rangle \sim 1$ for the 77 Sbc–Sd galaxies, which should present the most reliable sample. Although this method is beset by many uncertainties and cannot give a unique solution for both $b(T_0)$ and the IMF (many of the possibilities are discussed by Kennicutt; see also Section 5.7 below), it is still encouraging that the result is consistent with the approximately constant birthrate inferred for our galaxy.

2.5.5. *Discussion*

The time dependence of the stellar birthrate has obvious implications for the theory of star formation. Of most interest is the common suggestion that the star formation rate depends on some power of the gas volume or surface density, $B(t) \propto \rho^n$, with $n > 0$. The weak physical motivation for this idea seems to be that at the beginning of the evolution of the galactic disk most of the matter was in the form of gas and the birthrate had some finite value, while at some time in the future the gas will be completely locked up in low-mass stars and stellar remnants, at which time the star formation rate must be zero. It is therefore usually assumed that the birthrate must be a monotonically decreasing function of time in this interval. This argument is far from convincing. Most studies of the physical processes controlling the star formation rate do not yield a dependence on the large-scale gas density, except possibly as a threshold effect. More importantly, all the observational evidence reviewed above is consistent with a roughly constant birthrate. A full discussion of this problem is beyond the scope of this review. Previous arguments that $B(t) \propto \rho^n$ with $n \sim 1$–2 were critically reviewed by MS. An important study of this question can be found in Madore (1977), who shows that *if* there is a density dependence, n must be less than about 0.5. Even then, this dependence probably refers only to local regions, not the larger scales of interest here. For other galaxies there is no correlation between the derived star formation rate and the total neutral hydrogen content (Kennicutt and Kent, 1983). A detailed discussion of the lack of any empirical evidence for a relation between star

formation rate and gas number or column density can be found in Freedman (1984).

Judging from the above discussion, it appears that the birthrate (averaged over ~ 0.5–1×10^9yr intervals) has been reasonably constant within a factor of about 2 over the history of the galactic disk. We shall proceed to compute the IMF under this assumption. Since the stellar age distribution results sample the birthrate history back to $\sim 5 \times 10^9$yr ago, the derived IMF will only be sensitive to detailed variations in $B(t)$ for masses in the rather small range 1.0–$1.2 M_\odot$, corresponding to $10^{10}\text{yr} \geq \tau(m) \geq 5 \times 10^9\text{yr}$.

2.6 The resulting IMF

The field star IMF is given in terms of the PDMF, the birthrate history, the stellar lifetime, and the age of the galactic disk by Eq. (2.9):

$$\xi(\log m) = \phi_{ms}(\log m) T_0 \Big/ \int_{T_0-\tau(m)}^{T_0} b(t)\,dt, \qquad \tau(m) < T_0. \tag{2.12}$$

For masses so small that $\tau(m) > T_0$, we have $\xi = \phi_{ms}$.

An upper limit to the age of the disk can be set by the ages of globular clusters, while a lower limit comes from the ages of the oldest known open clusters. Both estimates depend on the accuracy of the distance scale, details of stellar evolution calculations, and the adopted abundances for the clusters in question, and are correspondingly uncertain (see, for example, Janes and Demarque, 1983 and references therein; also Mihalas and Binney, 1981, ch. 3). Assuming that the oldest disk stars have ages somewhat in excess of the smallest determinations for the ages of the oldest open clusters, most estimates are consistent with values of T_0 in the range

$$9 \times 10^9\text{yr} \leq T_0 \leq 15 \times 10^9\text{yr}. \tag{2.13}$$

With $T_0 = 12 \times 10^9$yr as a standard value, this range implies an uncertainty of about ± 0.1 in $\log \xi$ for all masses $> 1 M_\odot$.

All the evidence discussed in Section 2.5 above is consistent with $0.5 \leq b(T_0) \leq 1.5$, and for illustration an exponential birthrate of the form

$$B(t) = B(o) \exp(t/\tau_B) \tag{2.14}$$

is used, with $\tau_B = -T_0$, ∞, and $+T_0$, which corresponds to $b(T_0) = 0.58$, 1.0 and 1.38. The resulting IMF (stars pc^{-2} log m^{-1}) is given in Table VII for these three choices and $T_0 = 15$, 12, and 9×10^9yr, respectively. These choices give a range in the important quantity $b(T_0)/T_0$ from 0.04 Gyr^{-1} to 0.16 Gyr^{-1}, extremes which are just consistent with the available observational evidence.

TABLE VII

log m	log ξ(log m)			ϵ(log ξ)
$b(T_0)$ =	0.6	1.0	1.4	
T_0 =	15 *Gyr*	12 *Gyr*	9 *Gyr*	
1.80	−1.22	−1.76	−2.35	0.43
1.62	−0.90	−1.44	−2.03	0.34
1.43	−0.72	−1.26	−1.80	0.32
1.26	0.49	−1.03	−1.62	0.31
1.08	−0.07	−0.61	−1.20	0.30
0.90	0.22	0.31	−0.90	0.25
0.72	0.52	−0.02	−0.60	0.25
0.54	0.82	+0.29	−0.30	0.23
0.40	1.12	0.65	+0.02	0.25
0.27	1.38	0.87	0.33	0.25
0.16	1.74	1.25	0.74	0.24
0.07	1.92	1.46	1.00	0.24
−0.01	1.83	1.46	1.46	0.17
−0.08	1.59	1.59		0.24
−0.14		1.50		+0.27, −0.21
−0.21		1.59		+0.26, −0.20
−0.27		1.70		+0.25, −0.19
−0.35		1.83		+0.24, −0.17
−0.44		1.88		+0.21, −0.16
−0.54		1.88		0.24
−0.65		1.88		0.24
−0.75		1.85		0.23
−0.85		1.65		+0.29, −0.36
−0.96		1.38		+0.41, −0.49
−1.06		1.06		0.7

2.6.1 *Comparison with the MS IMF*

The resulting IMF (stars pc^{-2} log^{-1}m) for $T_0 = 12$ and $b(T) = 1.0$ is illustrated in Figure 16, and is tabulated in Table VII for three combinations of T_0 and $b(T_0)$. The error estimates given reflect the contributions to the PDMF uncertainties discussed in Section 2.3.4 except that the uncertainties in log m at given M_v from the $m(M_v)$ relation have been decreased to account for the counteracting effect of a mass error on $\tau(m)$. In addition, an uncertainty of 30% in $\tau(m)$ at all masses was included, which seems reasonable in light of the discussion in Section 2.4. Uncertainties due to T_0 and $b(T_0)$ are not included, but their effects for $m \gtrsim 2$ are indicated in the figure.

Also shown in Figure 16 (as crosses) is the IMF derived by MS using the same T_0 and $b(T_0)$. The difference between this result and the presently-derived IMF are surprisingly large, especially for $m \gtrsim 2$, reaching a factor of four between 5 and $8M_\odot$. About half of the difference comes from the PDMF, which was larger in MS because of the adopted LF and, for $m \gtrsim 12$, because of the shallower $m(M_v)$ relation, giving larger masses for a given M_v. The other half stems from the adopted stellar lifetimes. Even neglecting the effects of overshoot, the MS lifetimes were almost certainly too small, by a factor of about 1.6 at log $m = 0.9$. The effect of overshoot in prolonging core hydrogen-burning raises this to about a factor of 2. The MS IMF approaches the present IMF at the highest masses because the GCC LF is flatter than the LF used by MS. For $0.5 \lesssim m \lesssim 1$ the MS IMF is larger because it relied heavily on Luyten's (1968) LF, which is an overestimate in this mass range. Also, MS ignored the dip in the LF of Wielen, now confirmed by several studies, which shows up at $m \approx 0.7$ in the present IMF. At very small masses the present IMF decreases rapidly compared to MS because of the recent body of evidence supporting a turnover in the LF at faint magnitudes (Section 2.2.2).

2.6.2 *The IMF at very small masses*

The peak in the IMF at $m \approx 0.3$ and decline at $m \lesssim 0.2$ directly reflects the same behavior in the adopted luminosity function for $M_v \gtrsim 12$, a form which has now been obtained directly using independent methods to estimate the LF, and is also inferred from indirect arguments (Probst and O'Connell, 1982; Probst, 1983b). While it is true that all methods for determining the LF are subject to incompleteness at the faintest magnitudes, the weight of evidence strongly suggests that the turnover is real. Such a sharp turnover in

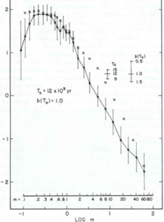

FIGURE 16 Derived field star IMF. Uncertainty estimates do not include relative birthrate $b(T_0)$ and disk age T_0, whose effects are indicated in the figure. Crosses represent the IMF derived in Miller and Scalo (1979).

the IMF could be avoided if $|dM_v/d\log m|$ becomes very large at small masses (D'Antona and Mazzitelli, 1983), but, as discussed earlier, it is unlikely that this effect could lead to an IMF which continues to increase with decreasing mass. At most it could give a flat IMF. Recent studies attempting to predict the number of very faint, possibly substellar, objects (e.g. Staller and de Jong, 1981; see van der Linden and Staller, 1983 for evolutionary models of very

low-mass stars) have used an IMF which continues to increase at small masses. If the IMF turnover shown in Figure 16 is real, or even if it is flat, then the number of such objects must be negligibly small, unless some process causes the IMF to increase drastically at $m \lesssim 0.08$, i.e. unless the formation process of substellar objects is much different than those of stars. Also, the mass density contributed by stellar objects less massive than $0.2M_\odot$ would be negligible, as pointed out by MS. More detailed low mass stellar models and more accurate bolometric corrections are crucial for a resolution of this question.

2.6.3 *A bimodal IMF?*

The shape and amplitude of the IMF are strongly affected by the birthrate history in the range 1.0–1.5$M_\odot$. Figure 17 shows the IMF in more detail between $m=0.4$ and 1.9 for $b(T_0)=0.6$, 1.0, and 1.4, each for 3 values of $T_0=9$, 12, and 15 Gyr. For a given T_0, the spread in ξ at $m \approx 1.2$ is a factor of five, and is a factor of ten if the range in T_0 is included. It seems impossible to obtain even an approximate estimate of the IMF in this mass range, especially when the uncertainties in the PDMF and lifetimes are considered, unless some additional constraint can be imposed. In MS it was argued that the IMF should be a monotonic decreasing function and used this requirement to constrain $b(T_0)$ and the IMF by pushing the uncertainties at $m<1$ and $m>1.2$ to their estimated limits. The resulting limits on $b(T_0)$ have been substantiated by more recent work (Section 2.5 above), but the argument for a smooth IMF is no longer compelling, for a number of reasons.

First, while it is true that the uncertainties in the IMF are large, it does not seem possible that the *differential* errors between neighboring masses, or between masses just above and below $1M_\odot$, could be large enough (factor of 2–3) to eliminate the peak at $m \approx 1.2$ in the $b(T_0)=0.6$ case. A smooth IMF would require an amazing conspiracy among the errors at each mass. Second, all three birthrates result in a feature at $m \approx 1.1$–1.3, from a strong peak for the $b(T_0)=0.6$ case, to a "plateau" for the constant and increasing birthrates. The plateaus could conceivably be removed by a suitable change in the input data. In particular, a steep decrease of the scale height occurs in the mass range $1.0 \lesssim m \lesssim 1.4$, and the plateaus can be mostly removed without

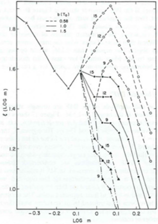

FIGURE 17 Form of the derived IMF around $1 M_\odot$, for nine combinations of the relative birthrate $b(T_0)$ and disk age T_0.

affecting the IMF outside this mass range if the M_v at which the sharp increase in $H(M_v)$ sets in is actually larger than adopted by about one magnitude. This can be seen by replacing $H(M_v)$ by $H(M_v-1)$ and rescaling the IMF. This procedure is barely within the uncertainties in $H(M_v)$. However, no reasonable alteration of the input relations can remove the peak in the case of a decreasing birthrate, and so, in order to obtain a smooth IMF above $m=1$ we would need to require

$b(T_0) \gtrsim 1.0$, *as well as* a change in $H(M_v)$. Since a value of $b(T_0)$ somewhat less than unity is certainly allowed by more direct estimates using stellar age distributions, these requirements seem quite artificial.

However, by far the most important consideration is the minimum in the IMF at $m \approx 0.7$. This feature, reflecting the dip in the adopted LF which has now been well-established, is very likely real. Its existence is independent of $\tau(m)$, T_0, and $b(T_0)$, and cannot be removed by any reasonable modification of $m(M_v)$, $g_{ms}(M_v)$, or $H(M_v)$. As discussed in Section 2.3.1, a flatter m–M_v relation than used here in the range $5 \leq M_v \leq 9$ could remove the feature (D'Antona and Mazzitelli, 1983), but seems unlikely. The mass at which the dip occurs is only uncertain by about 10%, the amplitude by about $(+0.02, -0.05)$ in $\log \xi$, and the width by 20–30% (see the discussion of Figure 4). Therefore, since the IMF shows a peak at $m \approx 0.8$, the assumption of a smooth IMF for $m > 1$ no longer has much motivation. Also, the width of the peak at $m \approx 0.8$ would be extremely small if $b(T_0) \gtrsim 1$, implying a very peculiar process which favors the formation of stars only over a quite narrow mass range. The most likely resolution is that the "peak" at $m \approx 0.8$ is not a peak at all, but a continuation to smaller masses of a broader feature in the IMF which has its maximum at $m \approx 1.2$. It therefore seems reasonable that the actual form of the IMF resembles the cases with $b(T_0) = 0.6$ and $T_0 = 12$ or 15 Gyr in Figure 17.

The now-likely existence of a maximum in the IMF at $m \approx 1.2$ (or at $m \approx 0.8$ if $b(T_0) \gtrsim 1$) and the second maximum at $m \approx 0.3$ *may* support suggestions of "bimodal" star formation in our galaxy. The bimodal form does *not* reflect only the local IMF because the lifetimes of most stars in the appropriate mass range are sufficiently long that these stars were formed over a significant area of the galactic disk. The question of whether the bimodality reflects separate physical star formation processes for stars born in a given region, or different mass functions for stars formed in different types of groups (e.g. open clusters and associations) or different places (e.g. in spiral arms and between the arms), or represents a single complicated process is a fundamental one whose answer will require a great deal more theoretical work, as well as additional estimates of the IMF in star clusters and other galaxies. Further discussion is given in Section 8 below.

2.6.4 *The IMF of massive stars*

The IMF for massive stars is particularly important in many applications, and is also especially uncertain. The method of derivation used above transformed a visual luminosity function, from the GCC catalogue of O stars extrapolated to join smoothly with other determinations at small luminosities, into a mass function with the aid of a brightening correction which accounts for the admixture of stars with a range of ages and masses at a given M_v. The correction was implemented in an approximate manner by using the relation between initial mass and average hydrogen-burning luminosity. This method uses only the gross features of the theoretical calculations, namely the brightening in M_v during core hydrogen-burning, which does depend on the bolometric correction and effective temperature scale, but operates only on the observed M_v luminosity function, which comes directly from the observations.

A different approach to the problem is to estimate bolometric luminosities and effective temperatures for each star in the sample from its M_v, spectral type, and luminosity class. The present-day mass function can then be estimated by counting the number of stars in the *H–R* diagram between theoretical evolution tracks computed for models with different masses. The IMF follows by division of the number in each mass range by the main sequence lifetime. This spectroscopic method, first discussed in detail by Lequeux (1979), uses the full information from the theoretical models, but suffers from the uncertainties in the bolometric corrections and effective temperatures which must be assigned to each star on the basis of its spectral type and luminosity class. This method has been used to estimate the field star IMF by Lequeux (1979), Garmany *et al.* (1982, GCC), Bisiacchi, Firmani, and Sarmiento (1983, BFS), Humphreys and McElroy (1984, HM), Van Buren (1984), and Vanbeveren (1984). (A few applications of the method to cluster and association IMFs are presented in Section 3). In this section we compare these determinations among themselves and with the IMF derived from the luminosity function given earlier, which will be referred to as IMF(LF). In doing so we shall try whenever possible to normalize the stellar lifetimes to the same scale adopted in Section 2.4, which emphasized the importance of convective overshoot. In this way the comparison is relatively independent of differences in adopted lifetimes; the absolute numbers can be easily revised for a different

adopted $\tau(m)$ relation. However, because it was assumed here that overshoot causes brightening during the core-hydrogen burning phase, the present mass scale will be smaller than in the other determinations, which results in a shift of the other IMFs to larger masses compared to the present IMF.

It must be stated at the outset that the various IMF determinations listed above have not yet converged to a definitive result, and in some cases it is not possible to fully resolve the discrepancies or even identify their causes. The discussion given here is meant primarily as a graphical comparison and a summary of the various treatments of the ingredients which enter each determination.

Lequeux (1979) used an apparent magnitude-limited sample obtained by combining a number of catalogues. Details concerning the sample selection, adopted calibrations of M_v, bolometric corrections and effective temperatures, corrections for reddening, and other considerations can be found in Lequeux's paper. The numbers of stars per kpc^2 in each mass range were derived by comparison with tracks of Chiosi *et al.* (1978, large mass loss rate models) for $m > 15$. The resulting IMF is shown in Figure 18 as filled squares (Lequeux derived the IMF down to $m = 2.5$, but the results are not shown in the figure). The plotted symbols give the number of stars formed kpc^{-2} yr^{-1} per unit $\log_{10} m$. It should be noted that the counts had been smoothed by Lequeux. In constructing this IMF I used the $\tau(m)$ relation given in Table V, in order to make a more direct comparison with the IMF based on the visual luminosity function; Lequeux's adopted lifetimes are smaller by about 30%. It was also assumed that the contribution of old evolved O stars was negligible, as discussed earlier. According to a private communication quoted in GCC and the discussion in Van Buren (1984), the IMF values are probably too small because of an overestimate of the surface area due to an underestimate of interstellar extinction.

GCC followed the method of Lequeux, but applied it to a volume-limited sample of 424 O stars within a distance of 2.5kpc. (This is the same sample used earlier to construct the IMF from the luminosity function.) The distribution in the *H–R* diagram was compared with three sets of evolutionary tracks which differed in the inclusion of mass loss and convective overshoot, although all the tracks were calculated using essentially the same evolutionary code. Although GCC only give the indices of power law fits to the resulting IMFs, the actual values at each mass are easily obtained from their Table III, and are shown in Figure 18. The lifetimes used by GCC were increased by 30% in order to make a more direct comparison with the LF-based IMF. Counting uncertainties are also indicated for the two largest mass intervals for their model *a*.

Another study using a similar approach with a different sample has been presented by Bisiacchi, Firmani, and Sarmiento (1983, BFS in what follows). They used Humphrey's (1978) catalogue of supergiants and O stars in associations and clusters as the basic sample. This sample is not complete because of the omission of stars not in catalogued clusters and associations, but the incompleteness should not be a function of spectral type or luminosity class. BFS therefore normalized the counts using the catalogue of Cruz-Gonzales *et al.* (1974). Two samples, which contained associations and clusters in two different distance intervals, were examined. *H–R* diagrams were constructed using Humphrey's spectral type-T_{eff} scale and compared with theoretical tracks fom Chiosi *et al.* (1978). The IMFs calculated from their star counts using the lifetimes in Table V are plotted in Figure 18 for both samples, which agree well with each other. BFS only give a lower limit of $m=60$ for the counts at the highest masses, and I chose a range $60 \leq m \leq 100$ for these counts. Also, no correction for later evolutionary stages is included ($g_{ms}=1$; BFS took $g_{ms}=0.9$).

A still more recent determination of the massive star IMF has been presented by Humphreys and McElroy (1984, HM), who compiled a catalogue of over 5000 stars which included O stars, supergiants of all spectral types, and the less luminous B stars with known MK spectral types and luminosity classes. This comprises a much larger sample than previous work and, as in BSF, includes stars of later spectral types than in the GCC sample, which contained only O stars. (As noted in Section 2.2.3, the LF of the stars in the HM sample is consistent with the LF used here to derive the IMF). The spectroscopic method was applied using Maeder's evolutionary tracks with moderate to large mass loss rates. The most important point stressed by HM is that the star counts for the less luminous stars, mostly B stars of LC V to III, are incomplete even at a distance of 1 kpc. Figure 18 shows their derived IMF with no correcton for incompleteness as plus signs. The lifetimes have been increased by 30% to account for convective overshoot. The flattening at $20M_{\odot}$ and

decline at smaller masses are due to incompleteness. HM estimated a correction for incompleteness at $m=20$ by extrapolating the bolometric luminosity function for higher luminosities, for which the sample should be complete to about 3 kpc. The correction is a factor of 2.5, and this corrected IMF point is shown as the asterisk in Figure 18. The IMF index for $20<m<70$ is $\Gamma=-2.2$, in good agreement with BSF. If the point at $100M_{\odot}$ is included, HM find a weighted least

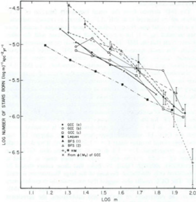

FIGURE 18 Comparison of a number of determinations of the IMF of massive stars. Crosses connected by dark solid line is the IMF derived in the present work from the luminosity function; all other determinations used the method of spectroscopic matching described in the text.

squares power law fit with $\Gamma = -2.4$. It should be noted that HM adopted lower effective temperatures for the early O stars than in the work described above, giving smaller luminosities at the largest masses; the effect on the IMF is to shift its value at the largest mass interval to a lower mass than would be obtained using the warmer temperatures. As noted by HM, their slope is very similar to that derived in MS. Some of this agreement is certainly fortuitous. It does appear that, by restricting the limiting distance of the sample, MS avoided problems with incompleteness; however, the price paid was a very small sample size.

The IMF derived from the visual luminosity function of GCC, which will be referred to as IMF (LF), is shown as crosses connected by a heavy solid line. No correction for post-hydrogen-burning stars was included ($g_{ms} = 1$) for a more direct comparison with the other results. Note that the IMF (LF) does not depend on an assumed scale height. The result agrees well with the GCC IMF derived from evolutionary tracks, especially for their cases *a* (no mass loss or overshoot) and *b* (mass loss and overshoot included). The IMF (LF) is smoother than the GCC results because the visual LF is smooth, and because we applied an approximate brightening correction at each mass, while the GCC counts in each mass interval depend on the details of the evolutionary tracks. The IMF (LF) would be shifted in absolute value and slope if brightening corrections derived from different sets of evolutionary calculations were applied. The index of the IMF (LF) for the 3 largest masses (the ones for which the LF was from GCC) is $\Gamma = -1.4$. If the next lowest mass is included (recall that the GCC LF was incomplete here and the adopted LF was smoothly joined to other data), $\Gamma \approx -1.55$; however, if we do include the g_{ms} corrections, $\Gamma = -1.4$ down to this mass also. GCC give indices of -1.55, -1.36, and -1.65 for their cases a, b, and c, respectively, although Figure 18 shows that these values should be considered only illustrative, because of the large fluctuations in each IMF. The GCC results also suggest that uncertainties in evolutionary tracks can be a significant source of error in the high-mass IMF. Given the differences in method and calibrations, the agreement between GCC and IMF (LF) determined from the GCC catalogue must be considered excellent, and shows that a reliable IMF can be derived from photometric data alone. This result is especially important for IMF estimates from star counts in other galaxies, where spectroscopy of large numbers of stars to the requisite limiting absolute magnitude is presently impossible.

The Lequeux IMF lies below the other determinations, presumably because of the reddening problem mentioned earlier. The index of the Lequeux IMF shown in Fig. 18 is $\Gamma = -1.3$ (recall that the counts had already been smoothed). This is about the same value which would be obtained using Lequeux's adopted lifetimes. Lequeux's result of $\Gamma = -2.0$ was obtained assuming that a large fraction of O stars are evolved stars from an old population. As discussed earlier current evidence does not support a large value for this fraction, although its actual value remains unknown. It is therefore seen that the shape of the IMF found by Lequeux ($\Gamma \sim -1.3$), GCC ($\Gamma = -1.3$ to -1.7), and IMF (LF) ($\Gamma = -1.4$ to -1.6) are in fairly good agreement.

The IMFs of BFS and HM are steeper than the IMFs of Lequeux, GCC, and IMF (LF), and the IMF values are significantly larger at the lower masses. The IMF indices are about -2.0 for BFS and -2.2 for Humphreys and McElroy (omitting the point at highest mass, whose location is uncertain due to the uncertainty in the T_{eff} calibration). According to the discussions of BFS and HM, this difference must be due mostly to the inclusion of stars of later spectral types, which were not contained in GCC's O star catalogue. For example, the total surface densities for the BFS and GCC samples are 41 and 22 stars kpc^{-2}, while the surface densities of O stars alone are in good agreement. A still more recent study by Vanbeveren (1984) which also included B stars, finds $\Gamma \approx -2.2$ to -2.4, although Vanbeveren finds a large difference between field stars and stars in clusters, as discussed further below. All these studies suggest that the values of Γ from Lequeux, GCC, and IMF (LF) are too flat. This is not a firm conclusion, however, since the thorough study of Van Buren (1984), to be discussed in detail below, gives $\Gamma \approx -1.4$.

Another difference between all the spectroscopic determinations shown lies in the adopted calibrations of effective temperatures, which can alter the slope of the derived IMF as well as shift it horizontally. (For recent work on the T_{eff} scale for hot stars, see Böhm-Vitense, 1980; Conti, 1984; Simon *et al.*, 1983; and Tobin, 1983.) The drastic effects of uncertainties in the T_{eff} calibration can be seen by comparison of Figures 3 and 5 in GCC. If IMF determinations are to be profitably compared in the future, it is imperative that a provisional standard T_{eff} scale be decided upon, since it is impossible to *post facto* unravel the discrepancies in the IMF determinations caused by the differing T_{eff} scales. The IMF (LF) is less sensitive to these calibrations, which only enter the brightening correction, and then only differentially. I believe this is an advantage of the direct use of the visual luminosity function.

There are additional problems such as the unknown fraction of young stars hidden in opaque interstellar clouds. This effect, if important, would flatten the IMF at large masses, as discussed in detail by GCC (see also Section 2.8 below). The appropriate lifetimes also remain uncertain by at least 30%.

IMFs derived here (Table VII) and in GCC agree well in shape but differ by a factor of around two in absolute value, even though they are both based on the same data. There are basically three reasons for the difference. 1. The adopted lifetimes here are larger than in GCC. 2. At a given mass, the luminosities used here are larger because of the weight given to stellar models that included convective overshoot. 3. A correction of 30% was applied here for the presence of evolved stars in the sample; this value is still uncertain. 4. The IMF was extracted from the data in different ways; basically GCC applied bolometric corrections and an effective temperature scale to each star's M_v, spectral type, and luminosity class, while the present result uses only the distribution of observed M_v's and applies the bolometric correction and effective temperature calibration to the brightening of the theoretical tracks. It appears that the first two differences account for most of the discrepancy, as discussed presently.

After this comparison was completed, two additional estimates of the high-mass IMF by Van Buren (1984; see Van Buren, 1983) and by Vanbeveren (1984) became available.

Van Buren applied a variant of the spectroscopic method to a sample consisting of the O stars in the GCC catalogue and the $\sim 10^5$ stars in the Michigan HD catalogue to determine the IMF down to $3M_\odot$. Extinction was treated more carefully than in previous work by using Lucke's (1978) reddening maps and assuming an exponential z-distribution of dust. The details of the method differ somewhat from the papers discussed above, in that a mass-luminosity relation was used for each luminosity class. Two different sets of mass-luminosity relations were employed. The first is a fit to binary star data for stars in each luminosity class. An important point stressed by Van Buren is

that this relation gives each star's *present* mass, which is an underestimate if mass loss is important. Van Buren's IMF derived for this case is shown in Figure 19 as the open triangles connected by dotted lines. I have again rescaled the results so that they correspond to the same lifetimes as adopted here. Van Buren did not examine any models which included convective overshoot, so his lifetimes are smaller; the differences are less than 15% for $10 < m < 30$, but are 15–25% for larger masses, and increase from 20–80% as mass decreases from 8 to $3M_\odot$. Since overshoot only increases lifetimes by 20–30%, the large discrepancy at the smallest masses underscores the additional uncertainties in stellar lifetimes as discussed in Section 2.4 above. The observationally-based $m(M_v)$ relation used by Van Buren is shown in Figure 20 for LC V (dashed line) and LC IV (dotted line). In constructing these relations I used Van Buren's $m(L)$ relation and his adopted M_v-spectral type and BC-spectral type relations. The LC V relation agrees fairly well with the relation used here.

This observational IMF refers to present masses, not initial masses. Van Buren used a number of published evolutionary calculations which included mass loss to derive a theoretical initial mass-luminosity relation for each luminosity class. The resulting IMF is shown in Figure 19 as filled triangles connected by dashed lines, again rescaled to the lifetimes of Table V. The error bars shown were measured from Van Buren's figures, and include $N^{-1/2}$ counting uncertainties, a 10% uncertainty in the sampling volumes, a 15% uncertainty in the assigned masses, and a 20% uncertainty in lifetimes. The shifting of stars to higher initial masses markedly flattens the derived IMF. The IMF derived from the visual LF and given in Table VII is shown in Figure 19 as open circles connected by solid lines. The agreement is poor for $m \gtrsim 15$, with Van Buren's IMF being larger and flatter; $\Gamma \approx -1.2$ for $m > 10$, compared with -1.5 found here.

The major source of disagreement does not lie in the sample size, extinction corrections, etc., but is probably due to the different $m(M_v)$ relations which were used. Van Buren's $m(M_v)$ relation, extracted from his tables, is shown in Figure 20 for LC V (solid line) and LC IV (dot-dashed line). For $m \gtrsim 20$ this relation gives progressively larger masses than the present relation. The difference is *not* related to mass loss, since the present relation, which was fit to model calculations, does refer to the initial model masses. The discrepancy is mostly due to the fact that I assumed that models which include convective overshoot are brighter by about 0.3 to 0.7 mag while none of the models used by Van Buren included overshoot. If the overshoot brightening were neglected here, it would "stretch out" the derived IMF, moving each IMF value to larger masses, by $\Delta \log m \sim 0.2$ at large masses. Inspection of Figure 20 clearly shows that this change would bring the two results into better agreement, although Van Buren's IMF would still be slightly larger and flatter, with $\Gamma \sim -1.3$ to -1.4.

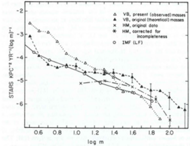

FIGURE 19 Comparison of high-mass IMFs derived by Van Buren (1984, 1985), Humphreys and McElroy (1985), and the present work.

However, the discussion of HM suggests that Van Buren's sample may be incomplete for $m \lesssim 30$. The HM IMFs with and without an incompleteness correction, are shown in Fig. 19. However, after a study of Van Buren's careful treatment of incompleteness for each spectral type-luminosity class, it is my opinion that the discrepancy is *not* due to incompleteness in Van Buren's work. The discrepancy in absolute value between Van Buren and HM at large masses is due to a combination of different $T_{\text{eff}} - \text{BC}$ scales, adopted evolutionary tracks, and extinction corrections. In particular, Van Buren's more

detailed treatment of reddening gives a smaller sample volume, and so a larger IMF.

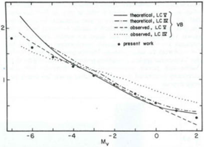

FIGURE 20 Comparison of mass-luminosity relations used by Van Buren (1984, 1985) with relation adopted in present work.

Since none of the other calculations shown include overshoot brightening, it seems that much of the discrepancy in absolute value between these determinations and the present work is due to convective overshoot brightening, which shifts the IMF to lower masses.

Finally, a study of the IMF has been presented by Vanbeveren (1984), which includes in an approximate manner the effect of atmospheric extension on the effective temperature. Vanbeveren shows that this effect can help explain the large width of the observed core hydrogen-burning band in the *H–R* diagram. In order to estimate the IMF, a sample was constructed which consisted of cluster OB stars out to a distance of about 2.5 kpc, and "field stars" from the stars not in the GCC catalogue, but included in the Humphreys catalogue; known binaries, OC, and ON stars were omitted. The IMF for the combined cluster-field star sample is shown in Figure 21 as filled squares. These IMF values were derived using models which include convective overshoot. The results for models without overshoot are shown as open squares; the form is essentially the same but the absolute values are larger because of the smaller lifetimes. However, the models used by Vanbeveren did not exhibit the overshoot brightening which was adopted here, which is why, in part, his IMF lies above IMF (LF), which is shown as the crosses connected by a solid line. The IMF estimated by HM (which is similar to that of BFS) is also shown. The absolute levels and slopes are similar, and Vanbeveren estimates $\Gamma = -2.4$ (-2.2 without overshooting), although I find $\Gamma = -1.9$ from the same numbers. The discrepancy is due to the fact that Vanbeveren applied a weighting procedure in deriving his slopes (Vanbeveren, private communication), and illustrates how much uncertainty is involved in simply estimating power law slopes for a single data set.

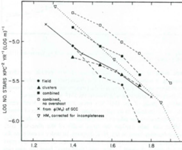

FIGURE 21 Comparison of high-mass IMFs derived by Vanbeveren (1985) for different samples and assumptions concerning convective overshoot, Humphreys and McElroy (1985), and the present work.

Vanbeveren finds a much steeper slope for the field stars ($\Gamma = -3.5$ for models with overshoot) than for the clusters ($\Gamma = -1.6$). The derived IMFs are shown in Figure 21 as filled circles (clusters) and filled triangles (field stars). Part of this difference may be due to the problems with assigning an absolute magnitude to each spectral type-luminosity class, as pointed out by Vanbeveren. Another possible problem arises because of the crude correction of the field star sample for B stars, which was based on the ratio of B-to-O stars in the cluster sample. However, the major problem lies in understanding why the cluster sample ($\Gamma \sim -1.6$) gives an IMF which is so much flatter than that determined by BSF ($\Gamma \sim -2.0$) which was based on the *same* sample. This difference may be due to the effects of atmospheric extension on the effective temperature scale, which was not considered in BSF; however, the information given by Vanbeveren is not sufficient to ascertain whether this is an important effect on the IMF. Alternately, the discrepancy could be due to the different evolutionary tracks and different $BC - T_{eff} - M_{bol}$ scales adopted in the two papers.

Obviously the situation concerning the high-mass IMF remains in a very confused state. The several determinations of the IMF index Γ from the analyses discussed above are listed in Table VIII. The quoted values apply to masses greater than about 15 to $25 M_\odot$ for all the determinations; the upper mass limit varies from 60 to $100 M_\odot$.

From this discussion we can draw the following conclusions for high-mass ($m \gtrsim 10$) stars.

1. The IMF derived from the visual LF agrees well with the IMF derived from two-dimensional spectroscopic matching, both in slope and amplitude, when the same lifetimes and luminosities at a given mass are used. This supports the feasibility of deriving IMFs for nearby galaxies from luminosity functions alone, since large scale spectral classification will be impossible for stars this faint. However, the spectroscopic method is potentially more accurate than the LF method, if both methods were applied to the same number of stars, because a small uncertainty in the slope of the LF results in a much larger uncertainty in the slope of the IMF.

2. If the effects of convective overshoot on the lifetimes and luminosities are completely neglected, the results of Lequeux (1979), Garmany *et al.* (1982), Van Buren (1984), and the present work suggest

that Γ is around -1.0 to -1.4 for $m \gtrsim 10$–15, or -1.3 to -1.6 for $m \gtrsim 20$. However, the results of Bisiacchi *et al.* (1983), Humphreys and McElroy (1984), and Vanbeveren (1984) suggest that these data are incomplete below $30 M_\odot$, and that $\Gamma \approx -2$ for $m \gtrsim 20$. The discrepancies do not only reflect the effect of including the B stars in the sample, since they were included in Van Buren's study which gave the flattest slope. In addition, Van Buren made a careful study of incompleteness in each of his Sp–LC bins.

TABLE VIII
Estimates of Γ for high-mass stars

Study	Γ	Notes
Lequeux	-1.3	
GCC	-1.4 to -1.7	a,b
BSF	-2.0	
HM	-2.2	c
Van Buren	-1.3	
Vanbeveren	-2.4(-1.9)	d
IMF (LF)	-1.5	e

[a] Range for 3 different sets of evolutionary tracks
[b] Does not include B stars
[c] Corrected for incompleteness in the 15-30 $m_\odot$ bin.
[d] For combined cluster and field star sample; value in parentheses was derived from Vanbeveren's results without weighting
[e] From LF of GCC for $m > 25$, joined to adopted LF at smaller masses.

3. If overshoot does extend main sequence lifetimes of massive stars, as assumed here, the IMF is steepened somewhat, with $\Delta\Gamma \approx -0.1$ to -0.2 and is smaller in magnitude by a factor of 1.2 to 1.5, roughly independent of mass; a similar result is found in Vanbeveren's (1984) independent IMF comparison based on models with and without overshoot.

4. If overshoot also causes overluminosity during core hydrogen burning, the change in the mass-luminosity calibration causes a further slight steepening of the IMF by $\Delta\Gamma \approx -0.1$, and a further decrease in the amplitude at a given mass which reaches about a factor of 1.5 at the largest masses.

All the existing studies of overshoot, by Cloutman and Whitaker (1980), Cloutman (1983), Maeder (1976), Bressan *et al.* (1981), and Matraka *et al.* (1982), support the lifetime extension, and all but Bressan *et al.* support the brightening effect. In addition, the inclusion of overshoot improves the agreement between the width of the observed and theoretical main sequence band, although it does not completely account for it. If this is correct, then a reasonable "best" estimate of the high-mass IMF may be the IMF (LF) given in Table VII for $\log m \lesssim 1.08$, and an extrapolation with $\Gamma = -1.5$ to -2 to larger masses, although the above discussion shows that this estimate must be considered very crude.

It is disappointing that, after much effort, the high-mass IMF is still so uncertain. The additional uncertainty due to the possibilities that the T_{eff} scale needs modification, and that a significant fraction of massive stars are hidden within dense interstellar clouds, gives further cause for concern. There has been significant progress which at least more clearly defines the set of problems, such as sample completeness, convective overshoot and rotational mixing, T_{eff} and BC scales, which need to be examined in more detail. However, it is clear that any study of the integrated properties of stars in our own or other galaxies whose conclusions depend on the shape of the IMF at large masses must be viewed with caution. In later sections additional information from luminosity functions of star clusters and galaxies will be brought to bear on these problems.

2.6.5 *Derived quantities*

In this section we give several useful quantities which can be derived from the IMF.

The fraction by number of stars more massive than a mass m is

$$F_N(>m) = \frac{\int_m^{m_u} \xi(\log m)\, d\log m}{\int_{m_l}^{m_u} \xi(\log m)\, d\log m} \tag{2.15}$$

where $m_l = 0.087\ m_\odot$ and $m_u = 100\ m_\odot$ (the IMFs were extrapolated from 63 to 100 $m_\odot$. The quantity in the denominator is the total number of stars pc^{-2} ever formed in the disk, which is denoted N_{tot}. The present total stellar birthrate by number is

$$B_N = \frac{b(T_0)}{T_0} N_{\text{tot}} \text{ stars pc}^{-2}\,\text{yr}^{-1} \tag{2.16}$$

and the present birthrate of stars more massive than m is just $B_N F_N(>m)$.

Similarly, the fraction by mass of stars more massive than m is

$$F_M(>m) = \frac{\int_m^{m_u} m\xi(\log m)\,d\log m}{\int_{m_l}^{m_u} m\xi(\log m)\,d\log m} \tag{2.17}$$

The denominator is the total mass of stars pc^{-2} ever formed in the disk, M_{tot}, and the present total mass consumption rate due to star formation is

$$B_M = \frac{b(T_0)}{T_0} M_{\text{tot}} M_\odot \text{ pc}^{-2}\,\text{yr}^{-1}. \tag{2.18}$$

The mass consumption rate of stars more massive than m is $B_M F_M(>m)$.

The time necessary to consume the interstellar gas in the solar neighborhood, assuming no inflow or outflow, is given by

$$\tau_g = \frac{M_{\text{ISM}}}{B_M} \tag{2.19}$$

where M_{ISM} is the mass of interstellar material pc^{-2} in the solar neighborhood, taken as $8 M_\odot$ pc^{-2} (see Tinsley, 1980), with an uncertainty of perhaps 30%.

The cumulative distributions $F_N(>m)$ and $F_M(>m)$ are shown in Figure 22 for the 3 choices of $b(T_0)$ and T_0 used in Table VII. The

result of MS for $b(T_0)=1$, $T_0 = 12$ Gyr is shown as a light solid line for comparison. The three IMFs result in a range in $F_N(>m)$ and $F_M(>m)$ of a factor of 10 and 5, respectively, for all masses $> 1 M_\odot$. Considering further the estimated uncertainties in the IMF, it is clear that we cannot yet use the IMF to reliably predict these fractions, although the cases shown may provide approximate upper and lower limits.

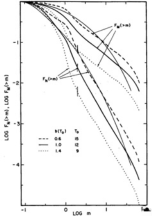

FIGURE 22 Cumulative distributions by number, $F_N(>m)$, and by mass $F_M(>m)$, for three combinations of birthrate history $b(T_0)$ and disk age T_0. The thin solid lines are the distributions corresponding to the IMF derived by Miller and Scalo (1979).

The quantities N_{tot}, M_{tot}, B_N, B_M, *and* τ_g are given for all 3 IMFs in Table IX. The number and mass are about 30–40% smaller than in MS, while the uncertainty has been reduced because of the tighter constraint on the quantity $T_0/b(T_0)$ (6–25 Gyr here, 6–50 Gyr in MS). The birthrates B_N, B_M, and the gas consumption timescales τ_g are approximately the same as found by MS, although the range is again smaller. For an effective disk radius of 15 kpc, the total galactic star formation rate can be crudely estimated as about 2–7 stars yr^{-1} or 1.5–$3M_\odot yr^{-1}$. An improved estimate could be obtained by using a galactic model for the surface density as a function of galactocentric distance. As in MS, the small values for τ_g imply that the gas must be replenished by infall or radial flows, or that our galaxy will essentially cease star formation in a few billion years. The possibility that the present birthrate is a positive fluctuation is not a likely alternate because most of the contribution to the IMF comes from stars which have fairly large mean ages and were born over a substantial fraction of the disk. An alternative interpretation, given recently by Larson (1985), involves a bimodal IMF whose higher-mass mode has decreased its amplitude with time; the resulting gas consumption timescales are significantly larger than given in Table IX. Further discussion of this idea is postponed to Section 8 below.

TABLE IX
Integrated properties of the field star IMF

$b(T_0)$	T_0(Gyr)	$N_{tot}(pc^{-2})$	$M_{tot}(m_\odot pc^{-2})$	$B_N(pc^{-2}yr^{-1})$	$B_M(m_\odot pc^{-2}yr^{-1})$	τ_g(yr)
0.6	15	79	53	3.2×10^{-9}	2.1×10^{-9}	3.8×10^{9}
1.0	12	64	33	5.3×10^{-9}	2.7×10^{-9}	2.9×10^{9}
1.4	9	58	24	9.0×10^{-9}	3.8×10^{-9}	2.1×10^{9}

2.7 Population II field star IMF

The field stars in the samples used to construct the LF and IMF above were nearly all formed in the disk of our galaxy over the past $\sim 10^{10}$yr. A distinctly different population of stars resides in the spheroidal, or halo, component of the galaxy. These "Population II" stars have large velocity dispersions and small metal abundances relative to disk srars, and were almost certainly formed during the first 10^8–10^9yr of galactic history (see the review by Mould, 1982). Although the present observable halo stars all have masses less than $1M_\odot$, information on their IMF would yield valuable clues concerning any dependence of the IMF on physical conditions, especially metal abundance. One approach to this question is the determination of LFs in globular clusters. This difficult problem is reviewed in Section 3 below. However, not all halo stars are contained in globular clusters; some are field stars whose orbits happen to take them through the solar neighborhood. The mass density contributed by these stars is probably less than a few percent of the density of disk stars, but if there was some method for identifying them and obtaining their distances, a luminosity function, and IMF, could be constructed.

There have been several attempts to obtain such information, but they all suffer from the fact that criteria for the identification of halo field stars are highly model-dependent. A kinematic criterion, such as a minimum transverse velocity or a minimum orbital eccentricity inferred from radial and transverse velocities, depends on an assumed model for the velocity distribution function and rotational velocity of the halo, as demonstrated clearly by Richstone and Graham (1981). Spectrophotometric criteria based on the different metal abundances in disk and halo stars are less fundamental both because metal abundances are difficult to estimate and because they must be based on a model for the poorly-understood chemical evolution of the galaxy, as emphasized by Mould (1982).

Schmidt (1975) used a sample of 121 stars with measured trigonometric parallaxes and proper motions which satisfied the criteria $m_{pg} < 16$, $\mu \geq 1.3''yr^{-1}$, and $\delta \geq 0°$. The halo stars were identified by a kinematic criterion which assumed that, like the metal-poor RR Lyrae stars, half of the halo stars would have transverse velocities $v_T > 250$ km s^{-1}. Schmidt attempted to construct a LF for the halo stars using the V_{max}^{-1} method described briefly in Section 2.2.1 and in more detail in Schmidt's paper. Unfortunately the adopted kinematic criterion left only 18 halo stars, enough to estimate their total mass density, which is of importance for understanding the dynamics of the halo population and its possible stabilization of the disk, but too few to derive a reliable luminosity or mass function.

Chiu (1980) determined luminosity functions for both disk and halo stars in three selected areas, using a modified version of the V_{max}^{-1} method. In Chiu's approach each star is assigned a probability for membership in the disk and halo populations, and the results depend on the assumed density distribution of the halo. It is difficult, however, to assess the reliability of the population assignments, a point stressed by Bahcall, Schmidt, and Soneira (1983).

The most recent study of the problem has been presented by Eggen (1983), who used a complete sample of stars with $\mu \geq 0.''7\ \mathrm{yr}^{-1}$, $m_v \leq 15$, and $\delta < +30°$. For the stars with measured parallaxes, halo stars were identified by comparing their position in the $(M_v, R-I)$ plane with a previously established subdwarf sequence in this plane. For the stars without measured parallaxes, luminosities were derived from intermediate-band photometric criteria. Besides using the subdwarf sequence, halo stars were also identified by requiring that the iron-to-hydrogen abundance ratio, as derived from another calibration of intermediate-band photometry, be at least four times smaller than the solar ratio, or that the star's orbital eccentricity as inferred from its radial and transverse velocities be greater than 0.42. This procedure results in a sample of 215 halo stars (excluding a white dwarf), and Eggen used Schmidt's V_{max}^{-1} method to determine the LF. The price paid for the enlarged sample size is again the increased uncertainty in halo population assignment, which in this case involves photometric, kinematic, and abundance criteria. However, the median transverse velocity of the resulting halo sample was large (290 km s^{-1} for $5 < M_v < 12$,375 km s^{-1} for $7 < M_v < 10$), suggesting that, if the photometric distances are trustworthy, most of these stars are indeed halo stars.

Mould (1982) has given a useful graphical comparison of the LFs of Schmidt, Chiu, and Eggen, as well as the abundance-based halo sample of Fenkart (1977), and Mould's graph is reproduced in Figure 23. (A similar comparison has been given by Reid 1984.) The local field star LF of disk stars adopted earlier is shown (dashed line, arbitrary normalization) for comparison. (Because of the slightly different mass-luminosity relation for population II stars, shown in Figure 8, a proper comparison of IMFs should have the disk LF shifted to brighter M_v by $\lesssim 1$mag, but this would not affect our conclusions.) It is seen that the halo LF of Eggen agrees surprisingly well with the disk star LF over most of the range, especially considering the large

statistical uncertainties for the faintest two points in Eggen's LF. Unless Eggen's halo sample actually is contaminated by a substantial fraction of disk stars, the results seem consistent with the hypothesis that the halo and disk IMFs are the same for $m < 1$.

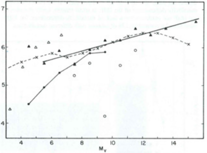

FIGURE 23 Various determinations of the luminosity function of halo field stars, from Mould (1982). For sources of data, see text. The crosses connected by dashed lines is the disk luminosity function adopted in the present work.

In order to better illustrate this point, Figure 24 compares the IMF derived from Eggen's halo LF, using a Pop. II $m(M_v)$ relation from Gunn and Griffin (1974), with the disk field star IMF adopted in the present work. It might appear that the halo IMF is marginally steeper than the disk IMF, as suggested by Reid (1984) based on a similar comparison. However, Eggen's method for obtaining the halo LF is quite different from the methods used for the adopted *disk* LF. The IMF derived from Eggen's disk LF, which was estimated by the same method as he used for the halo stars, is also shown in Figure 24. The agreement is very good, especially considering that the faintest two points in Eggen's halo LF contain only one or two stars with correspondingly low weight. This comparison is consistent with the hypothesis that the disk and halo field star IMFs are the same in shape between 0.3 and $0.8M_{\odot}$. The halo sample covers a large range of (uncertain) metallicities, but most of the stars probably have metal abundances by mass $Z \sim 10^{-3}$ to 10^{-4}. Thus there is no indication of a metallicity-dependence of the IMF at small masses. Later (Section 4) we shall see evidence for a lack of metallicity-dependence for high-mass stars by comparing LFs of galaxies with different metallicities.

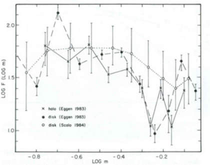

FIGURE 24 IMF of halo and disk field stars derived by Eggen (1983); disk IMF found in the present work is also shown.

2.8 Concluding Remarks

The field star IMF has the major advantage of covering the entire range of stellar masses with a single method. Its disadvantage is the dependence on and sensitivity to so many inadequately-known observational and theoretical quantities. In addition, the derived result is only meaningful if the ensemble average IMF is a universal function, independent of space and time. I believe that the importance of the lengthy derivation given above lies not only in the final result, which may be short-lived, but in the enumeration of the steps and assumptions involved and especially the very real uncertainties which arise at every step along the way. While the relative errors between values of the IMF at neighboring mass points are probably much smaller than the uncertainty attached to the individual values, the magnitude of the estimated uncertainties in localized mass ranges must be considered seriously in any application. For example, the actual mean index Γ of the IMF between 2 and $20M_{\odot}$, which is about -1.9 for the data shown, could easily be in the range -1.5 to -2.3. As another example, one can imagine one or more bends, bumps, or dips anywhere above $1M_{\odot}$ which may have been disguised by the smoothing and interpolation which was necessarily performed in estimating the luminosity function. The existence of such dips has been suggested by Piskunov and Vereshchagin (1985). There is room for improvements, but these must probably await the operation of the Space Telescope, the European astrometric satellite HIPPARCOS (see Crézé, 1983; Upgren, 1983b), improvements in the scales of effective temperatures and bolometric corrections for massive stars, and advances in the theory of stellar evolution, particularly in the areas of convection and rotation. Nevertheless, the three choices of IMFs given above probably span a range which includes the true ensemble IMF, although the slopes in given mass ranges may be in error.

In addition, there are several potentially significant effects which we have not considered. One is the effect of unresolved binaries. If the angular separion of a binary is less than some limit which depends on magnitude difference, telescope, seeing conditions, etc., the binary will be identified as a single star. This has the effect of placing one object in the apparent luminosity function at the combined luminosity of the pair instead of two objects at fainter luminosities. The net effect of this erroneous redistribution of luminosity will be to give an IMF which is weighted too heavily toward massive stars; i.e. the effective index Γ will be too large. Hartmann (1970) attempted to estimate the size of this effect by comparing the LFs of samples with different limiting distances, and found no significant effect; however, the LFs themselves were very uncertain. Armandroff

(1981) compared the LF of Weilen's catalogue of nearby stars constructed by combining luminosities of pairs with the LF in the case where each star is included individually. The differences were small but statistically significant. This question has also been briefly discussed by Reid (1982), Mezzetti *et al.* (1983), and Zinnecker (1984), but no detailed analysis has been carried out to assess the effect on the full luminosity function. That the duplicity effect might be significant can be seen by noting that more than 50% of stars may be binaries and, of these, a large fraction may be unresolved; a rough estimate by Mezzetti *et al.* (1983) suggests ~40% for this fraction. One expects the unresolved fraction to increase with luminosity, since the average distance of luminous stars is large because of their small space densities. A proper investigation of the duplicity correction will also require careful consideration of selection effects.

An interesting effect also related to stellar duplicity has been discussed by Vanbeveren (1982). If protostellar fragments have a given mass function, but only some fraction of them form stars without fissioning into a binary system, then, if the probability of fission depends on the original fragment mass, the IMF of the single stars will differ from that of the primaries or secondaries of the binary stars, and neither will be identical to the mass function of the fragments. The magnitude of the effect depends on a number of uncertain parameters, and Vanbeveren has given some examples relevant to massive stars. The difficulty which this result presents for interpretation of the field star IMF is that the observed function combines single stars and binaries into one sample, and so this IMF includes the effects of any fission process on the IMF as well as the physical effects which determined the original protostellar fragment mass function. To recover the "true" mass function in this model, we would have to include the close binaries in the mass function using the combined mass of each pair.

Another potentially important effect concerns the fact that stars may not be visible during a significant portion of their lifetimes. It is well known that stars are formed within dense interstellar clouds which are visually opaque, often presenting more than 5–10 magnitudes of extinction. Very young stars in such clouds can only be detected by the infrared radiation of the surrounding dust which they heat, or by radio emission from their HII regions for massive stars. The lifetimes of large cloud complexes are estimated from indirect

arguments to be as large as 10^7–10^8yr (for a summary of the evidence, see Scalo, 1985), which suggests that obscuration may greatly reduce the number of high-mass stars which can be detected. The true IMF at large masses would in this case be significantly flatter than the function derived from visual star counts. GCC have shown that the hypothesis that stars remain obscured for even a few million years can produce large changes in the slope of the upper IMF. A theoretical investigation of this question is not currently possible because of lack of knowledge concerning cloud lifetimes and structure. An empirical constraint is possible due to the fact that visually-obscured O stars should still be detectable over much of their lifetime by the radio emission from the HII regions which they ionize. Mezger and Smith (1976) used the observed numbers and other properties of radio HII regions, to estimate that the fraction of O and early B stars which are unobserved is only about 30%, but the uncertainty in this estimate is large. On the other hand, Vanbeveren (1985) has pointed out that when the positions of bright stars in the *H–R* diagram are compared with theoretical isochrones, no stars are found with ages less than about 2×10^6yr. Although this discrepancy *could* be due to errors in effective temperature scales, evolutionary tracks, etc., it still strongly suggests that the "hidden star" problem may be quite serious.

Finally, we must remember that the IMF has been derived by assuming that its form is independent of time and position in the galaxy. The field star sample contains stars with a wide variety of ages and places of birth, and so significant temporal or spatial variations in the IMF would obscure the meaning of the function derived here. For example, if the true IMF is stochastic in space and time, the derived IMF will only be meaningful if the range in ages and birth locations of the stellar sample is large enough that the sample can be considered representative of the average IMF. More likely is the possibility that IMF variations do not represent a stochastic process which is stationary in time and homogeneous in space, in which case the derived IMF is ill-defined. The important subject of IMF variations will become a continuing theme in the remaining sections of this review.

Studies of luminosity functions and mass functions in star clusters avoid many of the sources of error involved in the field star IMF, but contain quite different uncertainties which are just as severe. We next examine the cluster IMFs in detail and compare them with the field star IMF.

3. STAR CLUSTERS

3.1 Basic considerations

The function we are trying to determine is usually thought of as the probability of occurrence of stars in a given mass interval among a group of stars all formed at the same time. This idealization is most closely realized in the numerous star clusters of our galaxy, each of which offers us a single realization of the ensemble average IMF.

For stars in the galactic disk population there are two major types of groupings: Open clusters, which usually contain about 100 to 1000 observable stars and cover a wide range of ages, from $\sim 10^6$yr to $\sim 10^{10}$yr (see Mermilliod, 1981; Lynga, 1982; Janes and Demarque, 1983 for detailed discussions of their properties); and OB associations, which are very loose clusters containing young, massive stars (Blaauw, 1964). The number of stars in associations is unknown because the low star density makes it difficult to assign membership to any but the O and B stars; typically 10–100 OB stars are seen. The OB associations exhibit the interesting property of subgroupings into a few regions of different ages. Many very young open clusters form a part of an association. Additional classes of young stellar groups are clusterings of T Tauri and related stars, objects which are so young that they have not yet reached the hydrogen-burning main sequence (see Strom, Strom, and Grasdalen, 1975) and R associations, which are sparse groups of young stars recognized by their association with reflection nebulosity (see Herbst, 1975). Because of their susceptibility to destruction, only a small fraction of the stars in the disk are found in these groups, but the fraction increases with increasing stellar mass (decreasing age), and it is well established that most, if not all, stars form in such groups (Roberts, 1957; Ebert *et al.*, 1960; Miller and Scalo, 1978).

Populating the halo of our galaxy are the globular clusters, characterized by large mass ($\sim 10^5 M_\odot$), extreme central condensation, metal abundances significantly smaller than that in the galactic disk in most cases, and ages around 10^{10}yr (see Harris and Racine, 1979). Globular clusters are most interesting for studies of the IMF because they were formed during a short time interval (probably $\lesssim 10^9$yr) during the early evolution of the galaxy, when physical conditions and star formation processes may have been much different than in the galactic disk. They also might reveal a dependence of the IMF on metal abundance.

Star clusters present an excellent opportunity to study the IMF, its possible variations on small spatial scales and with time, and possible differences between different types of clusters and between clusters and the field star IMF. The usefulness of clusters arises primarily because all stars in a given cluster have approximately the same distance and age. If the range of formation times of the cluster members is much less than the cluster age, then their observed LFs directly reflect their IMF below the main sequence turnoff, without the necessity for birthrate history corrections or stellar lifetimes. In principle, there is no need to assume a time-independent IMF, as is necessary in deriving the field star IMF; indeed, comparisons of the IMFs of clusters of different ages provide the only direct tool for uncovering such a time-dependence. Finally, the stars in a cluster were all born in the same small region of space, unlike most of the field stars, whose birthsites may have spanned much of the galaxy. For these reasons, most of the numerous problems associated with the field star IMF can be avoided for clusters; we need only convert a luminosity function into a mass function.

Unfortunately, these advantages are offset by a number of severe difficulties. Open clusters and associations usually contain only a small number (~ 100–1000) of observable stars, so statistical uncertainties are large. Since most open clusters and associations are situated in the galactic plane, contamination by foreground and background field stars is serious and membership is difficult to establish without proper motion studies and faint star photometry. Another problem arises because of the likely existence of stellar mass segregation. As discussed in more detail below, it is known that in open clusters there is a tendency for stars of lower mass to reside in the outer parts of clusters and the more massive stars to favor the central regions. Therefore, in order to observationally determine a cluster mass function, the outer parts, where it is most difficult to establish membership, must be included. Dynamical modeling of mass segregation in clusters with ~ 100 members is difficult because the crossing (orbital) time scale is comparable to the relaxation time, close encounters are as important as distant cumulative encounters, and because a number of physical processes, such as 2-body relaxation, galactic tidal forces, tidal shocks by interstellar clouds, stellar mass loss, and binary formation may be important in causing radial variations in the cluster LF.

An additional problem which arises for moderately young open clusters and for OB associations involves evidence that the spread in formation times of stars in some clusters is very large, so that evolutionary corrections to the cluster LF, similar to those applied to the field star PDMF, may be important. The evidence for non-coeval star formation in clusters is based on the result that the cluster age estimated from stars near the turnoff mass of the upper main sequence (the "nuclear age", τ_N) often comes out significantly smaller than the gravitational contraction times of lower-mass stars which have not yet reached the lower main sequence (the "contraction age", τ_C). This means that star formation has been occurring over an interval greater than $\Delta\tau = \tau_C - \tau_N$, if our understanding of pre-main-sequence evolution is correct. For several young clusters with nuclear ages ~ 5–20×10^6 yr, the inferred age spread is $\Delta\tau \approx 10$–20×10^6 yr (e.g. Iben and Talbot, 1966; Vogt, 1971; Warner, Strom, and Strom, 1977; Herbst and Miller, 1983). For the Pleiades cluster, with $\tau_N \sim 5$–10×10^7 yr, the suggested value of $\Delta\tau$ inferred from a number of arguments may be as large as 0.5–5×10^8 yr (see Landolt, 1979; Stauffer, 1980, 1982, 1984; Stauffer *et al.*, 1984). If the condition $\Delta\tau \gtrsim \tau_N$ applies to most young clusters, then the apparent IMF derived from the LF could be a significant distortion of the true IMF, which could not be estimated without knowledge of the birthrate history in each cluster. To make matters worse, it is strongly suspected that the average stellar mass increases during the formation interval $\Delta\tau$ (e.g., Iben and Talbot, 1966; Cohen and Kuhi, 1979; Doom, *et al.*, 1985; see Stahler, 1985 for an argument against this interpretation), so the IMF may be time-dependent within individual clusters. In these cases most of the advantages of cluster IMF determinations over the field star IMF are lost, and in fact we have no method for uncovering the "true" IMF. Although these effects will be neglected in the following presentation of cluster IMFs, they should be kept in mind for the younger open clusters and for OB associations, and deserve a careful study.

Despite all these problems, some progress has been made in uncovering the basic features of cluster IMFs, which will be summarized in this section, updating an earlier brief summary on open clusters by Scalo (1978). We discuss the available information on the IMF

of open clusters, OB associations, pre-main sequence stars, and globular clusters. Most of this material has not been previously reviewed. In most cases the original published star counts have been converted to mass functions using the mass-luminosity relation adopted in the previous section, and, when possible, an attempt has been made to exclude evolved stars on the basis of the color-magnitude diagram. In some cases, the data had to be measured from the published graphical luminosity functions, but the measurements errors are negligible.

The major questions of interest are: 1. Does the average cluster IMF differ fom the field star IMF? 2. Are there significant cluster-to-cluster IMF variations, and, if so, can these be related systematically to cluster properties such as age, star density, or metal abundance, or are they stochastic in nature? 3. Are the apparent "turnovers" which are seen in many open cluster luminosity functions actually related to the physical processes related to the IMF, or are they a result of incompleteness at faint magnitudes, cluster dynamical evolution, and/or incomplete sampling of the outer regions of the cluster?

An important and influential study of some of these questions was given by Van den Bergh and Sher (1960), who estimated the LFs of 20 open clusters using star counts down to $m_{pg} \approx 20$. The data reached $M_{pg} \approx 10$ in NGC 188, $M_{pg} \approx 11$ in M67, and $5 < M_{pg} < 8$ in the remaining clusters. The main importance of this work was that it demonstrated apparent differences in LFs among clusters and the possible existence of turnovers at faint magnitudes. Similar effects had been found earlier in 8 clusters by Roberts (1958). Additional important early papers on open clusters are Sandage (1957), Jaschek and Jaschek (1957), and Walker (1957). A figure illustrating the IMFs for five of the Van den Bergh and Sher clusters can be found in Scalo (1978). Van den Bergh (1961) interpreted these results as showing that the LF of field stars is much different than that of open clusters. McCuskey's (1966) review also contains a discussion of open cluster LFs which is based on the gradient of the cumulative LF instead of the LF itself. De Vaucouleurs (1956) had suggested that this gradient function better avoids statistical effects and differences between volume elements, magnitude scales, etc., among various determinations. McCuskey concluded that younger clusters (e.g. *h* Persei, Pleiades) may conform to the field star LF, but the older clusters differ. Because of the importance of these questions, the accumulation of new data since that time, and the increasing evidence for radial mass segregation, we give a fairly detailed reexamination of these questions here. The reader should be forewarned that in most cases no clear answers will emerge from the following discussion, which serves primarily to underscore the severe uncertainties involved. Nevertheless, it is my opinion that these uncertainties are no more severe than those entering the determination of the field star IMF, and so the cluster results should be considered complementary rather than secondary.

Before proceeding to examine the cluster data, it will be useful to review the observational evidence for mass segregation and the implications of theoretical studies of dynamical cluster evolution, since these topics bear directly on all studies of cluster mass functions.

3.2 Mass segregation in open clusters

Whatever the cause, there is clear evidence that the mean stellar mass is a decreasing function of radial distance in many open clusters. This effect has long been emphasized by the Russian workers (see, for example, Kholopov, 1969). Figure 25 shows mass functions derived from the data of Kholopov and Artyukhina (1972) for the Pleiades, Artyukhina (1972) for the α Per cluster, and Archemashoili (1976) for M37. The core and halo regions are shown separately for each cluster and the number of stars used for each region is indicated. Assuming that errors in corrections for non-members are not serious, all three clusters show evidence for differing IMFs between the core and halo with a greater proportion of low-mass stars in the outer halo regions.

Evidence for radial mass segregation has also been presented by van Leeuwen (1980) for the Pleiades, Vogt (1971) for h and χ Persei, Solomon and McNamara (1980) and Mathieu (1983) for M11 and M35, Stone (1980) for NGC 654, and Herbst and Miller (1983) for NGC 3293. A statistical comparison of 13 cluster LFs, most from Van den Bergh and Sher (1960), by Starikova (1963) also gave evidence for radial mass segregation. See also King and Tinsley (1976) for indirect evidence based on dynamical considerations related to the distribution of red giants in clusters. On the other hand, Burki (1978) has found the opposite effect in six very young clusters: the

fraction of stars with $m > 20$, relative to the fraction with $m > 4$, is over twice as large in the outer cluster regions compared to the central regions. These results all suggest that one should view individual cluster IMFs with some caution unless a relatively large area is surveyed, irregardless of cluster age.

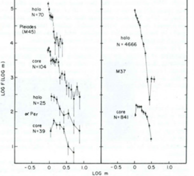

FIGURE 25 IMFs for several clusters derived from luminosity functions presented in Kholopov and Artyukhina (1972), Artyukhina (1972), and Archemashoili (1976), illustrating the existence of mass segregation.

For the study of cluster IMFs, it is obviously important to decide whether mass segregation is due to dynamical evolution or is an imprint of the star formation process itself. In the former case, we would have to contend with the possibility that the observed mass functions of individual clusters are a function of their age, and we would need quite detailed models for cluster evolution in order to correct for this effect in estimating the true IMF. Although no completely satisfactory answers have yet emerged (see King, 1980, and Wielen, 1975 for good reviews), some tentative conclusions can be drawn.

The age distribution of open clusters (Wielen, 1971; Van den bergh, 1983) demonstrates that they must dissolve quite efficiently. Only about 50% survive to an age of $\sim 10^8$ yr, while less than 5% live as long as 10^9 yr. The most important destruction processes are stellar gravitational encounters within clusters, galactic tidal forces, tidal shocks by interstellar cloud complexes, tidal shocks as clusters pass through the galactic disk, and mass loss from evolving stars.

The most obvious potential culprit for mass segregation is the relaxation of a cluster through cumulative long-range gravitational scattering. Because this relaxation leads to equipartition of kinetic energy, low-mass stars will come to possess the largest random velocities, and will tend to occupy a larger volume than the high-mass stars. We can write the relaxation time roughly as

$$\tau_{rel} \approx 2 \times 10^5 N^{1/2} r_c^{3/2} / m^{1/2} \text{yr}$$

where N is the number of cluster stars, r_c the cluster radius in parsecs, and m the stellar mass. As an example, if $N = 500$, $R_c = 2$ pc, and $m = 1$, then $\tau_{rel} \approx 2 \times 10^7$ yr. For a multiple mass system, the relaxation time may be up to an order of magnitude smaller. The cluster lifetime will be of order $40\tau_{rel}$. Thus mass segregation due to gravitational scattering may be an important process even in relatively young clusters.

For massive clusters like M67, in which close encounters can be neglected, Prata's (1971a) calculations, which include tidal effects and mass loss as well as 2-body relaxation, show that the stellar escape rate is not as large as would be inferred from a single-mass model. The relative number of low mass stars can be decreased significantly over $3\text{–}5 \times 10^9$ yr, but Prata concludes that the effect is not large enough to have converted the M67 mass function from a "normal" monotonic form to a "turnover" form in the required time. Typically, only 1% or so of solar mass stars escape during a relaxation time scale.

These results must be regarded with caution, however, since they are based on solutions of approximate rate equations for the response of stars of different masses to the changing gravitational field. N-body calculations give somewhat different results for smaller clusters because they are able to treat close gravitational encounters (which are more important than long-range gravitational relaxation for $N \lesssim 100$) and binary formation. Evolution is more rapid than τ_{rel} would indicate, and the presence of a mass spectrum further accelerates the relaxation and dissolution. The effects of the galactic tidal field and tidal shocks which occur as clusters pass through the disk dominate the disruption process for larger clusters, and it now appears that the age distribution of clusters can be satisfactorily accounted for by a combination of these processes (see Figures 3 and 4 of Wielen 1975). Although the relative stellar escape rate in these N-body calculations is found not to depend significantly on stellar mass for masses smaller than the average mass, it must be borne in mind that these external forces act primarily on the halo, which, after a relaxation time, will contain mostly low-mass stars (Mathieu, 1984, private communication).

One must conclude that our present understanding does not allow a clear decision as to whether mass segregation is due to dynamical processes or the physics of star formation in clusters, or both. In either case, estimates of cluster IMFs must establish cluster membership in as large a volume as possible; otherwise the prevalence of mass segregation may lead to spurious "turnovers" in the derived IMFs.

3.3 Composite cluster mass functions

Because of the small number of stars in an individual open cluster, it is natural to seek a decrease in the statistical uncertainty of the open cluster IMF by combining the star counts for a fairly large number of clusters to obtain an average, or "composite", cluster IMF. The construction of a meaningful composite mass function from the data is not at all straightforward, even though each individual cluster may give a true IMF between certain mass limits. The problem occurs because the clusters do not form a complete volume-limited sample of stars, and the clusters differ in age, number of stars, upper and lower mass limits to which the individual IMFs can be estimated, and possibly the IMFs themselves. Since the age distribution of open clusters is heavily weighted toward young clusters compared to a uniform age distribution, a simple average of all the individual IMFs would not give the field star IMF, even if all the individual IMFs were identical and if all field stars formed in open clusters. Even if the age distribution was uniform, the result would be affected by stellar evolution (variation in the individual upper mass limits) and incompleteness (variations in the individual lower mass limits set by the limiting magnitude of the photographic plates). These problems are illustrated in Figure 26. If, in addition, the IMFs differ among clusters, the problems become more severe.

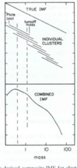

FIGURE 26 Distortions in derived composite IMF for clusters due to variations in limiting absolute magnitude (plate limit) and turnoff mass.

Vanbeveren (1982) has pointed out another effect by which composite cluster or association IMFs will differ from the individual IMFs

even when all the individual IMFs are the same. The effect, discussed earlier by Reddish (1978), occurs if the upper stellar mass limit in a cluster is limited by the available mass in the cluster. If the stellar mass spectrum varies as $f(m) \propto m^{\gamma}$, then for $\gamma < -1$, the maximum stellar mass is related to the available mass m_{cl} of the cluster by $m_{max} \propto m_{cl}^{-(1/\gamma+1)}$. If the masses of the clusters or associations, m_{cl}, are distributed as $f_{cl}(m) \propto m_{cl}^{\gamma_1}$, then the apparent mass spectrum of all these stars will be proportional to $m^{-\gamma_1(1+\gamma)-1}$. The true index γ is then related to the apparent index γ by $\gamma = -(1+\gamma+\gamma_1)/\gamma_1$. For example, if the *apparent* mass spectrum has index $\gamma = -2$ and the spectrum of cluster masses has the same slope, then the true mass spectrum could have an index $\gamma = -1.5$. For reasonable parameters, a cluster mass spectrum which decreases with increasing mass always gives an apparent stellar mass spectrum which is too steep, because the cluster mass spectrum gives smaller probability for obtaining more massive stars.

Finally, composite cluster IMFs are usually based on heterogeneous photographic data which may cover arbitrary survey areas, and employ different ZAMS calibrations, main sequence fitting techniques, and reddening corrections, as pointed out by an anonymous referee.

It should be clear that the estimate of a composite cluster IMF is a complex problem. The only attempt to account for some of these effects is due to Taff (1974; the statistical effect due to a cluster mass distribution is not accounted for, however). Because these problems are largely unappreciated, Taff's iterative method is outlined here. It must be emphasized, however, that the method rests on the assumption that all clusters were formed with *identical* IMFs. I know of no method for the more general case.

For each cluster, c, the number of stars $N_c(m)$ in each mass interval Δm can be obtained from the cluster luminosity function. The upper mass limit for the counts is the turnoff mass m_{to}^{c} and the lower mass limit is m_l^c, determined by the plate limit and the cluster distance. We can write

$$N(m) = I_c(m) N_c(m) \tag{3.2}$$

where

$$I_c(m) = H(m_{to}^c - m) H(m - m_l^c) \tag{3.3}$$

and $H(x)$ is the Heaviside function $[H(x)=1$ if $x>0$, $H(x)=0$ if $x<0]$. This just says that the contribution to $N(m)$ is zero if m is outside the range m_l^c to m_{to}^c. In order to correct for evolution and incompleteness, we must estimate the total number of stars *originally* in the cluster, denoted n_c. This requires that the cluster IMF for *all* masses be known. Define $f(m)$ as the true differential mass spectrum, normalized to unity so that $f(m)\Delta m$ is the fraction of stars of all masses in the mass interval $(m, m+\Delta m)$, and assume that $f(m)$ is the same for all clusters when they formed. Let $f_0(m)$ be an initial estimate of the true mass spectrum. The corresponding estimate for the fraction of the original number of stars presently observed is $\sum I_c(m)\, f_0(m)\, \Delta m$, so if the number of observed stars is N_c, an estimate for the initial number of stars is

$$n_{c,0} = N_c / \sum I_c(m) f(m) \Delta m. \tag{3.4}$$

An improved estimate for $f(m)$ at mass m is then

$$f_1(m) = \frac{\sum_c I_c(m) N_c(m)}{\sum_c I_c(m) n_{c,0}} \tag{3.5}$$

which is the ratio of the number of stars of mass m around Δm on the main sequence in all clusters for which $m_l < m < m_{to}$ to the total *original* number of stars in the same clusters. This new $f_1(m)$ can then be used to calculate an improved $n_{c,1}$, the iteration proceeding until some desired measure of convergence is achieved. If the process converges, clusters which do not satisfy the universality assumption on $f(m)$ can be rejected using the χ^2 test described by Taff.

This method yields a composite mass function which is free of evolutionary and limiting magnitude effects, and is independent of the sample cluster age distribution, but depends on the assumption of a universal IMF among clusters.

Taff (1974) applied this method to a sample of 62 clusters to obtain a composite IMF. Many more clusters were rejected on the basis of small membership ($\lesssim 50$), cluster age (to insure against cluster disruption effects), large differential reddening, and other factors; more than half of the 62 clusters contained over a hundred

stars. Details concerning selection criteria can be found in Taff's paper. The result (using the mass-luminosity relation of Section 2.4 above) is shown in Figure 27 as the crosses connected by a solid line. The LF for $M_v < -6$ was omitted because of the small number of stars. A rough power law fit to the data between $m=1$ and 10 gives a slope of $\Gamma = -1.8$. The field star IMF is shown as the plus signs; results for three combinations of $b(T_0)$ and T_0 of (0.6, 15 Gyr), (1.0, 12 Gyr), and (1.4, 9 Gyr) are shown. (The two extreme cases are

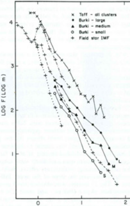

FIGURE 27 Estimates of composite open cluster IMFs by Taff (1974) and Burki (1978); the adopted field star IMF is also shown. Normalization is arbitrary.

terminated at log $m=0.7$; all three are parallel for larger masses.) Taff's cluster IMF fits the field star IMF extremely well between about $m=1$ and 10, but the cluster mass function shows an apparent excess at larger masses, with a flatter slope for $m \gtrsim 10$. However, remembering the large uncertainties in both the field star and cluster IMFs, the overall agreement is remarkably good. Note that the marginal flattening which occurs around $m \sim 0.7$ in Taff's IMF might be consistent with the "dip" in the field star IMF for $b(T_0)=1$ or 1.4 which occurs at the same mass, although it is more likely due to incompleteness at faint magnitudes or the tendency of observational studies to exclude the outer regions of clusters, i.e. the effect of mass segregation. Taff finds no correlation of IMF with richness or concentration class for $m \gtrsim 1$ and no statistical evidence against the hypothesis of universality, i.e. that all clusters have the same IMF. Taff's IMF does not show any peak at $1.2M_\odot$, as occurs in the field star IMF for decreasing birthrate.

Piskunov (1976, in Russian) also constructed a composite cluster IMF, using 7000 members of 61 clusters to derive a mean IMF slope of $\Gamma=-1.3 \pm 0.14$ for $1<m<25$, with no evidence for large cluster-to-cluster differences. The slope would be altered if the present mass-luminosity relation were used. However, it does not appear that Piskunov corrected in any way for the effects described above, but simply constructed a weighted mean.

Burki (1977) has presented composite luminosity and mass functions for a sample of 27 young open clusters with ages $\leq 15 \times 10^6$ yr. (Only 9 of these clusters are in common with Taff's study.) The luminosity functions were averaged without explicitly correcting for evolution and incompleteness (plate limit) effects, but the problems may not be serious because Burki was careful to combine only the clusters which had the same estimated limiting M_v at the faint end of the LF, and because the clusters span a relatively small range in ages, minimizing (but not eliminating) evolutionary effects. Burki found an interesting correlation between the slope of the upper IMF and the cluster diameter D. The 27 clusters were divided into 3 groups: large ($D>8$ pc), intermediate (4 pc $>D \leq 8$ pc), and small ($D \leq 4$ pc), and their composite LFs were compared in the range corresponding to $5 \leq m \leq 50$. Each group contained around 300 stars. Burki found that the ratio of the number of stars with masses greater than $12M_\odot$ to the number with masses above $5M_\odot$ increases with increasing cluster

diameter, and showed by means of Monte-Carlo simulations that this result is probably not a statistical effect due to the small number of stars in the small clusters. Also, since there is no correlation between diameter and age, the result cannot be due to evolution of the more massive stars in small clusters.

Figure 27 shows the mass functions for the 3 groups. Burki's luminosity functions for $M_v<1$ ($m \gtrsim 2.5$) were measured from his Figure 1c and then converted to mass functions using the M_v-mass relation given earlier. The mean slopes of the mass functions between $m \approx 2.5$ and $m \approx 25$ (small clusters) to 50 (large clusters) are found to be $\Gamma=-1.7$ (small), -1.5 (medium), and -1.2 (large). The slopes must be affected somewhat by evolutionary effects, since the sample clusters differed in turnoff mass, but the magnitude of the effect cannot be estimated from the available data. It may be noteworthy that the composite mass spectrum of the large and intermediate-size clusters (flatter) agrees best with Taff's (1974) composite cluster IMF in this mass range, while that of the small clusters (steeper) agrees better with the field star IMF.

Since mean cluster size increases significantly with galactocentric distance (Burki and Maeder, 1976), Burki interprets the dependence on cluster size as indicating that the upper part of the IMF becomes flatter in the outer parts of the galaxy. It is unfortunate that Burki did not combine the clusters into groups with differing galactocentric distance to directly test this interpretation. No such effect is found for the young clusters studied by Tarrab (1982), as demonstrated in Section 7 below. Garmany *et al.* (1982) reached just the opposite conclusion for the OB star mass function using a catalogue which included both cluster members and field stars. This discrepancy emphasizes the uncertainty in both conclusions. Recall that Taff's statistical method supported a universal IMF, although the method may not be sensitive enough to detect the rather small differences found by Burki, and Taff did not explicitly consider dependences on cluster diameter or galactocentric distance. We shall return to the subject of spatial variations of the IMF in Section 7. For now, it is encouraging that the shape of the IMF determined for field stars and for composite cluster members agrees so well, at least for masses in the range 1–$10M_\odot$. A clearer visual comparison of these IMFs is shown in Figure 28 (arbitrary normalization at $\sim 3.5M_\odot$). In the next sections we shall see that a detailed examination of individual clusters gives evidence for cluster-to-cluster fluctuations in the IMF, which are to be expected if the IMF represents a stochastic process.

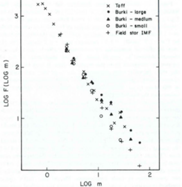

FIGURE 28 Same as Figure 27, but normalized so that agreement occurs at $\sim 3.5 M_{\odot}$.

3.4 *Young clusters and associations*

A comparison of the IMFs for several young clusters and associations is shown in Figure 29. The nuclear ages of all these regions are less than about 3×10^7 yr. The composite cluster IMF of Taff (1974, dark solid line) and the field star IMF (dot-dashed line) are shown for

comparison. Since the data and methods employed differed somewhat among the determinations, we comment upon them each briefly.

The determination of mass distributions for OB associations is particularly difficult because of the small star density, large angular size, and small proper motions, all of which make membership problematical, especially for the lower-mass stars. The only published study of the IMF in associations is due to Claudius and Grosbol (1980) who compared M_v's and spectral types obtained from uvbyβ photometry with theoretical isochrones in order to count the number of stars in each mass interval for 8 OB associations or subregions or associations. This is the same method used by Lequeux (1979), Garmany *et al.* (1982), and others in studies of the field star IMF. The scale of bolometric corrections, effective temperatures, and the evolutionary tracks are major sources of uncertainty, as in all IMF estimates for high-mass stars using this method. Because the number of stars in each region was so small (20–64), I have combined the regions in order to reduce the statistical fluctuations. This procedure seemed suitable, especially for the Orion subgroups, because the stars span about the same mass range ($0.4 \leq \log m \leq 1.0$) in each subgroup. For each region, LFs or mass functions were measured from the published graphs, with an estimated accuracy much better than the observational uncertainties. Combining the Ori a, Ori c, Ori b, and Ori b2 regions yielded 209 stars, whose mass function is shown in Figure 29 as filled circles. The flattening at $m \lesssim 3$ is probably due to incompleteness. For comparison, the IMF of the Ori OB1 association determined by MS directly from the LF of 389 stars in the catalogue of Warren and Hesser (1978) is also shown (crosses). Again, the turnover at $m \lesssim 3$ is due to incompleteness. The two IMFs agree fairly well within the errors, although the Claudius and Grosbol result is marginally steeper for $m \gtrsim 6$. Notice the good agreement with both the Taff composite IMF and the field star IMF in the range 3–$10 M_{\odot}$, where the data should be complete.

The Claudius and Gorsbol (1980) data for the α Per, NGC 2264, Centaurus, and Scorpius regions were also combined and treated in the same manner as above, giving a sample of 117 stars. The resulting IMF is shown as the open circles in Figure 29. The agreement with the Orion regions is very good for $5 \leq m \leq 10$, but there is a deficiency of lower-mass stars, the IMF being essentially flat between 2.5 and $5 M_{\odot}$. It is impossible to say with any certainty whether or not this is an incompleteness effect, but the deficiency does appear for each individual region. However, the study of NGC 2264 by Adams *et al.* (1984), to be discussed shortly, indicates that the IMF continues to rise down to small masses, indicating incompleteness in the Claudius and Grosbol data.

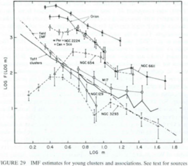

FIGURE 29 IMF estimates for young clusters and associations. See text for sources of data.

Most other studies of very young open cluster LFs sample fewer stars but extend to larger masses. The IMF constructed from Stone's (1970) study of NGC 654 is shown as the open triangles in Figure 29. Stone was careful to include the outer part of the cluster as well as the core, to guard against mass segregation effects, although membership is a difficult problem in the outer region. Stone also determined the variable reddening toward each sample star. The procedure I followed to construct the IMF was to retain only the 57 stars (out of 83) with membership probabilities greater than 0.70, and, from Stone's

$M_v-(B-V)$ diagram, evolved stars were eliminated, leaving 54 stars in the range $-4.92 \leq M_v \leq 0.23$. These data were divided into 6 bins with $\Delta M_v = 1.0$, and the IMF was then computed. The lowest mass points are almost certainly affected by incompleteness, so the apparent turnover is not real.

The young cluster NGC 6611 was studied by Sagar and Joshi (1978). To construct the IMF, only stars in the magnitude range $-6.8 < M_v < 1.9$ were used. Retaining only the probable members, the final sample consisted of only 47 stars, which were divided into 5 bins of $\Delta M_v = 1.0$. The resulting IMF is shown in Figure 29 as the filled triangles.

Chini, Elasser, and Neckel (1980) have presented a study of the young stars in M17 which allows a construction of a LF, which had to be measured from their Figure 7. Chini *et al.* state that the data is probably only complete in the range $-5 < M_v < -3$, with 34 stars in this interval. This region corresponds to the 3 highest mass points in the M17 IMF shown in Figure 29 (open squares), although their fainter data are also plotted. The statistical uncertainties shown were computed using the quoted total volume (9 pc^3) to which their plotted star densities apply. Chini *et al.* emphasize that the LF (and IMF in Figure 29) is nearly flat for the brightest three points, for which the data should be complete. Within the statistical uncertainties for IMF for M17 is consistent with the results for NGC 654 and NGC 6611, as well as the Taff cluster IMF. However, for $m \gtrsim 10$, all four of these IMFs are flatter than the field star IMF.

The LF of the cluster NGC 129 has been determined by Frolov (1975), who identified 141 members on the basis of proper motions and B, V photometry down to $B = 15.65$ of 325 stars in a $25' \times 25'$ field. The cluster age is around 4×10^7 yr. The LF (which Frolov smoothed) was measured from his Figure 1 and converted to the mass function shown in Figure 29 as open inverted triangles. The IMF of NGC 129 is steeper than most of the other young clusters in the mass range 2.2 to $8 M_\odot$. The effect of possible mass segregation would be to further steepen the IMF.

In a final presentation of a young cluster IMF, we discuss the recent study of NGC 3293 by Herbst and Miller (1983). These authors used UBV photographic photometry to $V = 16.5$ ($M_v = +3.5$) in order to determine the age spread, mass function, and other properties of this cluster. Herbst and Miller recognized the possibility of a core-halo structure with some segregation (even though the nuclear age is only about 6×10^6yr), and so studied each region separately. The mass function presented here refers to the combined regions. In order to obtain the LF, eye estimates of magnitudes were necessary in crowded regions, and an approximate (and fairly large) correction for contamination by field stars was made. The counts are believed to be complete to $M_v = +3.5$ ($\approx 1.3 M_\odot$). The IMF for NGC 3293 shown in Figure 29 (plus signs) is quite interesting because it exhibits a turnover at about $m = 3$. Although it is possible that this turnover results from overcorrection for field stars, the discussion of Herbst and Miller suggests that this turnover is a real physical effect. This cluster is the youngest cluster in which such a turnover has been found (for older clusters, see below) and it is highly unlikely that there has been sufficient time for dynamical effects to be the culprit. Herbst (1983) has presented a LF for the very young cluster NGC 6193 which also suggests a turnover at small masses, but the number of members studied is so small and the uncertainties large enough that it was not included in Figure 29. This result suggests that cluster IMF turnovers reflect initial conditions and not dynamical evolution. The pronounced dip at $m \sim 8$ should also be noted. Except for this dip, the NGC 3293 IMF agrees very well with the Taff composite IMF over the range 4–40$M_\odot$, but once again the cluster IMF is flatter than the field star IMF for $m \gtrsim 10$.

For visual comparison, all the IMFs of Figure 29 are redrawn with arbitrary normalization in Figure 30. Only the points which could be considered reasonably complete are included. Lines with slopes $\Gamma = -1.5$, -2.0, and -2.5 are also shown.

After this comparison was complete, Sagar *et al.* (1985) presented an investigation of the IMFs of 11 young clusters using UBV photometry and a comparison of positions in the *H–R* diagram with evolutionary tracks. For the 5 most populated (~ 100 members) clusters, their main results are: (a) The average value of $\Gamma = -1.5 \pm 0.3$ in the mass range 1.25–60$M_\odot$ (actually most of the fits apply to masses below 10–20$M_\odot$); this value of Γ might be slightly decreased by the effects of mass loss. No evidence for significant cluster-to-cluster variations was found; (b) the IMF of these clusters does not appear to steepen at high masses ($m \gtrsim 10$); (c) among these well-populated clusters no evidence was found for a variation of Γ with galactocentric distance (8.2 to 11.8 kpc); two inner clusters, not in this group,

appear to have flatter IMFs, but these clusters have only a small number of observable members.

It is clearly difficult to draw any firm conclusions from Figures 29 or 30 concerning IMF variations because of the problems with completeness and correction for field stars. It does appear that except for the turnover and dip in NGC 3293, the young clusters and associations agree fairly well among themselves and with the Taff composite and field star IMF between about 3 and 10$M_\odot$, but most of the young cluster IMFs are *flatter* than the adopted field star IMF for $m \gtrsim 10$.

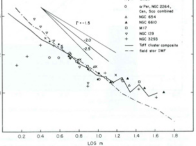

FIGURE 30 Same as Figure 29, but with different normalization. Composite cluster IMF of Taff (1974) and adopted field star IMF are shown for comparison.

3.5 Intermediate-age open clusters

Mass functions of several intermediate-age clusters with sufficient published data have been constructed and are displayed in Figures

31 (Hyades and Praesepe) and 32 (NGC 6811, NGC 2506, Pleiades, NGC 2420, M67, M11 and M35). The ages of these clusters range from roughly 7×10^7yr (Pleiades, M11, M35), to 8×10^8yr (Hyades, NGC 6811), to a few times 10^9yr (Praesepe, NGC 2420, NGC 2506, M67). We discuss each cluster in turn.

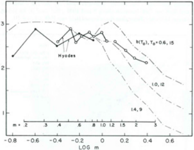

FIGURE 31 IMFs of Hyades and Praesepe clusters compared with field star IMF for three choices of relative birthrate and disk age.

Because of its proximity, the Hyades cluster offers the best opportunity to study an individual cluster IMF down to very small masses $\sim 0.2 M_\odot$. Since it is not too old, the IMF can be determined from this limit up to about $2.5 M_\odot$. Two determinations of the Hyades IMF are shown in Figure 31. Van Altena (1969) published star counts to $V \approx 15 (m \approx 0.3)$, but only stars near the cluster center were counted, which may have resulted in a deficiency of faint stars. His Table IIIA gives V and $(B-V)$ for 90 probable main sequence members which were divided into bins of $\Delta M_v = 2.0$ in order to construct a mass function (filled circles). The statistical uncertainties due to the

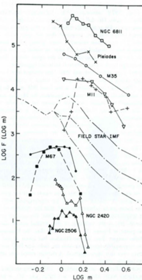

FIGURE 32 IMFs of several of the best-studied open clusters. See text for sources of data.

number of stars in each bin ranged from about 0.07 to 0.12 in the logarithm. Oort (1979) tabulated a blue luminosity function for a larger number of stars. His ΔB intervals were converted to ΔV using the main sequence color-magnitude relation for this cluster published by van Altena (1969). It was assumed that all stars with $V \geq 4.0$ ($M_v \geq 0.8$, $m \lesssim 2.7$) were main sequence stars, giving a final sample of 308 stars which were divided into 12 bins of width $\Delta M_v = 0.85$ and converted to the mass function shown as the open circles. Statistical uncertainties range from about 0.06 to 0.10 in the logarithm.

The adopted solar neighborhood IMF (dot-dashed lines) over the relevant mass range is also shown for our usual 3 combinations of $b(T_0)$ and T_0. (The large uncertainties in the local IMF must be kept in mind.) The agreement or disagreement between the Hyades and field star IMFs depends on which birthrate history for the field stars is chosen. If the decreasing birthrate (upper curve) is compared, the only disagreement is that the Hyades shows no evidence for the large dip centered on $0.7 M_\odot$. If a constant or increasing birthrate is used, the dip amplitude is reduced to within the counting errors for the Hyades data, but the Hyades is then somewhat flatter than the field star IMF. This could, however, be an artifact caused by the lack of counts in the outer regions of the cluster (i.e., mass segregation).

Also shown for comparison in Figure 31 is the IMF of the Praesepe cluster (= M44 = NGC 2632), derived from the LF presented by Jones and Cudworth (1983). Their LF weights each star by a membership probability based on proper motions and is further corrected for the fact that measurements were made only for part of the entire cluster area. A total of 441 stars are represented, with ~ 100 stars per bin. Jones and Cudworth remark that the number of stars in the faintest magnitude interval is a lower limit because of probable incompleteness; this is the meaning of the vertical arrow above the lowest mass point in Figure 31. Considering this, the Praesepe IMF may be a little steeper than for the Hyades, but given all the uncertainties, is in reasonable agreement with the field star IMF for a constant birthrate over this mass interval. A similar result was obtained by Anthony-Twarog (1984).

Barkhatova, Zakharova, and Shashkina (1978) have studied the LF of the open cluster NGC 6811 (age $\sim 8 \times 10^8$ yr, $(m-M)_0 = 10.3$) out to a radial distance of 20′. Photographic UBV observations of 2000 stars brighter than $V = 15.1$ were obtained and calibrated using photoelectric photometry of a small subset of these stars. Sanders' (1971) proper motion study was used to determine membership, and evolved stars were excluded. Additional main sequence stars in the nuclear region, for which proper motions were unavailable, were also included, giving a total of about 230 members after a uniform background density was subtracted. The mass function derived from the published luminosity function is shown in Figure 32 as open squares. The statistical uncertainties are typically ± 0.05. Notice that the mass function is very similar to the field star IMF. The decrease at the lowest mass point suggests a similarity with the peak for the decreasing birthrate case, but the turnover is more likely due to incompleteness.

The IMF for NGC 2420 was constructed using star counts published by McClure *et al.* (1974). The adopted $(m-M)_0$ was 11.5. Probable main-sequence stars were identified by requiring $M_v \geq 3.25$ ($m \lesssim 3$) or, if $M_v < 3.25$, by requiring $(B-V) \leq 0.55$. Their Table 3 was used to eliminate probable non-members. The final sample contained 244 stars ($2.2 < M_v < 6.0$), divided into 13 bins of $\Delta M_v = 0.3$ to construct the mass function shown as open triangles. The typical uncertainties are 0.07 to 0.12, but reach 0.20 and 0.23 for the two points at highest mass. Note the extremely peculiar form of the IMF for this cluster, with a very steep high-mass side and an apparent "dip" at intermediate masses ~ $1.2 M_\odot$. It may or may not be significant in this regard that NGC 2420 is mildly metal-poor. Of course, if the point at $\log m = 0.18$ has been overestimated by a factor of 2 or so, the feature would largely disappear.

The star counts used in preparing the NGC 2506 IMF (filled triangles) are from Chini and van Altena (1978), who adopted $(m-M)_0 = 11.70$ and $E(B-V) = 0.10$. In order to isolate main-sequence stars, all stars with $V \geq 15$ ($m \lesssim 1.3$) were retained, while if $V < 15$, only those with $(B-V) < 0.60$ were used. The resulting sample contained 252 stars which were divided into 12 bins of $\Delta M_v = 0.35$. (The 2 stars with $M_v < 2$ were omitted.) Statistical uncertainties ranged from 0.07 to 0.16. The most significant feature of NGC 2506, besides the steep high-mass slope it shares in common with NGC 2420, is the maximum in the IMF at $m \approx 1.2$, just where the field star IMF with decreasing birthrate shows the same effect. This type of turnover, which as been suspected in several other clusters covering a wide range of ages, has been the subject of considerable observational and theoretical interest. The probable peak in the IMF of the young cluster NGC 3293, which occurs at a larger mass, was discussed in the previous section.

I have included M67 as another cluster with an apparently well-established turnover. The LF for 564 stars given by McNamara and Sanders (1978) is based on Sanders' (1971) proper motion survey of this cluster. Only stars whose proper motions were determined from at least 4 independent plate pairs were used, and then Sanders' maximum likelihood technique for establishing membership was applied. The limiting magnitude of the Sanders proper motion study by $B \leq 18$, and I have only used the counts to $B = 18$ given by McNamara and Sanders (1978) to determine the IMF (filled squares), even though they give additional counts to $B = 22$ derived from Racine's data. The statistical uncertainty is only large at the point with the smallest mass in Figure 32, which is $(+0.11, -0.15)$. Also shown (filled circles) is the IMF for M67 derived in the careful study of Mathieu (1983), whose similar work on M11 is described in more detail below. Although the different membership conditions imposed by Mathieu result in an altered IMF compared to the McNamara and Sanders study, a turnover still exists. It would appear, then, that the turnover in M67, as in NGC 2506, is a real physical effect.

Recent discussions by van Leeuwen (1980) and Mathieu (1983) have emphasized dangers inherent in analyses of open cluster LFs. Van Leeuwen showed that the LF in the Pleiades is a function of the distance to the center, with more faint stars in the outer regions, as discussed earlier. This can be clearly seen in Van Leeuwen's Figure 2 and in his Figure 3 where he shows the LFs (in M_{pg}) for the central 1 pc area and for the total cluster out to 10 pc. Based on the proper motion survey of Pels *et al.* (1975) and photoelectric measurements of selected stars, van Leeuwen shows how previous LF determinations for the Pleiades had found a flat or decreasing LF at faint magnitudes (see Figure 1 in Scalo 1978) because they only studied the cluster core, but for a total field with a diameter of about 9° (~ 20 pc at a distance of 125 pc), the LF is still increasing at the faint end. A search for members even more distant from the center would be very difficult, because only a small fraction are expected to be members. Van Leeuwen even suggests that the flattening at $M_{pg} > 4$ in Taff's (1974) composite cluster IMF may be due to the fact that only the central cluster regions are usually studied.

The LF for the total Pleiades cluster given by van Leeuwen in his Figure 3 was converted to an IMF (crosses in Figure 32) by measuring the number in each M_{pg} range, converted to $M_v \approx 0.85\, M_{pg} + 0.31$ for the ZAMS, and assuming that the Pleiades stars are on the main sequence if $M_v \geq 1.5$ and $(B-V)_0 \geq 0.05$. This left 219 stars which were divided into 6 M_v bins. Uncertainties in log N are only ~ 0.05 to 0.10. Note that van Leeuwen's limiting M_{pg} was about 13 in this work, but he states that work is underway to extend this limit by 1.5 mag. This extension would be very important, because the IMF in Figure 32 based on his published study only reaches $m \approx 0.8$, while the previously reported turnover occurs at smaller masses. Van Leeuwen points out that data on faint flare stars suggest that the LF may continue to increase at smaller luminosities. While the IMF of the Pleiades may not turn over, its form certainly appears different (steeper) than the field star IMF in the same mass range, similar to the result for NGC 2420 and NGC 2506. The discrepancy could be partially removed if the birthrate of field stars has been an *increasing* function of time, but then the peaks in the IMFs of M67 and NGC 2506 would be anomalous compared with the field stars. It should also be remembered that there is strong evidence for a large spread in formation times for the Pleiades, so evolutionary effects may also be involved.

Perhaps the best example of the dangers caused by radial segregation and other problems is afforded by the cluster M11. I have shown two IMF determinations for M11 in Figure 32. The first (plus signs, dashed line) is based on the proper motion survey and photometry of McNamara *et al.* (1976) and McNamara and Sanders (1977), with $m - M = 12.3$. They tabulate m_v for all stars with membership probabilities (based on proper motion statistics) ≥ 0.5. The limiting magnitude of the survey was $V \approx 16.5$, so with a main-sequence turnoff at $M_v = -1.0$, only stars with $V > 11.3$ were assumed to be main-sequence stars, but this criterion only rejected 9 stars. The final sample which I used to construct the IMF consisted of 700 stars in 10 half-magnitude bins from $M_v = -1.1$ to $M_v = 4.0$. Typical statistical uncertainties were 0.04 to 0.11 in log $F(\log m)$. The IMF shows a clear turnover at $m \approx 1.6$. Since the sample should be complete below this mass, one would conclude that the turnover is real.

This cluster has recently been reexamined by Mathieu (1984). Mathieu's main point is that a proper motion membership probability of ≥ 0.5 is arbitrary and problematical, because (a) a criterion this large reduced the number of stars which can be studied, especially in the outer cluster regions and for low-precision faint stars; (b) because the value of the probability is very sensitive to measurement and reduction techniques when it is this large; and (c) because field stars exist whose proper motions are nearly equal to those of cluster members, so field stars cannot be easily identified. Instead, Mathieu keeps all stars in the McNamara and Sanders proper motion survey with membership probabilities ≥ 0.1, obtained photometry for these lower-probability objects (~ 1100 stars), and then used the color-magnitude diagram for all these stars from deep ($m_v < 20$) $4m$ KPNO plates to weed out the non-members. Mathieu also made estimates of incompleteness due to plate limit and central crowding effects using the deep plates. He finds 100% completeness to $V = 15.0$, 60% for $15.0 \leq V \leq 15.5$. Using these procedures, Mathieu finds that only 50–80% of the > 0.5 probability stars were actually members, and discovered about 15–40% additional members using the color-magnitude diagram as an additional constraint.

His resulting LFs for the inner ($r < 2'$) and outer regions of the cluster show clear differences due to mass segregation, with the inner region being flatter. The combined LF was converted to a mass function and is displayed in Figure 32 as the inverted triangles connected by solid lines. (The uncertainties are smaller than the triangles.) Although the result is not much different from the earlier work for $m \geq 2$, Mathieu's function does *not* turn over, although it is flat between $m = 1$ and 2. Note the reasonably good agreement with the field star IMF between 1.6 and $5 M_\odot$, independent of birthrate history.

Mathieu's (1983) IMF for M35 (NGC 2168, age ~ 2–4×10^7 yr), derived using a very similar approach, is also displayed in Figure 32 (open circles). Although less "curved" than the M11 IMF, the M35 IMF still bears a strong resemblance to the field star IMF, although this conclusion is admittedly subjective.

Cayrel de Strobel and Delhaye (1983) described preliminary results of a program to study the photometric, spectroscopic, and kinematic properties of the four nearest clusters: Ursa Major, Hyades, Coma, and Pleiades. The luminosity functions were converted to mass functions which are plotted in Figure 33, with counting uncertainties. The numbers in parentheses give the number

of stars in each sample. The dashed lines are the mass functions for the Hyades and the Pleiades which were constructed earlier. The field star IMFs for 3 birthrate-disk age combinations are also shown for comparison (crosses connected by dotted lines). The IMFs for the Hyades and Pleiades agree well with the earlier results for $m > 1$, but the Cayrel de Strobel and Delhaye functions are incomplete below this mass, probably because the sample excluded the outer cluster members. Omitting the points below $1 M_\odot$, the IMF for Coma agrees fairly well with the Hyades and Pleiades, although it may be a little

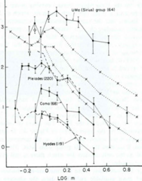

FIGURE 33 IMFs of the four nearest clusters, from the luminosity functions given by Cayrel de Strobel and Delhaye (1983). Numbers in parentheses are the number of stars used for each cluster. The dashed lines are the IMFs presented in Figure 31 for the Hyades and Figure 32 for the Pleiades. Dotted lines are the field star IMF for three combinations of relative birthrate and disk age.

flatter. The reasonable agreement with the field star IMF for $m \gtrsim 1.2$ (where birthrate uncertainties are unimportant) is again apparent. Including the lower-mass points $\geq 0.92 M_{\odot}$, these clusters agree best with the constant birthrate IMF, although possible incompleteness would be consistent with a slightly increasing birthrate. Although the turnovers in the Hyades and Pleiades found by Cayrel de Strobel and Delhaye are apparently artifacts caused by incompleteness, the situation for the Coma cluster is not so clear. Argue and Kenworthy (1969) noted that the main sequence of this cluster shows an abrupt termination at $M_v \sim 6.0$ ($m \approx 0.8$); however, they only studied the central region of the cluster, so mass segregation may again be responsible for the apparent turnover.

The IMF for the Ursa Major (Sirius) moving group is especially interesting because it is the only such group for which a LF is available. It is known that the solar neighborhood contains a group of stars, probably including the sun, which share a common streaming motion through the galaxy, implying that they shared a common origin (see Eggen, 1982, for further discussion of this "local supercluster"). The age of this group is estimated by Cayrel de Strobel and Delhaye (1983) to be 1.6×10^{8}yr, but the *H–R* diagram indicates a significant spread in age. The IMF for the UMa group derived from their LF appears somewhat flatter than the other IMFs in Figure 33, and shows a pronounced turnover at around $1.3 M_{\odot}$. Given the small number of stars, the flattening is probably not significant. Cayrel de Strobel and Delhaye checked for faint end incompleteness by searching the AGK 3 catalogue for stars with proper motion close to the group stars in the same direction, but found only 7 additional stars, which are included in the IMF. The effect of omitting these stars is illustrated by the open circles in Figure 33. It appears that incompleteness is not serious above $1 M_{\odot}$, so the turnover at $\sim 1.3 M_{\odot}$ may be real. If so, then the UMa group joins NGC 3193, M67, and NGC 2506 as the only clusters for which there is still evidence for a low-mass turnover.

Although IMFs of many more intermediate-age clusters could be constructed from available published data, the clusters shown in Figures 31 to 33 are the best-studied. The IMFs of the Hyades, Praesepe, NGC 6811, M35, and M11 are roughly consistent with the field star IMF and Taff's composite cluster IMF, but NGC 2420, NGC 2506, M67 and the Pleiades appear peculiar to varying degrees. The peculiarities and differences are not correlated with any cluster property such as richness or age. Although the existence of turnovers has still not been definitely established, M67, NGC 2506, and UMa, along with the younger NGC 3193, are the outstanding candidates for the effect. Another cluster requiring further study is IC 4635, for which Sanders and van Altena (1972 and references therein) find no probable members fainter than $M_v \approx +3.5$ or $m \approx 1.3$, even though their counts extend to $M_v \approx +5.5$; an additional interesting property of this cluster which may be relevant to turnovers is the fact that 18 of the 19 brightest members are binaries. If the turnovers in these clusters are real, they would be consistent with the idea that the birthrate of field stars has decreased somewhat during the history of the disk, and that the resulting peak at $m \approx 1.2$ in the field star IMF reflects a large contribution from clusters like these. However, in this case, all the other clusters with estimated IMFs down to $1 M_{\odot}$ would then have to be considered peculiar with respect to most of the field stars.

The establishment of reliable LFs for open clusters is an extremely difficult observational problem. Incompleteness, contamination by non-members, and radial mass segregation are the most severe effects to contend with, and much more work on proper motions, radial velocities, and photometry to very faint limits will be required. Significant advances in this area can be expected in the near future (see, for example, Weis and Upgren, 1982 and Weiss, 1983, on the Hyades). On the other hand, even bearing the uncertainties in mind, the cluster IMFs shown in Figure 32 indicate that variations among clusters and between clusters and the field star IMF probably do exist in some cases. Such variations might be expected if the IMF represents a stochastic process, and the lack of correlation of these variations with cluster properties suggests that this may indeed be the case.

3.6 More on variations in open clusters

We have seen that individual open clusters in a few cases show significant variations in the form of their IMF. That the IMF does vary greatly on small spatial scales is suggested by the work of Tarrab (1982), who studied the IMF in 75 fairly young open clusters with ages from about 6×10^{8}yr (e.g., the Hyades) to less than 10^{7}yr, divided into 14 age groups. The IMFs were constructed by counting the number of stars between evolutionary tracks of models of various masses computed by Maeder and Mermilliod (1981) for $1.25 \leq m \leq 9$ and Maeder (1981) for $m = 15$ and 30, transformed to the M_v, $(B-V)$ diagram using the tables of Flower (1977). The catalogue of UBV photometry and MK spectral types of Mermilliod was the basic data source. Membership was inferred from proper motions and radial velocities when available, while in other cases stars were counted as members only if they fell on the main sequence band of the $V-(U-B)$ diagram. The counts may be incomplete at faint magnitudes, although considerable care was taken in this regard, and in some cases rejection was based on a non-increasing IMF toward lower masses. However, the individual IMFs may be quite noisy, judging from the Orion result shown in Figure 1 of Tarrab.

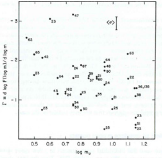

FIGURE 34 Maximum likelihood estimates of slope of assumed power-law IMFs of clusters as a function of the upper mass limit for which the fit was carried out, based on results of Tarrab (1982). Numbers beside each point give number of stars used in the fit. Typical standard error is indicated.

Tarrab used the method of maximum likelihood to calculate the slope of an assumed power law IMF for each cluster, and tabulated these slopes and their standard error. Figure 34 shows the derived values of the slopes for all clusters as a function of the upper mass limit for which the fit was carried out. The numbers beside each point give the number of stars used in the fit. A typical standard error for an individual slope determination is also indicated. The range in slopes is enormous, from about -0.2 to -3.4. Even given the problems with incompleteness and possible non-power law forms, much of this variation must be real. However, this result contradicts most of the evidence on cluster IMFs presented earlier, in which no such enormous differences were found. Also, comparing the few clusters in common with Tarrab's work and the studies discussed earlier, I find poor agreement, and have been unable to resolve the discrepancies.

The average slope for clusters in each of the 13 age groups is shown as a function of mean cluster age of that group in Figure 35. The arrows to the left of the four youngest groups indicate that only upper age limits were given. Again, a wide range of slopes is seen, although the range is not so large because of the averaging of clusters within each group. The figure also gives some weak evidence that the oldest clusters have the steepest IMFs.

According to Tarrab, if one considers only clusters with more than 60 members (10 clusters), the averaged slope is -1.7 in the mass range $1.25 < m < 14$. It must be remembered, however, that this is a straight average which neglects the effects of differing upper and lower luminosity limits and IMFs between clusters, as discussed in Section 3.3. The value $\Gamma = -1.7$ is similar to the indices of the field star IMF, Taff's (1974) composite cluster IMF, and Burki's (1977) composite IMF for small clusters, for the same mass range. The differences among individual clusters must be a combination of real variations, statistical uncertainties, and systematic errors.

By now it must be evident that no definitive picture of the nature of open cluster and association IMFs has emerged. On the one hand, the most careful studies of individual clusters and associations give the impression of approximate uniformity, considering the uncertainties, in *most* cases. However, a few of these well-studied groups do exhibit exceptional behavior, such as turnovers at low masses. On the other hand, studies such as that of Tarrab (1982) indicate *extreme* cluster-

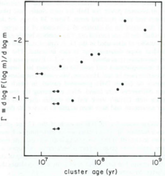

FIGURE 35 Average slope for clusters in each of 13 age groups as a function of mean cluster age, based on results of Tarrab (1982). Arrows signify that only upper age limits were given.

to-cluster variations which are difficult to reconcile with the individual studies. Nevertheless, when the cluster data is combined to give a composite cluster IMF, all the studies agree reasonably well. Whatever differences appear are tantalizingly close to the uncertainties in the various estimates. It does appear that, at large masses, the open cluster IMF is somewhat flatter than *some* estimates of the field star IMF, implying that stellar associations, which donate most of the field stars (e.g. Miller and Scalo, 1978), produce steeper high-mass IMFs than open clusters. However, confirmation of this conjecture must await a better understanding of the large uncertainties involved in estimating the field star IMF. *If* the IMF on the small spatial scales of clusters and associations does in fact exhibit significant variations, possibly stochastic in nature, then the appropriate questions for

studies of galactic evolution can be stated: Is the ensemble average of the IMF universal? This question can only be studied by star counts on a galactic scale, which is the subject of Section 4.3.

3.7 IMF of pre-main sequence stars

As discussed earlier, an understanding of the IMF is relevant to two research areas with disparate scales: physical processes involved in the formation of individual stars and clusters, and galactic evolution. For those interested in star formation processes, it is the small-scale IMF which is of most interest. Unfortunately, we have seen above how little has been learned concerning the IMF on the scale of open clusters and associations because of a variety of problems. It is therefore of great interest to the theory of star formation to attempt estimates of the IMF in regions of our galaxy which are currently forming stars. Although little is presently known concerning this subject, the recent and future availability of high-sensitivity high-resolution infrared and radio observations (e.g., IRAS and VLA) suggests that a review of the available techniques for IMF estimation in star-forming regions may be useful.

The IMF of pre-main-sequence stars is obviously of importance for the theory of star formation. However, we must remember that the IMF is a distribution function whose form tells us how mass is parceled out to a group of stars after their formation process is essentially complete, and assumes that the function is independent of time for a given group. Thus, if star formation proceeds from lowest to highest masses during the early evolutionary stages of a star cluster, as is commonly believed, we must exercise care in interpreting the IMF observed there at any given time. As an example, suppose we could determine the IMF in the Southern Coalsack, the Taurus complex, the ρ Oph cloud, and Orion. In the Coalsack, we would observe few, if any, stars, while in the other three regions the most massive star observed might be 3, 8, and $40 M_{\odot}$, respectively. If these regions represent a sequence of evolutionary stages, then the IMFs which we observe would only tell us how the IMF varies with time over short time scales within a small group. The distinction between this sort of study and most of the other studies discussed in this paper is essential to bear in mind.

3.7.1 *Optical Spectroscopic Matching*

The major source of data on the mass functions of pre-main-sequence stars comes from the comprehensive study of Cohen and Kuhi (1979), who estimated IMF slopes in the Taurus–Auriga, Orion, NGC 2264, and NGC 7000/IC 5070 regions. Cohen and Kuhi used infrared photometry and optical data to determine M_{bol}, and spectral classes to estimate effective temperatures, a very uncertain procedure mostly because the proper conversion between spectral type and T_{eff} is uncertain for premain sequence stars, as was recognized by Cohen and Kuhi. Next, these authors estimated masses by comparison with theoretical isochrones constructed from convective–radiative tracks. This last step is especially dangerous because, first, it is not known whether T Tauri and related objects evolve along convective–radiative tracks, and secondly because the convective portions of these tracks (along which most of the studied stars lie) are theoretically uncertain and do not discriminate masses well.

For example, a typical set of convective evolutionary tracks in the *H–R* diagram can be represented as $T_e = K\, m^{0.19}\, L^{-0.13}$, where K is a constant, m is the mass, and L is the luminosity (Scalo, Despain, and Ulrich, 1975; for an analytical derivation of a similar result, see Stein, 1971). Even if we assume that the luminosity is known exactly, the derived mass $m \propto T_e^{5.2}$. A 10% uncertainty in the observationally determined temperature (which seems optimistic) leads to a 50% uncertainty in the derived mass. Furthermore, it is well known that the positions of convective evolutionary tracks are uncertain because of problems with the treatment of subphotospheric convection and the radiative atmosphere; this causes an uncertainty of at least 10% in the constant K, so the best mass estimates we can hope for will be uncertain by *at least* a factor of two, even if pre-main-sequence stars do evolve along convective tracks and if their luminosities are exactly known. A more realistic uncertainty may be a factor of four. On the other hand, it is possible that *relative* masses in a single group of stars can be estimated to better accuracy using this procedure. It should also be noted that the above problems may not alter the more general conclusions of Cohen and Kuhi concerning the process of star formation.

However, a possibly more severe problem, emphasized recently by Appenzeller (1983), is that the form of the evolutionary tracks during

the convective protostellar phase appears to be sensitive to the initial conditions adopted in the numerical calculations. Since we expect variations in initial conditions for real protostars, this implies that a given point in the *H–R* diagram cannot be uniquely associated with a particular mass and age. A specific example of this problem is provided by the work of Mercer-Smith, Cameron, and Epstein (1984), who show that, if protostars accrete from a disk, a protostar will begin its evolution down a convective track at a smaller luminosity than if the energy radiated away during disk accretion is neglected; just where a protostar begins its descent down a convective track depends on the details of the accretion process, which may depend on a number of environmental factors. Mercer-Smith *et al.* conclude that the *H–R* diagram is not a useful tool for studying protostellar evolution. In particular, if their arguments are correct, there is little basis for assigning protostellar masses by positions in the *H–R* diagram. These points must be kept in mind in the following discussion.

Cohen and Kuhi presented their mass distributions in cumulative form and then attempted to derive mass function slopes by fits to these cumulative distributions. The slopes ranged from -1.4 to -2.9 for the various regions, but they feel that the most reliable values are for Taurus–Auriga ($-1.5^{+0.3}_{-1.0}$), NCG 2264 non-emission line stars (-1.7 ± 0.1), and the combined Orion stars (-1.4 ± 0.1).

Larson (1982) constructed differential frequency distributions from the Cohen and Kuhi data on T Tauri stars, and his results are shown in Figure 36, along with the field star IMF (for constant birthrate) estimated earlier. Larson has emphasized the difference between the Taurus and Orion mass functions, suggesting that the Taurus function resembles the field star IMF while Orion has relatively fewer low mass stars. It is true that Orion, NGC 2264 and NGC 7000/IC 5070 all have derived mass functions which appear deficient in low mass ($< 1 M_\odot$) stars, but it must be remembered that, first, these three regions are more distant than Taurus, making low mass (i.e., low luminosity) star detection more difficult, and second that Taurus is probably the youngest of the four regions and may simply not yet have formed higher-mass stars. As discussed below, recent work on NGC 2264 by Adams, Strom, and Strom (1983) suggests that incompleteness is indeed a problem. Mass-dependent selection effects might also arise because Larson restricted his IMFs to T Tauri stars, a phase whose existence and duration may depend on mass (Larson, 1985, private communication). Given these considerations, it appears premature to conclude that the Taurus and Orion IMFs differ (although certainly the upper mass limits differ), or that either differs from the field star IMF.

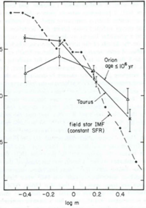

FIGURE 36 IMF estimates for pre-main sequence stars in Taurus and Orion by Larson (1983) based on masses given by Cohen and Kuhi (1979). Field star IMF is shown for comparison.

While it has been long known that the upper mass limit of stars varies among star-forming regions, a basic question which remains unsettled concerns the IMFs in these regions at some future time after star formation has been completed by consumption or disruption of the available gas. On the one hand, the differences in upper mass limits could be interpreted as indicating that Taurus has and will only produce relatively low mass stars, while only higher-mass stars are formed in Orion and NGC 2264; i.e. that the final forms of the IMFs will differ. However, Cohen and Kuhi's (1979) study gives support for the idea that star formation proceeds from lower to higher masses with time, as originally found by Iben and Talbot (1966; see, however, Stahler, 1985). If this is so, then it is plausible that the Taurus IMF will eventually extend to higher masses and the final IMFs of star-forming regions span similar mass ranges.

The only work which allows a tentative resolution of this question is the detailed study of the PMS stars in the NGC 2264 cluster by Adams, Strom, and Strom (1984), who identified about 300 probable PMS members in the range $17 \le V \le 22$ ($7.5 \le M_v \le 12.5$) on the basis of either $H\alpha$ emission, variability, or UV excess using automated star counting. By assigning effective temperatures from primarily the $V-I$ colors, and bolometric corrections either from a $BC-M_v$ calibration for main sequence stars or from the infrared excess, masses and ages could be estimated for each star by comparison with theoretical evolutionary tracks and isochrones, as was done by Cohen and Kuhi. The enlarged sample size and deep limiting magnitude allow a more definitive estimate of the IMF over a larger mass range than in any previous work, although the same cautions regarding the inferred masses still apply.

Adams *et al.* do not give masses for individual stars, but they point out that the visual luminosity function in NGC 2264 is very similar to the field star luminosity function. To emphasize this similarity I have converted their luminosity function to a mass function using the values of $dM_v/d \log m$ given in Table IV. This procedure, as well as the comparison of the LFs, is not really justified because most of the stars lie above the main sequence, but hopefully the brightening correction would not seriously distort the shape of the IMF. The result is shown in Figure 37 along with the field star IMF for three birthrate histories. The error bars represent the counting uncertainties. Except for the possible deficiency of stars around $1.5 M_\odot$, the major result is the striking similarity between the NGC 2264 IMF and the field star IMF for constant birthrate. Furthermore, the turnover at $\sim 2 M_\odot$ which can be found in the Cohen and Kuhi (1979) data for NGC 2264 is seen to be a result of incompleteness. It thus seems likely that all of the turnovers in the differential IMFs of Cohen and Kuhi are artifacts, especially since the mass at the turnover is found to be correlated with the cluster distance. This disagrees with Larson's (1982) arguments for Taurus and Orion.

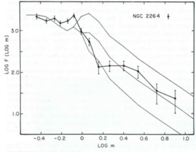

FIGURE 37 Mass function of pre-main sequence stars in NGC 2264 using the luminosity function found by Adams, Strom, and Strom (1984), and assuming a main sequence mass-luminosity relation.

It would be presumptuous to conclude from this that all star-forming regions produce the same IMF; indeed, we have already seen some evidence that IMFs vary among open clusters. Nevertheless, the work of Adams *et al.* does show that different cloud complexes probably do not produce IMFs which are peaked at different masses. Instead these results suggest that the main difference between regions like Taurus and Orion or NGC 2264 is related to age, so that the Taurus IMF will someday extend to large masses.

3.7.2 *Infrared Luminosity Functions*

Visual studies of PMS stars tell us nothing about stars still masked by optically thick dust envelopes or buried deep within their parent clouds. An alternative approach which does not have this difficulty uses infrared observations. If the infrared luminosity of a source arises solely from dust reradiation of stellar photons, then an integration of the infrared flux distribution gives the luminosity of the protostellar source. A luminosity function of protostellar sources can then be estimated. A problem in this case is the spatial resolution, since a given infrared source may have more than one embedded protostar; i.e. the luminosities are upper limits. Nevertheless, the approach is valuable because it can be used for all PMS stars (not just T Tauri-type and related stars) with masses greater than that corresponding to the limiting detectable infrared luminosity.

Although there have been numerous infrared surveys of selected star-forming regions, the only attempt so far to estimate an IMF is the study of the dense core of the ρ Oph cloud by Wilking and Lada (1984). The ρ Oph region contains no stars earlier than B2 V ($m \sim 10$), and so may represent a case intermediate between Taurus and Orion or NGC 2264. If the suggestions of the previous subsection are correct, then ρ Oph may show an IMF in the process of extension to larger masses.

Wilking and Lada emphasize the apparent lack of stars in the 2–$4M_\odot$ range, perhaps implying a bimodal IMF. The argument runs as follows. Far-infrared observations show the presence of only 3 objects earlier than B8 V–B9 V, and their optical counterparts yield spectral classes of B2 V, B3 V, and B6 V. The spectral type-mass relation given by MS gives masses of about 10, 8, and $4M_\odot$ for these stars. Four T Tauri stars also exist in the region, and their masses were estimated by the method of Cohen and Kuhi (1979). Wilking and Lada argue that the remaining 37 embedded near-infrared sources, which have no optical counterparts, must be low-luminosity premain-sequence stars to explain the absence of extended far-infrared emission. Lower limits on the luminosities of these stars are then obtained by extrapolating the observed near-infrared energy distribution.

The resulting luminosities are nearly all fairly small, in the range $0.5L_\odot$ to $13L_\odot$, with two others at $35L_\odot$ and $109L_\odot$. Comparing with evolutionary tracks, the most massive objects which could correspond to these luminosities are about $m \approx 3$, and all but the two brightest have derived masses $m \approx 0.5$–2. The point is that there are no stars between spectral types B7 and B9, and only two between A0 ($m \approx 2.8$) and A3 ($m \approx 2.0$) while there are 35 stars in the $m = 1$–2 range, implying a deficiency of stars in the mass range 2–4$M_{\odot}$, corresponding to spectral types between B7 and A3. It is difficult to say whether this result is statistically significant. For example, if the mass function was a power law with index -1 (say), the number of stars expected in the mass range $m = 0.5$–2 relative to the number in the $m = 4$ to 10 range would be 10. If the 35 low-luminosity stars are actually in the 0.5 to 2 range, then 3–4 stars earlier than B6 V are expected, as is observed. The expected number in the $m = 2$–3 range would come out to be about 5, while only 2 are observed, but considering the uncertainties involved in the observational mass estimates, it does not appear necessary that the result be interpreted as evidence for a bimodal mass spectrum. In addition, since it seems likely that the IMF in star-forming regions is time-dependent, proceeding from small to large masses, we should perhaps expect the high-mass end to exhibit stochastic fluctuations. We should also recall similar apparent deficiencies in restricted mass ranges, such as in NGC 3293 (at around $8M_{\odot}$) and the combined α Per – NGC 2224 – Cen – Sco IMF (at $\sim 3m_{\odot}$), as shown in Figure 29, and in NGC 2264 (at $\sim 1.5m_{\odot}$; see Figure 37).

3.7.3 *Radio Luminosities*

A promising technique for estimating the IMF of very young massive stars is the study at radio wavelengths of "ultracompact" HII regions (Ho and Haschick, 1981), HII regions with sizes ≤ 0.1pc. Ho and Haschick used VLA observations to obtain high spatial resolution maps (1″ at 6 cm, 0.″3 at 2 cm) of three such regions, which were resolved into a number of components. If these components are interpreted as the brightest members of a young cluster, then, since the radio emission is a direct measure of the ultraviolet luminosity of the underlying source, the spectral type and hence mass of the star responsible for the ionization can be obtained. If a statistical sample of such components were observed, the distribution of spectral types would yield the IMF, assuming that the stars are on the main sequence. Ho and

Haschick applied this method to eight components with spectral types between B0 and O6 in one ultracompact HII region and found an IMF somewhat steeper than the field star IMF given in Section II. They also discuss the sensitivity of the result to the choice of spectral type bins and the chosen spatial decomposition of the map into individual sources. Being based on only eight objects, the result must be considered as very preliminary, but this work does suggest that a larger survey could provide a useful method for obtaining the IMF at high masses. Compared to the method of infrared luminosities this approach has the advantage of better spatial resolution, but suffers from insensitivity to spectral types later than B0.

It is also possible to learn something about the IMF by a combination of IR and radio continuum observations of unresolved protostellar HII regions. The IR luminosity reflects the total luminosity of embedded stars while the radio continuum luminosity can be related to the luminosity in Lyman continuum photons, which depends only on the number of stars massive enough ($\gtrsim 20M_{\odot}$) to significantly ionize hydrogen. The ratio of IR-to-radio luminosities, usually called the infrared excess or IRE, should therefore decrease with an increasing fraction of massive stars. This quantity, depending on integrated light instead of source counting, is discussed in detail in Section 5 below. We note here, however, its potential use in studying individual galactic star formation regions. For example, Rengarajan *et al.* (1984) have estimated far-IR luminosities and IREs for the four major components of the W51 HII region complex. The IREs are small, 4–6, leading them to conclude that the IMF in W51 is deficient in stars with $m \lesssim 20$–40 for a reasonable range of power-law indices for the high-mass IMF. A similar conclusion was reached by Haschick and Ho (1983) for the core of the W33 complex. The problems involved in relating the IRE to the IMF are discussed in Section 5.

3.8 Globular clusters

Globular clusters are believed to be the oldest objects in our galaxy. Since their metal abundances are smaller and their interior stellar densities are much larger than in disk open clusters, globular cluster IMFs might reveal differences which depend on metallicity or protocluster density. However, mass segregation processes may be important, so it is difficult to know whether observationally determined mass functions actually refer to their initial mass functions because the central regions cannot be sampled. Comparisons of M/L ratios predicted by an assumed LF with dynamically determined values (e.g. Illingworth 1976) indicate no deficiency in low-mass stars, but this approach is very uncertain.

A direct determination of the IMF requires star counts, but because of their large distances and the intrinsic faintness of the stars in globular clusters, little data is available. Sandage (1954), van den Bergh (1975), and Sandage and Katem (1977) have determined visual luminosity functions of M3 (to $M_v = +6.8$), M92 (to $M_v = +8.5$) and M15 (to $M_v = +6.5$), respectively. A much larger sample of nearly 20,000 stars is available from the automated star counts of Irwin and Trimble (1984) for the cluster M55. All these LFs have been converted to mass functions (below the turnoff mass) and are shown in Figure 38. The adopted relation between M_v and mass for Pop. II stars was taken from Table III of Gunn and Griffin (1979; see Figure 8). [A redetermination of the M92 LF by Sandage and Katem (1983) shows good agreement with the deeper counts of van den Bergh (1975), but is a little flatter for $4 \leq M_v \leq 6$. The recent study of M4 by Richer and Fahlman (1984) indicates that the LF is "rather flat" and definitely turns over at $M_v = 7.5$. These latter two studies are not shown in Figure 38.] The local field star IMF (with the Pop. I M_v-mass scale) for the three usual combinations of $b(T_0)$ and T_0 is shown as crosses connected by a dashed line for comparison. Note that the field star IMF is very flat for $m \lesssim 0.8$, independent of birthrate.

A promising approach to the problem is to compare the star counts and the surface brightness profile with observations of the radial dependence of velocity dispersion in order to obtain a best fit to a multi-mass dynamical model. Details of this method were given by Gunn and Griffin (1979), and Da Costa (1982) has used it to determine (among other things) the LFs of 47 Tuc, NGC 6397, and NGC 6752. Because these clusters are relatively nearby, the LFs could be determined to relatively faint limits ($M_v = +9.3$ to 10.2).

Da Costa's published cumulative luminosity functions were first converted to differential functions by plotting the cumulative functions, differencing them in $\Delta M_v = 0.5$ intervals, and then converting to mass functions. The results are shown in Figure 38. Note that the jaggedness in these graphs, especially for NGC 6397, is mostly just a

result of noise which entered when differencing the cumulative luminosity functions. The mass functions appear to steepen in the sequence NGC 6397, NGC 6752, 47 Tuc. Da Costa (1982) points out that NGC 6397 has evolved over about 6 more central relaxation times than NGC 6752 or 47 Tuc, and so its relative deficiency in low-mass stars may just reflect a larger degree of mass segregation.

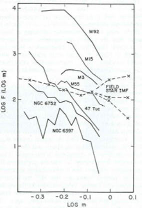

FIGURE 38 Estimated IMFs for globular clusters. See text for sources of data.

Alternatively, the differences may truly reflect different initial mass functions, perhaps related to differing metal abundances or total masses. Indeed, the mean logarithmic deficiency of Fe in these clusters relative to the solar Fe abundance decreases in the sequence (Zinn, 1980) NGC 6397 (−2.2), NGC 6752 (−1.5), 47 Tuc (−0.6). The implication is that the IMF becomes more depleted in low-mass stars with decreasing metal abundance. This suggestion has obvious problems: 1. The form of the IMF of 47 Tuc, with a metallicity most like the galactic disk, appears to differ most from the disk field star IMF; 2. The IMFs of M3, M15, and M92, with logarithmic Fe deficiencies of −1.7, −2.2, and −2.2, respectively, do not seem to follow this trend, and, if anything, show the opposite effect. Furthermore, a preliminary determination of the LF of 47 Tuc by Harris and Hesser (1985), using CCD photometry extending at least 2 magnitudes deeper than Da Costa's photographic work, shows a much *flatter* LF. It seems clear that the differences in IMFs between the clusters shown in Figure 38 could more plausibly be attributed to statistical and systematic errors, stochastic IMF differences between clusters (as almost certainly occurs in open clusters) or mass segregation, rather than a metal abundance effect.

Perhaps a more significant clue to be gleaned from Figure 38 is that globular clusters studied to date (except M3) *do* have roughly similar mass function slopes for $m \gtrsim 0.6$, with discrepancies arising only at very small masses where segregation, escape processes, and incompleteness may be most severe. There is no compelling reason to conclude from existing globular cluster data that their mass functions are *grossly* different from each other, certainly not to the degree suggested by Freeman (1977). They do appear steeper than the field star IFM in this mass range (but see Harris and Hesser, 1985, on 47 Tuc), but the importance of segregation in this regard is uncertain. It should be recalled from Section 2.7 that the population II field star luminosity function of Eggen (1983) is in excellent agreement with the disk luminosity function. Notice also that M55 has by far the largest sample size (Irwin and Trimble, 1984) and also the flattest slope.

Freeman (1977, 1980) has reported on luminosity functions derived for six young globular clusters in the LMC (ages $\sim 10^7$–10^8 yr, masses 10^4–$10^5 M_\odot$). Freeman states that the indices of the mass functions in the range $1 < m < 6$ vary greatly among these objects, from −0.2 to −2.5, with three of the clusters having indices larger (flatter) than about −0.5. Unfortunately, the details of this study were apparently never published.

Globular clusters in our galaxy only offer IMF information for masses less than about $0.9 M_\odot$. Did globular clusters originally have a large population of more massive stars which now lurk as invisible remnants? Or were the complete IMFs of globular clusters deficient in intermediate and high mass stars, as suggested by the steeper IMFs in Fig. 38? We will never have direct answers to such questions. Our only information must come from very indirect arguments such as luminosity functions of nearby irregular galaxies which have small metal abundances like globular clusters (Section 4) or from constraints imposed by relative abundances in halo stars (Section 6).

3.9 *Summary*

Freed from many of the problems involved in estimating the field star IMF, our foray into the realm of stellar clusters and associations has been, to say the least, disappointing, again illustrating the severity of a new set of practical problems rather than yielding any illuminating insights. The major problems involve small numbers, membership assignment, and radial mass segregation. In addition, non-coeval star formation and time-dependent IMFs may be severe effects for young clusters and associations. Indeed, most of the progress in this area has been the recognition of these problems and attempts to deal with them, for example the combination of proper motion surveys of open clusters with deep star counts by Mathieu (1983) and the use of automated star counts in globular clusters by Irwin and Trimble (1983).

The results reviewed in this section do suggest a few tentative conclusions:

1. Studies of composite IMFs for many clusters suggest $\Gamma \approx -1.5$ to -1.8 for $1 \lesssim m \lesssim 10$, similar to the field stars, but there are indications of a flattening at larger masses, with $\Gamma \sim -1.2$ or so.

2. The flattening at large masses appears in studies of some individual young clusters (e.g. M17, NGC 6611; see Figure 29). For $m \gtrsim 10$, therefore, one is tempted to conclude that open cluster IMFs generally contain larger fractions of high-mass stars than does the field star population, which presumably arise primarily from associations. Unfortunately, the true shape of the high-mass field star IMF is quite uncertain, as discussed earlier in Section 2.6.4.

3. The question of major IMF variations between different clusters

remains unresolved. Of the best-studied individual cases, the majority appear similar. However, there are also a few fairly convincing examples of clusters with peculiar IMFs, the most intriguing examples being the "turnovers" which appear in NGC 3293, M67, and NGC 2506. These turnovers do not occur at the same mass in each cluster, and are not correlated with cluster age or richness. Other peculiarities, which may or may not be real, include very steep IMFs near turnoff and "dips". These features appear in only a few clusters, and perhaps it is the *similarity* (within the uncertainties) of most cluster IMFs over a range of masses which should be emphasized, rather than the exceptions which have received most attention in the literature. Contrary to this point of view is the study of Tarrab (1982), whose results suggest enormous IMF variations among relatively young open clusters, contradicting the results found for well-studied individual clusters.

4. Of the globular clusters studied to date, most have similar IMFs over the rather small mass interval $0.5 \leq m \leq 0.9$, but are somewhat steeper than the disk field star IMF in this mass range. However, the possible importance of mass segregation coupled with the fact that only the outer cluster regions can be studied precludes a meaningful comparison. At smaller masses some variations between clusters appears, but again it is impossible to say whether these differences are real or artifacts due to segregation and incompleteness.

It appears that those astronomers interested in small-scale formation processes will have a rather long wait before empirical studies of cluster and association IMFs yield any unambiguous and useful constraints on the theory. In particular, the sought-after clue as to how the small-scale IMF depends on local conditions has not appeared in empirical investigations; either the variations, if they exist, are unsystematic (stochastic) or else they are currently masked by the uncertainties in the IMF estimates. Hoping to learn more by examining larger spatial scales, we now turn to studies of other galaxies.

4. LUMINOSITY AND MASS FUNCTIONS IN NEARBY GALAXIES

We have seen that it is uncertain whether major variations in the IMF do occur among star clusters. However in most practical applications

involving galactic evolution, we are interested only in possible variations in the IMF averaged over scales > 1 kpc. The most direct method for attacking this problem is to consider comparisons of star counts within and among nearby galaxies. The earliest such studies were of the luminosity functions of the Large and Small Magellanic Clouds by de Vaucouleurs (1956), Elasser (1959), and Hodge (1961).

There are several problems involved in the determination and comparison of luminosity functions in extragalactic systems. Only a few Local Group galaxies are near enough for star counts to be carried out with any reliability, and even these are so distant that only the very brightest part of the luminosity function can usually be sampled. The galaxies for which such data presently exist include the Large Magellanic Cloud (LMC), Small Magellanic Cloud (SMC), IC 1613, NGC 6822, M31, and M33. Because of the disparity in distances, there is often only a small overlap in absolute magnitude between the various luminosity functions, making comparisons difficult. Also, for the more distant galaxies, only a very small absolute magnitude range can be studied, and the total number of stars is relatively small, leading to large statistical uncertainties. Finally, it is likely that the galaxies have all experienced somewhat different histories of star formation, so it is not at all clear how the present-day LFs relate to the IMF. This is probably *not* a problem for the presently available star counts because of the bright limiting absolute magnitudes of the counts. A global birthrate variation occurring around a time τ in the past will not affect the conversion between LF and IMF shape for masses with lifetimes much less than τ [see Eq. (2.10)]. Given the limiting magnitudes of the LFs to be discussed here, we only require that the birthrate has been relatively constant over the past 10^7yr. Only for the faintest end of the LMC LF do we need to worry about variations over 10^9yr periods. The double asymptotic branch found by Frogel and Blanco (1983) in the LMC suggests a star formation burst which occurred about 10^8yr ago, but the mass of stars formed in this recent burst appears to be much smaller than in the major star formation episode which occurred $3\text{–}5 \times 10^9$yr ago. Therefore similarities or differences of galactic LFs should directly reflect similarities or differences in IMFs, at least for the portions of the LFs brighter than $M_v \sim -2$ to -3.

In addition there are practical problems with star counts in external galaxies, including crowding (obscuration of faint stars by brighter images in dense fields), incompleteness, corrections for foreground stars, magnitude scale calibration, and grain noise. Some of these problems, such as foreground stars, are not much of a problem if small regions of a galaxy are studied, but crowding effects and incompleteness become serious at faint magnitudes. A recent study of the effect of crowding on apparent LFs is given in Freedman (1983a, 1984). Many of these sources of error have been reduced in recent years using profile fitting routines and studies of artificial starfields using digital sampling of plates, as described below (see Tody, 1980). It should also be noted that in order to obtain star counts to very faint magnitudes (say $m_v \sim 22$ to 24) sufficient observing time on large telescopes and good seeing are required. Finally, a large number of stars is required for an accurate estimate of the LF; Freedman (1984) finds that if this number is smaller than about 500, the derived LF may appear too flat.

A typical procedure is to obtain a number of photographic plates, measure image intensities, calibrate these photographic images with photoelectric sequences in the same or other regions, estimate internal and galactic extinction, exclude evolved stars on the basis of a color-magnitude diagram, correct for galactic foreground contamination, and estimate corrections due to confusion and incompleteness at faint magnitudes. The techniques used for these corrections vary greatly in sophistication, but most of the effects are often not very serious except at faint magnitudes. The various plates can then be averaged to give a composite LF.

4.1 The brightest stars

4.1.1 *Spirals*

We begin by considering the bright parts of the LFs, $-9 < M_v < -3$. The only spiral galaxy for which a meaningful LF estimate can be made at present is M33 (type Sc). Following the procedure used by Berkhuijsen (1982), a LF was constructed by counting stars in Table 5 of Humphrey and Sandage's (1980) M33 bright star catalogue, which is "fairly complete" down to $V = 18.3$, keeping only stars with $B-V \leq 0.0$. A distance modulus of $(m-M)_0 = 24.3$ and extinction $A_v = 0.75$ was adopted (see Berkhuijsen, 1982). The sample included stars as faint as $V = 18.5$, giving 101 stars after omitting stars with

uncertain magnitudes or colors. Inclusion of stars with $0.0 < B-V \leq 0.2$ (52 more stars) did not significantly change the shape of the derived LF, which is shown in Figure 39 by plus signs.

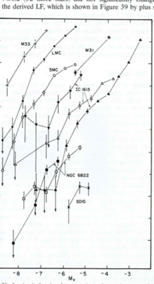

FIGURE 39 Luminosity functions for seven galaxies. See text for sources of data.

Unfortunately, because of the relatively great distance of M33 ($\sim 1 Mpc$), there is almost no overlap between the M33 LF and the local LF in our galaxy, so no comparison can be made. However for comparison the LF of the brightest stars in clusters in the spiral M31 (Andromeda) compiled by Hodge (1980b, converted from M_B to M_v) is also shown. (Counts were given by Hodge for an interval centered on $M_v = -2.75$, but the counts appear seriously incomplete for this interval and are therefore not shown.) Note that the M31 data has the same slope as an extrapolation of the M33 LF to fainter magnitudes.

4.1.2 *LMC and SMC*

Considerably more information is available for the irregular-type satellites of our galaxy, the Large and Small Magellanic Clouds (referred to as the LMC and the SMC in what follows). These galaxies are relatively small (diameters ≈ 12 kpc and 8 kpc for the LMC and SMC), blue, gas-rich, and metal-poor (metal abundance by mass $Z \approx 0.008$ and 0.002 for the LMC and SMC, compared with $Z \approx 0.02$ in the solar neighborhood). Instead of the current star-forming activity being organized into a spiral pattern, it is scattered rather irregularly in a small number of very active sites, perhaps generated by the stochastic self-propagating mechanism modeled by Gerola, Seiden, and Schulman (1980). Because of the substantial differences between the properties of irregular galaxies and our own galaxy, one might expect any variations of the stellar mass spectrum on the global scale to manifest itself in these systems. We consider the bright end of the LFs of the LMC and SMC here, and return to the fainter stars after discussing the bright star LF in three other irregular galaxies, IC 1613, NGC 6822, and the Sculptor Group Dwarf Irregular Galaxy.

Lequeux *et al.* (1980) constructed a LF in M_{pg} for a large field of the LMC using data from the catalogue of Rousseau *et al.* (1978), which is free from galactic contamination because the sample was based on radial velocities and spectral types. It is believed that the catalogue is complete to $m_{pg} \approx 13$ ($M_{pg} = -5.7$ or $M_v \approx -5.2$ for a LMC distance modulus of 18.7), although there is probably some incompleteness due to crowding effects at the faintest magnitudes. Selecting only stars with $B-V < -0.10$ (to eliminate red supergiants), the completeness factors are estimated as 100% in the field, 80% in dense associations, and 50% near small compact clusters. To check for crowding effects, they compare the total LF with the LF calculated by excluding the most crowded fields. The two samples are very similar, suggesting that crowding is not important. The extinction is fairly small (except in 30 Dor), and should not much affect the derived LF. Lequeux *et al.* note that the depth of the LMC system only introduces a spread $\Delta M \approx 0.2$ mag, which is not significant for the present applicaton.

The results of Lequeux *et al.* (1980) for the LMC differential LF converted to M_v is shown in Figure 39 as the closed circles. The normalization is arbitrary, since we are only concerned with the shape. The error bars only reflect statistical uncertainties due to the number of stars. Except for a marginal steepening at the brightest magnitudes, the LMC LF is remarkably similar to the M33 and M31 estimates. The "hump" referred to by Lequeux *et al.*, which occurs at $M_v \approx -7.4$, can be seen, but is not very pronounced.

Vangioni-Flam *et al.* (1980) applied a similar method to the SMC using the catalogue of Azzopardi and Vigneau (1975, 1979), which is estimated to be 80% complete to $B \approx 14$. No correction for crowding was applied, since the effect seems less severe than for the LMC. Likewise, the internal extinction is small, and so no correction was made. The distance modulus was taken as 19.2. The LF in M_B had to be measured from their Figure 3; the result after conversion to M_v is shown in Figure 39 as open circles. There is no gross difference in the LMC and SMC LFs (note that the faintest points shown may suffer from incompleteness), although, as pointed out by Vangioni-Flam *et al.*, there is a marginal excess of very bright stars in the SMC compared to the LMC; this difference, however, is at the 1σ level. The slight flattening around $M_v \approx -6$ may be real or a reflection of incompleteness.

4.1.3 *IC 1613, NGC 6822, and SDIG*

IC 1613 is a more distant dwarf irregular galaxy ($m-M \approx 24$) which is one of the faintest such galaxies in the local group ($M_v \approx -15$). Baade's unpublished star counts over an 11′ region, as analyzed by Sandage and Katem (1976), formed the most complete set of published data for the galaxy at the time of this writing. The early counts from Mount Wilson blue plates were converted to photoelectric B magnitudes by Sandage and Katem. Baade had already accounted for foreground stars. Crowding effects were apparently not considered. Sandage and Katem give the resulting differential M_B luminosity function, assuming $(m-M)=24.5$, in the range $-7.8 \le M_B \le -2.8$, and the results in terms of M_v are reproduced in Figure 39 as filled triangles. Note that the overlap in M_v with the LMC and SMC LFs is too small for a comparison. (The brightest 3 points contain only one star each.) The comparison of the IC 1613 LF of Sandage and Katem (1976) with the LMC LF of Hodge (1961), (which was not included in Figure 39) given by van den Bergh (1983) suggests that the IC 1613 LF is steeper.

Additional studies of IC 1613, considering a wide range of problems, have been published by Hodge (1978, 1980a), who was concerned with the evolutionary history of nearby dwarf irregulars. Hodge (1978) noted that his LF is not inconsistent with that of Sandage and Katem, and that it seems that the proportion of bright stars ($M_B < -3$) decreases as one moves outward in the galaxy, in agreement with a suggestion by Sandage and Katem.

In a later paper, Hodge (1980a) compared the bright star luminosity functions of the Local Group dwarf irregulars IC 1613 and NGC 6822. NGC 6822 has a distance modulus of about 23.2 and an absolute magnitude of about $M_v \approx -15$. Because of its small galactic latitude, contamination by foreground stars is a major problem. Adding up only the numbers of blue stars of individual OB associations in these two galaxies, Hodge obtained combined LF data for each system. These results are shown in Figure 39 as open triangles and filled squares for IC 1613 and NGC 6822, respectively. Note that while a point is shown for the 0.5 mag interval centered on $M_v = -8.25$ (1 star each in IC 1613 and NGC 6822), no stars were found in the $M_v = -7.75$ interval for either IC 1613 or NGC 6822, or in the $M_v = -7.25$ interval for IC 1613. The IC 1613 and NGC 6822 data are incomplete beyond $M_v \ge -3.25$ and $M_v \ge -5.75$, and these data are therefore not shown. These results should be considered tentative because problems with reddening, crowding, foreground contamination, etc., were not considered in detail. Hodge pointed out the similarity between the LFs of IC 1613, NGC 6822, the LMC, and the solar neighborhood.

A study of the Sculptor Dwarf Irregular Galaxy (SDIG) has been presented by Lequeux and West (1981). This galaxy, a member of the Sculptor Group of galaxies, is very distant $(m-M \approx -11)$. The

brightest star has $M_v = -6.3$, and the galaxy's linear extent is only about 1 kpc. A determination of its LF would therefore be very interesting, but quite difficult. Lequeux and West obtained photometry of the brightest stars in the SDIG. After subtraction of sky background and magnitude calibration, a preliminary cumulative LF of the blue stars was constructed. The extinction and crowding corrections were considered negligible. This LF was compared with the LFs of IC 1613 and NGC 6822 using data from Humphreys (1980). Unfortunately, the published cumulative LFs are misleading. (Cumulative distributions nearly always appear similar.) Differential LFs measured from their Figure 3 do not exhibit a smooth LF. The SDIG data contain only 20 stars, while the IC 1613 and NGC 6822 data contain 50 and 158 stars, respectively. Omitting the magnitude intervals which contain less than 2 stars, the differential LFs so obtained are plotted in Figure 39 as crosses (SDIG), inverted triangles (IC 1613), and open squares (NGC 6822). Excluding the two faintest points from NGC 6822 and SDIG, which are probably affected by incompleteness, this leaves only 2 usable points for the SDIG, so a meaningful LF cannot yet be estimated. The results for IC 1613 and NGC 6822 should be compared with Hodge's (1980b) LF for the brightest stars in the associations of these galaxies also shown in Figure 39 as discussed above.

4.1.4 *Comparison*

In order to facilitate the visual comparison of these galactic LFs, all the data points representing more than one star were normalized arbitrarily to obtain Figure 40. (The faintest SDIG point was omitted because of almost certain incompleteness.) Considering the varieties of search strategies, corrections (or non-corrections) for effects of absorption, crowding, foreground stars, etc., and the magnitude of the statistical uncertainties (see Figure 39), the agreement between the LFs of these galaxies seems remarkable. While marginal differences in form can be found, the similarity is the most striking feature. A linear fit to the data would have $d\log N/dM_v = 0.5$–0.6. The corresponding range in the IMF index

$$\Gamma = (d\log N/dM_v)(dM_v/d\log m) - (d\log \tau_{ms}/d\log m)$$

is about -2.0 to -2.6 for the relevant mass range. For further com-

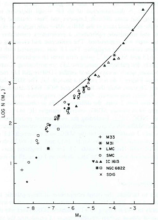

FIGURE 40 Luminosity functions of galaxies in Figure 39 normalized to exhibit their similarity. The adopted Galactic field star luminosity function is shown as the solid line.

parison, the solar neighborhood LF adopted in Section 2.2.2 above is shown as a solid line. For $M_v > -5.5$ the agreement with the overlapping data points is again surprisingly good. For the brighter stars the solar neighborhood LF appears flatter than most of the other galaxies which overlap in this magnitude range, with $d\log N/dM_v \approx 0.4$, corresponding to $\Gamma \approx -1.5$. However it should be remembered that the local LF remains fairly uncertain at the brightest luminosities (it

may be steeper if later spectral classes are included in the sample; see Section 2.6.4), and the slope in this magnitude range may fluctuate somewhat with position in the galaxy so that we cannot be sure what our own "galaxy-wide" LF would look like to an observer in another galaxy. We conclude that the available data is consistent with the universality of the galaxy-wide LF (and therefore probably the IMF) for $M_v < -3$, with suggestions of variations at the 1–2σ level for the brightest stars ($M_v < -6$).

A more definitive test of the idea of a universal IMF requires a larger and more homogeneous sample to fainter limiting magnitude. Freedman (1983, 1984, 1985) has analyzed deep photographic and CCD images of the galaxies M33, NGC 2403, M81, NGC 300, Ho

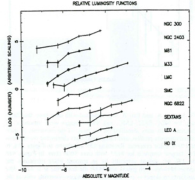

FIGURE 41 (a) Luminosity functions of galaxies determined by Freedman (1984, 1985);

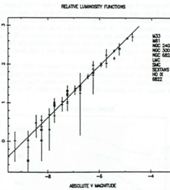

FIGURE 41 (b) same luminosity functions shifted vertically by an amount which minimizes the scatter between each galaxy and M33.

IX, Sextans A, and Leo A, supplemented with data from the literature for NGC 6822, LMC, and SMC. Images were measured by machine, with stars identified on the basis of the moments of individual intensity profiles, and foreground stars eliminated on the basis of a U-V color criterion. Resulting LFs are shown in Figure 41a, b. The largest sample is for M33, with over 5000 stars. In Figure 41b the LFs are shifted vertically by an amount while minimizes the scatter between each galaxy and M33; the line is the fit to M33. The similarity in slopes is evident, with differences occurring only at the brightest end where the numbers of stars is small. The slope for M33 is $d\log N/dM_v = 0.67 \pm 0.03$, a little steeper than the LFs in Figures 39 and 40, presumably because of better completeness, but also because Freedman's LFs extend to brighter M_v, where the IMF may steepen. Also, as printed out by Freedman, the derived slopes depend on the color criterion used to eliminate foreground stars; however, using the same criterion for all the galaxies, the *relative* slopes should be unaffected. If the differences in slope in Figure 41a, as estimated by Freedman, are taken literally, then, assuming no metallicity dependence of the $m(M_v)$ and $\tau(m)$ relations, the corresponding differences in IMF slope Γ would be around ± 0.5. However considering the uncertainties, Figure 41 is consistent with the conclusion that significant variations in the IMF of massive stars do not exist on the galactic scale, in agreement with the earlier result based on a more heterogeneous compilation of data. Again, it should be noted that the galaxies in Figure 41 represent a variety of morphological types and metallicities (five of the galaxies are Irr, while the remaining three are Sb or Sc).

Furthermore, Freedman finds no significant variations in slope with position or metallicity in the galaxies studied so far (see Section 7.1 below). In Section 4.2 below we shall see that the LF of fainter stars in the LMC also shows no significant variations with position. These results imply that approximate universality of the high-mass IMF may apply to all scales larger than ~ 1 kpc.

Hoessel and coworkers (see Hoessel *et al.* 1983; Hoessel and Danielson 1984) have also made much progress in deriving luminosity functions and other properties of a number dwarf irregular galaxies, using new CCD photometry for most the galaxies (for a summary, see Hoessel 1985). The resulting main sequence (defined as all stars with $B-V<0.5$) LFs for 11 dwarf irregulars are shown in Figure 42; the galaxies are qualitatively ordered from top to bottom by decreasing luminous stellar content. As noted by Hoessel (1985), the slopes at the bright end are consistent with a constant value. The average logarithmic slope is not well-determined, but the average $d\log N/dM_B$ for Holmberg II, Sextans A, and NGC 6822 is 0.55, a little less steep than found by Freedman, probably reflecting differences in reduction techniques, color criteria for inclusion, and treatment of crowding, but in good agreement with the compilation shown in Figures 39 and 40.

We have compared three independent compilations of bright star LFs for external galaxies. In every case the most striking result is the similarity of LFs between galaxies, even though the galaxies differ in morphology and metallicity. Considering that star formation rate histories in the irregular galaxies may have varied over the past $\sim 10^7$yr, affecting the present-day LF, this agreement points strongly to a nearly-universal massive star IMF in galaxies averaged over scales > 1 kpc. As mentioned above, power law IMFs fit to these data would give a corresponding scatter of less than about ± 0.5 in Γ.

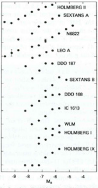

FIGURE 42 Luminosity functions (in M_B) for dwarf irregular galaxies determined by Hoessel and co-workers (from Hoessel, 1985).

It is difficult to reliably convert the LF slopes of Figures 39 to 42 to IMF indices because the LFs extend to much brighter M_vs than the calibrations adopted in Tables IV and V; the corresponding masses extend up to several hundred solar masses if $dM_v/d\log m = -5$. Especially uncertain are the lifetimes, which are probably significantly reduced by pulsational mass loss. For illustration, if we adopt

$\tau_{ms} \propto m^{-1/2}$ (the approximate relation for $25 < m < 60$), the IMF indices are $\Gamma \approx -3.1 \pm 0.5$ for Freedman's slopes; with a constant lifetime the IMFs would be steeper. This value is consistent with the steepening of the local IMF at $\sim 100 M_\odot$ found by Humphreys and McElroy (1984), although the latter result depends on the effective temperature calibration of the early O stars. For the data in Figures 39 and 40, and for the LFs of Hoessel *et al.* (Figure 42), the result would be $\Gamma \sim -2.0$ to -2.6. However the absolute (uncertain) values of Γ are less significant than the indications of uniformity of Γ.

Additional evidence for a universal LF in galaxies, at least at the bright end, has been given by Sandage and Tammann (1974), who showed that the absolute blue magnitude of the brightest blue star in a galaxy, $M_B(1)$, is well-correlated with the integrated photographic luminosity of the parent galaxy, M_{gal}, for 11 galaxies. Holmberg (1950) had shown that if the LF is a universal power law then a linear relation between $M_B(1)$ and M_{gal} is expected. A least squares fit to Sandage and Tammann's data gives $M_B(1) = 0.315 M_{pg}(\text{gal}) - 3.48$, with a highly significant correlation. Furthermore Sandage and Tammann point out that their derived slope is reasonably consistent with that expected from the bright end of the solar neighborhood LF. Thus their work supports the contention that the galaxy-wide IMF is universal, and that any deficit of very bright stars in smaller galaxies (as in IC 1613) can be ascribed to the smaller number of stars. In a more recent study, Humphreys (1983b) finds the same sort of correlation between luminosity of the brightest star and luminosity of parent galaxy, but states that the correlation of the brightest star luminosity with sample size or area of the galaxy is not as strong as might be expected if the effect is statistical. Instead, Humphreys suggests that the correlation might be due to flatter IMFs in smaller galaxies. The LFs presented here, while inadequate in many respects, give no indication of such a trend. Schild and Maeder (1983) have recently reexamined this question in more detail using simulated populations of stars drawn from identical IMFs, and conclude that the observed correlations can be accounted for by statistical effects alone. Their comparison of the observed correlation with the simulation prediction is shown in Figure 43.

This statistical interpretation suggests that there is no special process which limits the masses of stars. However it is also possible that the $M_B(1) - M_{gal}$ correlation is an artifact caused by crowding effects, which give *apparently* larger brightest star luminosities for larger populations and larger distances (Freedman 1983, 1984). If this interpretation is correct, then the upper mass limit of the IMF could be approximately the same in all galaxies, implying the existence of a physical effect which limits stellar masses. In either case, the observed correlation does not imply a systematic variation of either the shape of the IMF or the upper mass limit.

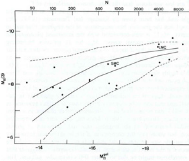

FIGURE 43 Relation between luminosity of third brightest star in a galaxy as a function total galaxy luminosity. Lines show the area which is predicted by simulations to be occupied if all galaxies have the same stellar luminosity function, so that the correlation is a result of sample size. Solid lines are 90% confidence limits, dashed lines 50% confidence limits. From Schild and Maeder (1983).

4.2 Fainter stars in the LMC

For the fainter portions of the LF, $-3 \le M_v \le 4$, only the LMC has been studied in enough detail to construct a LF. Surprisingly, even though photographic photometry to very faint magnitudes ($m_v \sim 22$–23) are required, the resulting LFs can be considered trustworthy. This is due in large part to the development of efficient interactive image processing systems, which fit mean image shapes to data images, and the generation of artificial starfields to estimate corrections for crowding and incompleteness. These procedures allow reliable star counts down to $V = 22$–23. The corrections remain small until $V \approx 23$, where they reach about 25% and increase rapidly at fainter magnitudes. This means that the LMC LF can be estimated down to $M_v \approx +3$ or $+4$.

These techniques were applied successfully by Butcher (1977) to two small LMC field regions, one near NGC 1866, about 4° north of the bar, the other a smooth field about 18′ south of NGC 1866. A 95″ region was used to study the bright stars, while a 48″ subregion was used to study the faint stars. The NGC 1866 region was chosen so that existing photoelectric photometry on NGC 1866 could be used to provide a standard magnitude sequence. The region was so small that foreground objects presented no problem; on the other hand, the study in this small region could not reveal the galaxy-wide LF. Giants and subgiants could be subtracted out on the basis of the color-magnitude diagram. Stryker and Butcher (1981) applied similar procedures to a region 4.5 northwest of the bar. Good agreement with Butcher's results were found, suggesting that his results apply to the galaxy-wide LF (see also Stryker, 1983). Butcher's results ($0 \le M_v \le 4$) are shown in Figure 44 as crosses. The adopted solar neighborhood LF is shown for comparison.

Hardy (1978) extended this work to the magnitude range $-2.5 \le M_v \le -0.2$. He obtained a number of *B* and *V* plates each in 8 areas (4 north, 4 south of the central region), each of 3.4′ diameter. He estimated completeness to $M_v \approx 0$, but the data with $M_v \le -1$ may be contaminated by giants. Figure 44 shows his LFs both for the combined north and south regions for all 8 averaged plates (filled circles), and for the north (filled triangles) and south (open triangles) regions separately. It can be seen that the north and south regions agree very well, suggesting that a galaxy-wide LF for the LMC is meaningful. A comparison with the solar neighborhood is uncertain because of the presence of giants in Hardy's LMC sample.

More recently Hardy *et al.* (1984) carried out a deep study of a region near the northwest end of the LMC bar, and presented a luminosity function which is shown as the open circles in Figure 44.

This result is quite important because the earlier LF determinations referred to outlying LMC regions, about 5–9 kpc from the center. Considering the uncertainties in both the solar neighborhood and LMC data, the agreement between the LFs of the NW bar, the peripheral LMC regions, and the solar neighborhood is surprisingly good, arguing again for a universal IMF both among and within galaxies.

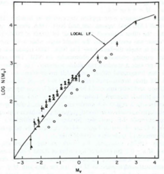

FIGURE 44 Estimates of luminosity function in several regions of the Large Magellanic Cloud, from Butcher (1977, crosses), Hardy (1978, triangles and filled circles), and Hardy *et al.* (1984, open circles).

There have been suggestions, based on indirect arguments to be presented in Section 5 below, that there is a deficiency of low-mass stars in blue dwarf galaxies. Available star count studies do not probe this low-mass region with $M_v > 4$, but future ground based CCD observations and Space Telescope observations should be able to test this hypothesis.

4.3 LMC and SMC IMFs from spectroscopic matching

In Section 4.1.2 it was seen that the available star counts for the LMC and SMC do not reveal any large differences between the LFs, and hence the IMFs, of these galaxies, nor between these objects and the field star LF, although the field star LF may be somewhat less steep for $M_v > -5$. Because of the large uncertainties in the LFs, it is important to compare the LMC and SMC mass functions derived by the method of spectroscopic matching, as was done in Section 2.6.4. for massive solar neighborhood stars. The major problem with the application of the spectroscopic matching method to external galaxies is that spectral classification requires relatively bright stars ($m_v < 14$–16 at present). For this reason, the samples, even for the nearest galaxies, are incomplete even for the O stars and the IMF determination is based mostly on evolved stars, for which evolutionary tracks are notoriously uncertain, as pointed out by Lequeux (1984, personal communication). The brief review of this work given here may still serve to emphasize the problems involved.

The first study of the LMC and SMC IMF using spectroscopic matching was presented by Dennefeld and Tammann (1980). These authors used a sample of supergiants in the LMC and SMC from different catalogues, converted to M_{bol} and T_{eff}, and then counted the number of stars lying between theoretical tracks of 9, 15, and 25 $M_\odot$ models to derive a mass function based on these points. Dennefeld and Tammann suggest that the SMC mass function at very high masses is flatter than the LMC mass function, similar to the finding of Vangioni-Flam *et al.* (1980). I attempted to reconstruct the mass functions from Dennefeld and Tammann's data, but encountered some difficulties. The data consists of only three mass intervals and the counts at the lowest masses are incomplete. At large masses the appropriate upper mass limit is unknown, and I adopted a limit of $m = 75$; the actual value may be much larger, but is not essential for the comparison. Using their results, I could find no evidence for a flatter mass function in the SMC, no matter which catalogue sample was used, or whether the blue, yellow, or combined supergiants were examined. The statement is made stronger when one considers the large uncertainties at each of the three mass intervals due to crowding, incompleteness, the bolometric correction and effective temperature scales, and the theoretical evolutionary tracks.

More recent LMC and SMC IMF studies using spectroscopic matching have been presented by Humphreys (1983a, b) and Humphreys and McElroy (1984). In the first paper Humphreys found good agreement between the LMC and the solar neighborhood, but evidence for a deficiency of high mass stars in the LMC, contrary to the claim of Dennefeld and Tammann (1980). In the second paper, Humphreys found that, including only stars earlier than O9.5 in order to compare with GCC, the IMFs of the LMC and SMC agree well with each other, but are extremely flat ($\Gamma \approx -0.6$ to -0.7) compared with the solar neighborhood IMF. The paper by Humphreys and McElroy (1984, HM) supersedes the previous papers because of the larger sample and the inclusion of later spectral types, but primarily because of the recognition of serious incompleteness at the smaller masses; it also supersedes the result presented in the review by Humphreys (1984). The IMF result of HM for the solar neighborhood was discussed in Section 2.6.4. This local IMF is

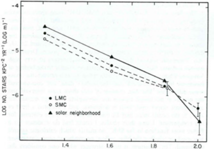

FIGURE 45 Estimates of the high-mass IMF in the LMC, SMC, and solar neighborhood using spectroscopic matching, from Humphreys and McElroy (1984). The points at lowest mass are based on an extrapolation of the luminosity function to account crudely for incompleteness.

shown in Figure 45 along with HM's IMFs for the LMC and SMC. The values at the lowest mass point were all corrected for incompleteness by an extrapolation of the luminosity functions from $M_{bol} < -8$ to fainter magnitudes, so the agreement of the IMFs below $\log m = 1.61$ only reflects the agreement of the IMFs at larger masses. For the two mass intervals in common, at $\log m = 1.61$ and 1.85, the LMC, SMC, and solar neighborhood slopes agree. The marginal steepening of the LMC IMF above $\log m = 1.85$ is at the 1σ level. While it is encouraging that this latest result agrees with the conclusions drawn from the luminosity functions, it seems clear that the method of spectroscopic matching is not suitable for determinations of extragalactic IMFs because of the required relatively bright limiting magnitudes. Estimates of IMFs from LFs can reach stars some 8–10 magnitudes fainter than the limit for spectral classification. The method of spectroscopic matching will remain important, however, for studies of the solar neighborhood.

5 INDIRECT EVIDENCE: INTEGRATED LIGHT OF GALAXIES

All the estimates of stellar mass spectra which we have discussed so far are based essentially on counts of stars as a function of luminosity. The term "indirect estimate" will be used for methods which do not employ star counts but still yield some information on the IMF. Such observable quantities as broad-band colors, mass-to-light ratios, elemental abundances and abundance ratios, spectral line strengths, etc., have been used in attempts to indirectly constrain the IMF of our own and other galaxies. One may well wonder how such methods can yield any useful information concerning the IMF when direct star counts have proven quite problematical. The answer is that most of these methods *are* relatively insensitive and ambiguous, but they sample distant volumes of space and large numbers of objects which cannot be studied by star counts. Besides the brightest stars, which can be counted only in the nearest galaxies, our knowledge of the IMF from star counts is essentially limited to the region within 20–1000 pc from the sun.

The problem with indirect methods is that the observable quantities on which they are based in all cases depend on one or (usually) more additional functions and/or theoretical input data which are uncertain to various degrees, such as the star formation rate (SFR) history, red giant evolutionary tracks, abundances of nucleosynthesis products ejected by massive stars, and so on. The resulting interpretation is therefore usually ambiguous and highly uncertain, but taken together, indirect methods may yield some clues to the gross properties of the IMF and especially its possible variations in space and time, information which in most cases cannot be obtained from star counts.

Because of the large number of published papers relevant to this section and the variety of approaches, often interrelated, which can be used to provide indirect IMF constraints, I have found no completely satisfactory way to order the presentation. In addition, it is not feasible to review all the work in this area. I have attempted to present a resaonably complete cross section, concentrating on recent studies, but I have omitted some indirect IMF constraints for which observational uncertainties and/or model dependence are very severe. Examples include the relation between a (possible) helium abundance-metal abundance correlation and the IMF, and attempts to relate supernova rates to the IMF. It will be seen that many of the arguments included in the following discussion unfortunately also fit this description.

The discussion begins with an examination of IMF constraints provided by photometry and spectrophotometry of the integrated light of external galaxies, proceeding generally from methods which provide information on the low-mass IMF to those which probe larger masses. The discussion then turns in Section 6 to IMF constraints derived by comparing observed elemental abundances with chemical evolution models, and finally, in Section 7, indirect (and direct) evidence related to internal IMF variations within our own and other galaxies. An attempt to summarize the results of all these diverse lines of evidence is given in the final section.

5.1 Giant/Dwarf Indicators

It is possible to place a constraint on galactic IMFs in the mass range $0.1 \lesssim m \lesssim 1$ using spectral features in the integrated light of galaxies which provide a measure of the relative numbers of giants and dwarfs. The light contributed by giants depends on the number of

stars in a very small mass range just above the turnoff mass, at least for old stellar systems, which is $\sim 1 M_\odot$, while the light from dwarfs comes from all masses less than the turnoff mass, so a steeper IMF will result in a smaller giant/dwarf ratio. Tinsley (1980) shows that for a model E galaxy in which the IMF is a power law with index Γ and in which the mass-luminosity relation is a power law with index $\alpha(\approx 5)$, the ratio of luminosities contributed by giants and dwarfs is proportional to $(\alpha+\Gamma)$. It is important to note that the ratio will be sensitive to Γ *only* when the IMF is steep, $\Gamma \lesssim -2$ or so.

There are several molecular spectral features which are known to depend on stellar surface gravity. These include the Wing–Ford FeH band at 0.99 μm, the H_2O bands, and the CO bands. Additional gravity-sensitive features are the TiO bands and the neutral Na I λ8190 doublet, but the use of these features as IMF probes is complicated, mostly by the fact that they are sensitive to the M giant population, whose inclusion in model galaxy calculations is still quite uncertain. The dependence of these features on surface gravity, or essentially atmospheric gas pressure, can be demonstrated analytically from the conservation equations of dissociation equilibrium (see Scalo 1974). More recently, Jones, Alloin, and Jones (1984) have shown that the Ca II infrared triplet is very sensitive to gravity and insensitive to metallicity, and so may provide a useful tool for studying the giant/dwarf ratio in future work.

Whitford (1977) presented a detailed study of the behavior of the Wing–Ford FeH band in galaxy models and compared these predictions with observed band strength ratios in seven galaxies. The predicted band strength index is shown as a function of Γ in Figure 46; the relative contributions of giants and dwarfs are indicated. Notice the insensitivity to Γ for $\Gamma \gtrsim -2$, as pointed out above. (The behavior of the FeH index as a function of time for three values of Γ can be found in Figure 3 of Tinsley and Gunn 1976.) The data point is the mean value of the FeH index for the seven galaxies. The galaxies include the three brightest E galaxies in the Virgo cluster, a dwarf elliptical (M32), and SO, two Sb's, and an Sab. The observed FeH indices range from 0.008 ± 0.009 to 0.017 ± 0.008. A dwarf-enriched population with $\Gamma \gtrsim -2$ is ruled out by this comparison. However, a more stringent limit cannot be imposed because the observed index is smaller than the predicted index even for $\Gamma \gtrsim 0$. Whitford lists a number of effects which might depress the FeH index, but at present the discrepancy remains unresolved. Nevertheless, the constraint $\Gamma \geq -2$ is consistent with the shape of the disk field star IMF, which has $\Gamma \sim 0$ over the relevant mass range, $0.15 \leq m \leq 1$.

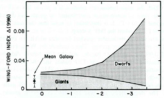

FIGURE 46 Predicted behavior of the Wing–Ford FeH band strength index as a function of IMF index Γ, from Whitford (1977). Contributions of dwarfs and giants are shown, as well as the mean observed index for seven galaxies.

The observed strengths of the CO and H_2O bands, at 2.4 μm and 1.9 μm respectively, can also be used to constrain the slope of the IMF in E galaxies, as shown by Frogel, Persson, and Cohen (1980, and earlier references given there). A plot of the narrow-band H_2O and CO indices in a sample of bright E and SO galaxies, along with the indices for Galactic and M31 globular clusters, from Frogel *et al.* (1980) is shown in Figure 47. The lines show the predicted loci for model galaxies which formed all their stars 10^{10} yr ago from a power law mass function. (For the dependence of CO index on age, see Figure 3 of Tinsley and Gunn 1976.) The parameter s in the figure is equal to $1-\Gamma$, with Γ the IMF index as defined here. The results are shown for 3 different values of $1-\Gamma$ and 4 values of the metallicity (logarithmic, relative to solar). Since H_2O is strongest for dwarfs while CO is strongest for giants, a steepening of the IMF causes a shift to the upper left in this diagram. Both H_2O and CO will strengthen with increasing metallicity, so a metallicity change causes a shift which is nearly orthogonal to the shift caused by an IMF change.

Figure 47 shows that a very steep IMF with $\Gamma \leq -2$ for $m \leq 1$ can

be ruled out for E galaxies; the large ratio of dwarfs to giants in such a case would give very strong H_2O and weak CO. However, just as for the FeH band strength, this method is insensitive to the dwarf/giant ratio for $\Gamma > -2$ because in that case the giants dominate the integrated light. Considering the large uncertainties in the measured band strengths as indicated in the figure, one can only conclude that $\Gamma \geq -2$ for E galaxies as well as globular clusters. A similar result is found from the $CO-(V-K)_0$ diagram (see Fig. 3 in Frogel *et al.* 1980).[1]

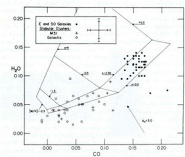

FIGURE 47 H_2O (1.9μm) − CO (2.4μm) band strength diagram, from Frogel *et al.* (1980), for E and SO galaxies and globular clusters. Lines of constant $s = 1-\Gamma$ and metallicity are indicated.

It is difficult to compare the result $\Gamma \geq -2$ for globular clusters, based on the integrated light, with the IMFs derived from luminosity functions in Section 3.8 because the latter IMFs are not power laws

[1]The color–color diagrams for E galaxies cannot be used to constrain Γ, apparently because of the presence of an excess population of asymptotic giant branch stars which are not accounted for by the galaxy models; see Frogel *et al.* (1980) for a discussion.

and show considerable variation (although these variations may not reflect real IMF differences, as discussed in Section 3.8). The result $\Gamma \gtrsim -2$ is probably consistent with the overall form of the cluster IMFs, although it should be noted that some of the cluster IMFs are steeper than this near the turnoff mass. The result is certainly consistent with the halo field star IMF given in Section 2.7.

In summary, studies of giant/dwarf indicators rule out the presence of a strongly dwarf-enriched IMF with $\Gamma \lesssim -2$ for all galaxies and globular clusters which have been studied. Most of these galaxies are bright ellipticals, but a few galaxies of different types are included in Whitford's (1977) work. It is unfortunate that the physics of stellar stucture makes these tests insensitive to Γ for $\Gamma \gtrsim -2$, precluding a more detailed comparison with the solar neighborhood IMF of Section II, which has $\Gamma \sim 0$ in this mass range. However, it should be noted that all of the observations used so far refer only to the central regions of the galaxies studied. If one tries to explain the increasing M/L ratios found in the outer parts of many disk galaxies as due to an IMF which steepens with galactocentric radius (see below), then the appropriate value of Γ in the other regions might be smaller than -2, values to which the giant/dwarf indicators are sensitive. Such measurements would require small aperture observations of the faint outer regions, necessitating extremely long exposures. Furthermore, the evidence for radially steepening IMFs from M/L ratios is far from compelling, as discussed presently.

Finally, it should be noted that the giant/dwarf ratio may be affected by stellar interactions in galactic nuclei. Tuchman (1984) has investigated the dynamics of dwarf-giant collisions and shows that in most cases the dwarf is capable of stripping off the loosely bound envelope of the giant, a suggestion made earlier by Lacy, Townes, and Hollenbach (1982). For stellar densities appropriate to galactic nuclei, Tuchman finds that the collision rate is large enough to significantly reduce the number of red giants, although the reduction factor is very uncertain.

5.2 Mass-to-light ratios

Another possible constraint on the shape of the average IMF in galaxies is the mass-to-light ratio, M/L (see Faber and Gallagher, 1979 for a detailed discussion of observational determinations of M/L).

This ratio is roughly a measure of the ratio of the number of low-mass stars (*and* remnants and other dark matter), which contribute most of the mass, to the number of higher-mass stars, which contribute most of the light. Thus M/L should be larger for a steeper IMF. Tinsley (1980) shows that for a simple burst model $M/L \propto (1+\Gamma)^{-1}$ for $\Gamma > -1$. For $\Gamma < -1$, $M/L \propto m_l^{(1+\Gamma)}$, where m_l is the lower limit of stellar masses, a quantity which cannot be determined photometrically. In the solar neighborhood $M/L_v \approx 2.1$ in solar units.

Figure 48, taken from Whitford (1977), shows how the M/L_v ratio for the stellar component of model galaxies varies with the slope of a power law IMF with index Γ, for a star formation burst which occurred about 11×10^9yr ago, as is relevant to E galaxies. Results are shown for two different choices of the lower mass limit m_l, and show the behavior expected from the simplified formula given above. The dashed line marked "L" is the M/L_v ratio calculated from Larson's (1973) lognormal IMF for the solar neighborhood, which is similar to the IMF derived earlier in Section 2. The relation shown in Figure 48 is consistent with independent calculations quoted by Aaronson *et al.* (1978), and with more detailed theoretical models by Larson and Tinsley (1978). The theoretical M/L ratios are uncertain primarily because of the uncertain treatment of stellar remnants.

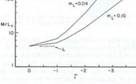

FIGURE 48 Theoretical variation of mass-to-light ratio with IMF index Γ for a star formation burst occurring 11×10^9yr ago, for two choices of the adopted lower mass limit. The dashed line is the ratio calculated from Larson's (1973) lognormal IMF, from Whitford (1977).

At the other extreme of ages, Figure 49 shows the theoretical $M/L_v - \Gamma$ relation for zero-age galaxies for $m_u = (40,100)$ and $m_l = (0.1, 1, 10)$, based on calculations by Melnick *et al.* (1984). This figure shows that M/L_v for galaxies which have just experienced a burst of star formation is insensitive to m_u even for a flat IMF, but retains the same type of dependence on m_l and Γ as for the E galaxy relation of Figure 48, shifted downward in M/L_v.

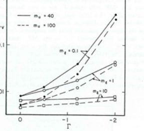

FIGURE 49 Theoretical variation of mass-to-light ratio with IMF index Γ for zero age galaxies for various values of m_l and m_u, from Melnick *et al.* (1984).

According to Faber and Gallagher (1979), the *mean* values of M/L_v within the Holmberg radius, based on rotation curves, as a function of morphological type vary from about 7 for SO galaxies to around 1 for late type galaxies (for a Hubble constant $H_0 = 50$ kms^{-1} Mpc^{-1}; M/L is proportional to H_0). The decrease can be at least qualitatively accounted for by the increasing fraction of blue stars, which control L_v in later type galaxies; there is marginal quantitative agreement with detailed models based on a constant IMF (see Faber and Gallagher, 1979, Table 2). The relevant systems for comparison with the initial burst calculations shown in Figure 48 are early-type galaxies, especially ellipticals. Although the derived M/L ratios are more uncertain for ellipticals because they rely on difficult measurements of the line-of-sight velocity dispersion, the mean value is $M/L_v \approx 6$ (12 for $H_0 = 100$). This value generally only refers to the core, but there does not seem to be any evidence for increases out to the Holmberg radius. From Figure 48 it can be seen that $M/L_v = 6$ to 12 again rules out a very steep IMF with $\Gamma \lesssim -2$ for $m \lesssim 1$. Taken at face value, Figure 48 suggests $\Gamma \sim -1$ to -2 for $m \lesssim 1$, steeper than the field star IMF, which predicts $M/L_v \sim 4$ to 6. However, given the uncertainties in both the observed and theoretical values, and the possibility of large amounts of dark nonstellar matter, this discrepancy should probably not be overemphasized.

Several galactic nuclei such as those of M82, NGC 253, and NGC 1068, have very small (and uncertain) M/L_{bol} ratios, inferred from their infrared radiation, in the range 0.003 to 0.04 (see Kleinmann, 1977; Rieke *et al.*, 1980). Such small M/L_{bol} values do not necessarily imply a deficiency of lower mass stars relative to the field star IMF, since they can be explained by a burst of star formation occurring in the recent ($\lesssim 5 \times 10^7$yr) past (e.g. Struck-Marcell and Tinsley, 1978, Table 1), and this "starburst" interpretation is now generally accepted (see Balzano, 1983, and references therein).

Somewhat stronger evidence for IMF differences comes from variations in M/L ratios within individual galaxies and among galaxies of the same morphological type. In spiral galaxies empirical M/L ratios within the Holmberg radius show a spread of a factor of about 2–3 at a given morphological type, with some values as large as 8–12 for early-type spirals (Faber and Gallagher, 1979). The spread might be attributed to observational uncertainties, variations in the size of the region for which the rotation curve was measured, and variations in the star formation rates, but the largest values, if real, suggest the presence of dark matter. The flat rotation curves of spiral galaxies at larger radii, determined both from optical and HI observations, give very large M/L ratios in these regions, and the existence of halos of dark matter is now generally accepted. *If* this dark matter is in the form of low mass stars, then either a steeper low-mass IMF or a smaller lower mass limit, compared to the solar neighborhood, is indicated. For example, Hegyi (1983) shows that in order to match the observed surface brightness data for the halo of NGC 4565, with $M/L_J > 60$, the value of Γ must be smaller than (IMF steeper than) -1.6 even with a lower mass limit as small as $m_l = 0.004 M_\odot$. An IMF index of $\Gamma = -1.35$ requires $m_l < 2 \times 10^{-4}$. Besides problems with understanding how large numbers of such low mass objects formed, there are more basic objections to attributing the halo mass to any baryonic component, especially constraints derived from calculations of big bang nucleosynthesis which show that if halos were baryonic, ^{4}He would be overproduced. These arguments only apply to the outer regions of spiral galaxies. The largest M/L ratios found within the Holmberg radius of some spirals could still be attributed to an IMF with an excess of very low mass stars, although nonbaryonic matter now seems just as plausible.

Variations in central M/L ratios determined from velocity dispersions in E galaxies have also been found, and are sometimes attributed to varying proportions of very low-mass stars. On the other hand the very large M/L ratio in the nucleus of M87 suggests the presence of a supermassive black hole (Young *et al.*, 1978), and Lauer (1984) finds similar structure in many bright E and SO galaxies. Correlations between M/L ratios and other properties of early type galaxies are not yet firmly established. For example, Faber and Jackson (1976) found that $M/L \propto L^{1/2}$ for ellipticals, suggesting a more elevated low-mass stellar fraction in brighter galaxies. However, a recent detailed study by Lauer (1984) indicates that M/L depends on central luminosity density ρ_c, not luminosity, with $M/L \propto \rho_c^{-0.17}$, a result which could be explained by a steeper low-mass IMF or a smaller lower mass limit in regions with smaller local mass density. Efstathiou and Fall (1984) have carried out a multivariate analysis of the observed blue luminosities, velocity dispersions, and line strengths in E galaxies and find that one of the parameters which control the correlations is M/L. This suggests that the low-mass IMF is affected by metallicity or by metallicity and the depth of the galaxy potential well. Terlevich and Melnick (1984) have also interpreted the correlation of M/L with Z in ellipticals as due to a Z-dependent IMF. Figure 50, from Terlevich and Melnick, shows a comparison of observations of Z and M/L_B for elliptical galaxies, giant HII regions in galaxies and isolated intergalactic HII regions, (discussed in Section 5.9 below), and globular clusters with model calculations based on a power-law IMF with $\Gamma = -4.0 - \log Z$. The light curve refers to the M/L ratio of the visible stars, while the dark curve is corrected for the presence of stellar remnants. The agreement is very good. However,

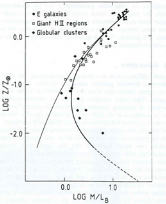

FIGURE 50 Observational and theoretical relation between metallicity and mass-to-light ratio, from Terlevich and Melnick (1984). The lines assume a power-law IMF with $\Gamma = -4.0 - \log Z$. Light curve refers to visible stars, dark curve is corrected for stellar remnants.

there are two problems. First, the predicted Γ for the ellipticals is $\Gamma \sim -2$ to -1.5, values which may be only marginally inconsistent with the giant/dwarf indicators discussed previously. Second, the M/L values for the HII regions are based on virial masses derived from emission line widths, and these masses may be inappropriate, as discussed in more detail in Section 5.9 below.

Still, the accumulating evidence does seem to point to a systematic dependence of the lower-mass IMF on some property of elliptical galaxies, but whether this property is the central mass density, the metallicity, or some other parameter, is not yet established. Alternately, the larger M/L ratios could be attributed to a large mass of higher-mass stellar remnants resulting from an enhancement of high-mass stars, perhaps due to a large value of m_b during the formation phase of E galaxies. We will encounter this idea again in the later discussion of chemical evolution.

5.3 Galaxy colors

Besides differences in morphological appearance, the most obvious difference between galaxies along the Hubble sequence concerns their colors, which vary from the red ellipticals to the very blue irregulars. This color variation presents an extreme example of the problem of deciding whether differences in galactic properties are due to variations in the IMF or variations in the star formation rate history, a problem I shall refer to as the "IMF–SFR ambiguity".

Certainly the color differences between E and Irr galaxies mean that the *present-day* mass functions differ, and, given no further information, one might speculate that the *initial* mass functions are responsible, with E galaxies forming only low-mass $\lesssim 1M_\odot$ stars and bluer galaxies forming increasing percentages of higher-mass stars. However, the color differences could also be due to a very small star formation rate in the recent past for the redder galaxies, since the existence of blue stars with a "normal" IMF requires active star formation within the past few times 10^7yr. The choice in this case is made clearer by the fact that the gas contents deduced from HI observations decrease for redder galaxies suggesting smaller present star formation rates in redder galaxies. On the other hand, Hunter, Gallagher, and Rautenkranz (1982) and Kennicutt (1983) find no correlation between the total SFR and the HI content in late-type galaxies.

A quantitative investigation of this problem was given in an influential paper by Searle, Sargent, and Bagnuolo (1973), who showed that the narrow distribution of most galaxies in the $(U–B)–(B–V)$ plane could be accounted for most simply if all galaxies formed at the same time and with the same IMF, but with different monotonically decreasing SFR histories. A similar conclusion was reached earlier by Tinsley (1968). The colors were found to depend mainly on the ratio of present SFR (i.e. averaged over the past 10^8yr) to average SFR

over the galaxy lifetime. Rocca-Volmerange *et al.* (1981) have found that this ratio controls the position of stars in the two-color diagram for basically *any* two colors.

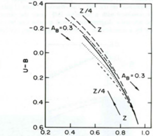

FIGURE 51 Theoretical two-color diagram for model galaxies with monotonic decreasing star formation rates, solar metallicity, but varying ages. Results are shown for different IMF shapes and upper mass limits.

The UBV colors are in fact not very sensitive to IMF variations. Figure 51, from Larson and Tinsley (1978), shows the theoretical two-color diagram for model galaxies with monotonic decreasing SFRs, solar metallicity, but different ages and IMFs. The IMFs used include a solar neighborhood IMF similar to the one derived in Section 2 (dark solid line) and power laws with $\Gamma = -1$ (long dashes) and -2 (short dashes); these three IMFs have an upper mass limit $m_u = 30$. Also shown is a case with $\Gamma = -1$ but $m_u = 10$ (dotted line). Notice the almost complete insensitivity of the colors of the redder galaxies with $B–V \gtrsim 0.8$ to the IMF. For the bluer galaxies, the IMFs used in Figure 51 are about the largest deviations from the local IMF which could be tolerated without predicting a greater color spread around the mean locus than is observed for normal galaxies. For example, Larson and Tinsley point out that $\Gamma = -2.6$ models would give colors well below the line for $\Gamma = -2$. However, it must be remembered that this could be compensated by increasing m_u to, say, $100 M_\odot$. Obviously UBV colors do not provide very stringent or discriminating constraints on the IMF. The observed colors of galaxies are certainly *consistent* with a universal IMF, since the observed spread in the two-color diagram for normal galaxies can be easily accounted for by a combination of observational errors, reddening

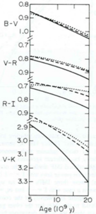

FIGURE 52 Theoretical colors as a function of time for $\Gamma = -2$ (solid lines), -1 (dashes), and 0 (dots). From Tinsley and Gunn (1976).

and model uncertainties. variations in metallicity, non-monotonic SFRs. However, colors alone do not allow a determination of Γ and/or m_u, let alone the distanglement of the effects of these two parameters. Colors involving infrared light, such as $V-K$, are somewhat more sensitive to the IMF if $\Gamma < -1$ as shown in Figure 52 (from Tinsley, 1980), but the infrared light is dominated by red giants whose modeling in the context of galactic photometric evolution is still very uncertain.

As shown by Larson and Tinsley (1978), the UBV colors of interacting galaxies show a much larger spread in the two-color diagram than do non-interacting galaxies. However, the now generally-accepted interpretation suggested by Larson and Tinsley is that these galaxies have suffered recent bursts of star formation induced by their interactions (see, for example, Kennicutt and Keel, 1984). Similarly, recent bursts of star formation can account for the very blue colors of some dwarf irregular galaxies; variations in the IMF, while still possible, are not required (see Gallagher and Hunter, 1984). Other lines of evidence concerning the high-mass IMF in "bursting" galaxies are discussed below.

5.4 Population synthesis: an example

All of the results discussed so far have been based on theoretical galaxy evolution models in which stellar evolutionary tracks are used to predict the galaxy properties for a given age, SFR history, IMF, and chemical composition. An alternative to this type of galaxy modeling is the method of population synthesis, which attempts to match the observed galaxy colors, spectrum, or line strengths by finding a "best" mixture of stars of various spectral types and luminosity classes. The properties of the various classes of stars are calibrated using observations of nearby stars, and so the method does not depend on stellar evolutionary tracks. All the methods for attaining a "best fit" try to minimize the residuals imposed on the solution. The question of tradeoff between uniqueness of the solution and the types of astrophysical constraints which should be imposed has remained a difficult problem. Detailed studies include Alloin *et al.* (1971), Faber (1972), Williams (1976), Turnrose (1976), and O'Connell (1976). More recent data, in the form of libraries of accurate stellar spectra with good coverage in wavelength, spectral type and luminosity class (Gunn and Stryker, 1983) will undoubtedly improve the situation.

Since the output of a population synthesis includes the number of main sequence stars of different spectral types, the reasonably well-established relation between spectral type and mass can be used to derive the present-day mass function. If the synthesis is based largely on the ultraviolet spectrum, which is controlled by relatively massive stars, the *initial* mass function can be derived by simply dividing the present-day mass function by the stellar lifetime at each mass [see Eq. (2.10)]. When other spectral regions are used (i.e. for masses $\lesssim 3M_{\odot}$) the conversion to the IMF will depend on the adopted SFR history, and so the IMF–SFR ambiguity is encountered.

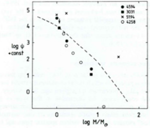

FIGURE 53 IMFs estimated for four galaxies using population synthesis by Ellis *et al.* (1982).

In practice, the use of the population synthesis technique to infer the IMF is quite difficult, and I will only discuss one recent attempt in this direction, by Ellis, Gondhalekar, and Efstathiou (1982), who analyzed absolute spectrophotometry from 1250Å to 4μm in the nuclei of four spiral galaxies of types Sa through Sbc. The synthesis algorithm used in this work only constrained the solution to produce positive fractional contributions to the composite spectrum from any

of the 28 stellar types which were included. Figure 53 shows the IMFs derived by Ellis *et al.* for the 4 galaxies studied, with arbitrary normalization. (The calculations assumed that the main sequence lifetimes are much smaller than the galaxy ages, an approximation which is not valid for the points with $m \lesssim 2$.) Also shown is the local field star IMF of Miller and Scalo (1979), which is similar to that of Section 2.

Ellis *et al.* give a realistic assessment of the limitations of the synthesis procedure for the estimation of IMFs, particularly the difficulty in distinguishing a small number of O stars from a larger population of B stars and the tendency for the models to produce populations clumped in only a few spectral types. These two effects are presumably responsible for the fact that for 3 of the 4 galaxies the models did not require any stars more massive than around $10M_{\odot}$, although it is also possible that very few more massive stars are present, especially for NGC 4594 (M101), which is discussed in Section 5.8 below.

5.5 Ultraviolet luminosities

The ultraviolet flux and spectrum from a young population must depend on the IMF and birthrate of massive ($m \gtrsim 3$) stars. The UV luminosity for $\lambda \lesssim 2000$Å is dominated by early B main sequence stars. The availability of satellite UV observations has led several groups to investigate how such measurements might be used to constrain the IMF.

One approach is to try to match the UV spectrum. Satellite observations of HII regions in the LMC (Israel and Koornneef, 1979) and other galaxies (Lequeux *et al.*, 1981) have been compared with theoretical calculations in this manner, but the results are sensitive to the uncertain extinction in the ultraviolet and are not very sensitive to the form of the IMF (see Lequeux *et al.*, 1981, Figure 1). Israel and Koornneef (1979) used a 2-segment power law IMF with $\Gamma = -1.1$ for $m < 20$ and variable Γ for larger masses and concluded that $\Gamma \approx -3 \pm 1$ for $m > 20$ gives an acceptable fit to the ultraviolet extinction curve, although values outside this range are possible considering the uncertainties. The value $\Gamma = -3$ is significantly smaller than even the steepest estimate for the local IMF for $m > 20$ discussed in Section 2.6.4.

Another approach tries to match only the absolute UV luminosity. Figure 54, based on Table 1 of Lequeux *et al.* (1981), shows the predicted luminosities at 1600 Å for clusters formed at $t=0$ as a function of Γ, for several different ages. The upper mass limit was taken as $m_u = 110$. (It should be noted that the variation of flux at ~1600 Å with Γ given in the Appendix of Israel and Koornneef for zero-age clusters is much less pronounced than the dependence found by Lequeux *et al.*, but I am unable to resolve the discrepancy.) For very young clusters, the 1600 Å luminosity increases by a factor of about 10 as Γ increases from -2.5 to -1.5, but the sensitivity decreases steadily with increasing age for $t \gtrsim 4 \times 10^9$ yr. Notice that without further information a given observed UV luminosity generally does not specify a unique Γ and age, another manifestation of the IMF–SFR ambiguity.

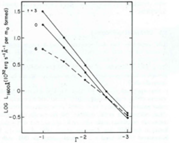

FIGURE 54 Theoretical UV luminosities for clusters formed at $t=0$ as a function of Γ for three ages.

A more recent study of the UV fluxes of 40 spiral and irregular galaxies has been given by Donas and Deharveng (1984), who estimate SFRs from the measured OAO-2 λ1910 fluxes. They adopt

a constant IMF with $\Gamma = -2$ for $m > 1.8$, and find that changes of Γ by ± 1 would change the UV luminosity by a factor of about 3. Given the large uncertainties in the derived SFRs due to the treatment of internal extinction and other effects, Donas and Deharveng suggest that the rather modest scatter in the derived SFR-gas mass correlation for these galaxies (roughly a factor of two) rules out fluctuations in Γ of more than 0.5 from galaxy to galaxy. Their result, $\Gamma \approx -2 \pm 0.5$, is consistent with the local field star IMF for $m \gtrsim 20$ discussed in Section 2.6.4. As they point out, however, a *systematic* variation of the IMF would be impossible to disentangle from the SFR variations. It is worth noting that the SFRs of Donas and Deharveng (1984) are much larger than these derived by Hunter *et al.* (1982) for two galaxies in common, apparently because of differences in the adopted mass–luminosity relation, according to Donas and Deharveng.

It is possible to weakly constrain the IMF using the observed strengths of ultraviolet atomic absorption lines which are unaffected by dust. In a multifrequency study of the very blue dIrr galaxies NGC 4214 and NGC 4670, Huchra *et al.* (1983) pointed out that the observed strengths of C III and Si IV rule out a flat IMF (or a population containing significant numbers of supermassive stars).

5.6 Methods based on Lyman Continuum Luminosity

Several of the studies to be discussed in the following sections attempt to constrain the IMF of massive stars in regions of active star formation by estimating the rate at which photons are emitted by stars in the Lyman continuum, N_{Lyc} (photons s^{-1}). Before proceeding, it will be useful to summarize the basic principles.

Given the value of N_{Lyc} for individual stars as a function of stellar mass, $N^*_{Lyc}(m)$, the total rate of emission of Lyc photons from a stellar population as a function of time can be computed from an integral of $N^*_{Lyc}(m)$ over the IMF and SFR, as in Eq. (1.21). When evolutionary tracks are used, the dependence of N^*_{Lyc} on luminosity and effective temperature is required. The derivation of such relations is complicated, depending on reliable model atmospheres and calibrations of the relations between effective temperature, M_v, bolometric correction, and so on. A useful discussion of the considerations involved is given by Panagia (1973). Figure 55 shows N^*_{Lyc} as a function of stellar mass for luminosity class V stars, using Panagia's calculations, his calibration of M_v as a function of spectral type, and the $m(M_v)$ relation given in Table VII of the present paper. Also shown is the relation derived by Melnick, Terlevich, and Eggleton (1984) using more recent model atmospheres; the discrepancy of a factor of about 4 at large masses is mostly due to the assumed importance of convective overshoot on the mass–luminosity relation used here. The important feature is that the O stars, with $m \gtrsim 20$, will completely dominate the integrated Lyc flux from any reasonable population, since roughly $N^*_{Lyc} \propto m^{10}$ for $m < 20$ and $N^*_{Lyc} \propto m^5$ for $m > 20$. An estimate of N_{Lyc} from a population of known total luminosity will therefore be sensitive to the IMF for $m \gtrsim 20$.

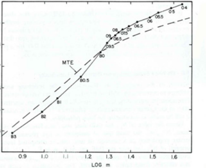

FIGURE 55 Lyman continuum emission rate as a function of stellar mass for luminosity class V stars. Solid line is based on Panagia's (1973) tabulation and the mass-luminosity relation adopted in the present work (Table 7). Dashed line is an independent calculation by Melnick *et al.* (1984).

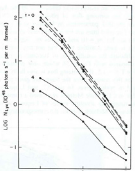

FIGURE 56 Lyman continuum emission rate per unit mass of stars formed for clusters of stars all formed at time $t = 0$ as a function of and four times. Dashed lines show effect of increasing m_u from 110 to 200 $M_\odot$ at two times. Data from Lequeux *et al.* (1981).

Figure 56 shows the behavior of N_{Lyc} per unit mass of stars formed for clusters of stars all formed at time $t = 0$ as a function of the IMF index Γ, at various times, based on the calculations of Lequeux *et al.* (1981). The IMFs all had $\Gamma = -0.6$ for $0.007 < m < 1.8$, and different values of Γ for $1.8 < m < 110$. The dashed lines show the effect of increasing the upper mass limit from 110 to $200 M_\odot$; the effect at times $\gtrsim 4 \times 10^6$yr is negligible. The value of N_{Lyc} at any time is extremely sensitive to Γ, decreasing by roughly an order of magnitude per unit decrease in Γ. The sensitivity is largely due to the sharp decrease in N^*_{Lyc} for $m \lesssim 20$. The Lyc luminosity can be seen to decrease rapidly between 2 and 4×10^6yr as the massive stars begin to die.

Figure 57 shows an independent calculation of the dependence of N_{Lyc} (actually the ionizing flux of photons with $\lambda < 912$ Å in erg $s^{-1} M_\odot^{-1}$) on the IMF parameters by Melnick *et al.* (1984) for zero-age clusters. The solid lines are for $m_l = 0.1$ and various m_u, while the dashed lines are for $m_u = 10$ and various m_l. Again we see that the ionizing flux is quite sensitive to Γ, but not too sensitive to m_u for $\Gamma \leq -1.5$, although the sensitivity to m_u becomes more significant for $m_u < 80$, compared with Figure 56 which only considered $m_u = 110$ and 200. For $\Gamma \leq -1.5$, the ionizing flux is also fairly sensitive to m_l. Note that, for this reason, since the fluxes are given per unit mass of stars formed in both Figures 56 and 57, and Lequeux *et al.* took $\Gamma = -0.6$ for $m < 1.8$ while Melnick *et al.* used a constant Γ over the entire mass range, the absolute values of Lequeux *et al.* are much larger than those of Melnick *et al.* for the corresponding cases.

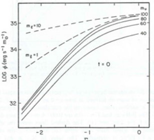

FIGURE 57 Lyman continuum flux per unit mass of stars formed for zero-age clusters as a function of Γ for various m_l and m_u. Data from Melnick *et al.* (1984).

How can N_{Lyc} be determined for an observed stellar population? One method uses an observable hydrogen line luminosity, usually Hα

or Hβ, which is proportional to N_{Lyc}, with proportionality constant which is relatively insensitive to the temperature and other parameters of the HII regions. However, the presence of dust greatly complicates the use of this relation in practice, since only a small fraction of the Hα or Hβ photons may escape the nebula without being absorbed by the dust and reradiated in the infrared (see Natta and Panagia, 1976). The reddening correction is often estimated by comparing the observed Hα/Hβ ratio with the value predicted by standard recombination theory. A better procedure for IMF estimates (e.g. Huchra, 1977; Kennicutt, 1983; Viallefond and Thuan,

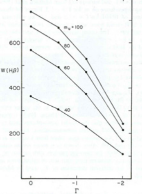

FIGURE 58 Hβ equivalent width as a function of for zero-age clusters with $m_l = 0.1$ and various m_u, based on results of Melnick *et al.* (1984).

1983) is to use the ratio of the Hα or Hβ flux to the flux in the continuum just outside the line, a ratio which is independent of reddening. These ratios are usually referred to as the Hα or Hβ equivalent widths. The Hα or Hβ emission is due to the massive O stars through N_{Lyc}, while the continuum radiation comes from lower mass stars, mostly B and A stars for the continuum around Hβ, and mostly $1-3M_{\odot}$ red giants for the continuum around Hα. Therefore, these equivalent widths are measures of the ratio of $m \gtrsim 20$ stars to intermediate-mass stars. However, they are also sensitive to the upper mass limit and the SFR history.

Figure 58 shows the dependence of $W(H\beta)$ on Γ for zero-age clusters with $m_l = 0.1$, and various m_u, from Melnick *et al.* (1984). Notice the strong dependence on m_u for $\Gamma \geq -1.5$. Figure 59 shows the time dependence of $W(H\beta)$ for $\Gamma = -1.5$ and -2, $m_u = 70$ and 110, for a constant SFR (solid lines) and a burst at $t = 0$ (dashed lines), from Viallefond (1983). The strong sensitivity to m_u and also the SFR history for $t \gtrsim 1-2 \times 10^6$ yr is apparent. A similar result would be obtained for $W(H\alpha)$. An example of an attempt to use $W(H\alpha)$ as an IMF indicator is given in Section 5.7 below.

Another potentially useful quantity for star-forming regions is "T_{eff}", the effective temperature of an imaginary star which produces a given ratio of Lyc photons above and below the He Lyman limit at 504 Å; i.e. T_{eff} is a measure of the ratio of He-ionizing flux to H-ionizing flux. T_{eff} can be observationally estimated from line intensity ratios like [O III]/Hβ (Stasinska, 1982). T_{eff} depends on the shape of the high mass IMF and is very sensitive to the upper mass limit m_u (Lequeux *et al.*, 1981; Viallefond and Thuan, 1983). Unfortunately it is also very sensitive that the model atmospheres used in its calculation (Lequeux, 1984, private communication). Figure 60 shows T_{eff} as a function of Γ for various ages, taken from Lequeux *et al.* (1981), for $m_u = 110$ and 200. Also shown is a more recent calculation of Melnick *et al.* (1984) for zero-age clusters with various m_u. The very large discrepancy between these two sets of calculations can only be attributed to the different definition of T_{eff} used by Melnick *et al.*, which was

$$T_{eff} \propto \int_0^{\infty} F(\lambda)d\lambda \Big/ \int_0^{\infty} hc/F(\lambda)d\lambda.$$

According to Lequeux (1984, private communication), this definition is inappropriate for comparison with observed T_{eff}s. Figure 61, from Viallefond (1984; see also Viallefond and Thuan, 1983), shows T_{eff} as a function of time for $\Gamma = -2$ and $\Gamma = -1.5$ for an instantaneous

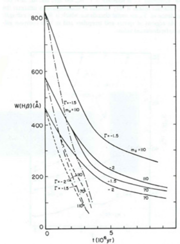

FIGURE 59 Hβ equivalent width as a function of time for a constant star formation rate (solid lines) or a burst at $t = 0$ (dashed and dot-dashed lines) for two values each of Γ and m_u. From Viallefond (1985).

burst and for continuous star formation, each for $m_u = 70$ and 110. (The reason for the increase in T_{eff} with time for some of the models is that the evolutionary tracks for massive stars which were used predict blueward evolution in the *H–R* diagram during the H-burning phase.) Evidently T_{eff} is sensitive to Γ, m_u, the age, and the SFR history. This fact makes it very difficult to unambiguously interpret the dependence of T_{eff} on metal abundance which is found in extragalactic HII regions of spirals and irregulars and in blue compact galaxies, to be discussed below.

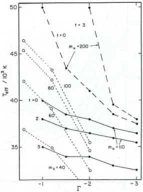

FIGURE 60 T_{eff} as a function of Γ for a number of ages and m_u values. Solid and dashed lines: results of Lequeux *et al.* (1981). Dotted lines: results of Melnick *et al.* (1984) for zero-age clusters.

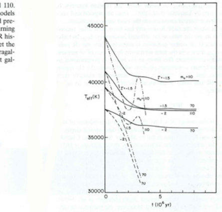

FIGURE 61 T_{eff} as a function of time for a constant star formation rate (solid lines) or a burst at $t = 0$ (dashed and dot-dashed lines) for two values each of Γ and m_u. From Viallefond (1985).

Another method to estimate N_{Lyc} uses the thermal radio continuum emission from HII regions. The continuum luminosity at wavelength λ from an HII region of volume V is $L_\lambda = n_e n_i j_\lambda(T_e) V$, where n_e and n_i are the electron and ion number densities and $j_\lambda(T_e)$ is the continuous emission coefficient as a function of gas temperature. If the HII region contains enough gas to be ionization bounded, then N_{Lyc} must approximately equal the recombination rate $\alpha(T_e)\, n_e n_i V$, where $\alpha(T_e)$ is the total recombination coefficient (see Osterbrock, 1974), so eliminating

V gives $L_\lambda = [j_\lambda(T_e)/\alpha(T_e)]N_{Lyc}$. A useful numerical relation between L_λ and N_{Lyc} is given by Lequeux *et al.* (1981). Dust absorption and contamination by nonthermal emission are the most serious problems.

The way in which the radio luminosity has been most often related to the IMF is to use the ratio of far infrared luminosity, L_{FIR}, to radio continuum flux. If all stellar radiation is converted into far IR radiation, then L_{FIR} measures the total luminosity from stars of all masses, while the radio continuum flux from an HII region is proportional to the number of Lyman continuum photons which ionize the HII region per unit time, and so is sensitive to the number of massive stars present. Far IR and radio observations therefore yield the so-called "infrared excess",

$$\mathrm{IRE} = L_{FIR}/N_i h\nu_{Ly\alpha} \tag{5.1}$$

where $h\nu_{Ly\alpha}$ is the energy of a Lyα photon. The dependence of this quantity on dust absorption cross sections and dust optical depth in the HII region was discussed in detail by Mezger, Smith, and Churchwell (1974; the infrared excess introduced by those authors is IRE−1). As explained in Lequeux (1984), if only massive spectral type O stars were present in an HII region, and if dust absorption of Lyc photons is ignored, then we would expect IRE ≈ 1, because every ionizing Lyc photon gives about one Lyα photon, which is in turn eventually absorbed by a dust grain. Accounting for the absorption of Lyc photons by dust in the HII region will increase the IRE by an amount which depends on the optical depth (Mezger *et al.*, 1974); typically IRE ≈ 2.5 might be expected. However, the presence of substantial numbers of lower-mass stars will provide an additional source of dust emission, as the grains absorb the longer-wavelength photons from these cooler stars, so the IRE could be much larger.

Lequeux (1984) has given an instructive plot of the IRE as a function of time for the cases in which a cloud is ionized by a burst of star formation at some time $t=0$ in the past, or in which the star formation rate has been constant since $t=0$, and is reproduced in Figure 62. The adopted IMF had $\Gamma = -2$ for $1.8 < m < 110$ and $\Gamma = -0.6$ for $0.007 < m < 1.8$. The IRE was calculated assuming no internal dust absorption in the HII region and that all stellar radiation is converted into far IR radiation. There are three features worth noting. First, the IRE is sensitive to the upper mass limit, although only until

$\sim 5 \times 10^6$ yr for the burst model. This is because N_{Lyc} is such a sensitive function of mass, as discussed earlier. With an upper mass limit $m_u = 20$, there is very little ionizing radiation compared to the total stellar radiaton which can be radiated by the dust. Second, the IRE increases with time as the massive ionizing stars die more quickly than the lower-mass stars; the effect is of course very pronounced in the burst case, since the dead stars are not replaced. Third, for any time greater than around 10^6 yr, the IRE depends on the history of the star formation rate. These predicted IREs do, of course, depend on the IMF the graph emphasizes the fact that, like most indirect IMF indicators, the IRE is sensitive to a number of parameters besides the shape of the IMF.

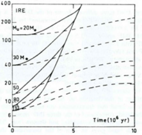

FIGURE 62 Infrared excess as a function of time for a burst of star formation at $t=0$ (solid lines) or a constant star formation rate (dashed lines), for various values of the upper mass limit. From Lequeux (1984).

An attempt to use the IRE to infer radial IMF variations in our galaxy is given in Section 7.3 below. The recent acquisition of data by IRAS should allow a study of the IRE in other galaxies in the near future.

5.7 The W(Hα)—(B−V) relation for late-type spirals

A good example of how the Hα equivalent width $W(\mathrm{H}\alpha)$ can be used to constrain the IMF is Kennicutt's (1983) study of SFRs in 115 spiral galaxies of all types. The basic idea is to compare the distribution of galaxies in the $W(\mathrm{H}\alpha)-(B\text{–}V)$ plane with the locus of model galaxies in order to limit the form of the IMF, assumed constant from galaxy to galaxy, and then use this IMF and $W(\mathrm{H}\alpha)$ to estimate the SFR in each galaxy. The greatest uncertainty in $W(\mathrm{H}\alpha)$ is the extinction correction, for which a rough average was estimated by comparing the observed $W(\mathrm{H}\alpha)$s to radio continuum fluxes. This 1.1 mag correction was then applied to all the galaxies. As pointed out by Kennicutt, this procedure results in large uncertainties for individual galaxies, but may be adequate for a study of the average properties of a large sample.

Kennicutt tried three different forms of the IMF: 1. A power-law approximation to the field star IMF estimated by MS, which has $\Gamma = -1.5$ for $1 < m < 10$ and $\Gamma = -2.3$ for $10 < m < 100$; 2. An "extended" MS IMF with $\Gamma = -1.5$ for $1 < m < 100$; and 3. A still shallower IMF with $\Gamma = -1$ for $1 < m < 100$. In all three cases the low-mass IMF was taken as $\Gamma = -0.4$ for $0.1 < m < 1$, although this value does not affect the results except by a scale factor in the derived total SFRs, *if* the low mass IMF is the same in all galaxies. Kennicutt shows that the lower mass cutoff must be smaller than $3M_\odot$; otherwise, excessive Hα strengths are predicted.

Figure 63 shows the $W(\mathrm{H}\alpha)-(B\text{–}V)$ comparison. The data points at the bottom of the diagram are Sa and Sab galaxies whose Hα widths are so small that uncertainties are larger than the measured values. The bands correspond to the three IMF choices listed above: MS (bottom), extended MS (middle), and shallow (top). The vertical width of each band gives an idea of the uncertainty due to dust extinction; the upper bound has no absorption while the lower bound has 0.8 mag of extinction. Each curve in Figure 63 shows the effect of varying the parameter t_0 in the assumed SFR time dependence, which was modeled as e^{-t/t_0}. The blue end actually corresponds to a SFR which is linearly increasing with time, while the red end refers to a burst of star formation which occurred 15×10^9 yr ago.

The best fit is seen to obtain for the intermediate IMF with $\Gamma = -1.5$; the steeper and shallower IMFs produce 2–5 times too

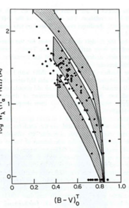

FIGURE 63 *Hα* equivalent width-color diagram from Kennicutt (1983). Dots are observed galaxies, bands are theoretical calculations for three IMFs with a range of star formation histories for each IMF choice. For details, see text.

little or too much Hα emission, respectively. It is also noteworthy that the steeper IMF would lead to unacceptably large SFRs in the late-type galaxies *if* the upper mass limit is $\lesssim 100M_\odot$. The value $\Gamma = -1.5$ is similar to the flatter estimates of the field star IMF discussed in Section 2.6.4. Given the uncertainties in the individual observed $W(\mathrm{H}\alpha)$ values, and the expected variation in extinction corrections, it appears that fluctuations in Γ larger than ± 0.3 or so can be excluded. *Systematic* variations in Γ are possible, but any substantial variation of Γ with color would probably destroy the good agreement of the slopes of the bands in Figure 63 with the observed $W(\mathrm{H}\alpha)$–$(B-V)$ correlation. The uniformity of the IMF in late-type spirals agrees with the direct evidence based on star counts discussed in Section 4.1.

Notice that the models do not account for the bluest galaxies, a familiar problem from earlier studies (see Tinsley, 1980); these galaxies are probably undergoing bursts of star formation, a possibility not taken into account in the model SFRs.

Note that Huchra (1977) found that IMFs with $\Gamma \gtrsim -1$ were suggested by his comparison of the colors and Hβ strengths of very blue galaxies with models containing both an old population and a young burst population; however, the constraint is dependent on the adopted upper mass limit; if $m_u \gtrsim 70$, then steeper IMFs would be allowed by Huchra's models.

The conclusion that $\Gamma - 1.5 \pm 0.3$ in most spiral galaxies (excluding the earliest types whose Hα widths are too small for use) is subject to one important caveat, and this concerns the adopted upper mass limit, which was $100 M_\odot$ for the calculations of Figure 63. As noted by Kennicutt, even the steepest IMF can be made to agree with the observations if $m_u \gtrsim 300$, although such a change would not much affect the derived SFRs. As mentioned in Section 1, there is no theoretical reason why such massive stars cannot exist, although their lifetimes may be reduced by instabilities and severe mass loss, and there is some circumstantial observational evidence for extremely massive stars. Alternately, if m_u is significantly less than $100 M_\odot$, a very flat IMF would be required (see Figure 58). Furthermore, it is already recognized that m_u probably increases with galaxy mass because of statistical effects involved with sampling from a finite number of stars (Section 4.1). For these reasons, future studies should include m_u as a third parameter.

Finally, we must remember that these results, as all others based on photometric or spectrophotometric galaxy modeling, rest on the validity of the stellar evolution and atmosphere models used to construct the model galaxy properties, a point which is easily forgotten in the midst of the large number of studies which routinely employ galaxy evolution models. Of particular concern is the treatment of red giants which, in the case of $W(\mathrm{H}\alpha)$, control the red continuum flux. In this respect the use of $W(\mathrm{H}\beta)$ is less sensitive to model uncertainties. In any case the Hα- or Hβ-color relation is not so useful a means to estimate the *absolute* values of IMF parameters as it is to test for real *differences* in IMF parameters between galaxies.

5.8 W(Hβ)—color diagrams for clusters in HII regions

De Gioia-Eastwood (1984) has suggested a similar method for estimating the high-mass IMF index from Lyc-color diagrams for clusters of stars formed coevally in a gas cloud. The Hβ flux and seven monochromatic continuum fluxes, two in the optical region (u at $\lambda 3560$ and b at $\lambda 4500$) and five in the UV, for use with the Space Telescope, were studied. The continuum wavelengths were chosen to avoid strong nebular emission lines and strong absorption lines from O and B stars. Lines of constant age and IMF index can then be constructed in the theoretical Hβ/b-color planes; two of these are shown in Figure 64. The calculations assume a power-law IMF, except for a case using the IMF of Miller and Scalo (1979); all the IMFs had an upper mass limit of $63 M_\odot$. The values of Γ used in the figure are, from left to right, $+0.95$, -0.35, -1.35, Miller and Scalo, -2.35, -2.85, -3.25, -3.65, and -3.95. The actual mass range to which these Γ values refer depend on Γ. For $\Gamma \gtrsim -2$ only stars with $m \gtrsim 10$ are important, and low mass stars with $m \sim 1$ only contribute for very steep IMFs with $\Gamma \lesssim -3$. For $\Gamma \lesssim -2.5$ it is unlikely that a single power law can represent the range of masses which contribute to the b fluxes, and the values of Γ derived from observations in these cases must be considered as an ill-defined mean; nevertheless even with steep IMFs the diagrams can be used to search for differences in IMFs between regions.

In principle the comparison of these diagrams with observations could give a unique estimate of both the age and Γ. In practice, there are several problems: 1. As pointed out by De Gioia-Eastwood, if $\Gamma \gtrsim -1.3$, then the curves will be distinguishable only for ages $\gtrsim 2 \times 10^7$ yr because of the importance of blue supergiants in younger clusters; steeper slopes can be distinguished for most ages. 2. The positions of the curves depend on the upper mass limit (see, for example, Figure 58), which must enter as a third parameter to be determined; there is no basis for adopting a constant value for m_u, especially in the regions of interest which contain a small enough number of stars that stochastic fluctuations in m_u from cluster to cluster are expected. 3. The use of the UV colors will be quite diffi-

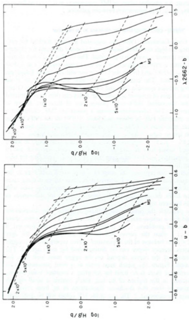

FIGURE 64 Theoretical $H\alpha$-color diagrams, showing lines of constant age and IMF index, from DeGioia-Eastwood (1984). See text for details.

cult because of uncertainties in the reddening. 4. The position of the lines in Figure 64 depend on the adopted evolutionary tracks, model atmospheres, mass-luminosity relation, effective temperature calibration, etc. For this reason these diagrams are again not so useful in determining the absolute value of Γ in any given region, but *variations* in Γ between different regions. Comments 2 and 4 apply to nearly all the indirect integrated light methods discussed in this section.

Despite these problems, the positions of objects in the $W(H\alpha)$ or $W(H\beta)$-color planes, as in Kennicutt (1983) and Di Gioia-Eastwood (1984), offer one of the best methods for uncovering possible systematic variations in the upper IMF, but explicit consideration of the upper mass limit as an additional parameter appears necessary.

5.9 Low-excitation disk galaxies: A deficiency of massive stars?

The gas in early-type spiral galaxies is known to be only weakly excited by the UV radiation of O stars. Of the 21 Sa and Sab galaxies listed in Kennicutt (1983), all but three have $H\alpha + N\textsc{ii}$ equivalent widths of 5 Å or less, compared with 10 − 100 Å for most of the later-type galaxies. The question of interest is: Is the low excitation due to a small current SFR or an IMF deficient in high-mass stars?

Van den Bergh (1976) first emphasized the lack of HII regions in the galaxy M104 (NGC 4594), the Sombrero galaxy. Subsequent observations by Schweizer (1978) revealed HII regions, but they are small and not very luminous. Van den Bergh reasoned that since NGC 4594 contains a significant amount of dust and therefore gas from which stars may form, it seemed likely that the IMF is deficient in stars with $m \geq 10$. However, it is now apparent that there is little correlation between the SFR and HI mass, at least for later-type galaxies (e.g. Kennicutt and Kent, 1984), so this interpretation is not so clear-cut. This question could be answered with very accurate measurements of the $H\alpha$ equivalent width in Sa and Sab galaxies. Figure 63 shows that the Sa and Sab galaxies (at the bottom of the diagram) probably have an IMF deficient in high-mass stars *if* the $H\alpha$ equivalent widths are smaller than about 2 Å. Unfortunately, the measured equivalent widths are uncertain by typically ± 2–3 Å, so the available data do not allow a conclusion. Future more precise measurements for these galaxies will clarify the situation, and work in this direction is now underway (Yamamaka, 1984, personal communication). However, it should be noted that an equivalent width ≤ 1 Å in an *individual* galaxy does not necessarily imply the IMF anomaly, since it is possible that the global SFR has fluctuated in the recent past.

Even more difficult is the choice between a steeper high-mass IMF and a "normal" IMF with a smaller upper mass limit. M104 (MGC 4594) is one of the galaxies studied by Ellis *et al.* (1982). The IMF derived from their population synthesis (see Figure 53), while very uncertain, does not appear anomalously steep between 1.5 and $8 M_\odot$, suggesting that a small upper mass limit may be responsible.

Besides the early-type spirals, van den Bergh (1981) pointed out that the so-called anemic spirals and smooth-armed spirals also exhibit a deficiency of OB stars and HII regions. Again, accurate measurements of Hα widths in these galaxies, along with their B–V colors, might be able to show whether the low excitation is due to a small SFR or an IMF deficient in high-mass stars.

A somewhat stronger case might be made for an IMF deficient in massive stars in the disk of M82 (NGC 3034). The extremely high surface brightness and *A*-type integrated light imply a recent burst of star formation, yet there are no bright HII regions or stars with $M_v \lesssim -5$ (van den Bergh, 1981). In this case it appears that a normal IMF would require that the burst subsided over the entire disk more than about 3×10^7 yr ago. However, it is difficult to rule out such a state of affairs. Seiden, Schulman, and Feitzinger (1982) have produced models for spiral galaxies which undergo coherent oscillations in their SFRs and morphologies. Furthermore, M82 is probably involved in a galactic interaction (e.g. Solinger, Morrison, and Markert, 1977) and it may be possible for interaction to generate star formation bursts which are at least initially coherent (Scalo and Struck-Marcell, 1985).

It should also be pointed out that the detailed modeling of the bursting *nuclear* region of M82 by Rieke *et al.* (1980), discussed below, allowed satisfactory agreement with the observations for an exponentially decreasing SFR and a power law IMF with $\Gamma \sim -2$ for $m_u = 16$ or 31. In fact, Rieke *et al.* found it necessary to impose a *lower* mass cutoff of $m_l \sim 3$. The upper mass limit of 16 or $31 M_\odot$ was used because there is no current evidence for stars hotter than around 30,000 K. However, if the time constant in their exponentially

decreasing birthrate is in the smaller part of the allowed range, 2–3×10^7 yr, then their derived burst age of 5×10^7 yr implies that a higher value of m_u might be acceptable.

5.10 Starburst nuclei

One of the most interesting attempts to model extragalactic stellar populations in regions undergoing active star formation is the detailed study of the nuclei of M82 and NGC 253 by Rieke *et al.* (1980). We concentrate here on summarizing their arguments concerning the form of the IMF, which they suggest contains essentially only stars more massive than about $3 M_\odot$. The same suggestion was made independently by Knapp *et al.* (1980) on the basis of the high star formation efficiency implied by a solar neighborhood IMF.

Rapid star formation in the M82 nucleus in inferred from the large far-IR luminosity ($\ge 4 \times 10^{10} L_\odot$) within the central 300 pc. The peculiar activity in M82 has been attributed to an interaction with M81 (Solinger, Morrison, and Markert, 1977), and there is mounting evidence that many nuclear "starburst" galaxies (see Weedman *et al.*, 1981; Balzano, 1983; Gehrz *et al.*, 1983) are triggered by interactions (e.g. Condon *et al.*, 1982).

The galaxy evolution calculations by Rieke *et al.* use a modified version of the program described by Huchra (1977), and give broadband colors, emission line strengths, and a CO band index as a function of time. The star formation rate was taken proportional to $\exp(-t/t_0)$, with t_0 a parameter, and the IMF as a power law (in most cases) with parameters Γ, m_l, and m_u. Because there is some evidence from emission lines that there are no stars hotter than $\sim 30{,}000$ K, m_u was chosen as 16 or 31. The major observational constraints for M82 are (the constraints and conclusions for NGC 253 are very similar): 1. The total nuclear luminosity, derived from IR measurements, is at least $4 \times 10^{10} L_\odot$. 2. The mass derived from the rotation curve is ~ 5–$8 \times 10^8 M_\odot$; the small M/L ratio $\lesssim 0.02$ implies that there cannot be too many low-mass stars. 3. The strength of the infrared Brα hydrogen line requires an ionizing flux of $N_{Lyc} \sim 2 \times 10^{53}\ s^{-1}$, which constrains the parameter t_0 to be in the range $\sim 2 \times 10^7$ yr to $\sim 10^8$ yr, and also rules out IMF slopes much steeper than $\Gamma \sim -1$, or else there would not be enough massive stars for ionization; the latter result could be altered somewhat if the adopted value of m_u were increased. 4. The most stringent constraint on the IMF comes from the observed 2.2 μm luminosity, $M_K \approx -23$. In order to account for this near-IR radiation, due to red giants and supergiants in the models, using the available mass, the lower-mass IMF cutoff m_l can be no smaller than about $3M_{\odot}$. For example, if a solar neighborhood-like IMF is used, with $m_l = 0.009$, models which satisfy the other constraints are too faint at 2 μm by about 1.5 mag, because the stars with $m \lesssim 3$ do not evolve to the giant phase within the derived age of the burst, $\sim 5 \times 10^7$ yr. With most of the required mass in these lower-mass stars, there are not enough higher-mass giants and supergiants to provide the 2 μm luminosity.[†] However, the discrepancy in 2 μm luminosity is only a factor of about 4, and one can think of several effects which might allow a small value of m_l.

1. As noted by Rieke *et al.*, the evolutionary tracks may be in error. Although it is well-known that stellar evolution in the red giant and especially the supergiant part of the *H–R* diagram is still uncertain, it is currently not possible to say whether these uncertainties are large enough to explain the excess 2 μm flux.

2. The extinction correction of about 2 mag at 2.2 μm was derived from the deviation of the observed Bα/Bγ ratio ($\sim 10 \pm 2$) from the value (2.8) predicted by recombination theory, and then applying a local reddening law to obtain the extinction in the *K* band; if the extinction was overestimated by more than about 1 mag, then the required m_l could be substantially decreased.

3. If star formation is presently occurring, then a large number of stars of all masses could still be embedded within dense interstellar or circumstellar clouds, and emit near-IR radiation which is not taken into account by the models. This possibility was noted by Struck-Marcell and Tinsley (1978). However, the 2 μm luminosity is about half the far-IR luminosity, while a ratio L(near-IR)/L(far-IR) ~ 0.1 is more typical of the nuclei of spirals (Solomon *et al.*, 1983).

4. Another possibility is that the present nuclear population does not represent the IMF because of stellar collisions. As mentioned in Section 5.1 above, calculations by Tuchman (1984) suggest that giant–dwarf encounters can strip the giants of their envelopes, and that the collision rate in nuclei may be sufficient to substantially reduce the number of red giants, and hence the 2.2 μm luminosity, although a factor of four reduction may require extremely large star densities.

5. Finally, the 2 μm emission may arise from very small, and hence warmer than average, dust grains (Lequeux 1984, private communication; see Sellgren *et al.*, 1982).

Although the proposed deficiency of lower-mass stars is the most intriguing result of the M82–NGC 253 study, the above listing suggests that it cannot yet be considered as conclusive, despite the very thorough analysis given by Rieke *et al.* (1980). Perhaps a firmer conclusion is that the index of the IMF must be larger than about $\Gamma = -2$ in order to produce a sufficient UV flux to account for the strength of Bα.

However, more recent analyses of bursting galaxies involved in collisions lend strong support to the claim that no lower mass stars are formed in such events. For example, a study of the extreme starburst galaxies Arp 220 and NGC 6240 by Rieke *et al.* (1984), using basically the same evolutionary code described above, requires an enhancement of massive stars for both galaxies, with $\Gamma \gtrsim -1.5$ and/or a low mass cutoff at ~ 2–$3M_{\odot}$. As in the study of M82 and MGC 253, this result depends on the interpretation of the 2 μm luminosity.

Olafsson, Bergvall, and Ekman (1984) have studied the colliding starburst system IC 2153 using galaxy evolution models. The main constraints on their model are the *B–V* color (-0.17), the Hβ emission equivalent width, and the equivalent widths of the Balmer absorption lines. The weak Balmer absorption lines require either a large population of very massive stars, which would, however, produce too much Hβ emission, or a large value for the lower mass cutoff, which is their preferred solution. Assuming a constant SFR during the burst and an IMF index $\Gamma = -1.35$, Olofsson *et al.* find that a value of $m_l \approx 10$ and a burst duration of 1.5×10^7 yr give a good fit to the observations. It is unclear how m_l would be changed for a different choice of Γ or a different adopted time dependence of the SFR, but it seems unlikely that a value $m_l \lesssim 5$ could satisfy the constraints. No constraint on m_u could be derived from the available data; optical specrophotometry and comparison of observed line

[†]It is sometimes stated that the Rieke *et al.* models require a deficiency of stars with $m \lesssim 3$ in the M82 nucleus in order to match the small observed *M/L* ratio. This is not true: *Bolometric M/L* ratios smaller than 0.02 can easily be obtained even using the local field star IMF if the burst age is smaller than around 2–5×10^7 yr. Some of the considerations are discussed in Struck-Marcell and Tinsley (1978).

ratios with photoionization models are desirable, since they could yield T_{eff} (Section 5.6 above) which is sensitive to m_u.

Augarde and Lequeux (1985) have presented a detailed rediscussion of evolutionary models for the interacting starburst complex Mk 171 (=NGC 3690+IC 694), previously studied by Gehrz *et al.* (1983). Line ratios interpreted with Stasinska's (1983) photoionization models yield an estimate of T_{eff} for the ionizing stars of $34,700 \pm 300$ K. This requires an upper mass limit of about $40M_{\odot}$. The Lyman continuum flux, derived from the Brγ flux, after a correction for extinction, then gives the number of stars from m_u down to about $20M_{\odot}$ (since less massive stars contribute little to N_{Lyc}; see Figure 55), assuming an IMF with $\Gamma = -2$. The value of m_l can then be estimated by requiring a match to L_{bol} (from the far-IR luminosity), the UV flux at 1900 Å, and M_v. The best fit to the data (including several other considerations) is obtained for a constant SFR over the past 8×10^6 yr with $m_l \approx 20$. There is, of course, some possible tradeoff between m_l, Γ, and the SFR parameters, but m_l cannot be much smaller than about $5M_{\odot}$ for any reasonable model. For comparison, the models of Gehrz *et al.* (1983) which best matched their less extensive data had $m_l = 6$, $m_u = 25$, $\Gamma = -2.5$.

These independent studies of several interacting starburst galaxies make, in my opinion, a convincing case for the idea that the IMF produced by a galaxy interaction-induced star formation burst has a low-mass cutoff *or* a mode (peak) at a mass which is at least an order or magnitude larger than for stars in the solar neighborhood. From the published studies it appears that this factor may be in the range 30–200 and probably varies from system to system. However, there is no compelling evidence that either the *shape* of the IMF above the minimum or mode or the upper mass limit is abnormal. Because of the growing awareness of the importance of galaxy encounters for several aspects of galaxy evolution, this result may have various ramifications, such as the production of remnant-dominated galactic nuclei (Weedman, 1983).

It is worth noting that the question of the mechanism by which a galactic interaction (in some cases only a tidal encounter) can induce such huge bursts of star formation is virtually unexplored. One attempt in this direction is given in Scalo and Struck-Marcell (1985).

In Section 7 below three indirect arguments will be reviewed which suggest that the same type of IMF "anomaly" found in interacting galaxies also occurs in spiral arms, although the minimum mass may be somewhat smaller (~ 2–$3M_{\odot}$) than in the starburst galaxies. It should also be noted that Lacy *et al.* (1982) have suggested an IMF which strongly favors stars in the 15–$25M_{\odot}$ range in our galactic center, based on a study of the observed excitation of the ionized gas.

5.11 Blue compact galaxies and related objects

Blue compact dwarf galaxies, first distinguished by Haro and Zwicky, have colors and line strengths that are similar to galactic HII regions, and are therefore sometimes referred to as extragalactic HII regions. They are often so compact that individual stars cannot be resolved. They usually exhibit very small metallicities, approaching a few percent of the metallicity of the Galactic disk. As mentioned earlier, their very blue colors, coupled with their small metal abundances, imply that star formation has occurred in a recent burst. This and other properties link the blue compact galaxies with supergiant HII regions observed in nearby spiral and irregular galaxies, starburst nuclei, and Magellanic Irregular galaxies (see Gallagher and Hunter, 1984 for a comprehensive review). Because their star-forming behavior (whose cause is not yet fully explained; but see Gerola and Seiden, 1982) seems so different from that of our galactic disk, the form of the IMF in such regions is of great interest, since we might learn whether and how metallicity and/or star formation mode influence the IMF. Of the substantial literature related to this type of extragalactic region, I will discuss two investigations which specifically address the IMF.

As was evident in the earlier discussion, it is generally quite difficult to disentangle the slope of the upper IMF, the upper and lower mass limits of the IMF, and the SFR history using a single observationally determined spectral or photometric quantity. Simultaneous studies of several of these quantities is clearly needed for further progress. One such investigation is the work by Viallefond and Thuan (1984) on the blue compact galaxy I Zw36. They used evolutionary models in which the SFR was either an instantaneous burst of age τ (ISB models) or a constant with duration τ (CSF models), and parameterized the IMF as a power law of index Γ with upper and lower mass limits m_u, m_l. The parameters were varied to obtain the best match to the following observed properties: 1. The Hβ equivalent width, which measures the ratio of the number of O stars (through the ionizing flux required to give the Hβ strength) to the number of B and A stars (through the continuum flux at Hβ); the Hβ equivalent width is sensitive to all the parameters except m_l if $m_l \ll 2$ (see Figures 58 and 59). 2. The effective temperature $T_{\rm eff}$, which depends strongly on Γ and m_u (see Figures 60 and 61). 3. Ratios of continuum intensities at pairs of wavelengths (λ_1, λ_2). The pairs (4087, 4462) and (4462, 4812), which were the primary ratios used, depend more on Γ and m_l (if $m_l > 2$) than on m_u, because the continuum in the 4000–5000 Å region comes mainly from B2–B9 and early A stars. The pair (1668, 4862) links the UV and optical regions and is sensitive to the number of B0–B3 stars, but was used only as a consistency check because the UV intensity depends so strongly on the extinction.

Applying this comparison to I Zw36, Viallefond and Thuan find that, for the continuous star formation model, the best fit is for $\Gamma \approx -1.5$, $m_u \approx 100$, $m_l \approx 4$, and a burst duration of 7×10^6yr. A flatter IMF (larger Γ) would give too flat an optical continuum, while the large value of m_l is needed to account for the observed value of the Hβ equivalent width, which is 238 ± 23 Å. For example, dropping m_l to $0.007 M_\odot$ would give good agreement with $T_{\rm eff}$ and the optical spectral indices, but predicts too large a value of W(Hβ). If the burst duration is increased to reduce W(Hβ), the optical spectral indices would become too large. The dervied value of m_l is smaller for the instantaneous SF burst models, in which the best agreement is found for $\Gamma \approx -1.5$ for $m > 1.8$ and $\Gamma \approx -0.6$ for $m < 1.8$, $m_u \approx 120$, $m_l \lesssim 4$, and a burst age of 3×10^6yr.

Viallefond and Thuan also give a comparison for two additional regions. In the blue compact galaxy I Zw18, the continuous star formation models require $\Gamma \approx -1.5$, $m_u \approx 100$, $m_l \lesssim 2$, and a burst duration of 3×10^7yr. The smaller limit on m_l is a consequence of the smaller observed W(Hβ). The result $\Gamma \approx -1.5$ for the two blue compact dwarfs can be compared with an earlier study by Lequeux *et al.* (1981) of two blue compact galaxies (I Zw18 and II Zw70) and several HII clumps in both spiral and irregular galaxies. They were unable to place a firm constraint on the IMF, but did find that the value of Γ must be in the range -1 to -2. Apparently the stronger constraint of Viallefond and Thuan (1983) is due to their use of optical continuum intensity ratios, since, except for this, the two studies are very similar. If $\Gamma \approx -1.5$, then the large empirical values of $T_{\rm eff}$ for

some regions suggest an upper mass limit around $150 M_\odot$, somewhat larger than found by Viallefond and Thuan, but the difference may not be significant considering the sensitivity of $T_{\rm eff}$ to the adopted model atmospheres. The results of these two studies of extragalactic HII regions disagrees with the result $\Gamma \approx -3 \pm 1$ for $m > 20$ found by Israel and Koornneef (1979) for HII regions in the LMC, but since this latter result is based solely on fits to the UV spectrum (see Section 5.5 above), which are not very sensitive to the IMF and suffer from reddening uncertainties, it should probably receive lower weight. For the giant HII region NGC 5471 in the spiral galaxy M101, the continuous star formation models of Viallefond and Thuan (1984) gave $\Gamma \approx -2$, steeper than in the blue compact galaxies, $m_u \approx 110$, $m_l \approx 0.007$, and a burst duration of 5×10^6yr. As pointed out by Viallefond and Thuan, it is interesting that the derived upper IMF slope turns out steeper in the M 101 HII region than in the two metal-poor blue compact galaxies which they studied, suggesting that the upper IMF flattens with decreasing metallicity. This suggestion recurs in many indirect IMF studies, especially chemical evolution arguments discussed below.

The strongest argument in favor of such a Z-dependent IMF slope has been recently presented by Terlevich and Melnick (1985), who examine the correlations between ionizing flux ϕ per unit mass (inferred from Hβ), M/L_B, $T_{\rm eff}$, and Z among giant HII regions in nearby galaxies and blue compact galaxies. The correlations are such that as Z decreases, ϕ and $T_{\rm eff}$ increase while M/L_B decreases. Using a detailed series of evolutionary models (Melnick, Terlevich, and Eggleton, 1984), Terlevich and Melnick show that these correlations cannot be accounted for in terms of variations in mass loss rates, age, or composition: A dependence of the IMF on Z is required. Futhermore, it is the *shape* of the IMF, not just m_u and/or m_l, which is implicated, since $T_{\rm eff}$ is insensitive to m_l, while M/L_B depends on the number of intermediate-mass stars, not m_u.

Using data for 24 HII galaxies and giant HII regions within galaxies, and $(m_l, m_u) = (0.1, 100)$, Terlevich and Melnick find a good fit to all three correlations with a Z-dependence of the IMF slope given by

$$\Gamma \approx -4.0 - \log Z. \tag{5.2}$$

This relation is shown in Figure 65 along with the values of Γ derived for individual regions from the observed ionizing flux per unit mass, assuming that m_l and m_u are fixed. (I have omitted the positions in this diagram which Terlevich and Melnick adopt for the solar neighborhood, the Orion OB association, and the SMC, in favor of the IMF slopes discussed earlier in this review; these slopes will be discussed below.)

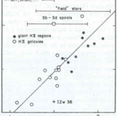

FIGURE 65 Filled and open circles: empirical log $Z-\Gamma$ relation proposed by Terlevich and Melnick (1981). Other symbols: approximate positions of young open clusters, high-mass field stars, spiral galaxies, and the blue compact I Zw 36 taken from sources discussed in the text.

Terlevich and Melnick point out several independent lines of evidence to support their finding: 1. Burki's (1977) finding that the upper IMFs of open clusters flatten with increasing galactocentric radius, coupled with our galactic Z-gradient, yields a $\Gamma-Z$ dependence whose *sign* is consistent with Eq. (5.2) (see, however, Section 7 below); 2. Da Costa (1982) found flatter IMFs for lower-Z globular clusters, with $\Delta\Gamma \approx -1.2\ \Delta \log Z$; however, recall from Section 3.8 that this interpretation is far from clear, and that the halo field stars do not seem to have a flatter IMF than the disk field stars (Section 2.7). 3. For elliptical galaxies, the apparent correlation of M/L with Z

is accounted for by Eq. (5.2) if the photometric M/L ratios are corrected for dark remnants (Figure 50).

A problem with Eq. (5.2) is that, except for the T_{eff}–Z relation, it is based on correlations whose form and even existence depends on the adopted values for the masses of the individual regions. Terlevich and Melnick (1981) had earlier proposed that giant HII regions and blue compact galaxies are in virial equilibrium, and the masses used in constructing the observed $\phi(Z)$ and $M/L_\beta(Z)$ relations were derived from the observed linewidths under this assumption. However, recent studies by Gallagher and Hunter (1983) and Rosa and Solf (1984) strongly suggest that the emission linewidths do *not* reflect the gravitational potential at least for the regions studied in detail. A useful discussion of other possible physical explanations for the linewidths, such as winds, explosions, and champagne flows, is given in Skillman and Balick (1984). The anticorrelation between T_{eff} and Z, which has been known for some time (see Alloin *et al.*, 1979; Stasinska, 1980), implicates a Z-dependence of the IMF in these young regions, but with this relation alone, it is not possible to decide whether the effect is due to a flatter IMF or a larger m_u at smaller Z. In addition, M/L will depend on the age of the star-forming region. A further confusion arises from the manner in which "T_{eff}" is defined by Melnick *et al.* (1984) and Terlevich and Melnick (1984), which is inappropriate for a comparison with excitation models (Lequeux, 1984; private communication; see Figure 60 for the sensitivity to definition).

A more serious problem with Eq. (5.2) becomes apparent when we compare its predictions with IMF slopes inferred from independent arguments. For example, the parameters of I Zw36 derived in the detailed study of Viallefond and Thuan (1984), discussed above, are indicated by a cross in Figure 65, and clearly fall below the proposed $\Gamma(Z)$ relation. Kennicutt (1983) found $\Gamma \approx -1.5$ for a sample of intermediate and late-type spirals, based on the $W(\mathrm{H}\alpha)-(B-V)$ correlation (Section 5.1.7 above); this result is shown as the open square in Figure 65, which has been placed rather arbitrarily at $Z = 10^{-2}$. Although Kennicutt's derived slope could be somewhat steeper if the upper mass limit is very large, it is unlikely that the average Z for his sample could be so small as to bring this point into agreement with Eq. (5.2).

We can also compare the prediction of Eq. (5.2) with the direct star counts available for field stars, young open clusters, and associations in the solar neighborhood. With $Z \approx 0.02$, Eq. (5.2) would predict $\Gamma = -2$ for $m \gtrsim 5$–10. For $m \gtrsim 10$ the value of Γ for the local field star population is very uncertain as discussed in Section 2.6.4. above; the range of suggested values is indicated by the line marked "field" stars in Figure 65. For young open clusters and associations the IMFs all appear much flatter than Eq. (5.2). For example, Taff's (1974) composite open cluster IMF has $\Gamma \approx -1.8$ for 1–10$M_\odot$, but appears much flatter for $m \gtrsim 10$, a property exhibited by several individual clusters and associations. The inferred Γs for M17, NGC 6611, NGC 3292, and the Orion association are all flatter than $\Gamma = -1.5$, approaching -0.5 for M17 and NGC G11 (Terlevich and Melnick give $\Gamma = -2.9$ for Orion). Other determinations of composite open cluster IMFs give Γ's larger (flatter) than predicted by Eq. (5.2) for the appropriate metallicities (e.g. $\Gamma = -1.3$ for Piskunov 1974, $-1.7 < \Gamma < -1.2$ for Burki, 1977). Burki's (1977) large clusters, which are typically at larger galactocentric distances and hence smaller Z, have $\Gamma \approx -1.2$; agreement with Eq. (5.2) would require Z approaching 10^{-3} for these clusters, which is clearly unreasonable since they are all located within about 2 kpc of the sun. Terlevich and Melnick place the SMC with $Z \approx 0.002$ in Figure 65 using the value $\Gamma \approx -1.5$ inferred by Dennefeld and Tammann (1980); however, as discussed in Section 4.3, this result is based on spectroscopic matching using only the brightest stars, and the LF of the SMC, as well as the LMC ($Z \approx 0.008$), does not appear significantly flatter than the upper LFs of higher-Z galaxies, including our own. Futhermore, Freedman (1984) finds the slope of the LF for metal-poor dwarfs such a Ho IX to be identical with with that of M33 and very similar to the other to the other spirals in her study.

Taken together, these considerations show that a $\Gamma(Z)$ relation like Eq. (5.2) cannot apply to the average *global* IMF in galaxies, and disagrees with the IMF slopes determined from star counts in local young clusters and associations. The relation *might* hold for the giant HII regions and blue compact galaxies studied by Terlevich and Melnick, but this conclusion rests partly on the assumption that masses can be derived from emission linewidths assuming virial equilibrium, an assumption which now appears doubtful. In addition, the value of Γ for I Zw36 derived by Viallefond and Thuan (1984), which is based on a number of spectral indicators, does not agree with the prediction of Eq. (5.2).

The anticorrelation between $T_{\rm eff}$ and Z does suggest that metal-poor HII regions have either flatter high mass IMFs, or larger upper mass limits, or both. However, $T_{\rm eff}$ is also sensitive to the adopted model atmospheres, the age of the region, and its definition (see Figure 61).

The blue compact galaxies have been frequently linked to the lower surface brightness irregular galaxies of the Magellanic type. However, at present, there is little convincing indirect evidence concerning the IMF in these latter systems. A major problem is that it is still not possible to decide whether most of these galaxies are undergoing *global* star formation bursts, although localized bursts definitely occur (as they do even in normal spirals; these local bursting regions appear similar to the bursting blue compact galaxies). For this reason the IMF–SFR ambiguity is particularly severe, since it is difficult to ascertain whether the present galaxy-wide average star formation rate reflects a large fluctuation.

Gallagher, Hunter, and Tutukov (1984) have investigated the star formation histories in blue, high surface brightness irregulars using the galaxy mass, blue luminosity, and ionizing luminosity as measures of the SFR averaged over different times in the past. They find that for most of the galaxies the observations are consistent with a constant mean SFR and IMF over the galaxy's life, and that this conclusion may not lead to excessively short gas consumption timescales. This last point is still problematic, however. For example, Rocca-Volmerange *et al.* (1981) were able to fit the spectrum of the LMC from the UV to the red with a power law IMF with $\Gamma = -2$ and a roughly constant SFR for the past 10^{10}yr; however, the gas content would have then decreased by a factor of 10, contrary to observations, so these authors were forced to conclude that either there has been continuous gas accretion onto the LMC (for which there is no evidence) or that the IMF has a low-mass cutoff at 1–2$M_\odot$, so that the total star formation rate would be reduced. It is now clear from the LMC *H–R* diagram that the SFR has not been monotonic (see Hardy *et al.* 1984 and references therein), but this example still illustrates the potential problem with gas consumption if most dIrr galaxies are not currently experiencing global bursts. In that case the IMF must be enhanced in high-mass stars, or deficient in low-mass stars. Since we know from the luminosity functions of the LMC, SMC, IC 1613, Ho IX, and other irregulars that the shape of the upper IMF cannot be much different than in other galaxies (see Section 4.1 above), and also because the strengths of C III and Si IV in two dIrr's studied by Huchra *et al.* (1983) seem to rule out a very flat upper IMF or a significant number of supermassive stars, the simplest way to achieve this is with a low-mass cutoff around $1-2M_\odot$. We shall see in Section 6 below that there is some weak evidence from chemical evolution arguments that dIrr galaxies may be deficient in low mass stars compared to the solar neighborhood.

6. INDIRECT EVIDENCE: CHEMICAL EVOLUTION MODELS

Studies of galactic chemical evolution compare observationally-determined abundances of the elements and their isotopes with the predictions of schematic evolutionary models. These predictions use the composition and mass of material ejected from dying stars of a given initial mass as given by stellar evolution and nucleosynthesis calculations, along with assumptions about the IMF and the SFR history, to obtain the average abundances at any time. Eq. (1.19) is an example of the type of equation which is used to model chemical evolution in a closed system. This approach is very similar to the methods used in interpreting the integrated light of galaxies, except that theory now provides nucleosynethetic yields of the elements as a function of mass and composition, rather than evolutionary tracks and model atmospheres. With regard to the information provided on the IMF, a fundamental difference between integrated light and chemical studies is that the former are sensitive to the SFR history while the chemical predictions are not, at least for primary elements ejected by massive stars. Unfortunately the IMF–SFR ambiguity encountered in studies of integrated light is replaced by a sensitivity of the predictions to the adopted model. For this reason certain discrepancies between observations and the simple models can be resolved either by postulating an anomalous IMF (compared to the solar neighborhood) or by introducing a new feature into the models, such as the accretion of metal-poor gas or non-local gas flows. In this section we discuss several such IMF constraints. General reviews of chemical evolution modeling can be found in Trimble (1975), Tinsley (1980), Pagel and Edmunds (1981), Chiosi and Jones (1983), and Güsten and Mezger (1983).

Figure 66, from Audouze and Vauclair (1980), shows a typical prescription for the fractional mass of newly synthesized elements and collapsed remnants as a function of the initial stellar mass. This diagram should be considered as schematic, since differences exist between different sets of calculations (compare Arnett, 1978; Weaver, Zimmerman, and Woosley, 1978; Chiosi and Caimi 1979; and Maeder, 1981). The contribution of intermediate and low-mass stars in the asymptotic branch (double shell source) phase of evolution is especially uncertain (see Renzini and Voli, 1981 for one prescription). The fact that the total mass of different metals ejected by stars depends on mass shows that the predictions of a chemical evolution model will generally depend on the IMF. Figure 67 is the result of multiplying the yields of Figure 66 by an IMF with $\Gamma = -1.55$, showing the relative contributions of stars of different masses to the enrichment of different elements.

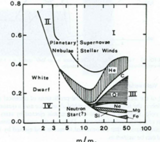

FIGURE 66 Typical prescription for the fractional mass of newly-synthesized elements and collapsed remnants as a function of initial stellar mass, from Audouze and Vauclair (1980).

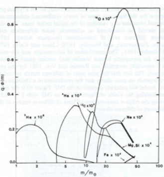

FIGURE 67 Yields of Figure 66 multiplied by an IMF with $\Gamma = -1.55$, showing relative contributions of stars of different masses.

6.1 Yield variations

One of the most important general predictions of chemical evolution models is the relation between metal abundance and a quantity called the yield, which is the mass of new metals ejected by stars per unit mass of matter locked into stars. Denoting the mass fraction of a star of initial mass m that is converted to metals and ejected by $P_z(m)$, the yield can be written as

$$y = (1-R)\int_{m_t(T)}^{m_u} mP_z(m)f(m)dm \Big/ \int_{m_l}^{m_u} mf(m)dm. \qquad (6.1)$$

where $m_t(T)$ is the turnoff mass corresponding to the system age T [assuming $m_t(T) > m_l$] and R is the fraction of mass that has formed stars and thereafter been ejected, the so-called "returned fraction". If the stars of initial mass m leave remnants of mass $w(m)$, then the returned fraction is

$$R = \int_{m_t(T)}^{m_u} [m - w(m)]f(m)dm \Big/ \int_{m_l}^{m_u} mf(m)dm. \qquad (6.2)$$

Estimates of R in the solar neighborhood are in the range 0.1 to 0.5. (The denominators of Eqs. (6.1) and (6.2) are absent from the equations of Tinsley [1980] because she normalized to $\int mf(m)dm = 1$, while the normalization used here is $\int f(m)dm = 1$.)

The importance of Eq. (6.1) for the present discussion is that, as long as $m_t(T)$ is smaller than the smallest mass of metal-forming stars, the yield y depends only on the IMF and the theoretical stellar metal production fractions $P_z(m)$.

In terms of y and R, the differential equation governing the metal abundance in a region of gas mass M_g is simply (see Tinsley, 1980)

$$M_g dZ/dt = y(1-R)B(t) + (Z_f - Z)f, \qquad (6.3)$$

where $B(t)$ is the stellar birthrate. This equation assumes $Z \ll 1$ and uses the instantaneous recycling approximation, which assumes that stars with $m < m_t(T)$ live forever, while those with $m > m_t(T)$ die as soon as they are born. The last term on the RHS represents infall of gas with metal abundance Z_f into the system at a rate f. A general result of chemical evolution models is that the predicted metal abundance is proportional to the yield and is independent of the past history of star formation, at least for primary elements produced in massive stars. Furthermore, the predicted Z depends only weakly on the parameters of the model, such as the gas fraction μ and the infall rate f. For example, in a model with no infall and zero initial Z, the result is

$$Z = y\ln(1/\mu). \qquad (6.4)$$

For a model in which infall just balances the SFR, the result is

$$Z = y[1 - \exp(-1-1/\mu)]. \qquad (6.5)$$

A more general solution for infall equal to a constant fraction of the SFR is given by Matteucci and Chiosi (1983).

The results that $Z \propto y$ and that Z/y is independent of SFR history hold for more complicated models in which the instantaneous recycling approximation is abandoned (e.g. Alloin *et al.*, 1979), and lead us to a choice between two interpretive approaches. Observations of Z and μ in galaxies could be used to test the nucleosynthesis calculations and constrain the evolutionary model, assuming a given IMF, or to probe for IMF variations and test the model assuming that the nucleosynthesis calculations are correct. This is a manifestation of the "IMF-model" ambiguity mentioned earlier. Because independent nucleosynthesis calculations give roughly consistent results and suggest only a weak dependence of the stellar production rates on metal abundance, the general practice has been to assume the validity of the nucleosynthesis calculations and focus on the IMF and model. A few examples of this approach will illustrate the possible implications for IMF variations and the difficulties involved.

Abundances derived from emission line strengths in HII regions are found to be spatially reasonably constant within individual Magellanic Irregular galaxies. This chemical homogeneity implies that these galaxies, and possibly the dwarf compact galaxies to which they may be related, are systems for which the simpler chemical evolution models are applicable. However, the fact that many of these galaxies have extensive HI halos (see Matteuchi and Chiosi, 1983; Gallagher and Hunter 1984 for references) suggests that infall may be important. Several studies have used the observed metal abundances and gas fractions μ to constrain the IMF in irregular and blue compact galaxies. Unfortunately the uncertainties in the empirical gas fractions are large, even for the LMC and SMC. The gas mass in the form of HI can be measured from 21 cm line observations, but the correction for molecular hydrogen is very uncertain. In addition, the HI distribution is usually much more extended than the HII regions used to derive the abundances, so it is not clear whether this outer gas should be included in the mass of gas which participates in the chemical evolution. Total masses can be estimated from HI rotation curves in some cases, but even then the estimate suffers from the complex structure and kinematics of these galaxies. Also it is not clear that the dynamical mass is equal to the mass of stars plus gas, since it is possible that these galaxies contain significant quantities of non-stellar dark matter. These uncertainties must be kept in mind in the following discussion.

Rocca-Volmerange *et al.* (1981) compared observed and theoretical oxygen yields for the LMC ($Z \approx 0.008$) and SMC ($Z \approx 0.003$), using a simple closed chemical evolution model. They show how the predicted oxygen yields depend on the IMF using three assumed IMFs. The first is a power-law approximation to the local IMF, with $\Gamma = -0.25$ for $0.25 < m < 1$, $\Gamma = -1.35$ for $1 < m < 2$, and $\Gamma = -2$ for $2 < m < 100$. The other two IMFs are power-laws with $\Gamma = -1.35$ or $\Gamma = -2$ for the entire mass range 0.25—$100 M_{\odot}$. Assuming no stars with $m < 0.25$, the predicted oxygen yields are 8×10^{-2} for the local IMF, 4×10^{-2} for the $\Gamma = -1.35$ case, and 2×10^{-3} for the $\Gamma = -2$ case. If half of the total stellar mass is in stars with $m < 0.25$ these yields are reduced by a factor of 2–3. The empirical yields estimated by Rocca-Volmeragne *et al.* (1981) for the simple closed model are 3.7×10^{-3} for the LMC and 1.2×10^{-3} for the SMC. This indicates that the $\Gamma = -2$ case with $m_l = 0.25$ gives a good fit, while the local IMF agrees if the fraction of mass in stars with $m < 0.25$ is significant. Considering the uncertainties, we can conclude that a value of $\Gamma \approx -2 \pm 0.5$ for $m \geq 2$ seems to be required, with a suggestion that the IMF is enhanced in very low mass stars compared to the solar neighborhood. Note that the fair agreement between the LMC and SMC yields indicates that their upper IMFs cannot be too dissimilar, in agreement with the star counts summarized earlier in Section 4.

An earlier study by Alloin *et al.* (1979) also used chemical evolution models to infer the IMF and other properties of extragalactic objects. Empirical O and N abundances and gas fractions for a variety of spiral disks and nuclei, irregulars, and blue compacts were compared with the predictions of a closed model. The theoretical O abundances depend on the IMF while N abundances depend on the IMF and on the assumed SFR history, because N was assumed to be partly a secondary element; however, the dependence of the N abundance on the SFR history was not very strong. Assuming that the closed model is valid and that the estimated gas fractions are accurate, the N and O abundances allow the determination of two parameters of the IMF, which were taken as the power law index Γ for $m>1$ and the fraction of the stellar mass with $m>1$, denoted ξ. Realizing that this procedure could only be applied to galaxies in which the gas fraction and abundances refer to the entire galaxy and in which $\mu \gtrsim 0.1$ to minimize the dependence of the N abundance on the SFR history, Alloin *et al.* restricted this part of their analysis to the five irregular and compact galaxies LMC, SMC, Mk 59, NGC 6822, and NGC 5253. They also compared the results with the same analysis applied to the solar neighborhood using abundances for the Orion Nebula. The values of Γ so derived came out to be surprisingly constant, in the range -1.52 to -1.65, for all the regions except NGC 5253, which gave $\Gamma=-2.3$. The fraction of mass with $m>1$ came out to be 0.13–0.16 for SMC, LMC, and NGC 6822, but larger, 0.23–0.25, for the solar neighborhood, NGC 5253, and Mk 59. For comparison, the local field star IMF of Section 2 gives $\xi=0.2$–0.6 for the range of birthrates considered. Considering uncertainties, Alloin *et al.* find that an abundance uncertainty of 50% corresponds to $\delta\Gamma \approx \pm 0.15$ and $\delta\xi \approx \pm 0.05$, while an uncertainty of a factor of 3 in the gas fraction corresponds to $\delta\Gamma \approx \pm 0.1$ and $\delta\xi \approx \pm 0.1$. Given the now-appreciated large uncertainties in μ, the results of Alloin *et al.* can be fairly summarized as $\Gamma=-1.6\pm0.3$, $\xi=0.2\pm0.1$ for all six galaxies except NGC 5253, which requires a steeper slope. I do not consider the slight differences in the derived values of ξ to be significant. The major problem with this result is that it rests on the validity of the closed model.

The applicability of simple closed models to dwarf irregulars and blue compact galaxies had been based partly on Lequeux *et al.*'s (1979) finding of a good correlation between Z and $\log\mu$ with $y \approx 4\times10^{-3}$, for a small sample of galaxies. However, subsequent studies using improved data for a large number of galaxies have shown that these galaxies are scattered below the relation found by Lequeux *et al.*, and have raised the question of significant IMF variations to explain this scatter.

Peimbert and Serrano (1982) studied this problem for about 25 irregular and dwarf compact galaxies, and also gave several estimates for yields in the solar neighborhood, galactic HII regions, and HII regions in M83. These authors noted two features of the distribution of objects in the $Z-\log\mu$ diagram. The first is the large scatter of the points compared to the straight line relation predicted by the simple closed model, implying IMF variations and/or inapplicability of the closed model (assuming that the μ estimates are accurate). They showed that models with constant yield $y=0.013$ and infall rates ranging from zero to $f=$ SFR could not account for the observed distribution (although it is not clear whether a smaller choice for the yield would remove most of the discrepancy); most galaxies would have to be accumulating mass somewhat faster than star formation can use it up, a possibility which they considered unattractive. The second point is a tendency for the empirical yields estimated for the simple model to increase with increasing metallicity. For example, the yields for irregular and dwarf compact galaxies are mostly in the range 2–4×10^{-3}, while the solar neighborhood and galactic HII regions with larger Z have $y \sim 5$–10×10^{-3}. The metal-rich HII regions in the galaxy M83 are found to have y as large as 20×10^{-3}. For these reasons Peimbert and Serrano suggested a Z-dependent yield of the form $y=0.002+0.6\ Z$, and showed that in this case all the objects except one could be explained by models in which the rate of infall plus stellar mass loss is smaller than the SFR.

Arguing that changes in stellar evolution properties with Z cannot explain the Z-dependent yield, Peimbert and Serrano suggest a Z-dependent IMF as the most likely culprit. A yield which increases with Z can be obtained by either an IMF whose high mass slope flattens with increasing Z or by an IMF in which the relative mass contained in low mass ($m \sim 1$–2) stars decreases with increasing Z. Noting that the bright star LFs of the Galaxy, the LMC, and IC 1613 do not show any dependence on Z (nor does the SMC or other galaxies—see Section 4), and that a change in the upper IMF slope with Z would cause a correlation of $\Delta Y/\Delta Z$ with Z which is not observed (although this is still somewhat controversial), they conclude that the fraction of low mass stars decreases with increasing Z. This conclusion is consistent with the LMC and SMC results of Rocca-Volmerange *et al.* (1981) discussed above. Since our galaxy and others exhibit a negative radial Z-gradient, this solution predicts that M/L ratios should increase with galactocentric distance, by factors of 2–5 out to a galactocentric distance of 10 kpc. Such gradients in M/L are in fact observed, but could also be attributed to nonstellar or even nonbaryonic matter (Section 5.2).

It should also be recalled that this proposed dependence of low-mass IMF on Z is just the opposite of what would be needed to account for the probable increase of M/L with Z in normal elliptical galaxies.

However, the case made by Peimbert and Serrano for a Z-dependent IMF and variable infall to explain the large dispersion of galaxies in the Z-log μ diagram has been considerably weakened by the thorough discussion of the properties and chemical evolution of 45 irregular and blue compact galaxies by Matteucci and Chiosi (1983), who considered the effects of a fluctuating star formation rate, infall, and galactic winds in their chemical evolution models. They do confirm the finding of Rocca-Volmerange *et al.* (1981) that the yields in the LMC and SMC require $\Gamma \approx -2$; $\Gamma = -1.35$ greatly over-produces oxygen, even if infall at the SFR is allowed. However, the models which match the LMC and SMC do not account for the rest of the galaxies, most of which have too small a Z for their estimated gas fractions, as shown in Figure 68. This result is similar to the plot given by Peimbert and Serrano, except that the large scatter is more apparent.

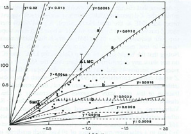

FIGURE 68 Metallacity–gas fraction diagram for various assumed yields, with and without fall, for observed irregular and blue compact galaxies, from Peimbert and Serrano (1982).

There are at least four possible explanations: 1. The gas fractions have been severely underestimated because most of the gas is molecular and/or because the dynamical mass is much larger than the star-plus-gas mass. 2. The yield, and hence the IMF, varies among the galaxies. Figure 69 shows lines of constant yield in the Z-ln μ plane for closed models (solid lines) and models in which the infall rate balances the SFR (dashed lines). The required variation in the IMF is very large; the relation $P_Z = 0.002 + 0.6\ Z$ suggested by Peimbert and Serrano (1982) does not give a sufficient yield variation even if variable rates of accretion up to the SFR are admitted, as pointed out by Matteucci and Chiosi. What seems to be required for the smallest $-Z$ galaxies (e.g. I Zw18) is that star formation prior to the present burst produced negligible numbers of massive stars, massive stars forming only during the present burst. The infrared light from red giants in some of these galaxies shows that an old population of low mass stars probably does exist (Thuan, 1983), but there is of course no way to test whether massive stars were also formed. 3. Infall of $Z = 0$ gas at rates exceeding the SFR has occurred. This solution requires inefficient star formation, but is perhaps suggested by the prevalence of large HI halos mentioned earlier. Figure 69 shows the predicted Z-log μ relation for an infall rate equal to 0, 1, 1.5, and 2 times the SFR. 4. Galactic winds energized by supernovae could reduce the gas fractions. Such winds have been suggested for other types of galaxies, and might be expected to be important in the loosely bound irregular and compact galaxies. Matteucci and Chiosi derive the Z-log μ relation for the case of a constant wind gas loss rate equal to some fraction λ of the net SFR. Figure 69 shows the result for $\lambda = 0, 1, 2$, and 4.

Evidently the IMF-model ambiguity will not be easily resolved for the irregular and blue compact galaxies. *If* the overly small metal abundances in some of these objects are solely due to IMF variations, then the IMF must be extremely deficient in massive stars, but not at the present epoch, since there is solid evidence from integrated light and a few luminosity functions that the present upper mass functions cannot be very abnormal. Considering the large uncertainties in the empirical gas fractions and the plausibility of substantial infall based on the existence of extensive HI halos, the case for substantial IMF variations remains unsettled. Further progress must await an understanding of the relation between the other properties of these galaxies (see Matteuchi and Chiosi, 1983), such as the possible correlation between metal abundance and total mass, in order to obtain a firmer physical model for their evolution.

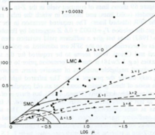

FIGURE 69 Metallicity–gas fraction diagram from Matteucci and Chiosi (1983). Yield is constant at 0.0032. Solid lines: Infall rate equal to λ times the star formation rate. Dashed lines: wind gas loss rate equal to Λ times the star formation rate.

At the other end of the metal abundance scale, we are faced with the large abundances found in spirals like M83 and M51 and in the central regions of large elliptical galaxies. If interpreted in terms of simple chemical models, these abundances imply IMFs which are progressively enriched in massive stars with increasing Z. It is incorrect, however, to interpret this as a causal dependence of the IMF on Z, since ellipticals presumably formed with near-zero metal abundances. Instead, the large present Z must be considered a *result* of a flat upper IMF, with the IMF controlled by physical conditions other than Z, such as density or turbulent velocity during elliptical galaxy formation.

It seems difficult to reconcile an IMF which flattens with increasing Z in ellipticals to explain their yields with the suggestion encountered in Section 5.2 above that the correlation of M/L with Z in ellipticals

is due to a proportion of *low*-mass stars which increases with Z. However, the two empirical constraints could be made compatible by postulating a low-mass cutoff which is initially large in ellipticals, say $m_l \sim 5$, and which decreases to small values ($m_l \sim 0.1$) only after the main burst of star formation has subsided. These low-mass stars might form from the gas expelled by more massive stars formed during the burst. In that case the M/L ratios could probably be accounted for by remnants of the massive stars, so the low-mass IMF would not need to be considerably different from the local IMF, in agreement with the constraint imposed by integrated light giant/dwarf indicators (Section 5.1 above). In addition, the *slope* of the upper IMF could be reasonably constant and independent of Z, as suggested by several lines of evidence discussed earlier, including direct star counts. It is interesting that a large value of m_l has also suggested for starburst galaxies (Section 5.9) and for density-wave induced star-formation (Section 7.4 below). These lines of argument, as well as the possible bimodality of the field star IMF (Section 2.6.3) lead to the conjecture that there are really two IMFs, one with $m_l \sim$ 1–10 which applies to regions in which star formation has been induced by some large-scale dynamical event, and the other with $m_l \simeq 0.1$ which obtains in relatively quiescent regions. We return to this idea below.

6.2 Metallicity distribution of disk dwarfs

The inability of the simplest chemical evolution models to account for the frequency distribution $p(Z)$ of metal abundances in low-mass disk dwarfs, independently discovered by van den Bergh and by Schmidt, is by now a classical problem (see Trimble, 1975 and Tinsley, 1980 for reviews). The discrepancy arises because the simplest model, assuming a closed homogeneous system which starts with no metals and evolves with a constant IMF, predicts too many stars with $Z \lesssim 0.3\ Z_\odot$ compared with the observed metallicity distribution of G-M dwarfs. As shown by Pagel and Patchett (1975) and others, the $p(Z)$ predicted by this simple model is independent of the history of the SFR and of the IMF, as long as the IMF is constant.

There are several proposed IMF variations which would resolve this difficulty, but they all basically involve an IMF at early times which was enhanced in high-mass stars. One can either postulate pre-enrichment of the disk by an earlier generation of massive stars, or assume that the disk star IMF itself was enhanced in massive stars at early times. Either way, very few low mass, low-Z stars would be formed. The IMF could have had an excess of metal-producing stars either because of flatter shape or a larger low mass cutoff m_l. It is easy to show that the required IMF need not be *too* peculiar compared to the present disk IMF by assuming that there is a lower limit to the mass of stars which produce and eject significant metals, and that the metal mass ejected by a star of initial mass m is given by a linear function of m, a good approximation to several stellar evolution calculations. Trimble (1975) shows that a simple variable yield model requires an initial yield $y_0 = 0.17$. For power law IMFs it is then straightforward to derive an expression for the ratio of initial yield to present day yield y_{now}, in terms of the parameters $m_{l,0}$, Γ_0, $m_{l,now}$, Γ_{now}. (We neglect the dependence of y on R here.) For example, if only the lower mass limit varies but the shape is constant, then for steep enough Γ,

$$m_{l,0} \approx m_{l,now}\,(y_{now}/y_0)^{1/\Gamma}. \tag{6.6}$$

With $\Gamma = -1.5$ to -2, the lower mass limit would only need to be 0.4–$0.7M_\odot$. With the field star IMF of Section 2.2, m_l would need to be ~ 2–$3M_\odot$. Alternately, if m_l is constant but Γ for $m > m_l$ varies, the required change in slope is

$$\Gamma_0 \approx \Gamma_{now} + \log(y_0/y_{now})/\log m_l \approx \Gamma_{now} + 1. \tag{6.7}$$

Obviously these approximations are simplistic, but they do suggest that radical changes in the IMF would not be necessary. A potential problem with the variable IMF model is that it may predict an embarrassingly large present Z unless the extra metals are locked up in remnants of massive stars, as pointed out by Trimble (1975).

The "G-dwarf" problem can also be resolved without invoking IMF variations. First, the early disk could have been enriched by metals expelled from halo stars with a normal IMF (Ostriker and Thuan, 1975). If the disk mass during the phase of halo star formation was small enough, the disk enrichment would be sufficient so that very few low-Z disk stars would have formed. The low-Z tail of $p(Z)$ is

then a reflection of the early mass growth of the disk. This idea is especially attractive because Larson's (1976) dynamical models for disk galaxy formation show significant early enrichment by halo stars, and in fact do reproduce the general form of $p(Z)$ in the solar neighborhood (Tinsley and Larson, 1978).

Instead of pre-enrichment of the disk by early infall, one can also use later infall of metal-poor gas (see Lynden-Bell, 1975). Parameterized studies of chemical evolution models with infall have been shown by numerous authors to provide a cure for the G-dwarf problem. A recent example is the work of Lacey and Fall (1983, see also Vader and de Jong, 1981), who use an exponentially declining infall rate and a SFR proportional to the n^{th} power of the gas volume density. Lacey and Fall show that for $n \approx 1$ and an infall time constant of about 5×10^9 yr (or slightly larger n and smaller time constant), the model reproduces the observed age-metallicity relation and the *differential* distribution $p(Z)$ (most previous work compared the cumulative distribution, which is somewhat easier to fit). Again, an important consideration is that Larson's (1976) dynamical models exhibit just the features desired with infall onto the disk continuing for several billion years. (In fact, many of the later papers which have more-or-less successfully accounted for properties of the solar neighborhood have in effect been simplified parameterized versions of Larson's models.) A possible problem with these late infall models is that they require a dependence of the SFR on gas density for which there is little observational evidence.

Another proposal for solving the G-dwarf problem assumes that the efficiency of star formation decreases strongly with decreasing metallicity. The specific form of this model discussed by Talbot and Arnett (1973) invokes large local chemical inhomogeneities, and so can also explain the spread in Z seen among stars of the same age. However, this spread can also be reasonably explained by inhomogeneous models which do not assume any Z-dependence (Audouze and White, 1984). There is also no observational or theoretical basis for a very small star formation efficiency in low-Z environments. One can argue that the metallicity controls the cooling function, temperature, and hence the Jeans mass, but then this model is equivalent to those assuming a larger low-mass cutoff at small Z.

In summary, there are a number of ways to account for the observed metallicity distribution and metallicity-age relation. While a flatter high-mass IMF and/or a larger low-mass IMF limit at early times can be invoked, models involving early disk enrichment by mass lost from halo stars and late infall of metal-poor gas appear less *ad hoc*, in the sense that their effects arise naturally in dynamical models for disk galaxy evolution. However, both IMF variations and infall effects may be important, and it is important to note that the suggested IMF variations are consistent with several other indirect arguments concerning IMF variations.

6.3 The "oxygen enhancement" in metal-poor stars

We have seen that attempts to constrain the IMF using the absolute values of metal abundances and their frequency distribution are ambiguous because of the sensitivity of the predicted abundances to the chemical model. This difficulty could be avoided if we could study the relative abundances of two (or more) elements whose yields depend differently on stellar mass. The difficulty with this approach is that it requires detailed predictions of stellar evolution and nucleosynthesis calculations as a function of stellar mass and metallicity, and the types of stellar ejection events which dominate the galactic enrichment of each element; this last point is especially problematic, as we shall now see.

Sneden, Lambert, and Whitaker (1979) summarized earlier work and presented new results showing that the O/Fe ratio is on average about 3–4 times larger in nearby metal-poor stars with $[Fe/H] \lesssim -0.5$ than in stars with larger [Fe/H], while $[C/Fe] \sim 0$, independent of [Fe/H]. This result was confirmed by Clegg, Lambert, and Tomkin (1983) for an enlarged sample of F and G dwarfs, and by Barbuy (1983) for two additional metal-poor stars. (A more recent review by Sneden [1985] suggests that [C/Fe] does increase at very small metallicities). Sneden *et al.* (1979) pointed out that the yields of these elements as a function of stellar mass given by Arnett (1978) predict that O/Fe increases with mass, while C/Fe is relatively independent of mass. The Fe yields are somewhat uncertain because of the uncertainty in how much iron is incorporated into a remnant as a function of mass, but the result that O/C increases with mass was confirmed in calculations which include mass loss by Maeder (1981, Figures 12–16) for 9–30$M_\odot$ models with $Z=0.03$ and by Ober, El Eid, and Fricke (1983) for 108–200$M_\odot$ models with $Z=0$. (At $m=200$ the calculations of Woosley and Weaver [1982], which do not include mass loss, give an O/C ratio which is about 5 times smaller than found by Ober *et al.*, although the absolute values of the O yields are similar). However, recent measurements indicate a much larger value for the $^{12}C(\alpha,\gamma)^{16}O$ cross-section, which will increase the yield of O relative to C (Lequeux, 1984, private communication).

These observed abundance trends *suggest* that the halo IMF was greatly enhanced in very massive stars relative to the disk IMF (Sneden *et al.*, 1979); in fact the IMF would have to contain most of its mass in stars with $m \gtrsim 50$ (see also Twarog and Wheeler, 1981). As with all other indirect IMF constraints, it is important to examine the possible alternative interpretations.

1. The elemental yields depend on the temperature–density structure of the stellar model, which may depend on Z, as pointed out by Clegg *et al.* (1983).

2. Even if the theoretical elemental yields are correct and do not depend on Z, the empirical abundance results only show that the dominant masses of stars which participate in chemical evolution were larger at low Z, a result which would also obtain if the mass range of stars which explode increased with decreasing Z. Given the extreme sensitivity of the available hydrodynamic explosion predictions to a number of factors (see Trimble, 1982; Wheeler, 1981, for reviews), this possibility cannot be presently ruled out.

3. The argument for an unusual halo IMF given above crucially depends on the assumption that C, O, and Fe are produced in short-lived massive stars. However, it is currently believed that Type I supernovae can be explained as explosions of accreting white dwarfs, which necessarily eject large quantities of Fe (see Nomoto, 1984; Woosley, Axelrod, and Weaver, 1984 and references therein), and possibly Si, S, and Ca (Nomoto, Thielemann, and Yokoi, 1984). Since white dwarf explosions may occur in stars with large ages, it can be seen that if O is produced in massive stars while most Fe comes from exploding white dwarfs, the O/Fe ratio will decrease with time. A chemical model based on such an idea was discussed by Tinsley (1979). In particular, the O/Fe ratio would be larger in halo stars, as observed, with no need for a peculiar IMF. This suggestion is also consistent with the observed constancy of [S/Fe] found by Clegg *et al.* (1983) if S is also produced primarily in exploding white dwarfs. The

statement that this model cannot enrich the halo from [Fe/H] ≈ −2.5 to −1.0 while keeping [O/Fe] constant (Twarog and Wheeler, 1981) is incorrect if *some* Fe is produced by massive stars.

In order to explain the increase in [O/C] with decreasing Z without invoking an IMF variation, a long-lived source of C is required. The ability of exploding white dwarfs to produce significant C is uncertain and requires further study. However, it is now realized that intermediate-mass carbon stars may also make a substantial contribution to the galactic C abundance (see Renzini and Voli, 1981). The estimated C production rates from this source are probably underestimates, since they are based on models which only predict C/O > for intermediate-mass stars, while observations clearly show that most carbon stars have masses $\sim 1 M_\odot$ (see Scalo, 1981, for a review).

Recently Matteucci and Tornambé (1984) have shown that single intermediate mass stars exploding by carbon deflagration (Type I−1/2 supernovae) can account for the observed [O/Fe]−[Fe/H] relation.

Evidently the use of abundance ratios of primary elements to constrain the IMF is not as clear-cut as is often supposed. The likelihood that exploding white dwarfs produce most of the Fe makes the [O/Fe] variaton irrelevant to the IMF. The strongest point in favor of a halo IMF enriched in massive stars is the increase of [O/C] with decreasing Z. If Type I supernovae or intermediate and low mass carbon stars are a significant source of galactic C, then the [O/C] variation can be accounted for without any necessity for an abnormal IMF. As pointed out by Lequeux (1984, private communication), the fact that the observed C/O ratios decrease in the sequence Milky Way–LMC–SMC strongly supports the idea that C is produced mainly by low-mass stars, since the present relative number of high-mass stars increases in this sequence.

6.4 Radial abundance gradients

Negative metal abundance gradients occur in many E and SO galaxies, inferred from color gradients, and in many S galaxies, including our own, determined from abundance analyses of HII regions and, for our galaxy, from abundances in late-type supergiants. The Galactic Z-gradient is $d\log Z/dr \approx -(0.07 \pm 0.02)\ \mathrm{kpc}^{-1}$ (e.g. Shaver *et al*., 1983) and similar gradients are found in other spiral galaxies (see Pagel and Edmunds, 1981). There is no consensus concerning the cause of these gradients, but since a variable IMF has been a frequently suggested agent, a brief review of the arguments is given here.

First of all, it is certain that a closed model with a constant IMF cannot explain the gradients. The gradients in the gas mass fraction are too small. The ability of models which include infall to produce the requisite gradients is apparently a controversial point. Chiosi (1980) and Diaz and Tosi (1984) find sizable Z gradients with a radially-independent infall rate, but the study of Lacey and Fall (1983) indicated that no combination of their model parameters could consistently account for the Galactic radial variation of Z, gas density, and SFR.

As emphasized by Tinsley (1980), Z gradients will be produced if there is a gradient in the metallicity of the infalling gas and/or the ratio of SFR to infall rate. In fact Larson's (1976) dynamical models for disk galaxies show both effects in the right direction and can produce Z-gradients which may be large enough to account for the observed gradients, as explained by Tinsley and Larson (1978), although Güsten and Mezger (1983) claim that the predicted gradients at the present time are too small.

Another effect of infall is that it must induce inward radial gas flows within the disk. Mayor and Vigroux (1981) showed that conservation of angular momentum demands that infall will lead to radial inflow at an estimated flow velocity of $\sim 10\ \mathrm{kms}^{-1}$ for an infall rate of $5 \times 10^{-3} M_\odot\ \mathrm{kpc}^{-2}\ \mathrm{yr}^{-1}$. They use a chemical evolution model incorporating the inflow, using $\mathrm{SFR} = \nu\sigma^k$ (σ = gas surface density) to show that the Z-gradient and gas surface density gradient can be account for if $k \approx 2$. Smaller values of k give smaller gradients. Tinsley (1980) shows that, to order of magnitude, $\partial(Z/y)/\partial \ln r \sim r/|v|\tau$. where v is the inflow velocity at position r and τ is the timescale for star formation to use up the gas. This shows that the inflow timescale $r/|v|$ must not be much smaller than the star formation timescale to produce significant gradients. Using data for the solar neighborhood, Tinsley shows that the required inflow velocity is a few $\mathrm{km\,s}^{-1}$, in agreement with the estimate of Mayor and Vigroux. Models with radial gas flows and constant IMF which consistently account for the Z-gradient have been recently presented by Lacy and Fall (1985).

Despite the marginal success claimed for some of these proposals, many workers feel that the most straightforward explanation for the observed Z-gradients is a radial gradient in the yield due to an IMF which contains a fraction of massive stars which decreases with increasing galactocentric radius. There are several ways to accomplish this behavior. For example, the shape of the mass function could steepen at larger radii. This suggestion seems unlikely considering the finding of Freedman (1985) that the bright star luminosity function in M33, which exhibits a modest Z-gradient, has a shape which is independent of galactocentric distance. A more detailed review of evidence relating to radial IMF variations is given in Section 7 below.

An interesting and compelling model to explain the Z-gradient in the spiral galaxies has been given by Güsten and Mezger (1983). In their model, the IMF has the same shape everywhere, but the lower mass limit is assumed to be large, $\sim 2-3\ M_\odot$, for stars formed in spiral arms and small, $\sim 0.1\ M_\odot$, for stars formed in interarm regions. The basic physical motivation for this model is that medium-mass clouds may only be able to grow to large mass clouds by collisional coalescence within spiral arms, although the evidence that only stars with $m \gtrsim 2-3$ form in these large clouds is very tentative. Given the assumed behavior of the lower mass limit, a radial Z-gradient arises because the SFR in arms at a given galactocentric distance R is assumed to be proportional to the rate at which interarm gas encounters arms, which is large at smaller R because of differential galactic rotation. Thus the ratio of arm to interarm star formation rates, and hence the ratio of stars formed with $m > 2-3$ stars formed with $m > 0.1$, increases at smaller R. The main effect causing larger yields at smaller galactocentric distance is the decrease of the fraction of locked-up matter, $(1-R)$, as m_l increases. The detailed models of Güsten and Mezger demonstrate that this "bimodal star formation" hypothesis gives good agreement with the observed Galactic ^{16}O gradient. In addition, this model increases the Lyc production rate per unit mass of gas forming stars because more massive stars are formed, thereby reducing the SFR deduced from radio continuum emission observations, which was uncomfortably large when interpreted using a constant IMF.

The proposal that m_l is much larger than $0.1 M_\odot$ in spiral arms, or more generally in any region in which large scale hydrodynamics induces a "burst" of star formation, is attractive. Suggestions for a larger m_l during the galaxy collapse phase and in starburst nuclei were encountered in earlier sections. Furthermore, surface photometric analyses of nearby spirals by Talbot *et al.* (1981) and Bash and Visser (1981) led these authors to conclude, from evidence completely independent of the Z-gradient arguments used by Güsten and Mezger, that only relatively massive stars are produced in spiral arms. These papers will be discussed in Section 7 below.

7 INTERNAL IMF VARIATIONS WITHIN GALAXIES

The most fundamental unknown about the IMF concerns the question of whether it varies from place and place, and how and why it might depend on local conditions. Although much of the empirical evidence concerning this question has been summarized in Sections 3–6 above, most of that discussion was concerned either with IMF variations on large scales $\gtrsim 1$ kpc, e.g. galaxy-to-galaxy variations, or with variations among star clusters on very small scales $\lesssim 100$ pc. For the most part we have not examined the evidence for and against internal galactic IMF variations on intermediate scales, and that is the subject of the present section. The discussion begins with the evidence related to the local IMF gradient in our galaxy, inferred from star counts, and a summary of the available information afforded by star counts in a few external galaxies. We then present the arguments which use indirect IMF indicators based on integrated light and chemical evolution models; the background for those methods has already been given in Sections 5 and 6.

7.1 IMF variations in the solar neighborhoods and external galaxies: star counts

Searches for variations in the local galactic stellar LF with direction or distance are only useful as probes of IMF variations for the most luminous stars. As we move to smaller luminosities the limiting volume for the LF determinations decreases rapidly. At the same time the average stellar age increases drastically, so that the present positions of these lower-luminosity stars may have little relation to their place of formation; any spatial IMF variations for these stars would probably have been washed out by orbital mixing caused by perturbations. In Section 2.2 it was seen that a number of independent LF estimates for intermediate luminosities based on different methods which sample different volumes of space generally showed reasonable agreement. Systematic searches for LF variations were discussed by McCuskey (1966). LFs for distances 100, 200, 400, and 600 pc, averaged over all longitudes (McCuskey, Figure 5) show only marginal systematic trends at the ~ 0.1–0.2 level in log $\phi(M)$. Variations of the LF with galactic longitude for various limiting distances up to 600 pc (McCuskey, Figure 6) suggest fluctuations less than a factor of two, considering the uncertainties in the individual LF determinations. These conclusions are supported by more recent LF determinations (e.g. Kipp, 1983), and by comparisons of galactic models with deep star counts (Pritchet, 1983; Bahcall and Soniera, 1984). Systematic variations in the LF with distance above the mid-plane do occur (McCuskey, Figure 7; see Gilmore and Reid, 1983), but are expected from the dependence of scale height on luminosity, as well as an increasing admixture of Population II stars, and so these variations have little to do with IMF variations.

Stars with masses $\gtrsim 15 M_\odot$ can be seen out to 2–3 kpc and are young enough so that they provide an adequate baseline for studying systematic variations of the IMF with galatocentric distance. Unfortunately the results have been ambiguous and even contradictory. As discussed in Section 3.3, Burki (1977) found a correlation between the LF slope and diameter for a sample of 27 young open clusters. Between $m \approx 2.5$ and 25–50, the corresponding IMF indices ranged from $\Gamma = -1.7$ for the small clusters to $\Gamma \approx -1.2$ for the large clusters. Burki argued that, because mean cluster size increases with galactocentric distance, this result could be interpreted as a flattening of the IMF with increasing galactocentric distance. However, since Burki did not specifically group the clusters according to galactocentric distance, it is difficult to judge the validity of his conclusion. I used Tarrab's (1982) maximum likelihood estimates of IMF indices obtained by spectroscopic matching to search for a correlation of Γ with galactocentric distance for the young clusters. The rather puzzling result is shown in Figure 70 for two different age groups (assuming $R_0 = 10$ kpc). The youngest clusters (age $< 2 \times 10^7$ yr, filled circles) show an abrupt increase in Γ for $R \gtrsim 11$, but for $R \lesssim 10$ kpc Γ appears to increase with *decreasing* R for both age groups. The fact that the minimum in Γ lies approximately at the solar galactocentric distance suggests some distance-dependent selection effect; a plot of

Γ as a function of distance shows only a weak correlation, with the scatter at any distance large, ~ 0.5 to 1. Evidently the question of a galactic IMF gradient cannot yet be answered using open clusters. However, it should be noted that Sagar *et al.* (1985) also found no evidence for a dependence of Γ on galactocentric distance for a smaller number of better-studied clusters.

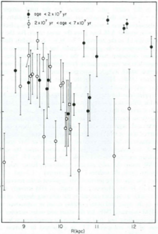

FIGURE 70 IMF index Γ as a function of galactocentric distance for the clusters studied by Tarrab (1982).

The field star LF adopted in Section 2.2 was based on the O star catalogue of Garmany *et al.* (1982; GCC) for $M_v \leq -5$. Data provided by Garmany for these stars were used to construct Figure 71, which shows the M_v distributions for stars inside (circles) and outside (squares) the solar circle, both for the complete sample (filled symbols) and for the luminosity class V stars along (open symbols). It can be seen that there is no significant difference between the form of the LFs in the center and anticenter for the total sample except at $M_v > -5$, where the counts are apparently incomplete. Notice that the incompleteness is worse for the stars toward the galactic center. A plot with smaller ΔM_v bins gives the same result. For the total O star sample the LF in the interval $-7 \leq M_v \leq -6$ is slightly flatter for stars in the direction of the galactic center, but the difference is within one standard deviation based on the counting uncertainties. A similar comparison for the cumulative *bolometric* LF of the O stars as well as a sample which includes supergiants and B stars by Humphreys and McElroy (1984; HM) gives the same result: The LFs toward the center and anticenter appear identical except for a greater degree of incompleteness for the stars toward the galactic center. HM suggest that the difference in completeness is due to the fact that most of the stars exterior to the sun appear in the northern sky (the Perseus arm) while those interior to the sun are mostly in the southern sky (the Carina and Sagittarius arms) which has not been as thoroughly observed and in which the extinction is generally higher. The LF of luminous stars therefore gives no evidence for an IMF gradient.

GCC estimated the IMF for their sample using the spectroscopic matching method (Section 2.6.4), not from the LF. They found that the IMF inside the solar circle is significantly flatter than that outside the solar circle, the indices Γ being around -1.3 and -2.1 respectively. (The sign of the inferred IMF gradient is the reverse of that suggested by Burki.) However, the study of HM strongly suggests that this result is an artifact caused by the differing degrees of incompleteness in the inner and outer samples noted in connection with Figure 71. HM estimated IMFs for the inner and outer samples by spectroscopic matching, but tried to correct for completeness by an extrapolation of the bolometric LF, as explained in Section 2.6.4. The resulting IMFs are shown in Figure 72, where the plus and cross represent the counts corrected in this way for incompleteness. The straight lines are least squares power law fits which are nearly identical, with $\Gamma = -2.5$. There *is* a larger *total* number of massive stars interior to the sun, but this increase is consistent with that expected from the overall increase in surface density of stars for an exponential disk with parameters appropriate to our galaxy, as pointed out by HM.

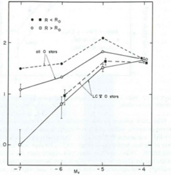

FIGURE 71 Luminosity functions for stars inside and outside the solar circle, from the O star catalogue of Garmany *et al.* (1982).

GCC and others have noted a radial gradient in the relative numbers of Wolf-Rayet stars in the galaxy, but it is not at all clear that this gradient is related to the IMF. Studies of the WR star populations in the LMC and SMC as well as indirect arguments suggest that much of the gradient may be due to the galactic metallicity gradient, possibly through the effect of metallicity on mass loss rates (see Maeder, Lequeux, and Azzopardi, 1980, and Meylan and Maeder, 1983).

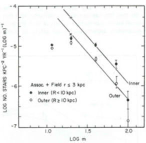

FIGURE 72 IMFs estimated by Humphreys and McElroy (1984) for stars inside and outside the solar circle.

What little information is available on luminosity functions at different positions within individual external galaxies gives no evidence for IMF variations. For the LMC, the studies of several regions outside of the bar region by Butcher (1977), Stryker and Butcher (1981), and Hardy (1978), and the study of a region near the northwest end of the bar by Hardy *et al.* (1984) all gave luminosity functions in surprisingly good agreement with each other and with the solar neighborhood function for various M_v ranges between ≈ -2 and $+4$, corresponding to a mass range from 8 $m_\odot$ to about 1.2 $m_\odot$. Freedman (1984, 1985) searched for radial variations in the LFs of several galaxies. The logarithmic slopes of the apparent LFs for four different radial intervals in M33 (the galaxy with the largest sample, over 5000 stars) are shown in Figure 73, assuming a distance modulus of 24.1. There is clearly no dependence of the slope on galactocentric distance within the uncertainties. In addition, the estimated M33 metallicity gradient ($d\log[\mathrm{O/H}]/dr \approx 0.13$ kpc^{-1}) therefore indicates no evidence for LF variations over a factor of 2 change in metal abundance. Similar studies for other galaxies in Freedman's sample also exhibit

no LF gradients, although the number of stars used in these cases is small. It is also important to note that in M33 Freedman found very similar LFs in the northern and southern regions, and in the arm and interarm regions. The north-south similarity disagrees with the conclusion of Boalerteix *et al.* (1982) based on [O III]/Hβ ratios.

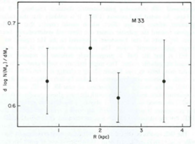

FIGURE 73 Logarithmic slope of the luminosity function as a function of galactocentric distance in M33, from the results of Freedman (1984, 1985).

7.2 A galactic gradient in the infrared excess?

In Section 5 the ratio of infrared flux to Lyman continuum flux, the so-called infrared excess or IRE, was discussed as a probe of the IMF. The IRE is a measure of the ratio of the total number of stars which contribute to the infrared luminosity by absorption and emission by dust to the number of massive stars which can ionize hydrogen. The IRE is sensitive to both Γ and m_u, but is difficult to interpret because of the unknown fraction of Lyc photons absorbed by dust. It is therefore of interest to examine the observed values of the IRE in different regions of our galaxy.

Boisse *et al.* (1981) presented the results of a balloon-borne survey in two wavelength bands around 100 μm for galactic longitudes from 0° to 85°. When combined with previous radio continuum observations at 5 GHz, the data allowed them to estimate the IRE for 13 HII complexes of approximately known distance. The basic result was that the IRE was very large (76) toward the galactic center, remained fairly large at galactocentric distances of 4–6 kpc (IRE ~ 20–60), and decreased with increasing galactocentric distance, reaching ~3 at 10 kpc. As noted by Lequeux (1982), it is unlikely that this radial gradient reflects an age effect, which would require that the HII regions toward the galactic center are observed systematically later after the onset of star formation compared to the HII regions with larger galactocentric radius. The conclusion drawn by Boisse *et al.* (1981) is that the IMF is progressively deficient in massive stars toward the galactic center. This might indicate a radial gradient in the upper mass limit m_u (see Figure 62), or a change in form of the IMF, or both. A similar conclusion was reached by Serra, Puget, and Ryter (1980) on the basis of a comparison of near-IR, far-IR, and radio continuum data, and also agrees with the open cluster results of Burki (1977) discussed in Section 7.1 above. A more recent survey of 34 HII complexes (Caux *et al.*, 1985) supports a radial gradient in the IRE, but the variation is much less pronounced: IRE ~7–17 at $R\sim$ 5 Kpc, IRE ~ 1–10 at $R\sim$ 10 Kpc.

The IRE results of Boisse *et al.* (1981) have been criticized by Scoville *et al.* (1983) and Lester *et al.* (1984). Scoville *et al.* point out that the radio continuum flux used by Boisse *et al.* for the galactic center is probably an underestimate by a factor of ~3, when scaled to the same beam size as the far IR data. Lester *et al.* have presented far-IR maps of the central core of the W43 complex, at a galactocentric distance of about 5 Kpc, and find IRE ≈ 2.4 to 3.3, depending on the assumed HII region temperature. This strongly contradicts Boisse *et al.* who found IRE = 26 for this region. Lester *et al.* argue that the large-beam measurements of Boisse *et al.* may be expected to overestimate the IRE because of the contribution by older subgroups in the complex, which have smaller turnoff masses and therefore much larger IREs (see Figure 62). If this hypothesis is correct for W43, then it would argue against any radial gradient in the IMF, since the Boisse *et al.* result would simply be due to a larger linear beam size (i.e. larger contribution from extended emission) at larger distances from

the sun. These problems are discussed in the more recent analysis of Caux *et al.* (1985).

I conclude that variations in the IRE for HII regions across our galaxy which could be linked to IMF variations are not firmly established; more high-resolution far-IR measurements of distant HII regions are needed to improve this situation. It should be remembered, however, that modest variations in the IRE can also be attributed to variations in the dust optical depth and the stellar birthrate.

7.3 Radial excitation gradients in galaxies

It is now well-established that spiral galaxies show radial gradients in excitation as measured by the [O III/Hβ] ratio, excitation increasing with galactocentric distance. Some of this gradient can be attributed to a metallicity gradient. Decreasing the oxygen abundance reduces the cooling rate from fine structure lines, leaving more energy to be radiated in optical forbidden lines; this effect causes the [O III] strength to increase with decreasing oxygen abundance. However, the *ratio* [O III]/Hβ is insensitive to the O abundance for $10^{-4}\leq$ O/H $\leq 4\times 10^{-4}$ (Stasinska, 1982), so gradients in this ratio must reflect a gradient in the effective temperatures of the exciting stars, at least for relatively low-Z galaxies (Lequeux, 1984, private communication).

Some part of the excitation gradient could therefore be due to an IMF gradient, requiring more massive, high-temperature stars at larger galactocentric distances. Motivated by the theoretical expectation that the upper mass limit m_u and hence maximum effective temperature T_u, should increase with decreasing metal abundance if m_u is controlled by radiation pressure and dust grains (Kahn 1974), Shields and Tinsley (1976; ST) investigated the contribution of a dependence of m_u on Z to the observed excitation gradient in M 101. As shown by ST, the theory predicts $m_u \propto Z^{-a/2}$, *with* $a\approx 1$, for $20 < m_u < 80$. Although ST were careful in their text to point out that their comparison with observations was only very marginally consistent with such a dependence of m_u on Z, and that their conclusions depend on several uncertain parameters, especially the adopted index of the IMF for massive stars, their abstract states that the observations are consistent with the $m_u \propto Z^{-1/2}$ result. For this reason their paper is often quoted as demonstrating that an m_u gradient exists in M 101 and probably other spirals which possess excitation gradients.

Because of this, a brief review of the argument presented by ST is in order.

For a given assumed relation $m_u \propto Z^{-a/2}$ and constant IMF index Γ, ST derived a theoretical expression for the change in T_u expected for a given change in Z (and helium abundance Y). Omitting the dependence on Y, this relation is, for $\Delta \log Z = -0.83 \pm 0.12$ appropriate for M 101,

$$\Delta \log T_u = (0.17 \pm 0.05)a + (0.05 \pm 0.02) \tag{7.1}$$

Notice that even with $a = 0$, $\Delta \log T_u \approx +0.05$ is expected because of the dependence of effective temperature on Z for massive stars, although this dependence is still not well established.

To test this prediction, ST derived a theoretical relation between the Hβ equivalent width and T_u, a relation which depends on the assumed index Γ of the IMF. (The dependence of $W(\mathrm{H}\alpha)$ on Γ and m_u based on more detailed stellar interior and atmosphere models was given in Section 5.9; see Figures 58 and 59.) An empirical estimate of the $W(\mathrm{H}\beta)$ gradient in M 101 gave $\Delta \log W(\mathrm{H}\beta) = 0.25 \pm 0.15$, which gives, from the theoretical $W(\mathrm{H}\beta)$ vs. T_u relation, $\Delta \log T_u = 0.02$ to 0.13, considering all the uncertainties. Comparing with the above expression for $\Delta \log T_u$ above, it is seen that consistency with the hypothesized $m_u(Z)$ relation, $a \approx 1$, requires that the $\Delta \log T_u$ derived from $W(\mathrm{H}\beta)$ be at the upper end of this range, while the coefficients in the theoretical relation above must be near their lower limits. However, a large semiempirical $\Delta \log T_u \approx 0.1$ requires a very steep IMF with $\Gamma \lesssim -3$ as used by ST. A shallower IMF slope gives a stronger dependence of $W(\mathrm{H}\beta)$ on T_u, and hence a smaller $\Delta \log T_u$ for a given $\Delta \log W(\mathrm{H}\beta)$, according to ST [their Figure 1; this also can be seen from inspection of Figure 58 for $W(\mathrm{H}\beta)$]. In fact, all of the various estimates of Γ for massive stars based on star counts of field stars (Section 2.6.4) and open clusters and associations (Sections 3.3 and 3.4), and nearly all of the indirect evidence based on integrated light (Section 5) and chemical evolution (Section 6) are consistent with Γ in the range -2.4 to -1. For $\Gamma \approx -2$ the semiempirical $\Delta \log T_u$ would be so small that $a \approx 0$ (i.e. no dependence of m_u on Z) is required. This conclusion depends somewhat on the theoretical relation between $W(\mathrm{H}\beta)$, T_u, and Γ. For example, assuming that $W(\mathrm{H}\beta) \propto W(\mathrm{H}\alpha)$, using an extrapolation of the $W(\mathrm{H}\alpha) - m_u$ relation derived from detailed models by Melnick *et al.* (1984), shown in Figure 58, and their adopted effective temperature scale I find $\Delta \log T_u \sim 0.05 - 0.1$, still smaller than the theoretical prediction for $a \sim 1$, but close enough to suggest that the currently large uncertainties in the stellar models as well as in the effective temperature scale might admit a mild dependence of m_u on $Z (a \lesssim 0.5)$. Unfortunately, since the theoretical dependence of $\Delta \log T_u$ on $\Delta \log m_u$ is also sensitive to the adopted models and temperature scale, it appears to me that the method used by ST to test for a dependence of m_u on Z is currently indeterminate. At any rate, the scaling relations used by ST and the empirical $W(\mathrm{H}\beta)$ gradient in M 101 are certainly inconsistent with any significant dependence of m_u on Z.

In a more recent analysis of HII regions in M 101, Shields and Searle (1978) emphasize the increase in the electron density-weighted mean fractional abundance of doubly-ionized oxygen with galactocentric radius. This gradient could be due to either a gradient in the effective temperature of the dominant ionizing star, or a gradient in the gas-to-dust ratio, as investigated by Sarazin (1976), but Shields and Searle were unable to decide between the two alternatives on the basis of the available data. However, even if the dust gradient hypothesis is rejected, it appears from the calculations of ST that the required gradient in maximum effective temperature can be obtained by considering only the effect of Z on the internal structure, without a need for invoking a dependence of m_u on Z.

In our galaxy, electron temperatures can be accurately determined from radio recombination lines (see Garay and Rodriguez, 1983; Shaver *et al.*, 1983; Wink, Wilson, and Bieging, 1983). The inferred galactic gradient in electron temperature, 400–500 K kpc^{-1}, is entirely consistent with the derived galactic metallicity gradient on the assumption that the temperature gradient is due solely to the metallicity gradient (Shaver *et al.*, 1983), with no need for a gradient in m_u.

Panagia (1980) has discussed effects which may account for the systematic decrease in the observed $\mathrm{He}^+/\mathrm{H}^+$ ratios in giant HII regions toward the galactic center. As discussed by Panagia, there are at least three ways in which such an ionization gradient can be explained as a consequence of the galactic metal abundance gradient: Depression of the He-ionizing continuum, decrease in effective temperature by an enhanced subphotospheric opacity, or a smaller upper mass limit for increasing Z. Panagia's calculations, based on apparently reasonable assumptions for these effects (although it is not clear how the Z-dependence of m_u was included; the reference to Kahn's calculations implies that $m_u \propto Z^{-1/2}$ was used), gave good agreement with the rather sparse evidence available at that time on He^+/H^+ as a function of galactocentric distance and the dominant effect is the variation of the upper mass limit, $m_u(Z)$. I have not attempted to reconcile this result with the fact that radio observations do not require such a dependence, or to evaluate the uncertainties in Panagia's calculations which include the dependence on the opacity details and the treatment of dust, and leave the matter of evidence for an m_u gradient from ionization and excitation gradients to future work.

An independent argument against a metallicity-dependent m_u was already offered in Section 4.1.4, where it was pointed out that such a relation would lead to an additional systematic effect in the correlation between luminosity of the brightest star in a galaxy and the total galaxy luminosity, an effect which is not seen. On the other hand, it was pointed out in Section 5 that there is an apparent anticorrelation between T_{eff} and Z among galaxies, suggesting an anticorrelation of either m_u or Γ with Z Except for the galactic IRE gradient, which may or may not exist as discussed above, this T_{eff}–Z anticorrelation is the only remaining compelling evidence for a possible dependence of the upper mass limit on metallicity. Evidently a great deal more work is required before we can claim to have established the existence or absence of internal radial IMF gradients in disk galaxies, including our own. The weight of the evidence suggests that the IMF variations are fairly small, but just how "small" is a question which awaits a future *coordinated* investigation of this problem, for which existing equipment appears adequate.

7.4 Spiral arm–interarm biomodality

It has occassionally been suggested that in spiral galaxies the IMF of stars formed in spiral arms differs from that of stars in the interarm regions. Most of these suggestions have been based either on qualitative theoretical arguments which lack much justification or on the idea that some local complexes produce only massive stars while others produce only low-mass stars, an idea which is also without firm basis (Section 3.7). However, there are three studies which, when

taken together, do strongly suggest that stars less massive than ~ 1–3 $M_\odot$ do not form efficiently in spiral arms compared to more massive stars, and these studies, two of which are based on photometry and one on chemical evolution, are summarized in this section.

Jensen, Talbot, and Dufour (1981; JTD) presented a detailed analysis of UBVR Hα surface photometry of the galaxy M83. The surface photometry was digitized as an image with a pixel size of 27 pc for a distance of 3.75 Mpc. After subtraction of a spheroid component and a disk component (defined to have inferred ages > 10^8yr), JTD were able to study the properties of the young stars found in the arms. The luminosity, age, and mass corresponding to each pixel was estimated by assuming that the light from each pixel is dominated by a group of stars which formed coevally (a "cluster") with a power-law IMF with $\Gamma = -1.35$ for $1.8 < m < 60$ and $\Gamma = -0.6$ for $0 < m < 1.8$, continuous at $m = 1.8$. These clusters were modeled theoretically using stellar evolutionary tracks to produce a curve in the $(U-B)$–$(B-V)$ diagram, each point on which corresponds to a definite age. The age of each pixel was then estimated by moving the observed position of the cluster in the two-color diagram, after correction for the disk contribution, back to the theoretical 2-color line assuming that the departure from this line was due to reddening following a normal solar neighborhood reddening law. The ages and the observed fluxes then allow an estimate of the SFR averaged over an annulus. Another estimate of the SFR comes from the Hα flux (corrected for extinction) over each annulus. Both SFR estimates assume the same IMF to include the low mass stars in the SFR, but of course the Hα rate is sensitive to more massive stars than the UBV rate. The reader is referred to the original paper for details of the procedure and the various sources of uncertainty.

JTD reach a number of interesting conclusions. First, the SFRs derived from UBV and Hα are so large that the gas would be used up in a very short time if the IMF is of the assumed form, suggesting that the IMF in the arms must be very deficient in low-mass stars. This conclusion would not be changed for any reasonable power law IMF. If viewed in terms of a lower mass limit, then $m_l \sim 0.5 - 3$, depending on the shape of the IMF. Second, the SFR from UBV colors greatly exceeds the SFR from Hα, suggesting a large deficiency of stars with $m \gtrsim 10$ compared to the assumed IMF. Steepening the IMF to $\Gamma = -2$ does not remove the discrepancy; the IMF must be very steep for $m \gtrsim 10$ or have an upper mass cutoff in the range $10-15M_{\odot}$. Alternatively, the effect might be attributed to excessive atmospheric blanketing compared to the models (the metallicities are very large in the regions of interest) or to most of the massive stars being hidden within dust cloud complexes. The hypothesis of a small upper mass limit has the advantage that it might circumvent a problem with excessive metal yields which might otherwise result from the large lower mass limit mentioned above. Finally, the derived distribution of cluster ages shows a broad peak at $20-40 \times 10^6$ yr. The deficiency of younger clusters must be due to either stars being hidden within their parent clouds for at least $20-30 \times 10^6$ yr or a small upper mass limit $m_u \sim 10$. JTD do not think it possible that most clusters remain hidden for more than about 10×10^6 yr, and so prefer the interpretation that $m_u \sim 10$. JTD suggest that the small value of m_u is controlled by radiation pressure on grains, although it was seen in Section 7.3 that there is currently no firm evidence for this effect. The decision between hidden clusters and small m_u does not seem so clear cut to me, especially considering the possibility of systematic errors in the derived ages due to the uncertainty in the extinction corrections, the effect of changing the assumed slope of the upper IMF, and the effect of noncoevality on the cluster color–age relations. It appears that the most secure conclusion is the first, that the lower mass limit is $\gtrsim 1M_{\odot}$ in the arms. This conclusion also agrees with the other two studies to be discussed presently.

Bash and Visser (1981) combined the two-armed spiral shock dynamical model for M81 by Visser with the "ballistic particle" model for star-forming CO clouds by Bash and co-workers in order to make predictions which can be compared with the spatial distribution and velocities of CO and HII regions. In the present procedure, Bash and Visser compared the predicted arm colors and widths with Schweizer's observations, a comparison which leads to an interesting conclusion about the IMF. The theoretical model basically consisted of CO clouds which are launched from spiral arms at the post-shock velocity given by Visser's dynamical models and then orbit ballistically in the axisymmetric potential of Visser's model. It was assumed on the basis of earlier work on this cloud model applied to our galaxy (see Bash, 1979; and references therein) that a cluster of stars forms in each cloud 25×16^6 yr after the cloud's formation in an arm. Assuming that stars in each cluster form coevally with an assumed

IMF, the color of each cluster can be followed as a function of time using theoretical evolutionary tracks. After subtraction of the disk light, this procedure allows a calculation of the mean arm colors in the galaxy model for different values of the density-wave amplitude in the old disk and for each of three adopted IMFs. The position of these models in the $(U-B)$–$(B-V)$ plane were then compared with Schweizer's (1976) observed arm colors dereddened by $E(B-V)=0.09$. The result was that the observed $U-B$ color is so blue (~ -0.5) that only a model with an IMF heavily weighted toward high-mass stars could yield agreement. Further support for this conclusion came from comparing the predicted and observed arm widths, which would be too broad if lower-mass stars formed in large numbers: however, this comparison is very sensitive to the model (i.e. the directions in which the clouds are "launched") and the modeling of the background disk light.

The IMF adopted by Bash and Visser had 83% of the stars by number (more than 99% by mass) more massive than $10M_{\odot}$. For comparison, the field IMFs of Section 2 all have less than 1% by number (less than 10% by mass) in stars above $10M_{\odot}$ (see Figure 22). The conclusion is that the spiral arms essentially make no stars with $m \lesssim 10$, or that the low-mass stars remain hidden in clouds while the high mass stars are visible, which seems unlikely. Bash and Visser also point out that if the IMF were normal, the implied SFR would be unreasonably large, basically the same result found by JTD. The required lower mass limit would be somewhere in the range $2-8M_{\odot}$ if the IMF at higher masses has the same form as in the solar neighborhood. Unfortunately, it is not possible from the published work to decide how sensitive this conclusion is to the adopted parametes, especially the parameters of the ballistic cloud model, the way in which the old disk light was subtracted, and the different definitions of "average arm color" to which the model and the observations refer. However, their conclusion does agree with that of JTD concerning the lack of low-mass stars formed in arms.

Further indirect support for a large lower mass limit in spiral arms comes from the study of chemical evolution by Güsten and Mezger (1983) already discussed in Section 6.4 above. In their model the shape of the IMF is the same everywhere, but the lower mass limit is $m_l \sim 2-3$ in the arms, compared to $m_l \sim 0.1$ for stars formed outside the arms. With this "bimodal" star formation model, and the assumption that the SFR is proportional to the rate at which interarm gas encounters a density wave, which increases with decreasing galactocentric distance because of differential rotation, Güsten and Mezger are able to account for the observed radial oxygen abundance in the Galaxy, since the fraction of massive stars, and hence the effective yield, increases toward the center. (An additional assumption that the SFR is also proportional to the first power of the gas density boosts the predicted gradient somewhat.) Models with a SFR depending on differential rotation which assume a constant IMF have difficulty accounting for the Z-gradient (Casse, Kunth, and Scalo, 1979). In addition, the model reduces the SFRs estimated from Lyc estimators such as Hα, Hβ, or radio continuum, which had implied uncomfortably small gas consumption timescales when interpreted in terms of a constant IMF; this remark applies not only to the Galactic SFR deduced from radio data discussed by Güsten and Mezger, but also to global SFRs estimated in other spiral galaxies (e.g. Kennicutt, 1983). It should also be noted that the ability of their model to reproduce the observed metallicity distribution and age–metallicity relation for solar neighborhood stars is due to the inclusion of infall, not the bimodal IMF.

Güsten and Mezger have demonstrated than an IMF in spiral arms which is deficient in low-mass stars can account for the Z-gradient, but the major question is: Is such an explanation really necessary, or can the Z-gradient be more "naturally" explained by gradients in the metallicity of infalling gas and/or the ratio of SFR to infall rate, as occur in Larson's (1976) dynamical models (see Tinsley and Larson, 1978), or by radial gas flows, whose plausible existence and ability to produce Z-gradients was demonstrated by Mayor and Vigroux (1981) (These proposals were discussed in Section 6.4). Güsten and Mezger argue that the Z-gradients produced by Larson's models are only significant during epochs when the accretion rate was large, and that the predicted present-day gradients are too small for our galaxy. Güsten and Mezger do not discuss the radial inflow hypothesis. Evidently this question cannot be presently resolved. However, the "bimodal m_l" model of Güsten and Mezger does seem very attractive, since, in addition to explaining the Z-gradients in spiral galaxies, it also reduces derived SFR's and is entirely consistent with the photometrically-based conclusions of JTD and Bash and Visser. It is also possible to relate the idea that the lower mass limit, but not the shape,

of the IMF is larger in regions which have suffered large-scale hydrodynamic disturbances to a surprisingly large number of observational results which have been discussed in the preceding sections. An attempt to draw all of the direct and indirect arguments together into a consistent empirical picture for the nature of the IMF is given in the next section.

8. CONCLUSIONS

Considering the wide range of topics and approaches which have been presented in the preceding sections, one cannot help but be impressed (or depressed) by how very little firm empirical knowledge we possess concerning the IMF. Large uncertainties and ambiguous interpretations abound. Nevertheless, an attempt will be made in this section to summarize the most reliable conclusions and synthesize them into a tentative picture for the behavior of the IMF which may be consistent with most of the available constraints.

We do know, or at least strongly suspect, a *few* things about the field star IMF. First, the local IMF probably peaks at $m \approx 0.3$ and declines at smaller masses, unless the mass-luminosity function has the severe form suggested by D'Antona and Mazzitelli (1983). Second, it is likely that the IMF is bimodal with a secondary peak at $\sim 1.2 M_\odot$. The IMF continues to decline at larger masses, but the form remains uncertain. A power law might have $\Gamma \sim -1.7$ for $2 \leq m \leq 10$, but the shape is extremely uncertain for $m \gtrsim 10$. A number of problems, from stellar evolution theory to the empirical effective temperature scale need to be attacked before further progress is possible. For these massive stars, the value of Γ (assuming that the IMF is actually of power law form) may lie between -1.3 and -2.4, and I feel there is as yet no basis to justify a particular choice in this range. Future work must concentrate on understanding the sources of uncertainty and their reduction, rather than aiming for definitive answers.

One significant result which may be correct is that the disk and halo field star IMFs appear very similar over the limited mass range $0.3 \leq m \leq 0.8$, implying no Z-dependence to the IMF at small masses.

Clusters and associations have given little new insight into the small-scale IMF and its relation to star formation processes. The difficulties involved in studying these objects, including membership, mass segregation, small numbers, and mass assignment, are severe. Several studies of *composite* cluster IMFs suggest $\Gamma \sim -1.7 \pm 0.2$ for $1.5 \leq m \leq 10$. At larger masses there are indications of significant flattening, especially from studies of individual young clusters. OB association IMFs seem to resemble the (very certain) field star IMF, but the data are too sparse for a firm conclusion. Concerning cluster-to-cluster variations, the weight of the evidence for individual well-studied clusters seems to point to general agreement, with, however, a few notable exceptions whose peculiarities (e.g. turnovers) are extremely difficult to confirm. The weight of the evidence, based on comparisons of individual clusters, certainly does not suggest that the *majority* of clusters are abnormal. On the other hand, one could conclude that wild IMF variations among clusters are common on the basis of Tarrab's (1982) work.

Given the available data and its uncertainties, globular cluster IMFs appear to be roughly similar; the differences which do appear may be real, or artifacts caused by incompleteness and/or mass segregation. At the upper end ($m \sim 0.6$–0.8), the globular cluster IMFs appear steeper than for either the disk or halo field stars, but again, this may be due to segregation.

Surprisingly (at least to me), star counts in other galaxies give a fairly convincing result, namely, that the luminosity functions of massive stars in galaxies of various morphologies, lumiosities, and metallicities are remarkably similar. Because of the differences in methodologies used in the various studies, no definitive conversion from LF to IMF can be made, but *differences* in Γ among most galaxies are probably less than ± 0.5, and possibly smaller. No systematic trends of LF with morphology or metallicity appear in the data. This result argues for a universal IMF shape, at least for massive stars with $m > 10$–20. At smaller masses, luminosity functions derived for several regions in the LMC agree with each other and with the solar neighborhood luminosity function, suggesting similar IMFs down to about $2M_{\odot}$.

Indirect arguments based on integrated light are problematical, yielding either indeterminate or ambiguous results concerning the IMF. However, there are a few useful and interesting results, most of which apply mainly to the high mass end of the IMF. Comparisons of galaxy evolution models with UV fluxes in many spiral and irregular galaxies (Donas and Deharveng, 1984), and the $W(\mathrm{H}\alpha)-(B\text{–}V)$ diagram for many late-type spirals (Kennicutt, 1983) appear to exclude variations in Γ between galaxies greater than about ± 0.3–0.5. For these two samples of galaxies, as well as for the two blue compact dwarfs studied by Viallefond and Thuan (1984), who used a number of spectral and continuum features, the derived values of Γ fall in the range -1.5 to -2; the derived values depend somewhat on the choice of upper mass limit, which should be treated as an additional parameter in future studies. These indirect results are in reasonable agreement with the IMF behavior inferred from star counts and again suggest universality of the IMF shape at large masses.

A particularly intriguing result found in many studies of interacting starburst galaxies is a deficiency of stars with masses less than about 3 to $20M_{\odot}$ (the actual value varies from galaxy to galaxy and is somewhat model-dependent). However, the *shape* of the IMF at greater masses does not show much evidence for abnormality. A similar result was suggested by Viallefond and Thuan's (1984) study of the blue compact galaxy I Zw36, which is also experiencing a burst of star formation. There are also indications that the IMF has a larger lower mass limit or mode within spiral arms, which can also be considered as regions experiencing "bursts" of star formation. These include the detailed study of surface photometry of M83 by Jensen *et al.* (1981), the comparison of arm colors and widths in M81 with models by Bash and Visser (1981), and the explanation of our galaxy's oxygen abundance gradient proposed by Güsten and Mezger (1983). The probable bimodality of the field star IMF is also consistent with this idea. Taken together, all these results suggest that the IMF terminates or turns over at fairly large masses (~ 2–$20M_{\odot}$) in regions in which large star formation rates have been instigated by large-scale hydrodynamic disturbances.

Most chemical evolution arguments, often invoked in the past to suggest IMF variations, have been found to be ambiguous. For example, yield variations in dwarf galaxies may be explained by combinations of infall, galactic winds, or uncertainties in estimated gas masses. The metallicity distribution of disk stars can be accounted for by pre-enrichment of the disk by early fall, later infall of metal-poor gas, or several other effects. The systematics of C, O, and Fe abundances in metal-poor stars can be understood if Type I supernovae in binary white dwarfs or carbon deflagration supernovae produce substantial Fe, as seems likely and if significant carbon is produced by Type I supernovae and/or carbon stars. If the latter condition is incorrect, then it may be necessary to invoke an early halo IMF enriched in high mass stars, as is frequently suggested. If this phase of proto-galactic evolution involved a large-scale burst of star formation, then this conclusion may be consistent with the evidence summarized earlier for an excess of high-mass stars in regions experiencing large global star formation rates. More refined calculations of models for Type I supernovae and carbon stars may be able to settle this question in the near future. Radial metal abundance gradients in galaxies might be explained by a combination of infall and radial flows, but an explanation in terms of a purely radial IMF gradient seems unlikely, especially considering the lack of evidence from star counts for radial IMF gradients in our own and other galaxies. The proposal of an arm–interarm IMF difference by Güsten and Mezger (1983) seems most promising, and is consistent with the type of IMF behavior suggested earlier for regions experiencing enhanced star formation rates.

I have found no convincing evidence for radial IMF variations within individual galaxies. The data used includes star counts and cluster IMFs in the solar vicinity, star counts in other galaxies, particularly M33 and the LMC, reported gradients in the Galactic IRE, and radial excitation gradients in our own and other galaxies, although these last two lines of evidence are still arguable. Similarly, I find no evidence for a dependence of the IMF shape at large *or* small masses on metal abundance. The dependence of excitation on metallicity found in several studies suggests an anticorrelation of the upper mass limit with metallicity, but the available results remain difficult to interpret. If such variations do exist, they are below the threshold of current observational and model uncertainties. A possible exception might be the elliptical galaxies. However, the large yields implied by the high metallicities in the central regions of large ellipticals would require a larger fraction of *high*-mass stars at larger Z, while an IMF-based explanation of the correlation of M/L with Z in ellipticals is that the fraction of *low*-mass stars increases with Z. Both arguments cannot be correct. As discussed earlier, both empirical constraints might be satisfied by the "variable m_l" IMF model suggested above if m_l is large during an early burst of star formation and small

($\sim 0.1 M_\odot$) after the burst has subsided, in which case the large M/L ratios might be accounted for by remnants of the massive stars.

Because the "variable m_l" model for the IMF is suggested by several lines of evidence and can resolve a number of apparent problems suggested by indirect studies, some further discussion is warranted. The basic suggestion is that in any large-scale region of star formation the IMF has a form which is independent of local or global conditions for masses well in excess of some characteristic mass m_0. The IMF is then assumed to terminate or turnover at (i.e., have a model at m_0. As a simple example, the IMF could have the form of a power law truncated exponentially low masses

$$C(\log m,t) = B(t)F(\log m,t) = B(t)Am^{\Gamma}\exp\left\{-[m_0(B(t)/m]^{\varepsilon}\right\} \qquad (8.1.)$$

The essential feature suggested by the considerations listed above is that the characteristic mass $m_0(t)$ must be an increasing function of the star formation rate $B(t)$, and so the creation function is no longer separable into an IMF and a birthrate. In an undisturbed spiral galaxy, the star formation rate might have essentially only two values: that in an arm and that in an interarm region; in this case, a bimodal IMF would arise, as suspected for the solar neighborhood field stars. A dwarf irregular galaxy which suffers a strongly fluctuating (in space and time) SFR will exhibit an IMF whose high-mass form is the same everywhere, but with bimodal or multimodal features at smaller masses, representing the superposition of all previous star formation episodes and their associated characteristic mass $m_0(t)$. Tidal or direct collisions between galaxies are apparently capable of causing extreme star formation bursts, and during such a burst m_0 will be large. It is important to emphasize that this proposed IMF is *not* intrinsically bimodal, but may appear bimodal after a given period of time due to the superposition of time-dependent IMFs which arise as $m_0[(t)]$ varies. The situation is similar to the superposition of open cluster IMFs illustrated in Figure 26. The observed present-day mass function is still given by Eqs. (2.2)–(2.4), except that $F(\log m)$ must be replaced by $F(\log m,t)$.

Although a detailed theoretical discussion is beyond the scope of this paper, it is worth noting that one simple model which could result in the above behavior is that outlined by Silk (1977), in which the enhanced cloud heating associated with an increasing number of high-mass stars increases the Jeans mass, and hence the characteristic mass. Any such coupling between the ultraviolet radiation field and fragment mass will result in the type of dependence of m_0 on $B(t)$ which is suggested by the observations, although m_0 would be a function not of the total SFR, but the SFR of stars massive enough to contribute to the gas heating ($\geq 20 M_\odot$).

Larson (1985) has independently investigated the consequences of a similar proposal for the IMF, but his suggested *form* is strictly bimodal and time-independent. His adopted creation function is

$$\begin{aligned} C(\log m,t) = {} & 1.43 m^{-2} \exp[-(0.3/m)^{3/2}] + \\ & 230 m^{-2} \exp(-t/3.4\ Gyr) \exp[(-2.2/m)^{3/2} \\ & \text{stars} (\log m)^{-1} \text{pc}^{-2}\, Gyr^{-1}. \end{aligned} \tag{8.2}$$

The first term represents a low-mass star formation mode whose rate is assumed constant with time, while the second term represents the high-mass mode whose contribution is assumed to decrease exponentially with time. The constants are chosen so that the high-mass mode gives sufficient remnants to account for the unseen mass in the solar neighborhood and so that the time integral of Eq. (8.2) gives a reasonable fit to the empirical field star IMF derived in Section 2.6 above.

Larson demonstrates that this creation function, besides giving sufficient remnants to account for the local unseen mass, results in good agreement with the age–metallicity relation of Twarog (1980), the SFRs in the inner regions of our galaxy and M33 without predicting more mass in low-mass stars than allowed rotation curves, the increase of both metallicity and M/L with mass among giant ellipticals (*if* the amplitude and characteristic mass of the high-mass mode increase with galactic mass), and possibly the dark matter in galaxy halos. It also increases the present timescales for gas consumption in our own and other spiral galaxies, which had seemed peculiarly small using "normal" IMFs (MS, Kennicutt, 1983; present work, Section 2.6.5).

Although Eqs. (8.1) and (8.2) have different forms, most of Larson's conclusions apply equally well to the time-dependent unimodal form of Eq. (8.1), since Larson requires variations in his parameter m_2 [$=2.2$ in Eq. (8.2)] and explicitly recognized that the for-

mation of massive stars must be favored in regions where the SFR is large. His theoretical speculation as to the cause of the bimodal IMF is also similar to that given in connection with Eq. (8.1); the difference is basically that Larson imagines that the gas will be heated very rapidly as soon as the first massive stars form, so that the Jeans mass will jump abruptly, giving a bimodal IMF. It would be possible to consolidate the two forms if a dependence of m_0 on the SFR per unit mass could be established using evolutionary models. Preliminary indications, culled from the papers already discussed, suggest $m_0 \sim 2$–3 in spiral arms, while estimates of m_0 range from $3M_\odot$ to $20M_\odot$ in starburst galaxies. There is some suggestion of a positive correlation of m_0 on SFR, but the number of parameters and uncertainties are presently too large for a definitive statement. In effect, the difference between the two forms is that, in Eq. (8.2), the characteristic mass is assumed to be given, while in Eq. (8.1), it is the star formation rate itself which controls the characteristic mass. I prefer the "variable m_0" model over the "bimodal" model because it seems more physically reasonable to adopt a dependence of a characteristic mass on the SFR than to posit a bimodal function whose mode masses, and their constancy, are left unexplained, but this is a matter of opinion at the present time.

Eq. (8.2), when integrated over the age of the disk, does give a useful representation of the empirical field star IMF, even if its application at any given time may not be valid. The only caveat is that the m^{-2} in the second (high mass mode) term should be written as m^{Γ}, with Γ an uncertain parameter somewhere between -1.3 and -2.4. In addition, the time constant in the second term was derived to fit the solar neighborhood and could have much smaller values in bursting galaxies; it must be treated as a parameter in extragalactic studies. Finally, for applications to individual external galaxies, it should be remembered that the exponential time dependence in the second term is only inserted for fitting the properties of the solar neighborhood conveniently, so that in (for example) starburst galaxies or blue compact galaxies, the time dependence of the high-mass mode must still be considered an open question.

Eq. (8.1) seems more realistic for applications to external galaxies because of its explicit dependence of m_0 on SFR, but is somewhat more difficult to deal with computationally because of the time- and SFR-dependence in the exponential. The available data are too meager to estimate the important function $m_0[B(t)]$. Inspection of published work in spiral arms and bursting galaxies does suggest an increasing function. If the feedback between star formation and IMF is due to only massive stars, then $m_0[B(t)]$ must be replaced by $m_0[B_M(t)]$, where $B_M(t)$ is the birthrate of massive stars alone, which depends on the instantaneous IMF form and so introduces a further implicit dependence. A simpler form which should probably be used in initial studies is a simple truncated power law with lower mass limit $m_l = m_l[B_M(t)]$.

In any case, the present considerations and Larson's (1985) work indicate that an IMF with constant shape at high masses but variable lower mass limit or mode mass depending on the SFR can explain many of the observed features of the solar neighborhood and other galaxies.

Besides this important effect, the available evidence on the *shape* of the IMF for masses $> m_0$ is consistent with universality for spatial scales $\gtrsim 1$ kpc. This result is equally important for theories of star formation. Unfortunately the uncertainties in the empirical estimates are large, and theorists appear capable of deriving agreeable IMF slopes using a wide range of physical ideas.

Acknowledgements

This manuscript was written over a period of three years, during which time a large number of people were kind enough to furnish preprints, figures, unpublished data, encouragement, and comments on particular parts of the text.

These include T. Armandroff, F. Bash, W. Freedman, C. Garmany, J. Hoessel, R. Humphreys, R. Larson, G. Miller, J. Mould, G. Shields, C. Sneden, L. Stryker, V. Trimble, D. Vanbeveren, D. Van Buren, C. Wheeler, B. Wilking, and H. Zinnecker.

I am especially grateful to G. Gilmore and R. Mathieu for their reading of and extensive comments on the early sections of the manuscript, and to the referee, J. Lequeux, for his constructive comments and suggestions concerning the entire text. I also want to acknowledge the work of G. Hickmann, S. Starrett, and C. Stepp, who typed and retyped numerous versions of this manuscript.

Finally, I wish to dedicate this work to the memory of Beatrice Tinsley, whose work on galaxy evolution provided much of the initial motivation for my interest in the initial mass function and its relation to other branches of astrophysics.

References

Aaronson, M., Cohen, J. G., Mould, J., and Malkan, M. (1978). *Astrophys. J.* **223,** 824.
Adams, M. T., Strom, K. M., and Strom, S. E. (1983). *Astrophys. J. Suppl.* **53,** 893.
Alcaino, G., and Thé, P. S. (1982). *PASP* **94,** 335.
Alloin, D., Collin-Souffrin, S., Joly, M., and Vigroux, L. (1979). *Astron. Astrophys.* **78,** 200.
Álvarez-Falcon, J. M. (1980). *Astron. Astrophys.* **89,** 291.
Anderson, J. (1983). *Astron. Astrophys.*, **118,** 255.
Andriesse, C. D. (1983). *Ap. Sp. Sci.* **89,** 401.
Andriesse, C. D., Packet, W., and de Loore, C. (1981). *Astron. Astrophys.* **95,** 202.
Anthony-Twarog, B. J. (1984). *Astron. J.* **89,** 267.
Applegate, J. H. (1983). *B.A.A.S.* **15,** 920.
Archemashvili, V. M. (1976). *Soviet Astrophys. J.* **20,** 116.
Argue, A. N., and Kenworthy, C. M. (1969). *MNRAS* **146,** 469.
Armandroff, T. E. (1982). Ph.D. dissertation, Wesleyan University.
Armandroff, T. E. (1983). In IAU Colloq. No. 76, *The Nearby Stars and The Stellar Luminosity Function*, A. G. Davis Philip and A. R. Upgren (Eds.), Schenectady: Van Vleck Observatory p. 229.
Arnett, W. D. (1978). *Astrophys. J.* **219,** 1008.
Artyukhina, N. M. (1972). *Soviet Astrophys. J.* **16,** 317.
Artyukhina, N. M. (1973). *Soviet Astrophys. J.* **17,** 65.
Audouze, J., and Vauclair, S. (1980). *An Introduction to Nuclear Astrophysics.* Dordrecht: Reidel.
Augarde, R., and Lequeux, J. (1985). *Astron. Astrophys.*, in press.
Bahcall, J. N. (1984). *Astrophys. J.* **276,** 169.
Bahcall, J. N., Schmidt, M., and Soneira, R. M. (1983). *Astrophys. J.* **265,** 730.
Bahcall, J. N., and Soneira, R. M. (1980). *Astrophys. J. Suppl.* **44,** 73.
Bahcall, J. N., and Soneira, R. M. (1981). *Astrophys. J. Suppl.* **47,** 337.
Bahcall, J., and Soneira, R. M. (1983). In *IAU Colloq. No. 76, The Nearby Stars and the Stellar Luminosity Function.* A. G. Davis Philip and A. R. Upgren (Eds.), Schenectady: Van Vleck Observatory, p. 209.
Bahcall, J. N., and Piran, T. (1983). *Astrophys. J. Letts.* **267,** L77.
Balzano, V. A. (1983). *Astrophys. J.* **268,** 602.
Barbuy, B. (1983). *Astron. Astrophys.* **123,** 1.
Barkhatova, K. A., Zakharova, P. E., and Shashkina, L. P. (1978). *Soviet Astr.* **22,** 31.
Barnes, T. G., Evans, D. S., and Moffett, T. J. (1978). *MNRAS* **185,** 285.
Barry, D. C., Cromwell, R. H., Hege, K., and Schoolman, S. A. (1981). *Astrophys. J.* **247,** 210.
Bartaya, R. A., and Kharadze, A. (1977). Astrofizika **13,** 123.
Bash, F. N., and Visser, H. C. D. (1981). *Astrophys. J.* **247,** 488.
Berkhuijsen, E. M. (1982). *Astron. Astrophys.* **112,** 369.
Berkhuijsen, E. M. (1983). *Astron. Astrophys.* **127,** 395.

Bertelli, G., Bressan, A., and Chiosi, C. (1984b). *IAU Symp. No. 105*, In *Observational Tests of Stellar Evolution Theory.* A. Maeder and A. Renzini (Eds.). Dordrecht: Reidel, p. 299.
Bertelli, G., Bressan, A. G., and Chiosi, C. (1984). *Astron. Astrophys.* **130,** 279.
Binette, L., Dopita, M. A., D'Odorico, S., and Benvenuti, P. (1982). *Astron. Astrophys.* **115,** 315.
Blaauw. (1964). *Ann. Rev. Astra. Ap.* **2,** 213.
Boeshaar, P. C., and Tyson, J. A. (1983). In *IAU Colloq. No. 76, The Nearby Stars and the Stellar Luminosity Function,* A. G. Davis Philip and A. R. Upgren (Eds.). Schenectady: Van Vleck Observatory, p. 85.
Boisse, P., Gispert, R., Coron, N., Wijnbergen, J. J., Serra, G., Ryter, C., and Puget, J. L. (1981). *Astron. Astrophys.* **94,** 265.
Brück, M. T. (1980). *Astron. Astrophys.* **87,** 92.
Bressan, A. G., Bertelli, G., and Chiosi, C. (1981). *Astron. Astrophys.* **102,** 25.
Brunish, W. M., and Truran, J. W. (1982a). *Astrophys. J.* **256,** 1247.
Brunish, W. M., and Truran, J. W. (1982b). *Astrophys. J. Suppl.* **49,** 447.
Bruzual, G. A (1983). *Astrophys. J.* **273,** 105.
Bruzual, G. A., Peimbert, M., and Torres-Peimbert, S. (1982). *Astrophys. J.* **260,** 495.
Burki, G. (1977). *Astron. Astrophys.* **57,** 135.
Burki, G. (1978). *Astron. Astrophys.* **62,** 159.
Burki, G., and Maeder, A. (1976). *Astron. Astrophys.* **51,** 247.
Butcher, H. (1977). *Astrophys. J.* **216,** 372.
Carrasco, L., Bisiacchi, G. F., Cruz-Gonzales, C., Firmani, C., and Costero, R. (1979), in IAU Symposium 83, *Mass Loss and Evolution of O-Type Stars,* ed. P. S. Conti and C. de Loore (Dordrecht-Reidel), 299.
Caux, E., Coron, N., Gispert, R., Puget, J. L., Ryter, C., and Serra, G. (1984). *Astra. Ap.* **137,** 1.
Caux, E., Puget, J. L., Serra, G., Gispert, R., and Ryter, C. (1985). *Astron. Astrophys.* **144,** 37.
Caryel de Strobel, G., and Delhaye, J. (1983). In *IAU Colloq. No. 76, The Nearby Stars and the Stellar Luminosity Function,* A. G. Davis Philip and A. R. Upgren (Eds.). Schenectady: Van Vleck Observatory, p. 241.
Cayrel, R., Cayrel de Strobel, G., Campbell, B., and Däppen, W. (1984). *Astrophys. J.* **283,** 205.
Cester, B. (1965). *Z. Ap.* **62,** 191.
Chan, K. L., and Sofia, S. (1983). *BAAS,* **15,** 913.
Chini, R., Elsässer, H., and Neckel, Th. (1980). *Astron. Astrophys.* **91,** 186.
Chiosi, C. (1981). In *The Most Massive Stars,* S. D'Odorico, D. Baade, and K. Kjär (Eds.). Munich: ESO, p. 27.
Chiosi, C. (1980). *Astron. Astrophys.* **83,** 206.
Chiosi, C. and Matteuchi, F. M. (1982). *Astron. Astrophys.* **105,** 140.
Chiosi, C., and Greggio, L. (1981). *Astron. Astrophys.* **98,** 336.
Chiosi, C. and Jones, B. (1983). In *The Origin and Evolution of Galaxies,* B. J. T. Jones and J. E. Jones (Eds.). Dordrecht: Reidel, p. 197.
Chiosi, C., and Matteucci, F. (1984). In *Formation and Evolution of Galaxies and Large Structures in the Universe,* J. Audouze and J. Tran Thanh Van (Eds.). Dordrecht: Reidel, p. 417.
Chiu, L.-T. G. (1980). *Astrophys. J.* **85,** 812.
Chiu, L.-T. and van Altena, W. F. (1981). *Astrophys. J.* **243,** 827.
Chu, Y.-H. and Daod, N. A. (1984). *PASP* **96,** 999.
Chu, Y.-H., Cassinelli, J. P., and Wolfire, M. G. (1984). *Astrophys. J.* 283, 560.
Claudius, M., and Grosbol, P. J. (1980). *Astron. Astrophys.* **87,** 339.

Clegg, R. E. S., Lambert, D. L., and Tomkin, J. (1981). *Astrophys. J.* **250,** 262.
Clegg, R. E. S., Lambert, D. L., and Tomkin, J. (1983). *Astrophys. J.* **250,** 262.
Cloutman, L. D., and Whitaker, R. W. (1980). *Astrophys. J.* **237,** 900.
Cloutman, L. D. (1983). *BAAS* **15,** 912.
Clube, S. V. M. (1983). In *AU Colloq. No. 76, The Nearby Stars and the Stellar Luminosity Function,* A. G. Davis Philip and A. R. Upgren (Eds.). Schenectady: Van Vleck Observatory, p. 289.
Cohen, M., and Kuhi, L. V. (1979). *Astrophys. J. Suppl.* **41,** 743.
Condon, J. J., Condon, M. A., Gisler, G., and Puschell, J. J. (1982). *Astrophys. J.* **252,** 102.
Conti, P. S. (1984). In *Observational Tests of Stellar Evolution Theory,* A. Maeder and A. Renzini (Eds.). Dordrecht: Reidel, p. 233.
Conti, P. S., and Burnichon, M.-L. (1975). *Astron. Astrophys.* **38,** 467.
Copeland, H., Jensen, J. O., and Jorgensen, H. E. (1970). *Astron. Astrophys.* **5,** 12.
Crézé, M. (1983). In *IAU Colloq. No. 76, The Nearby Stars and the Stellar Luminosity Function,* A. G. Davis Philip and A. R. Upgren (Eds.). Schenectady: Van Vleck Observatory, p. 181.
D'Antona, F., and Mazzitelli, J. (1978). *Astron. Astrophys.* **66,** 453.
D'Antona, F., and Mazzitelli, J. (1982). *Astron. Astrophys.* **113,** 303.
D'Antona, F., and Mazzitelli, J. (1983). *Astron. Astrophys.* **127,** 149.
Da Costa, G. (1982). *Astron. J.* **87,** 990.
Da Costa, G. S. and Freeman, K. C. (1976). *Astrophys. J.* **206,** 128.
De Gioia-Eastwood, K. (1984). *PASP,* **96,** 625.
De Gioia-Eastwood, K. (1985). *Astrophys. J.* **288,** 175.
Dennefeld, M., and Tammann, G. A. (1980). *Astra. Ap.* **83,** 275.
De Young, D. S., Lind, K., and Strom, S. E. (1983). *PASP,* **95,** 401.
Diaz, A. J., and Tosi, M. (1984). *MNRAS,* **208,** 365.
Dixon, M. E. (1970). *MNRAS,* **150,** 195.
Donas, J., and Deharveng, J. M. (1984). Preprint.
Donas, J., Milliard, B., Laget, M., Deharveng, J. M. (1981). *Astron. Astrophys.* **97,** L7.
Doom, C. (1982). *Astron. Astrophys.* **116,** 303.
Doom, C., and de Greve, J. P. (1983). *Astron. Astrophys.* **120,** 97.
Doom, C., de Greve, J. P., and de Loore, C. (1985). *Astrophys. J.* **290,** 185.
Duncan, D. K. (1981). *Astrophys. J.* **248,** 651.
Duncan, D. K., and Jones, B. F. (1983). *Astrophys. J.* **271,** 663.
Ebert, R., von Hoerner, S., and Temesvary, S. (1960). In *Die Enstehung von Sternen-durch Kondensation diffuser Materie.* Berlin: Springer-Verlag, p. 184.
Efstathiou, G., and Fall, S. M. (1984). *MNRAS* **206,** 453.
Eggen, O. J. (1982). *Astrophys. J. Suppl.* **50,** 221.
Eggen, O. J. (1983). *Astrophys. J. Suppl.* **51,** 183.
Ellis, R. S., Gondhalekar, P. M., and Efstathiou, G. (1982). *MNRAS* **201,** 223.
Faber, S. M. (1972). *Astron. Astrophys.* **20,** 361.
Faber, S. M., and Gallagher, J. S. (1976). *Astrophys. J.* **204,** 365.
Faber, S. M., and Gallagher, J. S. (1979). *Ann. Rev. Astron. Astrophys.* **17,** 135.
Faber, S. M., and Jackson, R. E. (1976). *Astrophys. J.* **204,** 668.
Falk, H. J., and Mitalis, R. (1983). *MNRAS* **202,** 19.
Fenkart, R. P. (1977). *Astron. Astrophys.* **56,** 91.
Freedman, W. L. (1984). Unpublished Ph.D. dissertation, University of Toronto.
Freedman, W. L. (1983a). In *Proc. IAU Colloq. 76, The Nearby Stars and the Stellar Luminosity Function,* A. G. Davis Philip and A. R. Upgren (Eds.). Schenectady: Van Vleck Observatory), p. 191.
Freedman, W. L. (1983b). *BAAS* **15,** 907.

Freedman, W. L. (1985). Preprint.

Freeman, K. C. (1977). In *The Evolution of Galaxies and Stellar Populations*, B. M. Tinsley and R. B. Larson (Eds.). New Haven: Yale University Observatory, p. 133.

Freeman, K. E. (1980). In IAU Symp. No. 85, in *Star Clusters*, J. E. Hesser (Ed.). Dordrecht: Reidel, p. 317.

Frogel, J. A., and Blanco, V. M. (1983). *Astrophys. J. Letters* **274**, L57.

Frogel, J. A., and Twarog, B. A. (1983). *Astrophys. J.* **274**, 270.

Frolov, V. N. (1975). *Soviet Astrophys. J. Letters* **1**, 156.

Gallagher, J. S., and Hunter, D. A. (1984). *Ann. Rev. Astron. Astrophys.* **22**, 37.

Gallagher, J. S., and Hunter, D. A. (1983). *Astrophys. J.* **274**, 141.

Gallagher, J. S., Hunter, D. A. and Tutukov, A. V. (1984). *Astrophys. J.* **284**, 544.

Garay, G., and Rodrigues, L. F. (1983). *Astrophys. J.* **266**, 263.

Garmany, C. D., Conti, P. S., and Chiosi, C. (1982). *Astrophys. J.* **263**, 777.

Gehrz, R. D., Sramek, R. A., and Weedman, D. W. (1983). *Astrophys. J.* **267**, 551.

Gerola, H., Seiden, P. E., and Schulman, L. S. (1980). *Astrophys. J.* **242**, 513.

Giampapa, M. S. (1984). *Astrophys. J.* **277**, 235.

Gilmore, G. (1983). In *Proc. IAU Colloq. 76, Nearby Stars and the Stellar Luminosity Function*, A. G. Davis Philip and A. R. Upgren (Eds.). Schenectady: Van Vleck Observatory, p. 197.

Gilmore, G., and Reid, N. (1983). *MNRAS* **202**, 1025.

Gispert, R., Puget, J. L., and Serra, G. (1982). *Astron. Astrophys.* **106**, 293.

Gliese, W. (1969). *Catalogue of Nearby Stars*, Astronomischer Rechen-Institute Heidelberg, No. 22.

Gunn, J. E., and Griffin, A. J. (1979). *Astron. J.* **84**, 752.

Gunn, J. E., Stryker, L. L., and Tinsley, B. M. (1981). *Astrophys. J.* **249**, 48.

Gunn, J. E., and Stryker, L. L. (1983). *Astrophys. J. Suppl.* **52**.

Güsten, R., and Mezger, P. G. (1983). *Vistas in Astronomy* **26**, 159.

Hardy, E. (1979). *Astron. J.* **83**, 319.

Hardy, E., Buonanno, R., Corsi, C. E., Janes, K. A., and Schommer, R. A. (1984). *Astrophys. J.* **278**, 592.

Harris, W. E., and Racine, R. (1979). *Ann. Rev. Astron. Astrophys.* **17**, 241.

Harris, W. E., and Hesser, J. E. (1985). In *Dynamics of Star Clusters*, IAU Symp. No. 113, J. Goodman and P. Hut (Eds.). Dordrecht: Reidel, p. 81.

Harris, W. E., and Canterna, R. (1980). *Astrophys. J.* **239**, 815.

Harris, W. E., Hesser, J. E., and Atwood, B. (1983). *PASP* **95**, 951.

Hartman, L., Soderblom, D. R., Noyes, R. W., Burnham, N., and Vaughan, A. H. (1984). *Astrophys. J.* **276**, 254.

Hartmann, W. K. (1970). *Mém. Soc. Roy. Sci. Liege* **14**, 49.

Haschick, A. D., and Ho, P. T. P. (1983). *Astrophys. J.* **267**, 638.

Heintz, W. D. (1972). *Astron. J.* **77**, 160.

Hellings, P., and Vanbeveren, D. (1981). *Astron. Astrophys.* **95**, 14.

Herbst, W. (1983), private communication.

Herbst, W. (1975). *Astron. J.* **80**, 683.

Herbst, W., and Dickman, R. L. (1983). In *IAU Colloq. No. 76, The Nearby Stars and the Stellar Luminosity Function*, A. G. Davis Philip and A. R. Upgren (Eds.). Schenectady: Van Vleck Observatory, p. 187.

Herbst, W., and Miller, D. P. (1982). *Astron. J.* **87**, 1478.

Herbst, W., and Sawyer, D. L. (1981). *Astrophys. J.* **243**, 935.

Hodge, P. W. (1961). *Astrophys. J. Suppl.* **6**, 235.

Hodge, P. W. (1979). *Astron. J.* **84**, 744.

Hodge, P. W. (1980). *Astrophys. J.* **241**, 125.

Hoessel, J. G., and Danielson, G. E. (1984). *Astrophys. J.* **286**, 159.

Hoessel, J. G., Schommer, R. A., and Danielson, G. E. (1983). *Astrophys. J.* **274**, 577.

Holmberg, E. (1950). *Medd. Lunds Obs.*, 1983, *Astrophys. J.* **266**, 263.

Ho, P. T. P., and Haschick, A. D. (1981). *Astrophys. J.* **248**, 622.

Huang, R. Q., and Weigert, A. (1983). *Astron. Astrophys.* **127**, 309.

Huchra, J. P. (1977). *Astrophys. J.* **217**, 928.

Huchra, J. P., Geller, M. J., Gallagher, J., Hunter, D., Hartmann, L., Fabbiano, G., and Aaronson, M. (1983). *Astrophys. J.* **274**, 125.

Humphreys, R. H. (1978). *Astrophys. J. Suppl.* **38**.

Humphreys, R. M. (1983a). *Astrophys. J.* **265**, 176.

Humphreys, R. M. (1983b). *Astrophys. J.* **269**, 335.

Humphreys, R. M. (1983c). In *The Most Massive Stars*, S. D'Odorico, D. Baade, and K. Kjär (Eds.). ESO: Munich, p. 5.

Humphreys, R. M., and McElroy, D. B. (1984). *Astrophys. J.* **284**, 565.

Humphreys, R. M., and Sandage, A. (1980). *Astrophys. J. Suppl.* **44**, 319.

Hunter, D. A., Gallagher, J. S., Rautenkranz, D. (1982). *Astrophys. J. Suppl.* **49**, 53.

Iben, I. (1967). *Astrophys. J.* **147**, 650.

Iben, I. and Talbot, R. J. (1966). *Astrophys. J.* **144**, 968.

Illingworth, G. (1976). *Astrophys. J.* **204**, 73.

Irwin, M. J., and Trimble, V. (1983). *Astron. J.* **89**, 83.

Israel, F. P. (1980). *Astron. Astrophys.* **90**, 246.

Israel, F. P., and Koornneef, J. (1979). *Astrophys. J.* **230**, 390.

Janes, K., and Adler, D. (1982). *Astrophys. J. Suppl.* **49**, 425.

Janes, K., and Demarque, P. (1983). *Astrophys. J.* **264**, 206.

Jarvis, J., and Tyson, A. (1981). *Astron. J.* **86**, 476.

Jaschek, C., and Jaschek, M. (1957). *Publ. ASP* **69**, 337.

Jensen, E. B., Talbot, R. J., and Dufour, R. J. (1981). *Astrophys. J.* **243**, 716.

Jones, B. F., and Cudworth, K. (1983). *Astron. J.* **88**, 215.

Jones, B. F., and Klemola, A. R. (1977). *Astron. J.* **82**, 593.

Jones, J. E., Alloin, D. M., and Jones, B. J. T. (1984). *Astrophys. J.* **283**, 457.

Kahn, F. D. (1974). *Astron. Astrophys.* **37**, 149.

Karimbadi, H., and Blitz, L. (1984). *Astrophys. J.* **283**, 169.

Kennicut, R. C., and Kent, S. M. (1983). *Astron. Astrophys.* **88**, 1094.

Kennicutt, R. (1984). *Astrophys. J.* **277**, 361.

Kennicutt, R. C. (1983). *Astrophys. J.* **272**, 54.

Kennicutt, R. C., and Keel, W. C. (1984). *Astrophys. J. Letters* **279**, L5.

Kholopov, P. N. (1969). *Soviet Astr.*, **12**, 625.

Kholopov, P. N., and Artyukhina, N. M. (1972). *Soviet Astrophys. J.* **15**, 760.

King, I. R. (1980). In *Star Clusters*, J. E. Hesser (Ed.). Dordrecht: Reidel, p. 139.

King, L., and Tinsley, B. M. (1976). *Astron. J.* **81**, 835.

Kipp, S. L. (1981). *BAAS* **13**, 539.

Kipp, S. L. (1983). In *IAU Colloq. No. 76, The Nearby Stars and the Stellar Luminosity Function*, A. G. Davis Philip and A. R. Upgren (Eds.). Schenectady: Van Vleck Observatory, p. 397.

Kormendy, J. (1977). In *The Evolution of Galaxies and Stellar Populations*, R. B. Larson, and B. M. Tinsley (Eds.). New Haven: Yale University Press, p. 131.

Kron, R. G. (1982). *Vistas in Astronomy* **26**, 37.

Kunkel, W. E., Liebert, J., and Boronson, T. A. (1984). *PASP* **96**, 896.

Lacey, C. G., and Fall, S. M. (1983). *M. N.* **204**, 791.

Lacey, C. G., and Fall, S. M. (1985). *Astrophys. J.* **290**, 154.

Lacy, C. H. (1977). *Astrophys. J. Suppl.* **34**, 479.

Lacy, J. H., Townes, C. H., and Hollenbach, D. J. (1982). *Astrophys. J.* **262**, 120.

Lada, C. J., and Wilking, B. A. (1984). *Astrophys. J.* **287**, 610.

Lambert, D. L., Dominy, J. F., and Sivertsen, S. (1980). *Astrophys. J.* **235**, 114.
Lamers, H. J. G. L. M., Paerels, F. B. S., and de Loore, C. (1980). *Astron. Astrophys.* **87**, 68.
Landolt, A. U. (1979). *Astrophys. J.* **231**, 468.
Larson, R. B. (1973). *MNRAS* **161**, 133.
Larson, R. B. (1976). *MNRAS* **176**, 31.
Larson, R. B. (1982). *MNRAS* **200**, 159.
Larson, R. B. (1985). Preprint.
Larson, R. B., and Starrfield, S. (1971). *Astron. Astrophys.* **13**, 190.
Larson, R. B., and Tinsley, B. M. (1978). *Astrophys. J.* **219**, 46.
Lauer, T. R. (1984). *BAAS* **16**, 455.
Lequeuex, J. (1983). Tenth Advanced Course of the Swiss Society of Astronomy and Astrophysics. In *Star Formation*, A. Maeder and L. Martinet (Eds.), p. 175.
Lequeux, J. (1979). *Astron. Astrophys.* **80**, 35.
Lequeux, J., Martin, N., Prévot, L., Prévot-Burnichon, M. L., Rebeirot, E., and Rousseau, J. (1980). *Astron. Astrophys.* **85**, 305.
Lequeux, J., Maucherat-Joubert, M., Deharveng, J. M., and Kunth, D. (1981). *Astron. Astrophys.* **103**, 305.
Lequeux, J., Peimbert, M., Rayo, J. F., Serrano, A., and Torres-Peimbert, S. (1979). *Astron. Astrophys.* **80**, 155.
Lequeux, J. (1979). *Revista Mexicana de Astronomie y Astrofisica* **4**, 325.
Lequeux, J., and Viallefond, F. F. (1980). *Astron. Astrophys.* **91**, 269.
Lequeux, J., and West, R. M. (1981). *Astron. Astrophys.* **103**, 319.
Lester, D. F., Dinerstein, H. L., Werner, M. W., and Harvey, P. M. (1984). *Astrophys. J.* In press.
Limber, D. N. (1960). *Astrophys. J.* **131**, 168.
Linde, P., Ardeberg, A., Lindgren, H., and Lynga, G. (1984). IAU Symp. No. 108, In *Structure and Evolution of the Magellanic Clouds*, S. van den Bergh and K. de Boer (Eds.). Dordrecht: Reidel, p. 99.
Lippincott, S. L., and Hershey, J. L. (1972). *Astron. J.* **77**, 679.
Lucke, P. B. (1972). Unpublished Ph.D. dissertation, University of Washington.
Lucke, P. B. (1978). *Astron. Astrophys.* **64**, 364.
Luyten, W. J. (1968). *MNRAS* **139**, 221.
Lynden-Bell, D. (1975). *Vistas in Astronomy* **19**, 299.
Lynga, G. (1982). *Astron. Astrophys.* **109**, 213.
Madore, B. F. (1970). Unpublished Master's dissertation, University of Toronto.
Madore, B. F. (1977). *MNRAS* **178**, 1.
Maeder, A. (1975a). *Astron. Astrophys.* **40**, 303.
Maeder, A. (1975b). *Astron. Astrophys.* **43**, 61.
Maeder, A. (1976). *Astron. Astrophys.* **47**, 389.
Maeder, A. (1980). *Astron. Astrophys.* **92**, 101.
Maeder, A. (1981). *Astron. Astrophys.* **101**, 385.
Maeder, A. (1981a). *Astron. Astrophys.* **99**, 97.
Maeder, A. (1982a). *Astron. Astrophys.* **101**, 385.
Maeder, A. (1982b). *Astron. Astrophys.* **105**, 149.
Maeder, A. (1983). *Astron. Astrophys.* **120**, 113.
Maeder, A. (1984). IAU Symp. No. 105, In *Observational Tests of Stellar Evolution Theory*, A. Maeder and A. Renzini (Eds.). Dordrecht: Reidel, p. 299.
Maeder, A., Lequeux, J., and Assopardi, M. (1980). *Astron. Astrophys.* **90**, L17.
Maeder, A., and Mermilliod, J. C. (1981). *Astron. Astrophys.* **93**, 136.
Marcus, P. S., Press, W. H., Teukolsky, S. A. (1983). *Astrophys. J.* **267**, 795.
Marcy, G. W. (1983). *BAAS* **15**, 947.

Massey, P., and Hutchings, J. B. (1983). *Astrophys. J.* **275**, 578.
Mathieu, R. D. (1983). Unpublished Ph.D. dissertation, University of California, Berkeley.
Mathieu, R. D. (1984). *Astrophys. J.* **284**, 643.
Matraka, B., Wassermann, C., and Weigert, A. (1982). *Astron. Astrophys.* **107**, 283.
Matteucci, F., and Tornambé, A. (1984). IAU Symp. No. 105, In *Observational Tests of Stellar Evolution Theory*, A. Maeder and A. Renzini (Eds.). Dordrecht: Reidel, p. 577.
Mayor, M. and Vigroux, L. (1981). *Astron. Astrophys.* **98**, 1.
McCarthy, D. W. (1983). In *IAU Colloq. No. 76, The Nearby Stars and the Stellar Luminosity Function*, A. G. Davis Philip and A. R. Upgren (Eds.). Schenectady: Van Vleck Observatory, p. 107.
McClure, R. D., Forrester, W. T., and Gibson, J. (1974). *Astrophys. J.* **189**, 409.
McCuskey, S. W. (1956). *Astrophys. J.* **123**, 458.
McCuskey, S. W. (1966). *Vistas in Astronomy* **7**, 141.
McNamara, B. J. (1976). *Astron. J.* **81**, 845.
McNamara, B. J., Pratt, N. M., and Sanders, W. L. (1977). *Astron. Astrophys. Suppl.* **27**, 117.
McNamara, B. J., and Sanders, W. L. (1977). *Astron. Astrophys.* **54**, 569.
McNamara, B. J., and Sanders, W. L. (1978). *Astron. Astrophys.* **62**, 259.
Melnick, J., Terlevich, R., and Eggleton, P. P. (1984). *MNRAS.* In press.
Mengel, J. G., Sweigert, A. V., Demarque, P., and Gross, P. G. (1979). *Astrophys. J. Suppl.* **40**, 733.
Mercer-Smith, J. A., Cameron, A. G. W., and Epstein, R. I. (1984). *Astrophys. J.* **279**, 363.
Mermilliod, J. C. (1981). *Astron. Astrophys.* **97**, 235.
Meylan, G., and Maeder, A. (1982). *Astron. Astrophys.* **108**, 148.
Meylan, G., and Maeder, A. (1983). *Astron. Astrophys.* **124**, 84.
Mezger, P. G., and Smith, L. F. (1976). In *Proceedings of the Third European Astronomical Meeting*, E. K. Kharadze (Ed.). Tbilsi: Georgian SSR Academy of Sciences, p. 369.
Mezger, P. G., Smith, L. F., and Churchwell, E. (1974), *Astron. Astrophys.* **32**, 969.
Mezzetti, M., Giuricin, G., and Mardirossan, F. (1983). *Astron. Astrophys.* **122**, 333.
Miller, G. E., and Scalo, J. M. (1978). *PASP* **90**, 506.
Miller, G. E., and Scalo, J. M. (1979). *Astrophys. J. Suppl.* **41**, 513.
Mould, J. R. (1982). *Ann. Rev. Astron. Astrophys.* **20**, 91.
Natta, A. and Panagia, N. (1976). *Astron. Astrophys.*, **50**, 191.
Neece, G. D. (1984). *Astrophys. J.* **277**, 738.
Nomoto, K. (1984). In *Stellar Nucleosynthesis*, C. Chiosi and A. Renzini (Eds.). Dordrecht: Reidel, pp. 205, 238.
Nomoto, K., Thielemann, F.-K., and Yokoi, K. (1984). Submitted to *Astrophys. J.*
O'Connell, R. W. (1976). *Astrophys. J.* **206**, 370.
Ober, W. W., El. Eid. M. F., and Fricke, K. J. (1983). *Astron. Astrophys.* **119**, 61.
Olofsson, K., Bergvall, N. and Ekman, A. (1984). *Astron. Astrophys.* **137**, 327.
Olson, G. L., and Pena, J. H. (1976). *Astrophys. J.* **205**, 527.
Oort, J. H. (1979). *Astron. Astrophys.* **78**, 312.
Osterbrock, D. E. (1974). *Astrophysics of Gaseous Nebulae*. San Francisco: W. H. Freeman.
Ostriker, J. P., and Thuan, T. X. (1975). *Astrophys. J.* **202**, 353.
Pagel, B. E. J., and Edmunds, M. G. (1981). *Ann. Rev. Astron. Astrophys.* **19**, 77.
Pagel, B. E. J., and Patchett, B. E. (1975). *MNRAS* **172**, 13.
Panagia, N. (1973). *Astron. J.* **78**, 929.

Panagia, N. (1980). In *Radio Recombination Line*, P. A. Shaver (Ed.). Dordrecht: Reidel, p. 99.

Panagia, N., Tanzi, E. G., and Tarenghi, M. (1983). *Astrophys. J.* **272,** 123.

Papp, K. A., Purton, C. R., and Kwok, S. (1983). *Astrophys. J.* **268,** 145.

Patenaude, M. (1978). *Astron. Astrophys.* **66,** 239.

Pawlowicz, L. M. and Herbst, W. (1980). *Astron. Astrophys.*, **86,** 68.

Peimbert, M., and Serrano, A. (1982). *MNRAS* **198,** 563.

Pels, G., Oort, J. H., and Pels-Louyver, H. A. (1975). *Astron. Astrophys.* **43,** 423.

Peruanskii, S. S., and Ryadchenko, V. P. (1978). *Soviet Astr.* **22,** 34.

Piskunov, A. E. (1976). *Nauch. Informatsii* **22,** 47.

Piskunov, A. E. (1981). *Astron. Zh., Sov. Astr. Lett.* **7,** 14.

Piskunov, A. E., and Vereshchagin, S. V. (1985). In *The Galaxy and the Solar System*, J. Bahcall, R. Smoluchowski, and M. Matthews (Eds.). Tucson: University of Arizona Press (in press).

Popper, D. M. (1980). *Ann. Rev. Astron. Astrophys.* **18,** 115.

Prata, S. W. (1971a). *Astron. J.* **76,** 1017.

Prata, S. W. (1971b). *Astron. J.* **76,** 1029.

Pritchet, C. (1983a). In *IAU Colloq. No. 76, The Nearby Stars and the Stellar Luminosity Function*, A. G. Davis Philip and A. R. Upgren (Eds.). Schenectady: Van Vleck Observatory, p. 171.

Pritchet, C. (1983b). *Astron. J.* **88,** 1476.

Probst, R. G. (1977). *Astron. J.* **82,** 656.

Probst, R. G. (1983c). *Astrophys. J.* **274,** 237.

Probst, R. G. (1983d). *Astrophys. J. Suppl.* **53,** 335.

Probst, R. G. (1983a). In *IAU Colloq. No. 76, The Nearby Stars and the Stellar Luminosity Function*, A. G. Davis Philip and A. R. Upgren (Eds.). Schenectady: Van Vleck Observatory, p. 369.

Probst, R. G. (1983b). In *IAU Colloq. No. 76, The Nearby Stars and the Stellar Luminosity Function*, A. G. Davis Philip and A. R. Upgren (Eds.). Schenectady: Van Vleck Observatory, p. 403.

Probst, R. G., and O'Connell, R. W. (1982). *Astrophys. J. Lett.* **252,** L69.

Quirk, W. J., and Tinsley, B. M. (1973). *Astrophys. J.* **179,** 169.

Reddish, V. C. (1978). Int. Series in Natural Philosophy, *Stellar Formation*, Vol. 97.

Reid, N. (1982). *MNRAS* **201,** 51.

Reid, N. (1983). In *IAU Colloq. No. 76, The Nearby Stars and the Stellar Luminosity Function*, A. G. Davis Philip and A. R. Upgren (Eds.). Schenectady: Van Vleck Observatory, p. 173.

Reid, N. (1984). *MNRAS* **206,** 1.

Reid, N., and Gilmore, G. (1982). *MNRAS* **201,** 73.

Reid, N., and Gilmore, G. (1984). *MNRAS* **206,** 19.

Rengarajan, T. N., Cheung, L. H., Fazio, G. G., Shivanandan, K., and McBreen, B. (1984). *Astrophys. J.* **286,** 573.

Renzini, A., and Voli, M. (1981). *Astron. Astrophys.* **94,** 175.

Rhijn, P. J. van (1939). Publ. Kapteyn Astron. Lab. Groningen, No. 49.

Rhijn, P. J. van (1965). In *Galactic Structure*, A. Blaauw and M. Schmidt (Eds.). Chicago: University of Chicago Press, p. 27.

Richer, H. B., and Fahlman, G. G. (1984). *Astrophys. J.* **277,** 227.

Richstone, D. O., and Graham, F. G. (1981). *Astrophys. J.* **248,** 516.

Rieke, G. H., Cutri, R. M., Black, J. H., Kailey, W. F., McAlary, C. W., Lebofsky, M. J., and Elston, R. (1985). *Astrophys. J.* **290,** 116.

Rieke, G. H., Lebofsky, M. J., Thompson, R. I., Low, F. J., and Tokunaga, A. T. (1980). *Astrophys. J.* **238,** 24.

Roberts, M. S. (1958). *PASP* **70,** 462.

Rocca-Volmerange, B., Lequeux, J., and Maucherat-Joubert, M. (198?). *Astron. Astrophys.* **104,** 177.

Rosa, M., and Solf, J. (1984). *Astron. Astrophys.* **130,** 29.

Rousseau, J., Martin, N., Préwt, L., Rebeirot, E., Robin, A., and Brunet, J. P. (1978). *Astron. Astrophys. Suppl.*, **31,** 243.

Roxburgh, J. W. (1978). *Astron. Astrophys.*, **65,** 281.

Sagar, R., and Joshi, U. C. (1979). *Ap. Sp. Sci.* **66,** 3.

Sagar, R., Piskunov, A. E., Myakutin, V. I., and Joshi, V. C. (1985). Preprint.

Salpeter, E. E. (1955). *Astrophys. J.* **121,** 161.

Sandage, A. (1957). *Astrophys. J.* **125,** 422.

Sandage, A., and Katem, B. (1983). *Astron. J.* **88,** 1146.

Sandage, A. R. (1954). *Astrophys. J.* **59,** 162.

Sandage, A. R., and Tammann, G. (1974). *Astrophys. J.* **191,** 603.

Sanders, W. L. (1977). *Astron. Astrophys. Suppl.* **27,** 89.

Sanders, W. L., and van Altena, W. F. (1972). *Astron. Astrophys.* **17,** 193.

Sargent, W. L. W., and Tinsley, B. M. (1974). *MNRAS* **168,** 19p.

Savage, B. D., Fitzpatrick, E. L., Cassinelli, J. P., and Ebbets, D. C. (1983). *Astrophys. J.* **273,** 597.

Scalo, J. M. (1974). *Astrophys. J.* **194,** 361.

Scalo, J. M. (1981). In *Physical Processes in Red Giants*, I. Iben, and A. Renzini (Eds.). Dordrecht: Reidel, p. 77.

Scalo, J. M., Despain, K. H., and Ulrich, R. K. (1975). *Astrophys. J.* **196,** 805.

Scalo, J. M. (1978). In *Protostars and Planets*, T. Gehrels (Ed.). Tucson: University of Arizona Press, p. 265.

Scalo, J. M., and Miller, G. E. (1979). *Astrophys. J.* **233,** 596.

Scalo, J. M., and Miller, G. E. (1980). *Astrophys. J.* **239,** 153.

Scalo, J. M., and Struck-Marcell, C. (1985). *Astrophys. J.* (in press).

Schatzman, E. (1977). *Astron. Astrophys.* **56,** 211.

Schild, H., and Maeder, A. (1983). *Astron. Astrophys.* **127,** 238.

Schmidt-Kaler, Th., and Feitzinger, J. V. (1981). In *The Most Massive Stars*, S. D'Odorico, D. Baade, and K. Kjär (Eds.). Munich: ESO, p. 105.

Schmidt, M. (1959). *Astrophys. J.* **129,** 243.

Schmidt, M. (1975). *Astrophys. J.* **202,** 22.

Schmidt, M. (1983). In *IAU Colloq. No. 76, The Nearby Stars and the Stellar Luminosity Function*, A. G. Davis Philip and A. R. Upgren (Eds.). Schenectady: Van Vleck Observatory, p. 155.

Schweizer, F. (1978). *Astrophys. J.* **220,** 98.

Scoville, N. Z., Becklin, E. E., Young, J. S., and Capps, R. N. (1983). *Astrophys. J.* **271,** 512.

Searle, L., Sargent, W. L. W., and Bagnuolo, W. G. (1973). *Astrophys. J.* **179,** 427.

Seiden, P. E., and Gerola, H. (1982). *Fund. Cos. Phys.* **7,** 241.

Seiden, P. E., Schulman, L. S., and Feitzinger, J. V. (1982). *Astrophys. J.* **253,** 91.

Serra, G., Puget, J. L., and Ryter, C. E. (1980). *Astron. Astrophys.* **84,** 220.

Shaver, P. A., McGee, R. X., Newton, L. M., Danks, A. C., and Pottasch, S. R. (1983). *MNRAS* **204,** 53.

Shields, G. A., and Searle, L. (1978). *Astrophys. J.* **222,** 821.

Shields, G. A., and Tinsley, B. M. (1976). *Astrophys. J.* **203,** 66.

Silk, J. (1978). In *Photostars and Planets*, T. Gehrels (Ed.). Tucson: University of Arizona Press, p. 172.

Simon, K. P., Jonas, G., Kudritzki, R. P., and Rahe, J. (1983). *Astron. Astrophys.* **125,** 34.

Skillman, E. D., and Baslick, B. (1984). *Astrophys. J.* **280,** 580.
Smith, L. F., Biermann, P., and Mezger, P. G. (1978). *Astron. Astrophys.* **66,** 65.
Smith, R. C. (1983). *Obs.* **103,** 1052, 29.
Sneden, C. (1985). In *ESO Workshop on Production and Distribution of C, N, O Elements* (in press).
Sneden, C., Lambert, D. L., and Whitaker, R. W. (1979). *Astrophys. J.* **234,** 964.
Solinger, A., Morrison, P., and Markert, T. (1977). *Astrophys. J.* **211,** 707.
Spite, F., and Spite, M. (1982). *Astron. Astrophys.* **115,** 357.
Spite, F., and Spite, M. (1984). *Astron. Astrophys.* **132,** 278.
Spitzer, L., and Schwarzchild, M. (1951). *Astrophys. J.* **114,** 385.
Stahler, S. W. (1983). *Astrophys. J.* **274,** 822.
Stahler, S. W. (1985). *Astrophys. J.* (in press).
Staller, R. F. A., and de Jong, T. (1981). *Astron. Astrophys.* **98,** 140.
Starikova, G. A. (1960). *Soviet Astron.* **4,** 451.
Starikova, G. A. (1963). *Soviet Astron.* **6,** 821.
Stasinska, G. (1980). *Astron. Astrophys.* **84,** 326.
Stasinska, G. (1982). *Astron. Astrophys. Suppl.* **48,** 299.
Stauffer, J. R. (1980). *Astron. J.* **85,** 1341.
Stauffer, J. R. (1982). *Astron. J.* **87,** 1507.
Stauffer, J. R. (1984). *Astrophys. J.* **280,** 189.
Stauffer, J. R., Hartmann, L., Soderblom, D. R., and Burnham, N. (1984). *Astrophys. J.* **208,** 202.
Stone, R. C. (1980). *PASP* **92,** 426.
Stothers, R. (1972). In *Stellar Evolution,* H.-Y. Chiu, and A. Muriel (Eds.). Cambridge: MIT Press, p. 141.
Straus, J. M., Blake, J. B., and Schramm, D. N. (1976). *Astrophys. J.* **204,** 481.
Strom, S. E., Strom, K. B., and Grasdalen, G. L. (1975). *Ann. Rev. Astron. Astrophys.* **13,** 187.
Struck-Marcell, C., and Tinsley, B. M. (1978). *Astrophys. J.* **221,** 562.
Stryker, L. L. (1984). IAU Symp. No. 108, In *Structure and Evolution of the Magellanic Clouds,* S. van den Bergh and K. de Boer (Eds.), p. 79.
Stryker, L. L., and Butcher, H. R. (1981). In *IAU Colloq. No. 68,* A. G. Davis Philip and D. S. Hayes (Eds.). Schenectady: Davis, p. 255.
Taff, L. G. (1974). *Astron. J.* **79,** 1280.
Talbot, R. J., and Arnett, W. D. (1973). *Astrophys. J.* **186,** 69.
Tammann, G. A., and Sandage, A. (1968). *Astrophys. J.* **151,** 825.
Tarrab, I. (1983). *Astron. Astrophys.* **125,** 308.
Tarrab, I. (1982a). *Astron. Astrophys.* **109,** 285.
Tarrab, I. (1982b). *Astron. Astrophys.* **113,** 57.
Terlevich, R., and Melnick, J. (1981). *MNRAS* **195,** 839.
Terlevich, R., and Melnick, J. (1985). *MNRAS* (in press).
Thuan, T. X. (1983). *Astrophys. J.* **268,** 667.
Tinsley, B. M. (1968). *Astrophys. J.* **151,** 547.
Tinsley, B. M. (1979). *Astrophys. J.* **229,** 1046.
Tinsley, B. M. (1974). *Astron. Astrophys.* **31,** 463.
Tinsley, B. M. (1977). *Astrophys. J.* **216,** 548.
Tinsley, B. M. (1980). *Func. Cos. Phys.* **5,** 287.
Tinsley, B. M., and Larson, R. B. (1978). *Astrophys. J.* **221,** 554.
Tinsley, and Gunn, J. E. (1976). *Astrophys. J.* **203,** 52.
Tobin, W. (1983). *Astron. Astrophys.* **125,** 168.
Tosi, M. (1982). *Astrophys. J.* **254,** 699.
Trimble, V. (1975). *Rev. Mod. Phys.* **47,** 877.

Trimble, V. (1982). *Rev. Mod. Phys.* **54,** 1183.
Trumpler, P. J., and Weaver, H. F. (1953). In *Statistical Astronomy,* Berkeley: University of California Press.
Truran, J. W. (1984). In *Formation and Evolution of Galaxies and Large Structures in the Universe,* J. Audouze and J. Tran Thanh Van (Eds.). Dordrecht: Reidel, p. 391.
Tuchman, Y. (1985). *Astrophys. J.* **288,** 248.
Turnrose, B. E. (1976). *Astrophys. J. Letters* **210,** L9.
Twarog, B. A. (1978). *Astrophys. J.* **220,** 890.
Twarog, B. A. (1980a). *Astrophys. J.* **242,** 12.
Twarog, B. A., and Wheeler, J. C. (1981). *Astrophys. J.* **261,** 636.
Upgren, A. R. (1963). *Astron. J.* **68,** 475.
Upgren, A. R. (1983a). In *IAU Colloq. No. 76, The Nearby Stars and the Stellar Luminosity Function,* A. G. Davis Philip and A. R. Upgren (Eds.). Schenectady: Van Vleck Observatory, p. 247.
Upgren, A. R. (1983b). In *Kinematics, Dynamics, and Structure of the Milky Way,* W. L. H. Shuter (Ed.). Dordrecht: Reidel, p. 15.
Upgren, A. R., and Armandroff, T. E. (1981). *Astron. J.* **86,** 1898.
Vader, J. P., and de Jong, T. (1981). *Astron. Astrophys.* **100,** 124.
van Altena, W. F. (1969). *Astron. J.* **74,** 2.
Vanbeveren, D. (1982). *Astron. Astrophys.* **115,** 65.
Vanbeveren, D. (1983). *Astron. Astrophys.* **124,** 71.
Vanbeveren, D. (1984). *Astron. Astrophys.* **139,** 545.
Vanbeveren, D. (1985). In *Massive Stars in Galaxies,* IAU Symp. No. 118 (in press).
Van Buren, D. (1983). *BAAS* **15,** 923.
Van Buren, D. (1983). Unpublished Ph. D. dissertation, University of California, Berkeley.
van den Bergh (1983).
van den Bergh, S. (1957). *Astrophys. J.* **125,** 445.
van den Bergh, S. (1961). *Astrophys. J.* **134,** 554.
van den bergh, S. (1976). *Astron. J.,* **81,** 797.
van den Bergh, S. (1981). *PASP* **93,** 712.
van den Bergh, S., and Sher, D. (1960). *Publ. DDO* **2,** 203.
van der Linden, T., and Staller, R. (1983). *Astron. Astrophys.* **118,** 285.
Van der Woerd, H., and van den Heuvel, E. P. J. (1984). *Astron. Astrophys.* **132,** 361.
Vangioni-Flam, E., Lequeux, J., Macherat-Joubert, M., Rocca-Volmerange, B. (1980). *Astron. Astrophys.* **90,** 73.
van Leeuwen, F. (1980). IAU Symp. No. 85 in *Star Clusters,* J. E. Hesser (Ed.). Boston: Reidel, p. 157.
Vaucouleurs, G. de (1956). *Irish Astron. J.* **4,** 13.
Vaucouleurs, G. de (1961). *Year Book Amer. Phil. Soc.,* p. 268.
Vaughan, A. H., and Preston, G. W. (1980). *Publ. ASP* **92,** 548.
Vaughan, A. H. and Preston, G. W. (1980). *PASP* **92,** 385.
Veeder, G. J. (1974). *Astron. J.* **79,** 1056.
Viallefond, F., and Thuan, T. X. (1983). *Astrophys. J.* **269,** 444.
Viallefond, F., and Thuan, T. X. (1984). *Astrophys. J.* **269,** 444.
Villumsen, J. V. (1983). *Astrophys. J.* **274,** 632.
Villumsen, J. V. (1985). *Astrophys. J.* **290,** 75.
Vogt, N. (1971). *Astron. Astrophys.* **11,** 359.
Walborn, N. R. (1982). *Astrophys. J. Lett.* **254,** L15.
Walker, M. P. (1957). *Astrophys. J.* **125,** 636.
Wanner, J. F. (1972). *MNRAS* **155,** 463.
Warner, J. W., Strom, S. E., and Strom, K. M. (1977). *Astrophys. J.* **213,** 427.

Warren, P. R. (1976). *MNRAS* **176**, 667.
Weaver, A., Zimmerman, G. B., and Woosley, S. E. (1978). *Astrophys. J.* **225**, 1021.
Webster, B. L. (1983). *MNRAS* **204**, 743.
Weedman, D. W. (1983). *Astrophys. J.* **266**, 479.
Weedman, D. W., Freedman, F. R., Balzano, V. A., Ramsey, L. W., Sramek, R. A., and Wu, C. C. (1981). *Astrophys. J*, **248**, 105.
Weiss, E. W. (1983). *PASP* **95**, 29.
Weiss, E. W., and Upgren, A. R. (1982). *PASP* **94**, 475.
Wheeler, J. C. (1981). *Rept. Prog. Phys.* **44**, 85.
White, S. D. M., and Audouze, J. (1984). *MNRAS* **203**, 603.
Whiteford, A. E. (1977). *Astrophys. J.* **211**, 527.
Wielen, R. (1971). *Astron. Astrophys.* **13**, 309.
Wielen, R. (1975). In *Dynamics of Stellar Systems*, A. Haylin (Ed.). Dordrecht: Reidel, p. 119.
Wielen, R., Jahreiss, H., and Krüger, R. (1983). In *IAU Colloq. No. 76, The Nearby Stars and the Stellar Luminosity Function*, A. G. Davis Philip and A. R. Upgren (Eds.). Schenectady: Van Vleck Observatory, p. 163.
Williams, I. P. and Cremin, A. W. (1969). *MNRAS* **144**, 359.
Williams, T. B. (1976). *Astrophys. J.* **209**, 716.
Wink, J. E., Wilson, T. L., and Bieging, J. H. (1983). *Astron. Astrophys.* **127**, 211.
Woosley, S. E., Axelrod, T. S., and Weaver, T. A. (1984). In *Stellar Nucleosynthesis*, C. Chiosi and A. Renzini. (Eds.). Dordrecht: Reidel.
Woosley, S. E., and Weaver, T. A. (1981). *Ann. N.Y. Acad. Sci.* **375**, 357.
Yang, J., Turner, M. S., Steigman, G., Schramm, D. N. and Olive, K. A. (1984). *Astrophys. J.* **281**, 493.
Young, P. J., Sargent, W. L. W., Boksenberg, A., Lynds, C. R., and Hartwick, F. D. A. (1978). *Astrophys. J.* **222**, 450.
Zappala, R. R. (1972). *Astrophys. J.* **172**, 57.
Zinnecker, H. (1981). Unpublished Ph. D. dissertation, Max-Planck Institut für Physik und Astrophysik.
Zinn R. (1980). *Astrophys. J. Suppl.* **42**, 19.